DIRECT GENERATION OF SEISMIC FLOOR RESPONSE SPECTRA FOR CLASSICALLY AND NONCLASSICALLY DAMPED STRUCTURES

by

Anil M. Sharma

and

Mahendra P. Singh

Technical Report of Research Supported by
The National Science Foundation Under
Grant No. CEE 8109100

Department of Engineering Science & Mechanics
Virginia Polytechnic Institute & State University
Blacksburg, VA 24061

November 1983

TABLE OF CONTENTS

Chapter 1

INTRODUCTION

1.1 BACKGROUND

The design of light equipment and nonstructural components to withstand dynamic/seismic loading is an important feature in the design of industrial facilities. Control equipment, piping systems, pumps, compressors, pressure vessels, generators, motors, tanks, furnaces, conveyor systems, cranes, mixers, antennas, stacks, bins, parapets and elevators are some examples of components which are found in nuclear power plant facilities, multistory buildings and industrial plants. These components are often referred to as secondary systems (also subsystems) so as to distinguish them from the primary structural systems on which they are supported.

These secondary systems are not of secondary importance, as their malfunctions during or after an earthquake are likely to have very serious repercussions; their survival is essential to provide and regulate much needed emergency services such as telecommunication, power transmission and transportation. Thus, it is important that these systems be designed properly to withstand some reasonable earthquake induced effects, even in the areas

where no earthquake activity has been reported in the recent past.

An important ingredient for a proper design of a secondary system is the definition of seismic design loading. Such a loading is commonly obtained in terms of floor response spectra which represent response characteristics of the motion of a floor of a building on which the secondary system is supported. Floor response spectra provide the same type of information about the motion of a floor as ground response spectra provide about the ground motion. The latter are commonly used as seismic inputs for the design of important primary systems. For the design of nuclear power plants in the United States the Nuclear Regulatory Commission has prescribed design ground response spectra in their Regulatory Guide No. 1.60 [51].

A primary structure and its supported secondary systems will experience the effects of the same ground motion during an earthquake. Thus if a primary structure is designed for a prescribed set of ground response spectra, its supported secondary systems also should be designed for a consistent seismic input. That is, the design floor spectra should be consistent with the ground response spectra which are used as design input for the supporting primary structures.

Procedures for establishing design ground response spectra are rather well defined and accepted by profession [7,20,31,32]. To obtain floor response spectra for a set of prescribed ground spectra, currently the time history analysis is most commonly used. In this method, usually a spectrum-consistent time history [17,48,50] -- a time history with its spectra closely enveloping the prescribed ground spectra -- is used as seismic input. Although this approach is analytically accurate for a given time history, it has been known to give unreliable and inconsistent results for design purposes. Specifically, it has been observed [5,6,39] that two independently synthesized spectrum-consistent time histories may give significantly different floor response spectra even though these time histories may be consistent with a given ground response spectrum in the same sense. To obtain a reliable design floor response spectrum, an ensemble of time histories should be used in the analysis. As a time history analysis to obtain floor spectra is costly even for a single time history, the analysis for a set of time histories becomes very expensive.

Upon realizing that the time history approach is impractical, several researchers have proposed simple approximate procedures to construct floor response spectra. Biggs [5] probably was the first person to develop a method for

obtaining floor response spectra directly from prescribed ground spectra. In this method magnification curves were obtained on the basis of observed behavior of oscillators subjected to a set of earthquake records. The use of these magnification curves reportedly gave conservative results. Kapur and Shao [23] also proposed a similar method. These two approaches were based on semi-empirical arguments. Several other investigators Penzien and Chopra [33], Newmark [32], Chakravorty and Vanmarcke [9], Schanlan and Sachs [36,37], Vanmarcke [53], Peters, Schmitz and Wagner [34], Atalik [2], Singh [39,43], Sackman and Kelly [35], Villaverde and Newmark [54], and Der Kiureghian et al. [14], and Vanmarcke [53] have addressed this problem and proposed different procedures, which are based on deterministic as well as random vibration principles.

Almost all of these approaches are applied to linear proportionally (or classically) damped [8,11,21,29] systems. They make different assumptions in their formulations. Some are based on deterministic method whereas others are based on random vibration principles. Most, usually, ignore the interaction between primary and secondary system, except those in References 14,24,35,43,54. In some isolated cases, the interaction may be important and must be considered. However, in a majority of cases omission of interaction from floor spectra generation procedure is quite

acceptable and provides a conservative estimate of floor spectra. Also interaction free spectra are easy to interpret and use in the design and qualification of secondary systems. In this investigation, only interaction free spectra development procedures are considered with the main objective of developing rational and analytically simple direct methods for generation of floor spectra.

1.2 SCOPE OF STUDY

The main aim of this study is to develop validated and simple-to-use floor spectra generation procedures for linear structural systems which are proportionally or non-proportionally damped. The main requirement of these procedures is that they should make a direct use of design input prescribed in the form of ground spectra, without employing spectrum consistent time histories or spectral density functions. For this, first an approach proposed by Singh [39,43] earlier has been critically examined, improved and validated by simulation studies. The special case of evaluation of floor spectra at resonance (i.e. at oscillator frequency equal to the structural frequency) is also considered. The effect of incorporation of peak factors in the calculation of floor spectra is investigated.

For seismic analysis, structural systems are often assumed to possess classical damping matrices [8,39]. This assumption is purely for mathematical convenience, and in some cases it may also be justified. Yet there may be cases where it cannot be justified and nonproportional or nonclassical nature of the damping matrix must be clearly recognized. Here the methods for generation of floor spectra for nonclassically damped primary system are also developed and validated by a simulation study.

Most of the approaches described above are based on the method of mode displacement of structural dynamics. Often only a first few modes are used in the analysis as the higher modes are considered unimportant. Some problems may, however, arise with these approaches if the response is affected by the high frequency modes. Herein, an alternative approach, based on the method of mode acceleration has been proposed in which the effect of high frequency modes is correctly included without their explicit evaluation. The seismic input in this approach is required to be prescribed in terms of relative acceleration and velocity spectra. This approach is very effective for the calculation of floor spectra for stiff structural systems which have significant contribution from the high frequency modes, and also for floors close to the base which are

usually affected by the higher modes. In other normal cases too, this approach has been shown to provide better results than the mode displacement approach for a given number of modes. The mode acceleration approaches have been developed for proportionally as well as non-proportionally damped structural systems.

To incorporate the uncertainties of the primary system in the generation of floor response spectra an analytical-cum-simulation approach has been used. Effect of mass and stiffness uncertainties on floor spectra is evaluated.

1.3 ORGANIZATION

In Chapter 2, a direct approach proposed for generation of seismic floor response spectra by Singh [39,43] is reevaluated and improved. Methods to incorporate the peak factors in generation of spectra have been examined. Generation of floor spectra for the important case of resonance between structural modes and oscillator has been developed. The verification of this approach is done by a numerical simulation study.

A method to generate the floor spectra for non-proportionally damped primary systems, using the mode

displacement method, is presented in Chapter 3. The formulation for the resonance case has also been developed. Verification of this direct approach is also done by a numerical simulation study.

In Chapters 4 and 5, the approaches based on the method of mode acceleration are developed for generation of floor response spectra for classically and nonclassically damped primary systems. Evaluation spectra at structural frequencies, i.e. at resonance, has also been considered. Verification of the approach is again done by a numerical simulation study.

To avoid distractions in presentation of the formulations, various coefficients required in the proposed methods and other analytical expressions are defined in the Appendices I, II, III, and IV, associated with Chapters 2, 3, 4, and 5, respectively.

The general summary and conclusions of the investigation are stated in Chapter 6.

Chapter 2

CLASSICALLY DAMPED SYSTEMS: MODE DISPLACEMENT METHOD

2.1 INTRODUCTION

To obtain the floor response spectrum, time history method of analysis is commonly used. However, it has been observed that this approach is unreliable and computationally expensive. Therefore direct approaches of generating floor spectra are becoming increasingly popular. In these direct approaches, the seismic input is defined in terms of ground spectra. One such direct approach was proposed by Singh [39,43]. This approach is based on mode displacement method of structural dynamics and primarily employs pseudo acceleration spectra and relative velocity spectra as input. Some simplified assumptions were made in the development of this approach. These assumptions are examined in this chapter with regard to their effects on generation of floor spectra. Various improvements are proposed, and finally the proposed approach is verified by a numerical simulation study. In the following section, a more general and complete formulation of the method is presented.

2.2 ANALYTICAL FORMULATION

The equation of motion of an n-degree-of-freedom structure subjected to ground excitation, $\ddot{X}_g(t)$, can be written in the standard form as

$$[M] \{\ddot{x}\} + [C] \{\dot{x}\} + [K] \{x\} = - [M] \{r\} \ddot{X}_g(t) \quad (2.1)$$

where [M], [C], and [K] are the mass, damping and stiffness matrices respectively; {x} = the relative displacement vector; {r} = displacement influence vector; $\ddot{X}_g(t)$ = ground acceleration; and dot over a term represents its derivative with respect to time.

Eq. 2.1 can be solved using normal mode approach where the response vector {x} is expressed as

$$\{x\} = [\phi] \{z'\} \quad (2.2)$$

where $[\phi]$ is the modal matrix, and {z'} is the vector of principal coordinates. By substitution of Eq. 2.2 in Eq. 2.1 and utilization of orthogonal properties of normal modes, the decoupled equations of the following form are obtained to solve for the principal coordinates.

$$\ddot{z}_j + 2 \beta_j \omega_j \dot{z}_j + \omega_j^2 z_j = - \ddot{X}_g(t) \quad (2.3)$$

where

$$z_j' = \gamma_j z_j \quad (2.4)$$

and γ_j = participation factor defined as = $\{\phi_j\}^T[M]\{r\}/m_j$, $m_j = \{\phi_j\}^T[M]\{\phi_j\}$, $\{\phi_j\}$ = jth mode displacement vector, ω_j = jth frequency, β_j = modal damping ratio defined as $= \{\phi_j\}^T[C]\{\phi_j\}/2\ \omega_j m_j$. This assumes that $\{\phi_j\}^T\ [C]\ \{\phi_k\} = 0$ for $j \neq k$ or the damping matrix is of classical or proportional type [8]. The cases when [C] is nonclassical are discussed in Chapters 3 and 5.

To obtain floor response spectra for the mth floor, we need to obtain the response of a series of oscillators placed on the floor. The equation of motion of one such oscillator with frequency, ω_o and damping ratio β_o, can be written as follows:

$$\ddot{\eta} + 2\ \beta_o\ \omega_o\ \dot{\eta} + \omega_o^2\ \eta = -\ \ddot{X}_a(t) \qquad (2.5)$$

in which η is the relative displacement of the oscillator and $\ddot{X}_a$ is the absolute acceleration of the floor. Here the effect of dynamic interaction between the oscillator and the supporting structure is neglected.

The absolute acceleration, $\ddot{X}_a$, is required to obtain the oscillator response. This can be obtained in terms of relative acceleration of the floor, $\ddot{x}_a$, and ground acceleration, $\ddot{X}_g$, as follows:

$$\ddot{X}_a = r_m\ \ddot{X}_g + \ddot{x}_m \qquad (2.6)$$

Using Eq. 2.2 and 2.4, $\ddot{X}_a$ can also be written as follows:

$$\ddot{X}_a = r_m \ddot{X}_g + \sum_{j=1}^{n} \gamma_j \phi_j(m) \ddot{z}_j(t) \qquad (2.7)$$

where $\phi_j(m)$ is the mth element of modal vector $\{\phi_j\}$. Using Eq. 2.3, it can also be expressed in the following form:

$$\ddot{X}_a = - \sum_{j=1}^{n} \gamma_j \phi_j [2 \beta_j \omega_j \dot{z}_j + \omega_j^2 z_j] \qquad (2.8)$$

in which $\phi_j(m)$ is simply replaced by ϕ_j. Hereafter ϕ_j will imply $\phi_j(m)$.

Eq. 2.8 defines the floor acceleration in terms of modal displacement, z_j, and modal velocity, $\dot{z}_j$. For small damping major contribution to $\ddot{X}_a$ comes from z_j, the mode displacement value. Thus, the formulation which employs Eq. 2.8, is called the mode displacement formulation. Most floor spectra generation approaches developed so far adopt this expression for floor acceleration, and therefore, can be classified as mode displacement approaches.

For design purposes, we are interested in the solution of the Eq. 2.5 for a class of earthquake motion that can be expected at a site. That is, we should evaluate the

response for an ensemble of earthquake motions. This suggests that we model $\ddot{X}_g(t)$ as a random process representing the ensemble. For earthquake motions modeled by a random process, the response of the oscillator will also be a random process. To define floor response spectra we need to obtain the maximum value of such random response. For engineering purposes, the maximum response can be obtained from the mean and autocorrelation characteristics of the response. Here, our aim therefore is to obtain these two characteristics of the response. More specifically we will obtain absolute acceleration response of the oscillator, as in practice acceleration floor spectra are more commonly used. If other response characteristics, like relative or pseudo velocity are desired, they can also be obtained similarly.

From Eq. 2.5, the absolute acceleration, $\ddot{\eta}_a$, of the oscillator can be defined as follows:

$$\ddot{\eta}_a = \ddot{X}_a(t) + \ddot{\eta} = - (2 \beta_o \omega_o \dot{\eta} + \omega_o^2 \eta) \qquad (2.9)$$

To define acceleration spectra, we need to obtain the mean and autocorrelation function of $\ddot{\eta}_a$ which in turn is defined in terms of the mean and autocorrelation function of $\ddot{X}_a(t)$. These characteristics of $\ddot{X}_a(t)$ are obtained in the following section.

2.3 AUTOCORRELATION AND POWER SPECTRAL DENSITY FUNCTION OF ABSOLUTE ACCELERATION OF A FLOOR

Here earthquake motion, $\ddot{X}_g(t)$, is modeled as a zero mean random process. Thus the mean value of $\ddot{X}_a(t)$, from Eq. 2.8, is zero. The autocorrelation function of $\ddot{X}_a(t)$ is obtained as:

$$E[\ddot{X}_a(t_1)\ \ddot{X}_a(t_2)] = \sum_{j=1}^{n}\sum_{k=1}^{n} \gamma_j\ \gamma_k\ \phi_j\ \phi_k \{4\ \beta_k\ \beta_j\ \omega_j\ \omega_k \cdot E[\dot{z}_j \cdot \dot{z}_k] + \omega_j^2\ \omega_k^2\ E[z_j \cdot z_k] + 2\ \beta_k\ \omega_k\ \omega_j^2 \cdot E[z_j\ \dot{z}_k] + 2\ \beta_j\ \omega_j\ \omega_k^2\ E[\dot{z}_j\ z_k]\} \qquad (2.10)$$

The auto and cross correlation of principal coordinates and their derivatives required in Eq. 2.10 can be obtained in terms of autocorrelation function of the ground motion from Eq. 2.3. Here to simplify the analysis it is assumed that ground motion is a stationary random process with spectral density function $\Phi_g(\omega)$. Although earthquake motions are not stationary, this assumption, as shown later by simulation study, will still provide us an acceptable and reliable method for generation of floor spectra. With this assumption, various expected value terms in Eq. 2.10 can now be obtained in terms of ground spectral density function, $\Phi_g(\omega)$. Furthermore, if we consider stationary response, these terms can be shown to be as given in

Appendix I-A, Eqs. I.5 and I.6.

Substituting these expressions of various expected value terms in Eq. 2.10, the autocorrelation function of the absolute acceleration $\ddot{X}_m$ can be shown to be as follows:

$$E[\ddot{X}_a(t_1)\ \ddot{X}_a(t_2)] = \int_{-\infty}^{\infty} e^{i\omega(t_1-t_2)}\ \Phi_m(\omega)\ d\omega \qquad (2.11)$$

where $\Phi_m(\omega)$ is the spectral density function of floor acceleration defined as:

$$\Phi_m(\omega) = \sum_{j=1}^{n}\sum_{k=1}^{n} \gamma_j\ \gamma_k\ \phi_j\ \phi_k\ [\omega_j^2\ \omega_k^2 + 4\ \beta_j\ \beta_k\ \omega_j\ \omega_k\ \omega^2 + 2\ i\omega\ \omega_j\ \omega_k(\omega_k\ \beta_j - \omega_j\ \beta_k)]\ H_j\ H_k^*\ \Phi_g(\omega) \qquad (2.12)$$

where H_j is the complex frequency response function for mode j, defined as

$$H_j = 1/(\omega_j^2 - \omega^2 + 2\ i\ \omega_j\ \beta_j\ \omega) \qquad (2.13)$$

and an asterisk denotes a complex conjugate. Here i is equal to $\sqrt{-1}$.

For further analytical manipulations, the spectral density function in Eq. 2.12 is spearated into terms with j=k and j≠k as follows:

$$\Phi_m(\omega) = \sum_{j=1}^{n} \gamma_j^2 \, \phi_j^2 \, (\omega_j^4 + 4 \, \beta_j^2 \, \omega_j^2 \, \omega^2) \, |H_j|^2 \, \Phi_g(\omega)$$

$$+ 2 \sum_{j=1}^{n} \sum_{k=j+1}^{n} \gamma_j \, \gamma_k \, \phi_j \, \phi_k \, N(\omega) \, |H_j|^2 \, |H_k|^2 \, \Phi_g(\omega) \tag{2.14}$$

in which

$$N(\omega) = (\omega_j^2 \, \omega_k^2 + 4 \, \beta_j \, \beta_k \, \omega_j \, \omega_k \, \omega^2) \cdot \{(\omega_j^2 - \omega^2)(\omega_k^2 - \omega^2)$$

$$+ 4 \, \beta_j \, \beta_k \, \omega_j \, \omega_k \, \omega^2\} + 4 \, \omega^2 \, \omega_j \, \omega_k (\omega_k \, \beta_j - \omega_j \, \beta_k)$$

$$\cdot \{\beta_j \, \omega_j (\omega_k^2 - \omega^2) - \beta_k \, \omega_k (\omega_j^2 - \omega^2)\} \tag{2.15}$$

The mean square value of the absolute acceleration, $\ddot{\eta}_a$, of an oscillator supported on floor can now be obtained in terms of floor acceleration spectral density function as follows:

$$\sigma^2_{\ddot{\eta}_a} = \int_{-\infty}^{\infty} \Phi_m(\omega) \, (\omega_o^4 + 4 \, \beta_o^2 \, \omega_o^2 \, \omega^2) \, |H_o|^2 \, d\omega \tag{2.16}$$

2.4 FLOOR RESPONSE SPECTRUM

Eq. 2.16 can be used to obtain the standard deviation of secondary system response which, when amplified by an appropriate peak factor, will give the maximum floor response value or response spectrum value as follows:

$$R_a^2(\omega_o, \beta_o) = P_F^2(\omega_o) \int_{-\infty}^{\infty} \Phi_m(\omega)(\omega_o^4 + 4\ \beta_o^2\ \omega_o^2\ \omega^2)\ |H_o|^2\ d\omega \tag{2.17}$$

where $R_a(\omega_o, \beta_o)$ = floor acceleration response spectrum value at frequency ω_o and damping β_o, $P_F(\omega_o)$ = a factor usually called a peak factor which when multiplied by the root mean square value of the floor spectral response gives the response spectrum value. Substituting for $\Phi_m(\omega_o)$ from Eq. 2.14,

$$\begin{aligned} R_a^2(\omega_o, \beta_o) = P_F^2(\omega_o) \Bigg[& \sum_{j=1}^{n} \gamma_j^2\ \phi_j^2 \int_{-\infty}^{\infty} (\omega_j^4 + 4\ \beta_j^2\ \omega_j^2\ \omega^2) \\ & \cdot (\omega_o^4 + 4\ \beta_o^2\ \omega_o^2\ \omega^2)\ |H_j|^2\ |H_o|^2\ \Phi_g(\omega)\ d\omega \\ & + 2 \sum_{j=1}^{n} \sum_{k=j+1}^{n} \gamma_j\ \gamma_k\ \phi_j\ \phi_k \int_{-\infty}^{\infty} N(\omega) \\ & \cdot (\omega_o^4 + 4\ \beta_o^2\ \omega_o^2\ \omega^2)\ |H_j|^2\ |H_k|^2\ |H_o|^2\ \Phi_g(\omega)\ d\omega \Bigg] \end{aligned} \tag{2.18}$$

To obtain the integrals in Eq. 2.18 in terms of ground spectra, which are commonly prescribed as seismic design inputs, the single and double summation terms will be resolved into partial fractions [39]. This will, however, not be possible when $\omega_j = \omega_o$ and $\beta_j = \beta_o$. Such a case is referred to as resonance case and is dealt with separately in Section 2.4.2.

2.4.1 Floor Spectrum: Nonresonance Case

Here the evaluation of single and double summation terms in terms of ground spectra is described.

Single Summation Terms

The integrand of a typical single summation term in Eq. 2.18 can be resolved into partial fractions as follows:

$$(\omega_o^4 + 4\,\beta_o^2\,\omega_o^2\,\omega^2)\,(\omega_j^4 + 4\,\beta_j^2\,\omega_j^2\,\omega^2)\,|H_j|^2\,|H_o|^2$$
$$= (A_1\,\omega_o^4 + A_2\,\omega_o^2\,\omega^2)\,|H_o|^2$$
$$+ (A_3\,\omega_j^4 + A_4\,\omega_j^2\,\omega^2)\,|H_j|^2 \qquad (2.19)$$

in which the coefficients A_1, A_2, A_3, and A_4 are defined in Appendix I-B, Eq. I.8. By multiplying Eq. 2.19 by $\Phi_g(\omega)$ and integrating over the frequency range, the following is obtained

$$I_s' = \int_{-\infty}^{\infty} \Phi_g(\omega)\ (\omega_o^4 + 4\ \beta_o^2\ \omega_o^2\ \omega^2)\ (\omega_j^4 + 4\ \beta_j^2\ \omega_j^2\ \omega^2) \cdot |H_j|^2\ |H_o|^2\ d\omega$$

$$= A_1 \int_{-\infty}^{\infty} \omega_o^4\ \Phi_g(\omega)\ |H_o|^2\ d\omega + A_2 \int_{-\infty}^{\infty} \omega_o^2\ \omega^2 \cdot \Phi_g(\omega)\ |H_o|^2\ d\omega + A_3 \int_{-\infty}^{\infty} \omega_j^4\ \Phi_g(\omega)\ |H_j|^2\ d\omega + A_4 \int_{-\infty}^{\infty} \omega_j^2\ \omega^2\ \Phi_g(\omega)\ |H_j|^2\ d\omega \qquad (2.20)$$

or

$$I_s' = A_1\ I_1(\omega_o) + A_2\ \omega_o^2\ I_2(\omega_o) + A_3\ I_1(\omega_j) + A_4\ \omega_j^2\ I_2(\omega_j) \qquad (2.21)$$

in which $I_1(\omega_j)$ and $I_2(\omega_j)$ are frequency integrals defined as

$$I_1(\omega_j) = \int_{-\infty}^{\infty} \omega_j^4\ \Phi_g(\omega)\ |H_j|^2\ d\omega \qquad (2.22)$$

$$I_2(\omega_j) = \int_{-\infty}^{\infty} \omega^2\ \Phi_g(\omega)\ |H_j|^2\ d\omega \qquad (2.23)$$

The frequency integral $I_1(\omega_j)$ and $I_2(\omega_j)$, respectively, represent the mean square values of pseudo acceleration and relative velocity responses of an oscillator of frequency, ω_o and damping ratio, β_o excited by the ground motion. The root mean square values when multiplied by their respective

peak factors will give the response spectrum values. That is

$$R_p^2(\omega_j) = S_p^2(\omega_j)\ I_1(\omega_j) \tag{2.24}$$

$$R_v^2(\omega_j) = S_v^2(\omega_j)\ I_2(\omega_j) \tag{2.25}$$

in which $R_p(\omega_j)$ = pseudo acceleration response spectrum value, $R_v(\omega_j)$ = relative velocity response spectrum value, $S_p(\omega_j)$ = peak factor for pseudo acceleration response and $S_v(\omega_j)$ = peak factor for relative velocity spectra, all obtained for the oscillator frequency of ω_o and damping ratio β_o.

Eqs. 2.24 and 2.25 are used to define $I_1(\omega_j)$ and $I_2(\omega_j)$ in terms of response spectrum values. Thus I'_s in Eq. 2.21 can also be defined directly in terms of response spectrum values.

Double Summation Terms

To evaluate the double summation terms in Eq. 2.18 in terms of ground response spectra, the integrand of a typical term in Eq. 2.18 is split into partial fractions as follows:

$$N(\omega)\ (\omega_o^4 + 4\ \beta_o^2\ \omega_o^2\ \omega^2)\ |H_j|^2\ |H_k|^2\ |H_o|^2$$

$$= (\omega_o^4 + 4\ \beta_o^2\ \omega_o^2\ \omega^2)\ |H_o|^2\ [(A_r\ \omega_j^4 + B_r\ \omega_j^2\ \omega^2)$$

$$\cdot\ |H_j|^2 + (C_r\ \omega_k^4 + D_r\ \omega_k^2\ \omega^2)\ |H_k|^2]\ d\omega \qquad (2.26)$$

where the coefficients A_r, B_r, etc. are defined in Appendix I-B, Eq. I.17.

The resonance case when the oscillator frequency and damping are equal to one of the structural frequencies and corresponding damping ratio will require a special treatment of the terms in Eq. 2.26. It is discussed in Section 2.5. For the nonresonance case the right hand side of Eq. 2.26 is further split into partial fractions as follows:

$$N(\omega)\ (\omega_o^4 + 4\ \beta_o^2\ \omega_o^2\ \omega^2)\ |H_j|^2\ |H_k|^2\ |H_o|^2$$

$$= (B_1\ \omega_o^4 + B_2\ \omega_o^2\ \omega^2)\ |H_o|^2 + (B_3\ \omega_j^4$$

$$+ B_4\ \omega_j^2\ \omega^2)\ |H_j|^2 + (C_1\ \omega_o^4 + C_2\ \omega_o^2\ \omega^2)\ |H_o|^2$$

$$+ (C_3\ \omega_k^4 + C_4\ \omega_k^2\ \omega^2)\ |H_k|^2 \qquad (2.27)$$

where the coefficients B_1, B_2, C_1, etc. are defined in Appendix I-B, Eq. I.12.

Multiplying Eq. 2.27 by $\Phi_g(\omega)$ and integrating over the frequency domain, the following is obtained for the

frequency integral of a typical double summation term in Eq. 2.18.

$$I_d' = \int_{-\infty}^{\infty} \Phi_g(\omega)\ N(\omega)\ (\omega_o^4 + 4\ \beta_o^2\ \omega_o^2\ \omega^2)\ |H_j|^2\ |H_k|^2 \cdot |H_o|^2\ d\omega$$

$$= (B_1 + C_1)\ I_1(\omega_o) + (B_2 + C_2)\ \omega_o^2\ I_2(\omega_o) + B_3\ I_1(\omega_j) + B_4\ \omega_j^2\ I_2(\omega_j) + C_3\ I_1(\omega_k) + C_4\ \omega_k^2\ I_2(\omega_k) \qquad (2.28)$$

where, again, $I_1(\omega_j)$ and $I_2(\omega_j)$ etc. are defined by the integrals in Eqs. 2.22 and 2.23. Using Eqs. 2.21 and 2.28, the floor response spectrum value in Eq. 2.18 can be written as follows:

$$R_a^2(\omega_o, \beta_o) = P_F^2(\omega_o) \left[\sum_{j=1}^{n} \gamma_j^2 \phi_j^2 \{A_1 I_1(\omega_o) + A_2 \omega_o^2 I_2(\omega_o) + A_3 I_1(\omega_j) + A_4 \omega_j^2 I_2(\omega_j)\} \right.$$

$$+ 2 \sum_{j=1}^{n} \sum_{k=j+1}^{n} \gamma_j \gamma_k \phi_j \phi_k \{(B_1 + C_1) I_1(\omega_o) + (B_2 + C_2) \omega_o^2 I_2(\omega_o) + B_3 I_1(\omega_j) + B_4 \omega_j^2 I_2(\omega_j)$$

$$\left. + C_3 I_1(\omega_k) + C_4 \omega_k^2 I_2(\omega_k)\} \right] \qquad (2.29)$$

As $I_1(\omega_j)$ and $I_2(\omega_j)$ are defined in terms of response spectrum values by Eqs. 2.24 and 2.25, Eq. 2.29 defines the expression for the floor response spectrum in terms of ground response spectrum values and associated peak factors. It differs from the expression derived by Singh [39] inasmuch as it contains the effect of different peak factors in generation of floor spectra. If all the peak factor values are assumed equal then this expression reverts back to the expression given by Singh [39].

2.4.2 FLOOR SPECTRUM: RESONANCE CASE

The factors A_1, A_2, B_1, C_1, etc. in Eq. 2.29 depend upon the frequency ratios and modal damping values. These are not defined for the special resonance case, i.e. when

$\omega_j = \omega_o$ and $\beta_j = \beta_o$. Here a procedure for the evaluation of a floor response spectrum value for this special case is presented. Specifically, the procedures for the evaluation of the frequency integrals in the single and double summation term of Eq. 2.18 in terms of ground spectrum values are described.

Single Summation Terms

For the special case of resonance, the frequency integral in a typical single summation term can be written as follows:

$$I_s = \int_{-\omega_c}^{\omega_c} \Phi_g(\omega) \; (\omega_o^4 + 4 \; \beta_o^2 \; \omega_o^2 \; \omega^2)^2 \; |H_o|^4 \; d\omega \qquad (2.30)$$

Here to be more realistic, the frequency range for the integral is limited to a cut-off frequency value of ω_c. In earthquake induced ground motion, this cut-off frequency will be about 25-30 cps. For example such a cut-off frequency limit is also implied by ground response spectra, prescribed by the N.R.C. for the design of nuclear power plants [51]. For the N.R.C. spectra, the ω_c value could be assumed to be about 33 cps, though actual limiting frequency will be somewhat smaller. Limiting the frequency range has special relevance in generation of floor spectra for oscillator frequencies higher than the limiting frequency.

Because of the peakedness of the function $|H_o|^4$ in Eq. 2.30, the integral can be fairly accurately approximated as follows [43,52]:

$$I_s = \Phi_g(\omega_o) \int_{-\omega_c}^{\omega_c} (\omega_o^4 + 4\ \beta_o^2\ \omega_o^2\ \omega^2)^2\ |H_o|^2\ d\omega$$

$$- 2\ \Phi_g(\omega_o)\ \omega_o + \int_{-\omega_c}^{\omega_c} \Phi_g(\omega)\ d\omega \qquad (2.31)$$

The first integral in Eq. 2.31 can be evaluated in closed form in terms of A_m as defined by Eq. I.22 in Appendix I-C as

$$\int_{-\omega_c}^{\omega_c} (\omega_o^4 + 4\ \beta_o^2\ \omega_o^2\ \omega^2)\ |H_o|^4\ d\omega = \omega_c\ A_m \qquad (2.32)$$

where

$$A_m = A_m(r,\ \beta_o,\ a_o,\ a_1,\ a_2,\ a_3) \qquad (2.33)$$

with $r = \omega_o/\omega_c$; $a_o = 0$; $a_1 = 16\ \beta_o^4$; $a_2 = 8\ \beta_o^2$; $a_3 = 1$.

The second frequency integral in Eq. 2.31 which represents the partial area under the PSDF is denoted by I_b, i.e.

$$I_b = \int_{-\omega_c}^{\omega_c} \Phi_g(\omega)\ d\omega \qquad (2.34)$$

Using Eqs. 2.32 and 2.34, Eq. 2.31 can be rewritten as follows:

$$I_s = \Phi_g(\omega_o)\ \omega_c\ (A_m - 2r) + I_b \tag{2.35}$$

To express $I_s(\omega_o)$ in terms of ground spectra it is now necessary to express $\Phi_g(\omega_o)$ and I_b in spectra terms. For this, as observed by Singh [43], the following relationship between the mean square values of pseudo acceleration and relative velocity is used:

$$I_1(\omega_o) \simeq \omega_o^2\ I_2(\omega_o) + I_b \tag{2.36}$$

or,

$$I_b = I_1(\omega_o) - \omega_o^2\ I_2(\omega_o) = I_1(\omega_o)\ \{1 - F(\omega_o)\} \tag{2.37}$$

where

$$F(\omega_o) = \omega_o^2\ I_2(\omega_o)/I_1(\omega_o) \tag{2.38}$$

is the ratio of the mean square value of the relative velocity to that of pseudo velocity. This ratio approaches zero for frequencies greater than ω_c. Eq. 2.37 with Eqs. 2.24 and 2.25 can now be used to express I_b in terms of response spectrum values.

To obtain $\Phi_g(\omega_o)$ in terms of response spectrum values, the following approximation for $I_1(\omega_o)$ is used:

$$I_1(\omega_o) = \omega_o^4 \int_{-\omega_c}^{\omega_c} \Phi_g(\omega) \, |H_o|^2 \, d\omega$$

$$\simeq \Phi_g(\omega_o) \, \omega_o^4 \int_{-\omega_c}^{\omega_c} |H_o|^2 \, d\omega - 2 \, \omega_o \, \Phi_g(\omega_o) + I_b \tag{2.39}$$

The integral in Eq. 2.39 can be evaluated in closed form as in Appendix I-C, Eq. I.27. Thus

$$I_1(\omega_o) \simeq \Phi_g(\omega_o) \, \omega_c \cdot B_m - 2 \, \omega_o \, \Phi_g(\omega_o) + I_b$$

$$= \Phi_g(\omega_o) \, \omega_c \, (B_m - 2r) + I_b \tag{2.40}$$

in which

$$B_m = B_m(r, \beta_o, b_o, b_1) \tag{2.41}$$

with $b_o = 0$, $b_1 = 1$. Substituting for the value of $\phi_g(\omega_o)\omega_c$ from Eq. 2.40 and for I_b from Eq. 2.37, into Eq. 2.31, the frequency integral in a single summation resonance term is obtained as

$$I_s = I_1(\omega_o) \, [A_m' + \{1 - F(\omega_o)\} \, (1 - A_m')] \tag{2.42}$$

in which A_m' is defined as

$$A_m' = \frac{A_m - 2r}{B_m - 2r} \tag{2.43}$$

If the frequency range is extended to ∞ i.e. $\omega_c = \infty$, the expressions for A_m, B_m, and A'_m become similar to those defined by Singh [43]. These expressions are given in Appendix I-D, Eq. I.31.

As $I_1(\omega_o)$ can be defined in terms of ground spectrum value by Eq. 2.24, Eq. 2.42 defines the single summation term in the resonance case in terms of ground response spectrum value.

Double Summation Terms

When one of the structural frequencies and corresponding modal damping values are equal to the oscillator frequency and damping, the evaluation of the integral of Eq. 2.26, after its multiplication by $\Phi_g(\omega)$, requires a similar approach as used for a single summation term in the preceding section. For example, if $\omega_j = \omega_o$ and $\beta_j = \beta_o$, the integral of the first term in Eq. 2.26 can be written as follows:

$$I_d = \int_{-\omega_c}^{\omega_c} \Phi_g(\omega)\ (\omega_o^4 + 4\ \beta_o^2\ \omega_o^2\ \omega^2)\ (A_r\ \omega_o^4 + B_r\ \omega_o^2\ \omega^2)\ |H_o|^4\ d\omega \qquad (2.44)$$

Again because of the peakedness of $|H_o|^4$ the approximation similar to the single summation term in Eq. 2.31 can also be made here. Proceeding similarly, the following is obtained for I_d:

$$I_d = I_1(\omega_o)\ [F(\omega_o)\ C'_m + A_r\ \{1 - F(\omega_o)\}] \tag{2.45}$$

where

$$\left.\begin{aligned} C'_m &= \frac{C_m - 2r\ A_r}{B_m - 2r} \\ C_m &= A_m(r,\ \beta_o,\ a'_o,\ a'_1,\ a'_2,\ a'_3) \\ a'_o &= 0\ ;\ a'_1 = 4\ \beta_o^2\ B_r\ ;\ a'_2 = (B_r + 4\ \beta_o^2\ A_r)\ ; \\ a'_3 &= A_r \end{aligned}\right\} \tag{2.46}$$

in which the functions A_m and B_m are as defined by Eqs. I.22 and I.27 in Appendix I-C. When $\omega_c = \infty$ these functions become similar to those defined by Singh [43] and are given by Eq. I.32 in Appendix I-D.

The integral associated with frequency $\omega_k \neq \omega_o$ in Eq. 2.26 can be evaluated by resolving into partial fractions as done for the non-resonance case.

Combining all the terms pertaining to the evaluation of floor response spectra value for the resonance case, i.e. when $\omega_j = \omega_o$ and $\beta_j = \beta_o$, the following is obtained

$$R_a^2(\omega_o,\beta_o) = P_F^2(\omega_o) \left[\sum_{j=1}^{n} r_j^2 \phi_j^2 I_s \right.$$

$$+ \sum_{j=1}^{n} \sum_{k=j+1}^{n} r_j r_k \phi_j \phi_k \{I_d + C_1 I_1(\omega_o)$$

$$\left. + C_2 \omega_o^2 I_2(\omega_o) + C_3 I_1(\omega_k) + C_4 \omega_k^2 I_2(\omega_k)\} \right] \quad (2.47)$$

where C_1, C_2, C_3 and C_4 are defined by Eq. I.13 in Appendix I-B.

2.5 EVALUATION OF PEAK FACTORS

Eqs. 2.29 and 2.47 define the floor response spectrum values in terms of $I_1(\omega_j)$ and $I_2(\omega_j)$, which in turn are defined in terms of response spectrum values and peak factors. If all the peak factors are assumed equal, then floor spectrum can just be defined in terms of ground spectra. This is what was done by Singh [39,43]. Here the peak factors are included in generation of floor spectra and the results are compared with the equal peak factor approach to see the effect of their inclusion.

To obtain peak factors $S_p(\omega_j)$ and $S_v(\omega_j)$ in Eqs. 2.24 and 2.25, a simple approach proposed by Vanmarcke [52] is

used. The expression relating the peak factor, S, with the probability of exceedance, p, level crossing rate, ν_a and duration t_d is as follows:

$$p = \exp(-\alpha\ t_d) \tag{2.48}$$

where the decay rate α is defined as

$$\alpha = 2\ \nu_a\ \frac{1 - \exp(-\sqrt{\pi/2}\ \delta_e\ S)}{1 - \exp(-S^2/2)} \tag{2.49}$$

in which the level crossing rate is defined as

$$\nu_a = \frac{1}{2\pi}\sqrt{\frac{\lambda_2}{\lambda_o}}\ \exp(-S^2/2) \tag{2.50}$$

and the band width parameter, δ_e, is defined as

$$\delta_e = \delta^{1.2} \tag{2.51}$$

with

$$\delta = \sqrt{1 - \lambda_2^2/\lambda_o\ \lambda_4} \tag{2.52}$$

The spectral moments λ_o, λ_2, and λ_4 of the response are defined as

$$\lambda_k = \int_{-\omega_c}^{\omega_c} \omega^k\ \Phi_R(\omega)\ d\omega \quad ; \quad k = 0,1,2,\ldots \tag{2.53}$$

in which $\Phi_R(\omega)$ is the spectral density function of the response quantity, R.

Herein the band width parameter, δ, is defined, rather, differently than in Ref. [52] where it was defined in terms of λ_o, λ_1, and λ_2. The present definition of δ is more suitable as it is possible to obtain the even moments in terms of response spectrum values. The evaluation of λ_1, on the other hand, requires knowledge of the spectral density function of a response.

For a given duration and probability of exceedance Eq. 2.48 is solved numerically to obtain the peak factor S.

It is seen that to obtain peak factors of a response quantity, R, its spectral density function is required. This spectral density function can be obtained in terms of the spectral density function of ground acceleration $\Phi_g(\omega)$. However, in practice $\Phi_g(\omega)$ will not be known. Here, to see how sensitive the floor spectra results are to the peak factor value, different forms of $\Phi_g(\omega)$ have been used to define the peak factors in Eqs. 2.29 and 2.47. The different spectral density functions that have been considered for calculation of peak factors are: 1) a broad-band 3-term Kanai-Tajimi [47], 1-term Kanai-Tajimi, and a white noise with cut-off frequency of 30 cps.

As in practice seismic input is usually defined in terms of ground response spectra, an approach is also

presented to calculate the peak factors in terms of ground response spectrum values.

In the following sections, the expression to evaluate spectral moments of pseudo acceleration, relative velocity and floor spectrum responses are given.

2.5.1 Spectral Moments of Pseudo Acceleration and Relative Velocity Responses

The spectral moment of 1st order of pseudo acceleration and relative velocity response for a given ground spectral density function are as follows:

$$\lambda_{p\ell}(\omega_j) = \omega_j^4 \int_{-\omega_c}^{\omega_c} \Phi_g(\omega)\ \omega^{\ell}\ |H_j|^2\ d\omega \tag{2.54}$$

$$\lambda_{v\ell}(\omega_j) = \int_{-\omega_c}^{\omega_c} \omega^{\ell+2}\ \Phi_g(\omega)\ |H_j|^2\ d\omega \tag{2.55}$$

where ℓ = 0, 2, and 4. For a given spectral density function these moments can be obtained in closed form. It may be noted that

$$\lambda_{p2}(\omega_j) = \omega_j^4\ \lambda_{vo}(\omega_j) \tag{2.56a}$$

$$\lambda_{p4}(\omega_j) = \omega_j^4\ \lambda_{v2}(\omega_j) \tag{2.56b}$$

Thus, only four integrals are required to be evaluated to obtain these spectral moments.

In absence of any knowledge about spectral density function of ground motion, a method for approximate evaluation of peak factors where the spectral moments are calculated from ground spectra was also tried. As the spectral moments represent the mean square value of a quantity, and as the mean square value is proportional to the response spectrum value of the quantity, the following approximations were used in the evaluation of spectral moments

$$\lambda_{po}(\omega_j) = K_1 \, R_p^2(\omega_j) \tag{2.57a}$$

$$\lambda_{p2}(\omega_j) = K_2 \, \omega_j^4 \, R_v^2(\omega_j) \tag{2.57b}$$

where the constants of proportionality were assumed to be the same.

To calculate the fourth spectral moment the following relationship between pseudo acceleration, relative velocity and relative acceleration mean square values can be used:

$$\lambda_{p4}(\omega_j) = \omega_j^4 \int_{-\omega_c}^{\omega_c} \omega^4 \, \Phi_g(\omega) \, |H_j|^2 \, d\omega$$

$$= \omega_j^4 \int_{-\omega_c}^{\omega_c} \phi_g(\omega) \, [1 - \{\omega_j^4 - 2 \, \omega_j^2 \, \omega^2 \cdot (1 - 2 \, \beta_j^2)\} \, |H_j|^2] d\omega \qquad (2.58)$$

The first integral in Eq. 2.58 represents the area under the spectral density function, and is directly proportional to the maximum ground acceleration. Similarly, the other integrals are proportional to the pseudo acceleration and relatively velocity spectrum values. Assuming that all the proportionality constants are equal to K, the fourth order moments can be obtained as

$$\lambda_{p4}(\omega_j) = \omega_j^4 \cdot K \, [A_g^2 - R_p^2(\omega_j) + 2 \, \omega_j^2 \, (1 - 2 \, \beta_j^2) \, R_v^2(\omega_j)] \qquad (2.59)$$

It may be noted that it is not necessary to know the exact value of K as it will cancel out in the evaluation of ν_a and δ in Eqs. 2.50 and 2.52.

Using Eqs. 2.56b, 2.57b, and 2.58, it is possible to obtain the first two moments of the relative velocity response. However, to obtain the fourth moment the following approach was considered:

$$\lambda_{v4}(\omega_j) = \int_{-\omega_c}^{\omega_c} \omega^6 \, \Phi_g(\omega) \, |H_j|^2 \, d\omega$$

$$= \int_{-\omega_c}^{\omega_c} \{\omega^2 - [\omega_j^4 \, \omega^2 - 2 \, \omega_j^2 \, (1 - 2 \, \beta_j^2) \, \omega^4]$$

$$\cdot \, |H_j|^2\} \, \Phi_g(\omega) \, d\omega \qquad (2.60)$$

Using Eqs. 2.54 and 2.55

$$\lambda_{v4}(\omega_j) = I_{b2} - \omega_j^4 \, \lambda_{vo}(\omega_j) + 2 \, \omega_j^2 \, (1 - \beta_j^2) \, \lambda_{v2}(\omega_j) \qquad (2.61)$$

where I_{b2} is defined as

$$I_{b2} = \int_{-\omega_c}^{\omega_c} \omega^2 \, \Phi_g(\omega) \, d\omega \qquad (2.62)$$

which represents the second spectral moment of the ground acceleration. It also represents the mean square value of the rate of change of ground acceleration or ground jerk. No ground spectrum contains this information in any form. Thus following approximation was considered.

Because of peakedness of function $|H_j|^2$, the following integral representing the second moment of pseudo acceleration can be approximated as follows:

$$\omega_j^4 \int_{-\omega_c}^{\omega_c} \omega^2 \, \Phi_g(\omega) \, |H_j|^2 = \Phi_g(\omega_j) \left[\omega_j^4 \int_{-\omega_c}^{\omega_c} \omega^2 \, |H_j|^2 \, d\omega - \frac{2 \omega_j^3}{3} \right] + \int_{-\omega_c}^{\omega_c} \omega^2 \, \Phi_g(\omega) \, d\omega \qquad (2.63)$$

where

$$D_m' = \frac{1}{\omega_c} \int_{-\omega_c}^{\omega_c} \omega_j^2 \, \omega^2 \, |H_j|^2 \, d\omega \qquad (2.64)$$

which is defined in Appendix I-C, Eq. I.27. Using Eq. 2.56b

$$I_{b2} = \lambda_{p2}(\omega_j) - \Phi_g(\omega_j) \, \omega_c \, \omega_j^2 \, [D_m' - 2r/3] \qquad (2.65)$$

Substituting for $\Phi_g(\omega) \, \omega_c$ from Eq. 2.40, the above equation can be written as

$$I_{b2} = \lambda_{p2}(\omega_j) - \omega_j^2 \, \frac{[D_m' - 2r^3/3]}{(B_m - 2r)} \, (I_1(\omega_j) - I_b) \qquad (2.66)$$

Using Eq. 2.36 in the above

$$I_{b2} = \lambda_{p2}(\omega_j) \left\{ 1 - \frac{(D_m' - 2r/3)}{(B_m - 2r)} \right\} \qquad (2.67)$$

Substituting this equation in Eq. 2.60, we can obtain $\lambda_{v4}(\omega_j)$.

The approximation for the evaluation of the 4th relative velocity spectral moment from generated spectra was

rather found to be very sensitive to the small changes in the spectrum values, especially at high frequency values. As such this approach was not used to obtain the peak factor for relative velocity spectral response. Rather, the relative peak factors were assumed equal to the pseudo acceleration peak factors. The floor response spectrum obtained with these assumptions are discussed in Sec. 2.4.

2.5.2 Moments of Floor Spectral Response: Nonresonance Case

To obtain the peak factor $P_F(\omega_o)$, the spectral moments of the floor spectral response are required. The zero order moment is given by Eq. 2.16. In general, the lth order moment can be obtained from

$$\lambda_{f\ell} = \int_{-\infty}^{\infty} \omega^{\ell} \left(\omega_o^4 + 4 \beta_o^2 \omega_o^2 \omega^2\right) |H_o|^2 \Phi_m(\omega) \, d\omega \qquad (2.68)$$

in which $\Phi_m(\omega)$ is defined by Eq. 2.14. It is simple to show that the lth moment for the nonresonance case, expressed in terms of the corresponding moments of the response of an oscillator on ground, is as follows:

$$\lambda_{f\ell} = \sum_{j=1}^{n} \gamma_j^2 \phi_j^2 [A_1 \lambda_{p\ell}(\omega_o) + A_2 \omega_o^2 \lambda_{v\ell}(\omega_o) + A_3 \lambda_{p\ell}(\omega_j) + A_4 \omega_j^2 \lambda_{v\ell}(\omega_j)] + 2 \sum_{j=1}^{n} \sum_{k=j+1}^{n} \gamma_j \gamma_k \phi_j \phi_k [(B_1 + C_1) \lambda_{p\ell}(\omega_o) + (B_2 + C_2) \omega_o^2 \lambda_{v\ell}(\omega_o) + B_3 \lambda_{p\ell}(\omega_j) + B_4 \omega_j^2 \lambda_{v\ell}(\omega_j) + C_3 \lambda_{p\ell}(\omega_k) + C_4 \omega_k^2 \lambda_{v\ell}(\omega_k)] \quad (2.69)$$

where $\ell = 0$, 2, and 4.

2.5.3 Moments of Floor Spectral Response: Resonance Case

Oth Moment of Floor Spectral Response:

The evaluation of these moments for the resonance case requires an approach similar to the one used in the development of Eq. 2.47. In fact, Eq. 2.47 without peak factor, $P_F(\omega_o)$ defines the zero order moment which stated in a slightly different form can be written as follows:

$$\lambda'_{fo} = \sum_{j=1}^{n} \gamma_j^2 \phi_j^2 [\lambda_{po}(\omega_o) \{A'_m + [1 - F_o(\omega_o)] (1 - A'_m)\}]$$

$$+ 2 \sum_{j=1}^{n} \sum_{k=j+1}^{n} \gamma_j \gamma_k \phi_j \phi_k [\lambda_{po}(\omega_o) \{F_o(\omega_o) C'_m$$

$$+ A_r [1 - F_o(\omega_o)]\} + C_1 \lambda_{po}(\omega_o) + C_2 \omega_o^2 \lambda_{vo}(\omega_o)$$

$$+ C_3 \lambda_{po}(\omega_k) + C_4 \omega_k^2 \lambda_{vo}(\omega_k)] \qquad (2.70)$$

where $F_o(\omega_o) = \omega_o^2 \lambda_{vo}(\omega_o)/\lambda_{po}(\omega_o)$.

2nd Moment of Floor Spectral Response:

To obtain the 2nd moment of floor spectra Eq. 2.18 without peak factor, $P_F(\omega_o)$ is multiplied by ω^2. The integrals in the single and double summation terms for $\omega_j = \omega_o$ and $\beta_j = \beta_o$ are evaluated as follows.

The frequency integral of a typical single summation term in the resonance case can be written as follows:

$$I'_s(\omega_o) = \int_{-\omega_c}^{\omega_c} \omega^2 \Phi_g(\omega) (\omega_o^4 + 4 \beta_o^2 \omega_o^2 \omega^2) |H_o|^2 \, d\omega \qquad (2.71)$$

which can be approximated as

$$I_s'(\omega_o) \simeq \Phi_g(\omega_o) \int_{-\omega_c}^{\omega_c} \omega^2 \, (\omega_o^4 + 4 \, \beta_o^2 \, \omega_o^2 \, \omega^2) \, |H_o|^2 \, d\omega$$

$$- 2/3 \, \omega_o^3 \, \Phi_g(\omega_o) + \int_{-\omega_o}^{\omega_o} \omega^2 \, \Phi_g(\omega) \, d\omega \qquad (2.72)$$

and can be rewritten as

$$I_s'(\omega_o) = I_1(\omega_o) = I_1(\omega_o) \, F(\omega_o) \, \omega_o^2 \cdot \frac{(D_m - 2/3 \, r)}{(B_m - 2 \, r)} + W_2 \qquad (2.73)$$

where D_m is defined as

$$D_m = A_m(r, \beta_o, b_o, b_1, b_2, b_3) \qquad (2.74)$$

in which $b_o = 16 \, \beta_o^4$, $b_1 = 8 \, \beta_o^2$, $b_2 = 1$, $b_3 = 0$. The above integral is similar to the integral in Eq. I.22, Appendix I-C. Also the frequency integral W_2 is defined as

$$W_2 = \int_{-\omega_o}^{\omega_o} \omega^2 \, \Phi_g(\omega) \, d\omega \qquad (2.75)$$

Also B_m is defined in Eq. 2.41. Using Eq. 2.37 and 2.44, Eq. 2.73 can be written as

$$I_s'(\omega_o) = I_1(\omega_o) \, \omega_o^2 \, F(\omega_o) \, D_m' + W_2 \qquad (2.76)$$

where

$$D_m' = (D_m - 2/3 \, r)/(B_m - 2 \, r) \qquad (2.77)$$

Similarly, the integral in a double summation term to be evaluated for the resonance can be written as

$$I_d(\omega_o) = \int_{-\omega_c}^{\omega_c} \omega^2 \, \Phi_g(\omega) \, (\omega_o^4 + 4 \, \beta_o^2 \, \omega_o^2 \, \omega^2) \cdot (A_r \, \omega_o^4 + B_r \, \omega_o^2 \, \omega^2) \, |H_o|^4 \, d\omega \tag{2.78}$$

which because of peakedness of $|H_o|^4$, can be approximated as follows:

$$I_d(\omega_o) \simeq \omega_o^2 \, \Phi_g(\omega) \int_{-\omega_c}^{\omega_c} N_1(\omega) \, |H_o|^4 \, d\omega - 2/3 \, A_r \, \omega_o^3 \, \Phi_g(\omega_o) + A_r \int_{-\omega_o}^{\omega_o} \omega^2 \, \Phi_g(\omega) \, d\omega \tag{2.79}$$

where

$$N_1(\omega) = A_r \, \omega_o^6 \, \omega^2 + (B_r + 4 \, \beta_o^2 \, A_r) \, \omega_o^4 \, \omega^4 + 4 \, \beta_o^2 \, B_r \, \omega_o^2 \, \omega^6 \tag{2.80}$$

in which the first integral is defined by Eq. I.22 in Appendix I-C. Eq. 2.7 can be written as

$$I_d(\omega_o) = \omega_o^2 \, I_1(\omega_o) \, F(\omega_o) \, \frac{E_m - 2/3 \, r \, A_r}{B_m - 2 \, r} + A_r \, W_2 \tag{2.81}$$

where the factor E_m is defined as

$$E_m = A_m(r,\ \beta_o,\ b'_o,\ b'_1,\ b'_2,\ b'_3) \tag{2.82}$$

in which $b'_o = 4\ \beta_o^2\ B_r$; $b_1 = B_r + 4\ \beta_o^2\ A_r$; $b'_2 = A_r$; $b'_3 = 0$; and A_m is defined by Eq. I.22. Eq. 2.81 can be further simplified as

$$I_d(\omega_o) = \omega_o^2\ I_1(\omega_o)\ F(\omega_o)\ E'_m + A_r\ W_2 \tag{2.83}$$

in which

$$E'_m = (E_m - 2/3\ r\ A_r)/(B_m - 2r) \tag{2.84}$$

and B_m is defined by Eq. 2.41. Using Eq. 2.29, 2.73, and 2.83, the expression for second moment of floor can be written as follows:

$$\begin{aligned}\lambda'_{f2} = &\sum_{j=1}^{n} \gamma_j^2\ \phi_j^2\ [\lambda_{p2}(\omega_o) \cdot \omega_o^2\ F_2(\omega_o) \cdot D'_m + W_2] \\ &+ 2 \sum_{j\neq k}^{n}\sum^{n} \gamma_j\ \gamma_k\ \phi_j\ \phi_k\ [\lambda_{p2}(\omega_o)\ \omega_o^2\ F_2(\omega_o)\ E'_m \\ &+ A_r\ W_2 + C_1\ \lambda_{p2}(\omega_o) + C_2\ \omega_o^2\ \lambda_{v2}(\omega_o) \\ &+ C_3\ \lambda_{p2}(\omega_k) + C_4\ \omega_k^2\ \lambda_{v2}(\omega_k)]\end{aligned} \tag{2.85}$$

where

$$F_2(\omega_o) = \omega_o^2\ \lambda_{v2}(\omega_o)/\lambda_{p2}(\omega_o) \tag{2.86}$$

4th Moment of Floor Spectral Response

The 4th moment will be obtained by multiplying Eq. 2.18 without peak factor $P_F(\omega_o)$ by ω^4. The resulting single and double summation terms for the case when $\omega_j = \omega_o$ and $\beta_j = \beta_o$ are obtained as follows.

The frequency integral of a typical single summation term in the resonance case can be written as:

$$I_s'(\omega_o) = \int_{-\omega_c}^{\omega_c} \omega^4 \, \Phi_g(\omega) \, (\omega_o^4 + 4 \, \beta_o^2 \, \omega_o^2 \, \omega^2)^2 \, |H_o|^4 \, d\omega \tag{2.87}$$

which can be written as

$$\begin{aligned} I_s'(\omega_o) = {} & 16 \, \beta_o^4 \, \omega_o^4 \int_{-\omega_c}^{\omega_c} \Phi_g(\omega) \, d\omega \\ & + \omega_o^4 \int_{-\omega_c}^{\omega_c} \Phi_g(\omega) \, (b_o \, \omega^2 \, \omega^6 + b_1 \, \omega_o^4 \, \omega^4 \\ & + b_2 \, \omega_o^2 \, \omega^6 + b_3 \, \omega_o^8) \, |H_o|^4 \, d\omega \end{aligned} \tag{2.88}$$

in which the coefficients b_o, b_1, b_2 and b_3 are defined as follows:

$$b_o = 8\ \beta_o^2 + 64\ \beta_o^4\ (1 - 2\ \beta_o^2);$$

$$b_1 = 1 - 32\ \beta_o^4\ \{1 + 2\ (1 - 2\ \beta_o^2)^2\};$$

$$b_2 = 64\ \beta_o^4\ (1 - 2\ \beta_o^2);\ b_3 = -\ 16\ \beta_o^4 \qquad (2.89)$$

The 2nd integral in Eq. 2.88 can be approximated using Eq. I.22 in Appendix I-C. Eq. 2.88 can be rewritten as

$$I_s'(\omega_o) = 16\ \beta_o^4\ \omega_o^4 \cdot I_b + \omega_o^4\ \{\Phi_g(\omega_o)\ \omega_c\ G_m' - 2\ \Phi_g(\omega_o)\ \omega_o\ b_3 + b_3\ W_1 \qquad (2.90)$$

where

$$G_m' = A_m\ (r,\ \beta_o,\ b_o,\ b_1,\ b_2,\ b_3) \qquad (2.91)$$

in which A_m is defined by Eq. I.22 in Appendix I-C. Also in Eq. 2.90 the integral I_b is defined by Eq. 2.34 and W_1 is defined as follows:

$$W_1 = \int_{-\omega_o}^{\omega_o} \omega^2\ \Phi_g(\omega)\ d\omega \qquad (2.92)$$

Using Eqs. 2.37 and 2.44, the single summation term in Eq. 2.90 can be written as follows:

$$I_s'(\omega_o) = \omega_o^4\ \{16\ \beta_o^4\ I_b + I_1(\omega_o)\ F(\omega_o)\ G_m' + b_3\ W_1\} \qquad (2.93)$$

in which the factor G_m' is defined as

$$G_m' = (G_m - 2r\ b_3)/(B_m - 2r) \tag{2.94}$$

Similarly, the integral in a double summation term is

$$I_d'(\omega_o) = \int_{-\infty}^{\infty} \omega^4\ \Phi_g(\omega)\ (\omega_o^4 + 4\ \beta_o^2\ \omega_o^2\ \omega^2) \cdot (A_r\ \omega_o^4 + B_r\ \omega_o^2\ \omega^2)\ |H_o|^4\ d\omega \tag{2.95}$$

which can be written as

$$I_d'(\omega_o) = 4\ \beta_o^2\ \omega_o^4\ B_r \int_{-\omega_c}^{\omega_c} \Phi_g(\omega)\ d\omega + \omega_o^4 \int_{-\omega_c}^{\omega_c} \Phi_g(\omega)\ N_1(\omega)\ |H_o|^4\ d\omega \tag{2.96}$$

where

$$N_1(\omega) = \omega_o^2\ \omega^6\ c_o' + \omega_o^4\ \omega^4\ c_1' + \omega_o^6\ \omega^2\ c_2' + \omega_o^8\ c_3' \tag{2.97}$$

in which $c_o' = B_r + 4\ \beta_o^2\ A_r + 16\ \beta_o^2\ B_r\ (1 - 2\ \beta_o^2)$; $c_1' = A_r - 8\ \beta_o^2\ B_r\ \{1 + 2\ (1 - 2\ \beta_o^2)^2\}$; $c_2' = 16\ \beta_o^2\ B_r \cdot (1 - 2\ \beta_o^2)$; $c_3' = -\ 4\ \beta_o^2\ A_r$.

Since the function $|H_o|^4$ is highly peaked, the 2nd integral in Eq. 2.96 can be approximated as

$$I'_d(\omega_o) = 4\ \beta_o^2\ \omega_o^4\ B_r \cdot I_b + \omega_o^4 \left[\Phi_g(\omega_o) \int_{-\omega_c}^{\omega_c} N_1(\omega) \cdot |H_o|^4\ d\omega - 2\ \Phi_g(\omega_o)\ \omega_o\ c'_3 + c'_3 \int_{-\omega_o}^{\omega_o} \Phi_g(\omega)\ d\omega \right] \tag{2.98}$$

Using Eqs. 2.37 and 2.40, Eq. 2.98 can be written as

$$I'_d(\omega_o) = \omega_o^4 \{4\ \beta_o^2\ B_r\ I_b + \Phi_g(\omega_o)\ \omega_c\ H_m - 2\ \Phi_g(\omega_o)\ \omega_o\ c'_3 + c'_3\ W_1 \tag{2.99}$$

where

$$H_m = A_m\ (r,\ \beta_o,\ c'_o,\ c'_1,\ c'_2,\ c'_3) \tag{2.100}$$

in which A_m is defined by Eq. I.22 in Appendix I-C. Using Eq. 2.40, Eq. 2.100 can be written as

$$I'_d(\omega_o) = \omega_o^4 \{4\ \beta_o^2\ B_r\ I_b + I_1(\omega_o)\ F(\omega_o)\ H'_m + c'_3\ W_1\} \tag{2.101}$$

in which the factor H'_m are defined as

$$H'_m = (H_m - 2\ r\ c_3)/(B_m - 2\ r) \tag{2.102}$$

in which B_m is defined by Eq. 2.41. Using Eqs. 2.29, 2.93, and 2.101, the expression for the 4th moment of floor spectra can be written as follows:

$$\lambda'_{f4} = \sum_{j=1}^{n} r_j^2 \phi_j^2 \omega_o^4 [16 \beta_o^4 I_b + \lambda_{p4}(\omega_o) \cdot F_4(\omega_o) G'_m + b_3 W_1]$$

$$+ 2 \sum_{j\neq k}^{n} \sum^{n} r_j^2 \phi_j^2 [\omega_o^4 \{4 \beta_o^2 B_r W_{g1} + \lambda_{p4}(\omega_o) F_4(\omega_o) H'_m + c'_3 W_1\} + c_1 \lambda_{p4}(\omega_o) + c_2 \omega_o^2 \lambda_{v4}(\omega_o) + c_3 \lambda_{p4}(\omega_k) + c_4 \omega_k^2 \lambda_{v4}(\omega_k)] \quad (2.103)$$

where

$$F_4(\omega_o) = \frac{\omega_o^2 \lambda_{v4}(\omega_o)}{\lambda_{p4}(\omega_o)} \quad (2.104)$$

Once the moments of floor spectra are available, the peak factors are obtained by the numerical solution of Eq. 2.39 for a given probability of exceedance, p, and earthquake duration of motion, t_d.

2.6 SIMULATION STUDY FOR VERIFICATION OF DIRECT APPROACH

Several implicit assumptions have been made in the development of the approach so that it can use ground spectra directly as design input. To verify the suitability of these assumptions and validity of the proposed approach,

the simulation study, described in this section, was conducted.

This study consisted of 1) synthetic generation of ensembles of accelerograms; 2) development of mean and mean-plus-one-standard-deviation ground response spectra; and 3) generation of floor spectra for each time history and ensemble averaging and statistical processing of results.

A method for generation of systhetic time histories is described in Ref. [17,47]. The frequency characterization of the time histories was in terms of a broad-band Kanai-Tajimi type of spectral density function of the following form:

$$\Phi_g(\omega) = \sum_{j=1}^{3} S_j \frac{\omega_j^4 + 4\,\beta_j^2\,\omega_j^2\,\omega^2}{(\omega_j^2 - \omega^2)^2 + 4\,\beta_j^2\,\omega_j^2\,\omega^2} \quad ;$$

$$-30 \text{ cps.} \leq \omega \leq 30 \text{ cps.} \qquad (2.105)$$

The parameters of this spectral density function are given in Table 2.1. To introduce nonstationary character in the synthetically generated time histories, envelop functions shown in Fig. 2.1 have been used. Three different envelop functions with total and strong motion phase

durations of (12 sec., 2 sec.), (15 sec., 4 sec.), and (30 sec., 15 sec.) were used to get three different sets of time history ensembles. There were 100 time histories in 12 sec. duration set, 75 in the 15 sec. set and 33 in the 30 sec. duration set. The selection of the number of time histories generated in an ensemble set was primarily governed by the computational cost. The response results for each set were processed separately. Figs. 2.2 - 2.4 show the time histories from the three sets.

The synthetically generated acceleration time histories were used for generation of base motion spectrum curves. Pseudo acceleration, relative acceleration and relative velocity spectra were generated for a total of 10 damping ratios ranging from 0.5% to 50% of the critical. For each damping value, the spectra curves of the time history ensemble were statistically processed to obtain the mean and mean-plus-one-standard-deviation spectrum curves. These averaged base motion spectra are used as base input in the direct approaches described in this chapter and Chapter 3 employed pseudo acceleration and relative velocity spectrum curves as inputs whereas the approaches of Chapters 4 and 5 employed relative acceleration and relative velocity spectra as inputs. Figs. 2.5 - 2.7 show these averaged spectra for 12 sec. duration, Figs. 2.8 - 2.10 for 15 sec. duration, and Figs. 2.11 - 2.13 for the

30 sec. duration sets. The curves for mean + one standard deviation are shown in Figs. 2.14 - 2.22.

To obtain floor spectra for acceleration time histories, modal time history analysis approach has been used. It involves solution of Eq. 2.3 for each mode by Duhamel integral approach [29]. This method provides an exact solution for a given digitized acceleration time history. Absolute floor acceleration time history is obtained from Eqs. 2.8 in the mode displacement approach (Chapter 2) and by Eq. 4.1 for mode acceleration approach (Chapter 4). The floor acceleration time history is then applied to the oscillator, Eq. 2.5, for generation of floor spectrum. Solution of Eq. 2.5 is also obtained by the Duhamel integral approach.

For each time history floor spectra are obtained for different damping values at the points of interest of a structure. The floor spectra obtained for a time history ensemble are then statistically processed to obtain the mean and mean + one standard deviation spectra. The mean time history spectra are compared with the spectra obtained by the direct approaches with mean ground spectra as seismic input. Similarly, the mean + one standard deviation time history spectra are also compared with the corresponding spectra by direct approaches for mean + one standard

deviation ground spectra as input. A good comparison of these two sets of spectra means that the direct approach is acceptable in spite of the simplifying assumptions made in its development.

2.7 NUMERICAL RESULTS

In this section the numerical results for two different models obtained by the time history analysis and the direct approach are presented and compared for the validation of the direct approach. The dynamic characteristics like natural frequencies, participation factors and modal displacements of the floor points of the two structural models are given in Tables 2.2 and 2.3. The first model has also been used in earlier studies [39,42]. The second model is a regular 10-story building with 10 degrees-of-freedom.

The structural damping for both structures was taken as 5 percent of critical in each structural mode. The oscillator damping for generation of floor spectra was varied between 0.5 to 50 percent. Large damping values were included to examine the applicability of the proposed approach for such damping values. However, floor spectra results, only for a selected damping values are shown.

Figs. 2.23 - 2.34 show the floor spectra for two floors of the first model (also referred to as the 11-FRQ) for 1 percent and 5 percent damping ratios, obtained by the direct approach and time history analysis. Figs. 2.23 - 2.26 are for 12-sec. time histories, Figs. 2.27 - 2.30 for 15-sec. time histories and Figs. 2.31 - 2.34 for 30-sec. time histories. In generation of these curves Eq. 2.29 which assumes equal peak factors was used.

The comparison of the two results for three sets of time histories shows that the direct approach predicts higher (conservative) response at dominant structural frequencies than the time history response. For floor 3 shift in curves is also noted between the oscillator periods of .08 sec. to 0.16 sec. In general, however, the results obtained by the direct approach and time history analysis compare very well. The main reasons for getting higher response in the direct approach are: 1) the assumption of equality of peak factors, 2) the inability of step-by-step time history analysis to reach the maximum (peak) response because of the finite size of the time step. (This effect could account for about 2 percent to 7 percent difference. This was verified by the calculation of response of two equal frequency oscillators in cascades subjected to a harmonic input. The closed form response obtain the harmonic input was compared with the step-by-step

time history response obtained with a time step size of 0.005 sec.)

To see if any improvements can be made by inclusion of peak factors in generation of floor spectra, Eq. 2.2 was used to obtain floor spectrum values. To obtain the spectral moments for the calculation of the peak factors, three different forms of spectral density functions were used: 1) the spectral density function defined by Eq. 2.105, 2) the spectral density function with only the first term of Eq. 2.105, and 3) a band-limited white noise with cut-off frequency of 30 cps. The first choice of the spectral density function is most consistent with the input spectra used, as they were obtained from this spectral density function. In the calculation of peak factors, the effective earthquake durations for 12, 15 and 30 second time histories was assumed to be 5 sec., 7 sec. and 19 sec. as suggested by Hou [19]. The use of duration values somewhat different from these, however, did not make any significant difference in the final results. The probability of exceedance with the mean spectra was taken as 0.5 which corresponds with the median of the maximum response. It was also observed that the final results were not sensitive to the choice of this probability either.

The floor spectra with peak factors are shown in Figs. 2.35 - 2.38 for the 12 sec. time history set, in Figs. 2.39 - 2.42 for the 15 sec. time history set and in Figs. 2.43 - 2.46 for the 30 sec. time history set. In these figures, the peak factors were obtained for the spectral density function of Eq. 2.105. It is seen that compared to the results presented before, these results show a definite improvement inasmuch as their comparison with the time history results is now better. Similar results comparing the mean + one standard deviation spectra are shown in Figs. 2.47 - 2.50.

In Figs. 2.51 - 2.54 are shown the floor spectra with peak factors obtained for the 1-term PSDF and in Figs. 2.55 - 2.58 for the white noise PSDF. Again, as the 1-term PSDF represents the frequency content of the input better than white noise, the results are better for the 1-term PSDF. The results obtained with white noise PSDF are in fact erratic sometime. Thus, it appears to be essential to have a correct representation of the frequency content of the input in terms of a PSDF to obtain peak factor for Eq. 2.29 and the assumption of white noise as PSDF for calculation of peak factor may not give consistent results.

As suggested in Sec. 2.5, the spectral moments were also obtained from ground spectra for the calculation of

peak factors. The floor spectra calculated with such peak factors are shown in Figs. 2.59 - 2.62. It is seen that the approach is not entirely inappropriate. However, because of the unevenness of ground spectra, Figs. 2.5 - 2.22, used in the evaluation, the peak factors calculated by this approach may not always lead to improved results (see Figs. 2.59 - 2.62). Thus the use of this approach is not recommended.

In practice, a PSDF representing the input spectra will usually not be known. It can, however, be obtained by iterative procedure (see Ref. 17) for a given spectrum. As an input is usually defined by a set of spectrum curves for the damping values of interest, such procedures will in general not give one PSDF for all the curve. In fact there may be as many PSDFs as there are spectrum curves. However, use of any one of these PSDFs for the calculation of spectral moments and then the peak factors should provide improved results of floor spectra.

A PSDF can also be directly used as input for generation of floor spectra, but since there is no one PSDF which is consistent with all input spectrum curves, choosing the right PSDF out of several becomes a problem. As such, the use of PSDF approach for generation of floor spectra is not advocated here. In fact in absence of a

proper PSDF, the use of Eq. 2.29 will provide quite acceptable and conservative results.

Another set of results obtained by the direct approach for the 10 story building are shown in Figs. 2.63 - 2.65 and compared with the corresponding time history results. Again for this structure also, the two sets of results are again seen to compare very well.

2.8 SUMMARY AND CONCLUSIONS

In this chapter, a direct approach initially developed by Singh [39,43] is reformulated and critically examined. Several improvements related to the development of floor spectra for the resonance case and inclusion of peak factors in floor spectra generation methodology have been formulated. A procedure for the evaluation of the peak factors for an oscillator on ground and another one on floor is described for its use in floor spectra generation procedure. A simulation study for validation of the direct approach proposed here is outlined.

Extensive numerical results, covering a wide range of parameters such as different duration time histories, different structural systems, different floors of a building,

range of damping values, etc. have been obtained. A critical evaluation of the results indicates that the proposed approach does provide an acceptable method for direct generation of floor spectra. Inclusion of in peak factors in generation of floor spectra is possible and can improve results if peak factors are evaluated for a proper PSDF. In absence of any knowledge about the PSDF, the assumption of equal peak factors for an oscillator on ground as well as on floor in the method of generation of floor spectra will also provide conservative and acceptable floor spectrum curves.

Chapter 3

NONCLASSICALLY DAMPED SYSTEMS: MODE DISPLACEMENT METHOD

3.1 INTRODUCTION

The direct approach developed in the preceding chapter and most other approaches developed so far by various investigators assume that primary systems are classically damped and the normal modes can be used to decouple their damping matrices. Thus strictly speaking these approaches cannot be used for structural systems with nonclassical damping matrices. A damping matrix is called nonproportional or nonclassical if it is not proportional to either mass or stiffness matrix or both or is not of a special form as described in Reference [29]. Here, in this investigation the term nonproportional is used in a general sense to include all the cases in which normal modes cannot be used to decouple the damping matrix.

For the convenience of dynamic analysis, the structures are generally assumed to be proportionally damped with modal damping ratio. It may be justified in some cases. However, there can also be situations where the nonclassical nature of damping matrix cannot be completely ignored. Such is usually the case when a structure is

made up of materials with different damping characteristics in different parts. A combined analytical model of a soil and structure system, commonly used to incorporate soil-structure interaction effects will usually be nonclassically damped. In such cases, methods which do consider the nonclassical nature of the system are required for generation of floor spectra.

Since the damping matrix cannot be decoupled in such cases, the time history analysis, employing step-by-step integration techniques can be used to obtain floor spectra if the time history of the input motion is known. However, the time history approach becomes impractical and expensive because to obtain reliable estimate of the design response an ensemble of time histories must be considered in the analysis.

To use normal modes, often the off-diagonal terms of $[\phi]^T [C] [\phi]$, representing modal coupling through damping matrix are completely disregarded and diagonal elements of the transformed matrix are used to obtain the modal damping ratios. This may sometimes introduce significant errors in the generation of floor response spectra.

For the calculation of member response of nonproportionally damped primary system, with response spectra as

seismic design input, an approach was developed by Singh [46]. Herein, this approach has been extended for generation of floor response spectra for nonproportionally damped primary systems. This approach is cast in the form of conventionally used modal analysis approach, such that the direct use of ground response spectra as seismic input is possible. Again, the mode displacement formulation is developed first. The mode acceleration formulation for nonproportionally damped primary systems is described in Chapter 5.

3.2 ANALYTICAL FORMULATION

When the damping matrix [C] in Eq. 2.1 is nonclassical, the 2n-dimensional state vector approach, as initially proposed by Foss [15], is used to obtain the response.

In this approach, Eq. 2.1 is cast into 2n-dimension equations, with the help of an identity equation [21], as follows:

$$[A]\{\dot{y}\} + [B]\{y\} = - [D] \left\{\frac{0}{r}\right\} \ddot{X}_g(t) \qquad (3.1)$$

where

$$[A] = \begin{bmatrix} [O] & [M] \\ [M] & [C] \end{bmatrix} \quad ; \quad [B] = \begin{bmatrix} -[M] & [O] \\ [O] & [K] \end{bmatrix} \quad ;$$

$$[D] = \begin{bmatrix} [O] & [O] \\ [O] & [M] \end{bmatrix} \tag{3.2}$$

Eq. 3.1 is called the reduced equation of motion of the system. $\{y\}$ is a 2n dimension state vector defined as

$$\{y\} = \begin{Bmatrix} \{\dot{x}\} \\ \{x\} \end{Bmatrix} \tag{3.3}$$

The solution of Eq. 3.1 can be obtained in terms of eigenvalues and eigenvectors of its associated eigenvalue equation,

$$p\,[A]\,[\phi] + [B]\,[\phi] = [O] \tag{3.4}$$

where $[\phi]$ = 2n×2n matrix of eigenvectors $\{\phi_j\}$, and p = eigenvalue. Eq. 3.4 gives 2n eigenvalues and corresponding eigenvectors which occur in the pairs of complex and conjugate.

Using the expansion theorem the response vector $\{y\}$ is written as follows

$$\{y\} = [\phi]\,\{z\} \tag{3.5}$$

where $\{z\}$ is a vector of complex valued principal coordinates, which are obtained from the solution of the following equation

$$[A^*]\ \{\dot{z}\} + [B^*]\ \{z\} = -\ [\phi]^T\ [D] \left\{-\frac{0}{r}-\right\} \ddot{X}_g(t) \qquad (3.6)$$

in which T over a vector or matrix represents its transpose. The matrices $[A^*] = [\phi]^T\ [A]\ [\phi]$ and $[B^*] = [\phi]^T\ [B]\ \ [\phi]$ are diagonal matrices with their diagonal elements related as

$$B_j^* = -\ p_j\ A_j^* \qquad (3.7)$$

in which p_j is the jth eigenvalue of Eq. 3.4. A decoupled jth equation of Eq. 3.6 is

$$\dot{z}_j - p_j\ z_j = -\ F_j\ \ddot{X}_g(t) \qquad (3.8)$$

in which F_j is an element of complex vector $\{F\}$ defined as follows:

$$\{F\} = [A^*]^{-1}\ [\phi]^T\ [D] \left\{-\frac{0}{r}-\right\} \qquad (3.9)$$

An element of $\{F\}$ can be shown to be

$$F_j = \{\phi_j\}_\ell^T\ [M]\ \{r\}/A_j^* \qquad (3.10)$$

where $\{\phi_j\}_\ell$ is the lower part of the complex eigenvector $\{\phi_j\}$.

The solution of Eq. 3.6 can be written as

$$z_j(t) = - F_j \int_0^t \ddot{X}_g(\tau)\, e^{p_j(t-\tau)}\, d\tau \qquad (3.11)$$

For generation of floor spectra the absolute acceleration vector, $\{\ddot{X}_a\}$, is of main interest which can be written in terms of relative and ground accelerations as follows:

$$\{\ddot{X}_a\} = \{\ddot{x}\} + \{r\}\, \ddot{X}_g(t) \qquad (3.12)$$

where $\{\ddot{x}\}$ = relative acceleration response vector of dimension n.

The above equation can also be written as

$$\begin{Bmatrix} \ddot{X}_a \\ \dot{x} \end{Bmatrix} = \begin{Bmatrix} \ddot{x} \\ \dot{x} \end{Bmatrix} + \begin{Bmatrix} r \\ 0 \end{Bmatrix} \ddot{X}_g(t) \qquad (3.13)$$

Using Eq. 3.3,

$$\begin{Bmatrix} \ddot{X}_a \\ \dot{x} \end{Bmatrix} = \{\dot{y}\} + \begin{Bmatrix} r \\ 0 \end{Bmatrix} \ddot{X}_g(t) \qquad (3.14)$$

which by virtue of Eq. 3.5, can also be written as

$$\{\ddot{X}_a\} = \sum_{j=1}^{2n} \{\phi_j\}_u\, \dot{z}_j + \{r\}\, \ddot{X}_g(t) \qquad (3.15)$$

where $\{\phi_j\}_u$ = upper part of $\{\phi_j\}$. By substitution of $\dot{z}_j$ from Eq. 3.8 in Eq. 3.15,

$$\{\ddot{X}_a\} = \sum_{j=1}^{2n} \{\phi_j\}_u (- F_j \ddot{X}_g(t) + p_j z_j) + \{r\} \ddot{X}_g(t) \tag{3.16}$$

or

$$\{\ddot{X}_a\} = \ddot{X}_g(t) \left[- \sum_{j=1}^{2n} F_j \{\phi_j\}_u + \{r\} \right] + \sum_{j=1}^{2n} p_j z_j \{\phi_j\}_u \tag{3.17}$$

It can now be shown that the first term in Eq. 3.17 is zero. Using the expansion theorem, vector $\begin{Bmatrix} r \\ 0 \end{Bmatrix}$ can be written in terms of complex modes $[\phi]$ as follows:

$$\begin{Bmatrix} r \\ 0 \end{Bmatrix} = [\phi] \{\rho\} \tag{3.18}$$

where the constants $\{\rho\}$ in this expansion are obtained by employing orthogonality of $\{\phi_j\}$ as follows. Premultiplying Eq. 3.18 by $[\phi]^T [A]$ we obtain

$$\{\rho\} = ([\phi]^T [A] [\phi])^{-1} [\phi]^T [A] \begin{Bmatrix} r \\ 0 \end{Bmatrix} \tag{3.19}$$

or

$$\{\rho\} = [A^*]^{-1} [\phi_j]^T \{[\overset{o}{M}] \{r\}\} = \{F\} \tag{3.20}$$

A jth term of Eq. 3.20 is given by

$$\rho_j = \{\phi_j\}_\ell^T [M] \{r\}/A_j^* \tag{3.21}$$

which from Eq. 3.10 is equal to F_j. On substitution of Eqs. 3.18 and 3.20 into Eq. 3.17 it is seen that the terms in the square bracket become zero and the absolute

acceleration response vector, $\{\ddot{X}_a\}$ is given as follows:

$$\{\ddot{X}_a\} = \sum_{j=1}^{2n} p_j \; z_j \{\phi_j\}_u \tag{3.22}$$

and the absolute acceleration of, say, the mth floor can be written as

$$\ddot{X}_{am} = \sum_{j=1}^{2n} p_j \; z_j \; \phi_j(m) \tag{3.23}$$

in which $\phi_j(m)$ is the mth element of $\{\phi_j\}_u$.

Eq. 3.23 forms the basis of the mode displacement formulation for generation of seismic floor response spectra for nonproportionally damped primary systems. This will be used to define the spectral density function of the floor acceleration which in turn is required to define a floor response spectrum value.

As nonproportionally damped systems do not possess normal modes, the modal frequencies and damping ratios defined in a conventional sense do not exist. However, an equivalent information is contained in the real and imaginary parts of eigenvalues, p_j. In order to use a set of prescribed spectra in generation of floor spectra, it is essential to identify these modal parameters for nonproportional systems. For this, as in the case of

proportionally damped systems, the real and imaginary parts of p_j are expressed as follows:

$$p_j = -\xi_j + i\,\theta_j = -\beta_j\,\omega_j + i\,\omega_j\sqrt{1-\beta_j^2} \tag{3.24}$$

where $-\xi_j$ and θ_j are the real and imaginary parts of p_j respectively and ω_j and β_j are now the modal frequency and damping ratio, which can be obtained in terms of ξ_j and θ_j as follows:

$$\omega_j = \sqrt{\xi_j^2 + \theta_j^2} \tag{3.25a}$$

$$\beta_j = \xi_j / \sqrt{\xi_j^2 + \theta_j^2} \tag{3.25b}$$

3.3 AUTOCORRELATION AND SPECTRAL DENSITY FUNCTIONS OF FLOOR ACCELERATION

As done in the previous chapter, the expression for the spectral density function of floor acceleration defined by Eq. 3.23 will now be established. This will then be used as the input to an oscillator to obtain floor spectrum value.

Pairing complex conjugate terms, Eq. 3.23 can be written as a summation over n terms as follows:

$$\ddot{X}_a(t) = \sum_{j=1}^{n} \left[p_j\,\phi_j\,z_j(t) + p_j^*\,\phi_j^*\,z_j^*(t)\right] \tag{3.26}$$

where for brevity $\ddot{X}_{am}(t)$ is replaced by $\ddot{X}_a(t)$ and $\phi(m)$ by ϕ_j. Hereafter this notation will be used in this chapter.

For a zero mean excitation, $\ddot{X}_g(t)$, the mean of $\ddot{X}_a(t)$ is zero whereas its autocorrelation characteristics can be obtained as

$$E[\ddot{X}_a(t_1)\ \ddot{X}_a(t_2)] = \sum_{j=1}^{n}\sum_{k=1}^{n} p_j\ \phi_j\ p_k\ \phi_k \cdot E[z_j(t_1)\cdot z_k(t_2)] + \sum_{j=1}^{n}\sum_{k=1}^{n} p_j^*\ \phi_j^*\ p_k^*\ \phi_k^* \cdot E[z_j^*(t_1)\ z_k^*(t_2)] + \sum_{j=1}^{n}\sum_{k=1}^{n} p_j\ \phi_j\ p_k^*\ \phi_k^* \cdot E[z_j(t_1)\ z_k^*(t_2)] + \sum_{j=1}^{n}\sum_{k=1}^{n} p_j^*\ \phi_j^*\ p_k\ \phi_k \cdot E[z_j^*(t_1)\ z_k(t_2)] \qquad (3.27)$$

Using Eq. 3.11, various expected values required in Eq. 3.27 can be obtained in terms of autocorrelation function or spectral density function of ground acceleration; these are defined in Appendix II-A.

To further simplify the evaluation of Eq. 3.27 the terms with j=k, called single summation terms and j≠k, called double summation or cross-terms, will now be

evaluated separately.

Terms with j=k of Eq. 3.27 denoted by R_s, can be written as

$$R_s = \sum_{j=1}^{n} p_j^2 \, \phi_j^2 \, E[z_j(t_1) \, z_j(t_2)]$$
$$+ \sum_{j=1}^{n} p_j^{*2} \, \phi_j^{*2} \, E[z_j^*(t_1) \, z_j^*(t_2)]$$
$$+ \sum_{j=1}^{n} p_j \, p_j^* \, \phi_j \, \phi_j^* \, E[z_j(t_1) \, z_j^*(t_2)]$$
$$+ \sum_{j=1}^{n} p_j^* \, p_j \, \phi_j^* \, \phi_j \, E[z_j^*(t_1) \, z_j(t_2)] \qquad (3.28)$$

Substituting for the expected values from Appendix II-A, Eq. 3.28 can be written as

$$R_s = \sum_{j=1}^{n} \int_{-\infty}^{\infty} \Phi_g(\omega) \, e^{i\omega\tau} \left[\frac{p_j^2 \, q_j^2}{(p_j^2 + \omega^2)} + \frac{p_j^{*2} \, q_j^{*2}}{(p_j^{*2} + \omega^2)} \right.$$
$$+ p_j \, p_j^* \, q_j \, q_j^* \left\{ \frac{1}{(-p_j^* + i\omega)(-p_j - i\omega)} \right.$$
$$\left. \left. + \frac{1}{(-p_j^* + i\omega)(-p_j - i\omega)} \right\} \right] d\omega \qquad (3.29)$$

where

$$q_j = F_j \, \phi_j \qquad (3.30)$$

With p_j expressed in terms of its real and imaginary parts as in Eq. 3.24 and q_j as

$$q_j = a_j + i\, b_j \tag{3.31}$$

and with appropriate combination of the 1st with the 2nd term, and the 3rd with the 4th term, and after some algebraic simplification, Eq. 3.29 can be written as follows:

$$\begin{aligned} R_s^2 = \sum_{j=1}^{n} 2 \int_{-\infty}^{\infty} \Phi_g(\omega)\, e^{i\omega\tau} \,[\omega^2 \{A_j' + \omega_j^2 (a_j^2 + b_j^2)\} \\ - \omega_j^2 (1 - 2\beta_j^2)\, A_j' + 2\, B_j'\, \beta_j \sqrt{1 - \beta_j^2}\, \omega_j \\ + \omega_j^4 (a_j^2 + b_j^2)]\, |H_j|^2\, d\omega \end{aligned} \tag{3.32}$$

in which

$$\begin{aligned} A_j' = - (a_j^2 - b_j^2)\, \omega_j^2\, (1 - 2\, \beta_j^2) \\ + 4\, a_j\, b_j\, \omega_j^2\, \beta_j \sqrt{1 - \beta_j^2} \end{aligned} \tag{3.33}$$

$$\begin{aligned} B_j' = 2(a_j^2 - b_j^2)\, \omega_j^2\, \beta_j \sqrt{1 - \beta_j^2} \\ + 2\, \omega_j^2\, a_j\, b_j\, (1 - 2\, \beta_j^2) \end{aligned} \tag{3.34}$$

where H_j is the frequency response function of a single-degree-of-freedom oscillator, defined by Eq. 2.3. Eq. 3.32 can be rewritten as

$$R_s = \sum_{j=1}^{n} 2 \int_{-\infty}^{\infty} \Phi_g(\omega)\ e^{i\omega\tau}\ (\omega^2\ C_j' + D_j')\ |H_j|^2\ d\omega \quad (3.35)$$

in which

$$C_j' = A_j' + \omega_j^2\ (a_j^2 + b_j^2) \quad (3.36)$$

$$D_j' = -\ \omega_j^2\ (1 - 2\ \beta_j^2)\ A_j' + 2\ B_j\ \omega_j^2\ \beta_j\sqrt{1 - \beta_j^2} + \omega_j^4\ (a_j^2 + b_j^2) \quad (3.37)$$

The double summation terms (cross terms) are also evaluated similarly. Substituting for the expected values from Appendix II-A the double summation term of Eq. 3.27, herein denoted as R_d, may be written as follows:

$$R_d = \sum_{j\neq k}^{n}\sum^{n} \int_{-\infty}^{\infty} \Phi_g(\omega)\ e^{i\omega\tau} \left[\frac{p_j\ p_k\ q_j\ q_k}{(-p_j+i\omega)(-p_k-i\omega)} + \frac{p_j^*\ p_k^*\ q_j^*\ q_k^*}{(-p_j^*+i\omega)(-p_k^*-i\omega)} + \frac{p_j\ p_k^*\ q_j\ q_k^*}{(-p_j+i\omega)(-p_k^*-i\omega)} + \frac{p_j^*\ p_k\ q_j^*\ q_k}{(-p_j^*+i\omega)(-p_k-i\omega)} \right] d\omega \quad (3.38)$$

Substituting q_j, q_k, p_j and p_k in terms of their real and imaginary parts, and with some algebraic manipulations, Eq. 3.48 can be written in the following form

$$R_d = \sum_{j}^{n} \sum_{k \neq j}^{n} \int_{-\infty}^{\infty} \Phi_g(\omega)\ e^{i\omega\tau}\ [X'_{jk}(\omega) + i\ Y'_{jk}(\omega)]\ H_j\ H_k^*\ d\omega \tag{3.39}$$

in which

$$X'_{jk} = 4\ \omega^2\ \omega_{jk} \left[a_j\ a_k\ \beta_j\ \beta_k + b_j\ b_k \sqrt{1 - \beta_j^2}\ \sqrt{1 - \beta_k^2} + a_j\ b_k\ \beta_j \sqrt{1 - \beta_k^2} + a_k\ b_j\ \beta_k \sqrt{1 - \beta_j^2}\right] + 4\ \omega_j^2\ \omega_k^2\ a_j\ a_k \tag{3.40}$$

$$Y'_{jk} = 4\omega\ \omega_j\ \omega_k \left[a_j\ a_k\ (\omega_k\ \beta_j - \omega_j\ \beta_k) - a_j\ b_k\ \omega_j \sqrt{1 - \beta_k^2} + a_k\ b_j\ \omega_k \sqrt{1 - \beta_j^2}\right] \tag{3.41}$$

Eq. 3.39 can be further transformed into the real forms of H_j and H_k^* as

$$R_d = \int_{-\infty}^{\infty} \Phi_g(\omega)\ e^{i\omega\tau}\ [X_{jk}(\omega) + i\ Y_{jk}(\omega)]\ |H_j|^2\ |H_k|^2\ d\omega \tag{3.42}$$

in which

$$\begin{aligned} X_{jk}(\omega) &= X'_{jk}\ U_{jk} - Y'_{jk}\ V_{jk} \\ Y_{jk}(\omega) &= X'_{jk}\ V_{jk} + Y'_{jk}\ U_{jk} \end{aligned} \tag{3.43}$$

where U_{jk} and V_{jk} are defined as

$$U_{jk} = (\omega_j^2 - \omega^2)(\omega_k^2 - \omega^2) + 4\ \omega^2\ \omega_j\ \omega_k\ \beta_j\ \beta_k \tag{3.44a}$$

$$V_{jk} = 2\omega[\omega_k\ \beta_k\ (\omega_j^2 - \omega^2) - \omega_j\ \beta_j\ (\omega_k^2 - \omega^2)] \tag{3.44b}$$

Noting that $X_{jk} = X_{kj}$ and $Y_{jk} = -Y_{kj}$, the cross-terms when combined together will eliminate the imaginary terms from the final expression. Using Eq. 3.35 and 3.42, the complete expression for the autocorrelation function of the stationary response of a floor acceleration is obtained as follows:

$$E[\ddot{X}_a(t_1)\ \ddot{X}_a(t_2)] = \sum_{j=1}^{n} 2 \int_{-\infty}^{\infty} \Phi_g(\omega)\ e^{i\omega\tau}\ (\omega^2 C_j' + D_j')\ |H_j|^2\ d\omega + 2 \sum_{j=1}^{n} \sum_{k=j+1}^{n} \int_{-\infty}^{\infty} \Phi_g(\omega)\ e^{i\omega\tau} \cdot X_{jk}(\omega)\ |H_j|^2\ |H_k|^2\ d\omega \qquad (3.45)$$

for $\tau = 0$ this equation also defines the mean square acceleration response of floor. From Eq. 3.45 it is seen that the PSDF of a floor acceleration response can be written as

$$\Phi_m(\omega) = 2 \left[\sum_{j=1}^{n} (\omega^2 C_j' + D_j')\ |H_j|^2 + \sum_{j \neq k}^{n} \sum^{n} X_{jk}(\omega)\ |H_j|^2\ |H_k|^2 \right] \Phi_g(\omega) \qquad (3.46)$$

3.4 FLOOR RESPONSE SPECTRUM

This PSDF characterizes the acceleration of a floor. The maximum response of an oscillator with this PSDF as input defines the floor response spectrum value. For example, the absolute acceleration response spectrum value at a frequency ω_o and damping β_o can be obtained from the mean square value as follows:

$$R_a^2(\omega_o, \beta_o) = P_F^2(\omega_o) \left[2 \sum_{j=1}^{n} \int_{-\infty}^{\infty} \Phi_g(\omega)(\omega^2 C_j' + D_j') \right.$$

$$\cdot (\omega_o^4 + 4 \beta_o^2 \omega_o^2 \omega^2) |H_j|^2 |H_o|^2 \, d\omega$$

$$+ 2 \sum_{j \neq k}^{n} \sum_{k}^{n} \int_{-\infty}^{\infty} \Phi_g(\omega) X_{jk}(\omega) (\omega_o^4$$

$$\left. + 4 \beta_o^2 \omega_o^2 \omega^2) |H_j|^2 |H_k|^2 |H_o|^2 \, d\omega \right] \qquad (3.47)$$

where $P_F(\omega_o)$ is the peak factor by which the root mean square value is amplified to obtain the response spectrum value.

To define the response spectrum value in terms of ground response spectra, each term of Eq. 3.47 is separated into partial fractions, as was done in the previous chapter. Here again the case with $\omega_j \neq \omega_o$ and $\omega_j = \omega_o$ with $\beta_j = \beta_o$

will be treated separately. The latter case with $\omega_j = \omega_o$ and $\beta_j = \beta_o$ will again be referred to as the resonance case.

3.4.1 FLOOR SPECTRUM VALUE FOR THE NONRESONANCE CASE

In Eq. 3.47 the separation of terms into their partial fractions is straight forward. With this separation the response spectrum expression can be written as follows:

$$R_a^2(\omega_o, \beta_o) = P_F^2(\omega_o) \left[2 \sum_{j=1}^{n} \left\{ \frac{A_1}{r_1^4} I_1(\omega_j) + \frac{A_2}{r_1^2} I_2(\omega_j) + A_3 I_1(\omega_o) + A_4 I_2(\omega_o) \right\} + 2 \sum_{j=1}^{n} \sum_{k=j+1}^{n} \left\{ \frac{A_j}{r_1^4} I_1(\omega_j) + \frac{B_j}{r_1^2} I_2(\omega_j) + \frac{A_k}{r_2^4} I_1(\omega_k) + \frac{B_k}{r_2^2} I_2(\omega_k) + (C_j + C_k) I_1(\omega_o) + (D_j + D_k) I_2(\omega_o) \right\} \right] \quad (3.48)$$

where A_1, A_2, A_j, etc. are the coefficients of partial fractions and are defined in Appendix II-B. $I_1(\omega_j)$ and $I_2(\omega_j)$ are the frequency integrals as defined in Chapter 2, Eqs. 2.22 - 2.25. Again these can be obtained from the pseudo acceleration and relative velocity response spectrum and their associated peak factor values.

Here this expression allows the incorporation of various modal peak factors in generation of floor spectra. However, if all the peak factors are assumed to be the same, an expression independent of peak factors is obtained as follows:

$$R_a^2(\omega_o, \beta_o) = 2 \sum_{j=1}^{n} \left\{ \frac{A_1}{r_1^4} R_p^2(\omega_j) + \frac{A_2}{r_1^2} \omega_j^2 R_v^2(\omega_j) + A_3 R_p^2(\omega_o) + A_4 \omega_o^2 R_v^2(\omega_o) \right\} + 2 \sum_{j=1}^{n} \sum_{k=j+1}^{n} \cdot \left\{ \frac{A_j}{r_1^4} R_p^2(\omega_j) + \frac{B_j}{r_1^2} \omega_j^2 R_v^2(\omega_j) + \frac{A_k}{r_2^4} R_p^2(\omega_k) + \frac{B_k}{r_2^2} \omega_k^2 R_v^2(\omega_k) + (C_j + C_k) R_p^2(\omega_o) + (D_j + D_k) \omega_o^2 R_v^2(\omega_o) \right\} \quad (3.49)$$

This expression has been used to obtain numerical results for nonproportionally damped system.

3.4.2 FLOOR SPECTRUM VALUE FOR THE RESONANCE CASE

For this special case when $\omega_j = \omega_o$ and $\beta_j = \beta_o$, the coefficients of partial fractions, A_1, A_2, etc. are undefined. However, this case may be treated in the same way

as in Sec. 2.4.2 for a proportionally damped system.

Single Summation Terms

A term with $\omega_j = \omega_o$ and $\beta_j = \beta_o$ in the single summation terms can be written as

$$I_s = \int_{-\omega_c}^{\omega_c} \Phi_g(\omega) \ (\omega^2 \ C_j' + D_j') \cdot (\omega_o^4 + 4 \ \beta_o^2 \ \omega_o^2 \ \omega^2) \ |H_o|^4 \ d\omega \qquad (3.50)$$

which can be approximated as

$$I_s \simeq \Phi_g(\omega_o) \int_{-\omega_c}^{\omega_c} (\omega^2 \ C_j' + D_j') \ (\omega_o^4 + 4 \ \beta_o^2 \ \omega_o^2 \ \omega^2) \cdot |H_o|^4 \ d\omega - 2 \ \phi_g(\omega_o) \ \omega_o \ D_j' + D_j' \ I_b \qquad (3.51)$$

The integral in the above equation can be evaluated using the integral in Appendix I-B, Eq. I.22. Thus Eq. 3.51 can be written as

$$I_s = \Phi_g(\omega_o) \ \omega_c \ \{A_m - 2 \ r \ D_j'\} + D_j' \ I_b \qquad (3.52)$$

in which A_m is defined in Appendix II-C, Eq. II.19. Using Eqs. 2.37 and 2.40 in Eq. 3.52 and after some algebraic manipulations, the following is obtained:

$$I_s = I_1(\omega_o) \{A'_m + [1 - F(\omega_o)] \cdot (D'_j - A'_m)\} \qquad (3.53)$$

where

$$A'_m = \frac{A_m - 2 r D'_j}{B_m - 2 r} \qquad (3.54)$$

in which B_m is defined by Eq. 2.41.

Double Summation Terms

The evaluation of a double summation term in resonance proceeds the same way as in Sec. 2.4.2 for proportionally damped case. In this evaluation an integral of the following form is encountered:

$$I_d = \int_{-\omega_c}^{\omega_c} (\omega_o^4 + 4 \beta_o^2 \omega_o^2 \omega^2) \cdot (F_1 \omega_o^4 + F_2 \omega_o^2 \omega^2) |H_o|^4 \cdot \Phi_g(\omega) \, d\omega \qquad (3.55)$$

where the coefficients F_1 and F_2 are defined in Appendix II-B. Eq. 3.55 can be approximated as

$$I_d = \Phi_g(\omega_o) \int_{-\omega_c}^{\omega_c} \left\{F_1 \omega_o^8 + (F_2 + 4 \beta_o^2 F_1) \omega_o^6 \omega^2 + 4 F_2 \beta_o^2 \omega_o^4 \omega^4\right\} |H_o|^4 \, d\omega - 2 \phi_g(\omega_o) \omega_o F_1 + F_1 I_b \qquad (3.56)$$

The frequency integral in above equation can be evaluated by using Eq. I.22 from Appendix I-C. Denoting this integral by D_m, Eq. 3.56 can be written as

$$I_d = \phi_g(\omega_o)\omega_c \{D_m - 2 r F_1\} + F_1 I_b \tag{3.57}$$

where D_m is defined in Appendix II-C, Eq. II.21. Using Eqs. 2.37 and 2.40 in Eq. 3.57 and after some simplifications the following is obtained:

$$I_d = I_1(\omega_o) \{D'_m + [1 - F(\omega_o)] \cdot (F_1 - D'_m)\} \tag{3.58}$$

in which D'_m is defined as follows:

$$D'_m = \frac{D_m - 2 r F_1}{B_m - 2 r} \tag{3.59}$$

With the integrals I_s and I_d defined by Eqs. 3.53 and 3.58, the floor spectrum value for the resonance case can be expressed as follows:

$$R_a^2(\omega_o, \beta_o) = 2 \sum_{j=1}^{n} I_s + 2 \sum_{j=1}^{n} \sum_{k=j+1}^{n} \left\{ I_d + \frac{A_k}{r_2^4} I_1(\omega_k) + \frac{B_k}{r_2^2} I_2(\omega_k) + C_k I_1(\omega_o) + D_k I_2(\omega_o) \right\} \tag{3.60}$$

3.5 NUMERICAL RESULTS

For the numerical consistency and veritication of the formulation developed in the preceding section, the floor spectra results were obtained for a proportionally damped system by this approach and approach developed in the previous chapter. The two results were exactly the same which verified the analytical correctness of the formulations and computer code.

To show the magnitude of the error which can be introduced in the floor spectra results when a nonproportionally damped system is assumed to be proportional by neglecting the off-diagonal terms of $[\phi]^T [C] [\phi]$, here numerical results are obtained with and without off-diagonal terms. Tables 3.2 and 3.3 show these results for a 5-story, 15 degrees-of-freedom torsional structure shown in Fig. 3.1. The structure consisted of rigid floors connected by columns. Each floor has 3 degrees of freedom -- 2-translation and 1-rotation. The eccentricity between mass and stiffness centers was adjusted to give closely spaced frequencies. The damping properties of the system were adjusted to give a nonproportionally damped system. The undamped frequencies, participation factors and the modal damping used in the normal mode approach are shown in Table 3.1. The corresponding quantities used in the

nonproportional formulation or complex mode approach are not shown here as they do not give any new insight into the characteristics of the system. The input for the results shown in Table 3.2 was defined in terms of PSDF defined by Eq. 2.105. Whereas, to obtain the results shown in Table 3.3, the input to the system was defined in the form of pseudo acceleration and relative velocity spectra shown in Figs. 2.10 and 2.11, obtained for an ensemble of 30 sec. duration time histories. The difference in the calculated spectrum values of various floors with and without off-diagonal terms, as indicated by the ratios in columns is between 0 to 47 percent. The assumption of proportionality is seen to predict higher response in this case. There could be other situations where this difference may be larger. Thus, if the system is non-proportionally damped the formulation proposed here should be used for generation of floor spectra.

Since assumptions like stationarity of input and response have been made in the development of this approach it is essential to validate the approach by simulation study. For this floor spectra were also generated for all 5 floors by time history analysis for the ensemble of 33 time histories of 30 sec. duration and by approach presented in this chapter.

In the time history approach, Eq. 3.8 was solved using Eq. 3.11. For a given ground acceleration time history, with linear variation of ordinates between digitized points, the solution of Eq. 3.8 was exact. That is, assumptions, such as linear variation of acceleration response which is commonly made in step-by-step integration approach, were not made. $z_j(t)$ obtained from Eq. 3.11 was used to define the floor acceleration time history, $\ddot{X}_a(t)$, by Eq. 3.23 which in turn was used as an input to the oscillator, Eq. 2.5, to obtain the maximum acceleration response or the floor spectrum value.

The floor acceleration spectrum values obtained for the time history ensemble were processed to obtain mean and mean + one standard deviation spectra for all floors. The mean spectra are plotted in Figs. 3.2 - 3.8 and compared with the spectra obtained by the direct approach proposed in this chapter. To obtain the mean floor spectra by the direct approach, the seismic input was defined in terms of the mean of ground spectra generated for the ensemble.

The Figs. 3.9 - 3.11 show the comparison of the mean + one standard deviation spectra obtained by time history analysis with floor spectra obtained by the direct approach with mean + one standard deviation spectra of the time history ensemble as ground input. In the generation of the

results by the direct approach all the peak factors were assumed to be equal.

The comparison of the spectrum curves obtained by the two approaches seems to be excellent. The floor spectra curves were obtained for a wide range of damping values, but not all are shown. The comparison between the results for damping not shown here, including very high damping values (50 percent), was also excellent. This comparison validates the proposed approach for direct generation of floor response spectra from ground spectra for non-proportionally damped systems.

3.6 SUMMARY AND CONCLUSIONS

A mode displacement approach is developed for direct generation of floor spectra for nonclassically damped structural systems. Although the normal modes do not exist for a nonclassical system, the developed approach can still be used with ground response spectra as seismic input. A good comparison of the results obtained by the proposed approach and the time history analysis for an ensemble of time histories validates the proposed approach.

Chapter 4

CLASSICALLY DAMPED SYSTEMS: MODE ACCELERATION METHOD

4.1 INTRODUCTION

A direct approach based on the mode displacement method of structural dynamics was described in Chapter 2. This approach is mathematically sound, and will provide accurate results as long as all structural modes of the system are considered. Because of the extra computational effort involved in obtaining higher modes accurately, and also the belief that such modes are not important, often only a limited number of modes are used in the analysis. This can induce some error in the calculation of member response as well as in the generation of floor response spectra, especially if the structure is stiff and also if the floor response spectra for floors near the base are to be generated. To alleviate this problem, here an alternative method based on the mode acceleration method is being proposed for direct generation of floor spectra. In the following sections a complete development of this approach is presented for the nonresonance and resonance cases of classically damped primary systems. The development of a mode acceleration approach for nonclassically damped systems is presented in Chapter 5. Numerical results validating

the proposed approach are also presented.

4.2 ABSOLUTE ACCELERATION OF FLOOR

The mode acceleration formulation, to be developed herein, employs Eq. 2.6 instead of Eq. 2.7 to obtain the absolute acceleration of a floor. That is,

$$\ddot{X}_a(t) = r_m \ddot{X}_g + \sum_{j=1}^{n} \gamma_j \phi_j \ddot{z}_j(t) \qquad (4.1)$$

It is seen that this expression for absolute acceleration contains $\ddot{z}_j(t)$ which is the acceleration of mode j, defined by Eq. 2.3. Hence this approach will be called as the mode acceleration approach.

In the following section, the spectral density function of floor acceleration, defined by Eq. 4.1 will be obtained. This spectral density will then be used as input to an oscillator to obtain the mean square value of its acceleration response and the floor spectrum value, as done in the previous chapters.

4.3 AUTOCORRELATION AND SPECTRAL DENSITY FUNCTION OF ACCELERATION

For a zero mean excitation, $\ddot{X}_g(t)$, the mean of $\ddot{X}_a(t)$ is zero whereas its autocorrelation function is given by

$$E[\ddot{X}_a(t_1)\ \ddot{X}_a(t_2)] = E\left[\left\{r_m\ \ddot{X}_g(t_1) + \sum_{j=1}^{n} \gamma_j\ \phi_j\ \ddot{z}_j(t_1)\right\} \cdot \left\{r_m\ \ddot{X}_g(t_2) + \sum_{k=1}^{n} \gamma_k\ \phi_k\ \ddot{z}_k(t_2)\right\}\right] \tag{4.2}$$

Eq. 4.2 can be rewritten as

$$\begin{aligned} E[\ddot{X}_a(t_1)\cdot\ddot{X}_a(t_2)] &= r_m\ E[\ddot{X}_g(t_1)\cdot\ddot{X}_g(t_2)] \\ &+ \sum_{j=1}^{n} \gamma_j\ \phi_j\ r_m\ E[\ddot{z}_j(t_1)\cdot\ddot{X}_g(t_2)] \\ &+ \sum_{k=1}^{n} \gamma_k\ \phi_k\ r_m\ E[\ddot{z}_k(t_2)\cdot\ddot{X}_g(t_1)] \\ &+ \sum_{j=1}^{n}\sum_{k=1}^{n} \gamma_j\ \gamma_k\ \phi_j\ \phi_k \cdot E[\ddot{z}_j(t_1)\cdot\ddot{z}_k(t_2)] \end{aligned} \tag{4.3}$$

The expected value terms in Eq. 4.3 can be evaluated in terms of ground acceleration PSDF and the modal frequency response functions of the structure. These expected value terms are given in Appendix III-A for the stationary response. Substituting these in Eq. 4.3, and after some algebraic manipulations, the following is obtained:

$$E[\ddot{X}_a(t_1)\ \ddot{X}_a(t_2)] = \int_{-\infty}^{\infty} \Phi_g\ e^{i\omega\tau} \left[r_m^2 \right.$$

$$+ \sum_{j=1}^{n} \gamma_j\ \phi_j\ r_m\ \omega^2\ \{H_j + H_j^*\}$$

$$+ \sum_{j=1}^{n} \gamma_j^2\ \phi_j^2\ \omega^4 \cdot |H_j|^2 + \sum_{j=1}^{n} \sum_{k=j+1}^{n} \gamma_j\ \gamma_k\ \phi_j\ \phi_k\ \omega^4$$

$$\left. \cdot\ [H_j\ H_k^* + H_j^*\ H_k] \right] d\omega \qquad (4.4)$$

The mean square value of floor acceleration can be obtained by substituting $\tau = 0$ in Eq. 4.4. Also, the PSDF of the stationary floor acceleration response can be shown to be given by the following equation:

$$\Phi_m(\omega) = \left[r_m^2 + \sum_{j=1}^{n} \gamma_j\ \phi_j\ \{2\ r_m(\omega_j^2 - \omega^2) \right.$$

$$+ \omega^2\ \gamma_j\ \phi_j\}\ \omega^2\ |H_j|^2$$

$$\left. + \sum_{j=1}^{n} \sum_{k=j+1}^{n} \gamma_j\ \gamma_k\ \phi_j\ \phi_k\ \omega^4\ H_j\ H_k^* \right] \Phi_g(\omega) \qquad (4.5)$$

4.4 FLOOR RESPONSE SPECTRUM

Using this expression of the PSDF, the mean square value of the oscillator response can be defined to obtain

the floor spectrum value. Substituting in Eq. 2.17 the absolute acceleration response spectrum value at frequency ω_o and damping β_o is obtained as follows:

$$R_a^2(\omega_o, \beta_o) = P_F^2(\omega_o) \int_{-\infty}^{\infty} \left[r_m^2 + \sum_{j=1}^{n} \gamma_j \phi_j \right.$$

$$\cdot \{2 r_m(\omega_j^2 - \omega^2) + \omega^2 \gamma_j \phi_j\} \omega^2 |H_j|^2$$

$$\left. + \sum_{j=1}^{n} \sum_{k=j+1}^{n} \gamma_j \gamma_k \phi_j \phi_k \omega^4 H_j H_k^* \right] \Phi_g(\omega)$$

$$\cdot (\omega_o^4 + 4 \beta_o^2 \omega_o^2 \omega^2) |H_o|^2 \, d\omega \qquad (4.6)$$

in which, again, $P_F(\omega_o)$ is the peak factor by which the root mean square response is multiplied to obtain the maximum response (floor spectrum value).

The integrals in Eq. 4.6 will now be evaluated in terms of ground response spectra. Here the seismic input is assumed to be prescribed in terms of relative acceleration and velocity response spectra and in the following sections the single and double summation terms of Eq. 4.6 are evaluated in terms of these spectra. Again the non-resonance and resonance cases will be considered separately.

4.4.1 FLOOR SPECTRUM VALUE FOR THE NONRESONANCE CASE

The first frequency integral in Eq. 4.6 can be written as

$$\int_{-\infty}^{\infty} \Phi_g(\omega) \ (\omega_o^4 + 4 \ \beta_o^2 \ \omega_o^2 \ \omega^2) \ |H_o|^2 \ d\omega$$

$$= I_g - I_3(\omega_o) + 2 \ \omega_o^2 \ I_2(\omega_o) \qquad (4.7)$$

where I_g is the variance of ground acceleration defined as

$$I_g = \int_{-\infty}^{\infty} \Phi_g(\omega) \ d\omega \qquad (4.8)$$

and $I_3(\omega_o)$ is the frequency integral defined as

$$I_3(\omega) = \int_{-\infty}^{\infty} \omega^4 \ \Phi_g(\omega) \ |H_o|^2 \ d\omega \qquad (4.9)$$

When multiplied by appropriate peak factor, S, these integrals define the maximum ground acceleration and the relative response spectrum values. That is

$$S_g^2 \ I_g = A_g^2 \qquad (4.10)$$

$$S_r^2 \ I_3(\omega_o) = R_r^2(\omega_o) \qquad (4.11)$$

where A_g = maximum ground acceleration, $R_r(\omega_o)$ = relative acceleration response spectrum value at frequency ω_o and damping β_o, S_g = peak factor for ground acceleration, and S_r = peak factor for relative acceleration response of an oscillator with frequency ω_o and damping β_o.

Single Summation Terms

Consider the integrand of the first part of the single summation terms in Eq. 4.6 and resolve it into partial fractions as follows:

$$(\omega_o^4 + 4\,\beta_o^2\,\omega_o^2\,\omega^2)\cdot(\omega_j^2 - \omega^2)\,|H_o|^2\,|H_j|^2\,\omega^2\,\Phi_g(\omega)$$
$$= [(\omega_o^2\,A_1 + \omega^2\,B_1)\,|H_o|^2 + (\omega_o^2\,C_1 + \omega^2\,D_1)\,|H_j|^2]\,\omega^2\,\Phi_g(\omega) \qquad (4.12)$$

where A_1, B_1, C_1, and D_1 are given in Appendix III, Eq. III.4. By integrating over the frequency domain and denoting it by, I_s', the first part of the single summation term can be written as,

$$I_s' = A_1 \int_{-\infty}^{\infty} \omega^2\,\omega_o^2\,\Phi_g(\omega)\,|H_o|^2\,d\omega$$
$$+ B_1 \int_{-\infty}^{\infty} \omega^4\,\Phi_g(\omega)\,|H_o|^2\,d\omega$$
$$+ C_1 \int_{-\infty}^{\infty} \omega^2\,\omega_o^2\,\Phi_g(\omega)\,|H_j|^2\,d\omega$$
$$+ D_1 \int_{-\infty}^{\infty} \omega^4\,\Phi_g(\omega)\,|H_j|^2\,d\omega \qquad (4.13)$$

By virtue of Eqs. 2.25 and 4.11, the above equation can be written as

$$I_s' = A_1\ \omega_o^2\ I_2(\omega_o) + B_1\ I_3(\omega_o) + C_1\ \omega_o^2\ I_2(\omega_j) + D_1\ I_3(\omega_j) \tag{4.14}$$

Following the same procedure, the integrand of the second part of the single summation term can also be resolved into partial fractions as follows:

$$\omega^4\ \Phi_g(\omega)\ (\omega_o^4 + 4\ \beta_o^2\ \omega_o^2\ \omega^2)\ |H_o|^2\ |H_j|^2 = \omega^2\ \Phi_g(\omega)\ [(A_2\ \omega_o^2 + B_2\ \omega^2)\ |H_o|^2 + (C_2\ \omega_o^2 + D_2\ \omega^2)\ |H_j|^2] \tag{4.15}$$

Integrating Eq. 4.15 over its frequency domain and using Eqs. 2.25 and 4.11, the frequency integral of the second part of the single summation term, herein denoted as I_s'', can be written as

$$I_s'' = A_2\ \omega_o^2\ I_2(\omega_o) + B_2\ I_3(\omega_o) + C_2\ \omega_o^2\ I_2(\omega_j) + D_2\ I_3(\omega_j) \tag{4.16}$$

in which the factors A_2, B_2, C_2, and D_2 are defined in Appendix III-B, Eq. III.7.

Double Summation Terms

Consider the complete double summation term, with pairing of the two Hermitian terms in the summation as follows:

$$I_{dd} = \sum_{j\neq k}^{n}\sum^{n} \gamma_j\ \gamma_k\ \phi_j\ \phi_k \int_{-\infty}^{\infty} \omega^4(\omega_o^4 + 4\ \beta_o^2\ \omega_o^2\ \omega^2) \cdot |H_o|^2\ H_j\ H_k^*\ \Phi_g(\omega)\ d\omega$$

$$= \sum_{j=1}^{n}\sum_{k=j+1}^{n} \gamma_j\ \gamma_k\ \phi_j\ \phi_k \int_{-\infty}^{\infty} \Phi_g(\omega)\ \omega^4 \cdot (\omega_o^4 + 4\ \beta_o^2\ \omega_o^2\ \omega^2)\ |H_o|^2\ (H_j\ H_k^* + H_j^*\ H_k)\ d\omega \qquad (4.17)$$

It can be further simplified, eliminating the complex term, as

$$I_{dd} = 2 \sum_{j=1}^{n}\sum_{k=j+1}^{n} \gamma_j\ \gamma_k\ \phi_j\ \phi_k \int_{-\infty}^{\infty} \omega^2\ \Phi_g(\omega)\ N'(\omega) \cdot (\omega_o^4 + 4\ \beta_o^2\ \omega_o^2\ \omega^2)\ |H_j|^2\ |H_k|^2\ |H_o|^2\ d\omega \qquad (4.18)$$

in which

$$N'(\omega) = \omega^2\ \{\omega_j^2\ \omega_k^2 - \omega^2(\omega_j^2 + \omega_k^2 - 4\ \beta_j\ \beta_k\ \omega_j\ \omega_k) + \omega^4\} \qquad (4.19)$$

Denote integral of Eq. 4.18 by I_d'. Resolving a part of the integrand into partial fractions, this integral can be written as

$$I_d' = \int_{-\infty}^{\infty} \omega^2 \, \Phi_g(\omega) \, N(\omega) \, |H_j|^2 \, |H_k|^2 \, (\omega_o^4 + 4 \, \beta_o^2 \, \omega_o^2 \, \omega^2) \, |H_o|^2 \, d\omega$$

$$= \int_{-\infty}^{\infty} \Phi_g(\omega) \cdot \omega^2 (\omega_o^4 + 4 \, \beta_o^2 \, \omega_o^2 \, \omega^2) \, |H_o|^2 \cdot \{(A_r \, \omega_o^2 + B_r \, \omega^2) \, |H_j|^2 + (C_r \, \omega_o^2 + D_r \, \omega^2) \, |H_k|^2\} \, d\omega \qquad (4.20)$$

where A_r, B_r, etc. are defined in Appendix III, Eq. III.15.

When $\omega_j = \omega_o$ and $\beta_j = \beta_o$, evaluation of the first term of Eq. 4.20 requires special consideration. This resonance case is described in Section 4.4.2. However, when $\omega_j \neq \omega_o$, each term in the integrand of Eq. 4.20 can be further broken into partial fractions to give the following

$$I_d' = \int_{-\infty}^{\infty} \Phi_g(\omega) \, \omega^2 [(A_j \, \omega_o^2 + B_j \, \omega^2) \, |H_o|^2 + (C_j \, \omega_o^2 + D_j \, \omega^2) \, |H_j|^2 + (A_k \, \omega_o^2 + B_k \, \omega^2) \, |H_o|^2 + (C_k \, \omega_o^2 + D_k \, \omega^2) \, |H_k|^2] \, d\omega \qquad (4.21)$$

where A_j, B_j, ..., A_k, B_k, etc. are defined by Eq. III.10 in Appendix III.

Using Eqs. 2.25 and 4.11, Eq. 4.21 can be written as

$$I'_d = \omega_o^2 (A_j + A_k) I_2(\omega_o) + (B_j + B_k) I_3(\omega_o) + \omega_o^2 \{C_j I_2(\omega_j) + C_k I_2(\omega_k)\} + D_j I_3(\omega_j) + D_k I_3(\omega_k) \quad (4.22)$$

By substituting Eqs. 4.7, 4.14, 4.16, and 4.21 in Eq. 4.6 the response spectrum value at oscillator frequency, ω_o and damping β_o can be obtained from the following equation:

$$R_a^2(\omega_o, \beta_o) = P_F^2(\omega_o) \left[r_m^2 \{I_g - I_3(\omega_o) + 2 \omega_o^2 I_2(\omega_o)\} + \sum_{j=1}^{n} \gamma_j \phi_j \{2 r_m I'_s + \gamma_j \phi_j I''_s\} + 2 \sum_{j=1}^{n} \sum_{k=j+1}^{n} \gamma_j \gamma_k \phi_j \phi_k I'_d\right] \quad (4.23)$$

I'_s, I''_s and I_d in Eqs. 4.14, 4.16, and 4.21 can be defined in terms of the frequency integral I_2 and I_3 which in turn are defined in terms of relative acceleration and relative velocity spectrum values and their peak factors by Eqs. 2.25 and 4.11.

Eq. 4.23 allows for the incorporation of peak factors in the generation of floor spectra. However, if all the peak factors are assumed to be equal, an expression independent of peak factors is obtained as follows:

$$
\begin{aligned}
R_a^2(\omega_o, \beta_o) = r_m^2 \, [A_g^2 - R_r^2(\omega_o) + 2 \, \omega_o^2 \, R_v^2(\omega_o)] \\
+ \sum_{j=1}^{n} \gamma_j \, \phi_j \, [\{2 \, r_m \, A_1 + \gamma_j \, \phi_j \, A_2\} \, \omega_o^2 \, R_v^2(\omega_o) \\
+ \{2 \, r_m \, B_1 + \gamma_j \, \phi_j \, B_2\} \, R_r^2(\omega_o) \\
+ \{2 \, r_m \, C_1 + \gamma_j \, \phi_j \, C_2\} \, \omega_o^2 \, R_v^2(\omega_j) \\
+ \{2 \, r_m \, D_1 + \gamma_j \, \phi_j \, D_2\} \, R_r^2(\omega_j)\}] \\
+ 2 \sum_{j=1}^{n} \sum_{k=j+1}^{n} \gamma_j \, \gamma_k \, \phi_j \, \phi_k \, [\omega_o^2 \, (A_j + A_k) \, R_v^2(\omega_o) \\
+ (B_j + B_k) \, R_r^2(\omega_o) + \omega_o^2 \, \{C_j \, R_v^2(\omega_j) + C_k \, R_v^2(\omega_k)\} \\
+ D_j \, R_r^2(\omega_j) + D_k \, R_r^2(\omega_k)] \qquad (4.24)
\end{aligned}
$$

Eq. 4.24 has been used to obtain floor spectra which are compared with the corresponding results obtained by the direct approach described in Chapter 2 and the time history analysis.

4.4.2 FLOOR SPECTRUM VALUE FOR THE RESONANCE CASE

The factors A_1, B_1, etc. in Eq. 4.17 depend upon the frequency ratios $r_1 = \omega_j/\omega_o$, $r_2 = \omega_k/\omega_o$ and damping coefficients β_j, β_k, and β_o. These factors are not defined for the resonance case. To define floor spectrum value at resonance a special treatment of the single and double summation terms, as in the previous chapters, is required. A more general formulation is developed here with the limits of frequency integration restricted to a cut-off frequency, ω_c. The expressions for the case when $\omega_c = \infty$ are also obtained.

Single Summation Terms

Consider the first single summation term in Eq. 4.6 when $\omega_j = \omega_k$ and $\beta_j = \beta_o$,

$$I_{s1} = \int_{-\omega_c}^{\omega_c} \Phi_g(\omega)\ \omega^2(\omega_o^2 - \omega^2)(\omega_o^4 + 4\ \beta_o^2\ \omega_o^2\ \omega^2)\ |H_o|^4\ d\omega \tag{4.25}$$

since the function $|H_o|^4$ is highly peaked, Eq. 4.25 can be approximated as [52]

$$I_{s1} \simeq \Phi_g(\omega_o) \int_{-\omega_c}^{\omega_c} \omega^2 \{\omega_o^6 - \omega^2 \omega_o^4 (1 - 4 \beta_o^2) - 4 \beta_o^2 \omega_o^2 \omega^4\} |H_o|^4 \, d\omega - \frac{2}{3} \omega_o \Phi_g(\omega_o) + 1/\omega_o^2 \int_{-\omega_o}^{\omega_o} \omega^2 \Phi_g(\omega) \, d\omega \qquad (4.26)$$

The integral in Eq. 4.26 is of the same form as integral in Appendix I-C, Eq. I.22. Hence it can be evaluated in closed form. Also because of the peakedness of $|H_o|^2$ the frequency integral $I_2(\omega_o)$ in Eq. 2.20 can also be approximated as

$$I_2(\omega_o) \simeq \Phi_g(\omega_o) \int_{-\omega_c}^{\omega_c} \omega^2 |H_o(\omega)|^2 \, d\omega - \frac{2}{3} \frac{\Phi_g(\omega_o)}{\omega_o} + 1/\omega_o^4 \int_{-\omega_o}^{\omega_o} \omega^2 \Phi_g(\omega) \, d\omega \qquad (4.27)$$

In the above equation the second and the third term are relatively very small and because of their opposite sign they cancel each other. This was verified for a 3-term modified form of Kanai-Tajimi PSDF defined by Eq. 2.105. By substituting for the 1st integral in Eq. 4.27 from Appendix I-C, in terms of V_m, the following is obtained

$$\Phi_g(\omega_o)\ \omega_c = \frac{\omega_o^2\ I_2(\omega_o)}{V_m} \tag{4.28}$$

where V_m is defined in Appendix III-C, Eq. III.16. Substituting Eq. 4.28 into Eq. 4.26 and after some algebraic manipulations the following is obtained

$$I_{s1} = \frac{\omega_o^2\ I_2(\omega_o)}{V_m}\ [F_m - \frac{2}{3}\ r] \tag{4.29}$$

where F_m is defined in Appendix III-C. Eq. 4.29 can be rewritten as

$$I_{s1} = F_m'\ I_2(\omega_o) \tag{4.30}$$

where

$$F_m' = \omega_o^2\ [F_m - 2/3\ r]/V_m \tag{4.31}$$

Proceeding similarly, the second single summation term at resonance can be written as

$$I_{s2} = \int_{-\omega_c}^{\omega_c} \Phi_g(\omega)\ \omega^4\ (\omega_o^4 + 4\ \beta_o^2\ \omega_o^2\ \omega^2)\ |H_o|^4\ d\omega \tag{4.32}$$

which for a sharply peaked $|H_o|^4$, can be approximated as follows:

$$I_{s2} \simeq \Phi_g(\omega_o) \int_{-\omega_c}^{\omega_c} \omega^4 \, (\omega_o^4 + 4 \, \beta_o^2 \, \omega_o^2 \, \omega^2) \, |H_o|^4 \, d\omega$$

$$- \frac{2}{3} \, \omega_o \, \Phi_g(\omega_o) + 1/\omega_o^4 \int_{-\omega_o}^{\omega_o} \omega^4 \, \Phi_g(\omega) \, d\omega \qquad (4.33)$$

In the above equation, the second integral is small and can be neglected. The 1st integral can be evaluated in closed form, Appendix I-C, Eq. I.22. Using Eq. 4.28 in Eq. 4.33 the second part of the single summation term at resonance can be written as follows:

$$I_{s2} = \omega_o^2 \, I_2(\omega_o) \, [G_m - 2/5 \, r]/V_m \qquad (4.34)$$

where G_m is defined in Appendix III-C, Eq. III.18. The above equation can be rewritten as

$$I_{s2} = G_m' \, I_2(\omega_o) \qquad (4.35)$$

in which

$$G_m' = \omega_o^2 \, [G_m - 2/5 \, r]/V_m \qquad (4.36)$$

Double Summation Terms

If $\omega_j = \omega_o$ and $\beta_j = \beta_o$, the first part of Eq. 4.20, and if $\omega_k = \omega_o$ and $\beta_k = \beta_o$, the second part of Eq. 4.20 require special considerations in their evaluation. Consider the case when $\omega_j = \omega_o$ and $\beta_j = \beta_o$. In this case

the first part of Eq. 4.20 can be written as

$$I_d = \int_{-\omega_c}^{\omega_c} \omega^2 \ (\omega_o^4 + 4 \ \beta_o^2 \ \omega_o^2 \ \omega^2) \ (A_r \ \omega_o^2 + B_r \ \omega^2) \ |H_o|^4 \cdot \Phi_g(\omega) \ d\omega \tag{4.37}$$

Again, because the function $|H_o|^4$ is highly peaked the terms with A_r can be approximated as follows:

$$A_r \int_{-\omega_c}^{\omega_c} \omega^2 \ (\omega_o^6 + 4 \ \beta_o^2 \ \omega_o^4 \ \omega^2) \ \phi_g(\omega) \ |H_o|^4 \ d\omega$$

$$\simeq \Phi_g(\omega_o) \ A_r \int_{-\omega_c}^{\omega_c} (\omega^2 \ \omega_o^6 + 4 \ \beta_o^2 \ \omega_o^4 \ \omega^4) \ |H_o|^4 \ d\omega$$

$$- 2/3 \ \omega_o \ \Phi_g(\omega_o) \ A_r \ \omega_o \tag{4.38}$$

Similarly the terms with B_r can be approximated as follows:

$$B_r \int_{-\infty}^{\infty} \omega^4 \ (\omega_o^4 + 4 \ \beta_o^2 \ \omega_o^2 \ \omega^2) \ \Phi_g(\omega) \ |H_o|^4 \ d\omega$$

$$\simeq \Phi_g(\omega_o) \ B_r \int_{-\omega_c}^{\omega_c} (\omega_o^4 \ \omega^4 + 4 \ \beta_o^2 \ \omega_o^2 \ \omega^6) \ |H_o|^4 \ d\omega$$

$$- 2/5 \ \Phi_g(\omega_o) \ B_r \ \omega_o \tag{4.39}$$

Using Eq. 4.38 and 4.39, Eq. 4.37 can now be written as

$$I_d = \Phi_g(\omega_o) \int_{-\omega_c}^{\omega_c} \{4\ \beta_o^2\ B_r\ \omega_o^2\ \omega^6 + (B_r + 4\ \beta_o^2\ A_r)\ \omega_o^4\ \omega^4 + A_r\ \omega_o^6\ \omega^2\}\ |H_o|^4\ d\omega - 2\ \omega_o\ \Phi_g(\omega_o)\ (A_r/3 + B_r/5) \tag{4.40}$$

The integral in Eq. 4.40 can be evaluated in closed form using the integral in Appendix I-C, Eq. I.22. Substituting Eq. 4.28, Eq. 4.40 can be written as

$$I_d = \frac{\omega_o^2\ I_2(\omega_o)}{V_m} \cdot \{H_m - 2r\ (A_r/3 + B_r/5)\} \tag{4.41}$$

in which the factor H_m is defined in Appendix III-C, Eq. III.19. Eq. 4.41 can be rewritten as

$$I_d = I_2(\omega_o)\ H_m' \tag{4.42}$$

in which

$$H_m' = \frac{\omega_o^2}{V_m} \{H_m - 2r\ (A_r/3 + B_r/5)\} \tag{4.43}$$

The second part of Eq. 4.20 can be evaluated as in non-resonance case, Eq. 4.21. Thus using Eqs. 4.30, 4.35 and 4.42, the response spectrum value for the resonance case can be written as follows:

$$R_a^2(\omega_o,\beta_o) = P_F^2(\omega_o)\ [I_g - I_3(\omega_o) + 2\ \omega_o^2\ I_2(\omega_o)$$

$$+ \sum_{j=1}^{n} \gamma_j\ \phi_j\ \{2\ r_m\ F'_m + \gamma_j\ \phi_j\ G'_m\}\ I_2(\omega_o)$$

$$+ 2 \sum_{j=1}^{n} \sum_{k=j+1}^{n} \gamma_j\ \gamma_k\ \phi_j\ \phi_k\ \{H'_m\ I_2(\omega_o)$$

$$+ A_k\ \omega_o^2\ I_2(\omega_o) + B_k\ I_3(\omega_o) + C_k\ \omega_o^2\ I_2(\omega_o)$$

$$+ D_k\ I_3(\omega_k)\} \qquad (4.44)$$

In this equation A_g, I_2, and I_3 can be substituted in terms of ground response spectrum values and their associated peak factors to define floor spectrum values. However, if all the peak factors are assumed to be equal then the following expression independent of peak factors is obtained:

$$R_a^2(\omega_o,\beta_o) = A_g^2 - R_r^2(\omega_o) + 2\ \omega_o^2\ R_v^2(\omega_o)$$

$$+ \sum_{j=1}^{n} \gamma_j\ \phi_j\ \{2\ r_m\ F'_m + \gamma_j\ \phi_j\ G'_m\}\ R_v^2(\omega_o)$$

$$+ 2 \sum_{j=1}^{n} \sum_{k=j+1}^{n} \gamma_j\ \gamma_k\ \phi_j\ \phi_k\ \{(H'_m + A_k\ \omega_o^2)\ R_v^2(\omega_o)$$

$$+ B_k\ R_r^2(\omega_o) + \omega_o^2\ C_k\ R_v^2(\omega_k) + D_k\ R_r^2(\omega_k)\} \qquad (4.45)$$

4.5 MODE ACCELERATION VS. MODE DISPLACEMENT APPROACH

The mode displacement approach presented in Chapter 2 and the mode acceleration approach presented here are mathematically consistent and equivalent. They just represent a response quantity in two different ways. As seismic input, the mode displacement approach requires the pseudo-acceleration and relative velocity spectra whereas the mode acceleration approach requires relative acceleration and relative velocity spectra. Numerically, they should provide same result if a complete set of modes are used to obtain the response and also if the two forms of input used in the two approaches are completely consistent. To verify this numerical consistency the mean square value of the floor spectral response of a structural system was obtained by the two approaches, using Eqs. 2.29 and 4.23 without the peak factor $P_F(\omega_o)$. The values $I_1(\omega_j)$ and $I_2(\omega_j)$ used in Eq. 2.29 and $I_2(\omega_j)$ and $I_3(\omega_j)$ used in Eq. 4.23 were obtained for the same spectral density function, Eq. 2.105. When all the modes were used, the two approaches provided exactly the same values of response. This verified the numerical consistency of the proposed approach as well as the computer code used for the evaluation of numerical results.

If all the modes are required to be used in the mode acceleration approach to obtain accurate response, then no specific advantage is gained. However, because of the special characteristics of the relative acceleration and velocity spectra which are the inputs to this approach it is possible to obtain a very accurate value of response even with only a first few modes. Thus the high frequency modes need not be obtained at all if this approach is used for generation of floor spectra. This, however, is not possible if the mode displacement approach is used. Omitting high frequency modes in the mode displacement approach can lead to larger errors in the calculated response especially if the structural system is stiff and floor response to be evaluated is affected by the high frequency modes. This happens when floor response spectra are to be generated for the floors which are near the ground. This is because of the so-called "missing mass" effect.

Figs. 2.12 and 2.13 show the average relative acceleration and relative velocity spectra for the ensemble of 30-sec duration earthquakes considered in this study. It is seen that for high frequencies, especially the ones higher than (the highest frequency in the motion) the relative spectra become very small. On the other hand the average pseudo-acceleration spectra shown in Fig. 2.11, which are

used in mode displacement approach, become constant equal to the maximum ground acceleration. Therefore, if the higher modes are omitted in the mode displacement analysis, a larger error will be caused than a similar omission in the mode acceleration approach.

In the mode acceleration method, the major part of the missing mass effect is included through the first terms in Eq. 4.23 and 4.45 which are associated with the rigid body effects of the ground motion.

Thus, the mode acceleration approach is computationally more efficient than the mode displacement approach, as a smaller number of modes are adequate in the calculation of accurate response. This advantage is clearly seen from the results presented in Table 4.2.

4.6 NUMERICAL RESULTS

In this section the numerical results obtained for a 10 story, 30 degrees-of-freedom structure (D.O.F.), as well as for the 11-frequency structural model considered in Chapter 2 are presented. The 30 degrees-of-freedom structure consists of 10 rigid floors connected by columns. The stiffness and mass parameters of this system can be

easily adjusted to create a stiff or soft system.

First to verify the mathematical correctness of the formulation developed in this chapter and also the claim that it is mathematically equivalent to the mode displacement approach presented in Chapter 2, the mean square values of floor spectral responses for 30-D.O.F. system were obtained by the mode displacement and the mode acceleration approaches with all 30 modes considered in the analyses. The input in both the analyses was in terms of the PSDF defined by Eq. 2.105. Both analyses provided exactly the same results. Thus verifying the mathematical equivalence of the two formulations as well as the logic of the computer codes.

To verify the claim made earlier in Sec. 4.5 that the mode acceleration approach is more effective than mode displacement approach inasmuch as the former provides a more accurate response than the latter for a given number of modes, here some mean square value results for the floor spectral responses of the 30 D.O.F. structure are presented. The stiffness properties of the structure were adjusted such that the frequencies are rather on higher side. The first 10 frequencies, partication factors and modal damping values are given in Table 4.1. To calculate the

mean square value the input was defined in terms of the PSDF in Eq. 2.105 with a cut-off frequency of 20 cps.

The results are shown in Table 4.2 for floors 1, 2, 5, 8 and 10. Floor 1 is the lowest floor and 10 the highest. The mean square floor response spectrum values obtained with all 30 modes in the analysis are given in Columns (2), (5), (8), (11) and (14) for various floors. In other columns, the response values obtained by the mode acceleration and mode displacement approaches, with only 4 modes used in the analysis, are shown in terms of their ratios to the values obtained with 30 modes (exact mean square value). Thus a ratio close to 1 means a more accurate result.

It is seen that the results obtained by the mode displacement approach are rather inaccurate, especially for the lower floors. This is because the floor spectra for the lower floors are affected by higher modes. For higher floors the effect of high frequency modes becomes small and thus neglecting them in the analysis should not give much error in the calculated response. This fact seems to be borne out from the results in Table 4.2 for the higher floors.

It is also seen that the results obtained by the mode acceleration approach are superior across the board. Even

for the lower floors, one need not worry about the higher modes in the calculation of response by this approach. The modes for which relative spectrum values are insignificant can be neglected. This will, in general, happen for modes with frequencies higher than the highest frequency in the input.

To verify the applicability of Eq. 4.24 and 4.45 for generation of floor spectra, in view of several simplifying assumptions made in their development, the floor spectra obtained from these equations are compared with the spectra obtained in the simulation study for the ensemble of time histories. For a proper comparison, the time history results were also obtained by mode acceleration formulation. That is, to obtain the floor acceleration time histories, Eq. 4.1 was employed instead of Eq. 2.7.

Figs. 4.2 - 4.5 show the mean floor spectra obtained for the 11-frequency model by time history analysis and the approach proposed in this chapter. The comparison of the two results is rather very good. This comparison validates Eqs. 4.24 and 4.45 for generation of floor spectra in spite of simplifying assumptions made in their development.

The results are also obtained for the 30-D.O.F. structure which further validate Eqs. 4.24 and 4.45 as well as substantiate the claim of effectiveness of the approach with limited modes. Figs. 4.6 - 4.12 are for 15 sec. time history spectra as input and Figs. 4.13 - 4.16 for 30 sec. time history spectra as input. These are obtained by the mode acceleration approach with only 10 modes out of 30 modes used in the analysis. These results compare very well with the time history results. In fact the results obtained with only the first 4 modes, shown in Figs. 4.17 - 4.26, also compare very well with the time history results. This clearly indicates that mode acceleration approach can be used to generate accurate floor spectra directly from ground spectra only with a limited number of modes. On the other hand, the mode displacement approach cannot be used with limited modes to obtain accurate results, as is shown by the results in Figs. 4.27 - 4.31 obtained with 4 modes for 15 sec. time histories. The mode displacement results even with 10 modes, Figs. 4.32 - 4.36, do not compare well with time history results. For floors far from the base where higher mode effects are not important, the mode displacement approach with a first few modes, however, can also provide reasonable results. Nonetheless, the superiority of the mode acceleration approach is consistently better.

These results were obtained without inclusion of the peak factors in Eq. 4.23. These indicate that there is probably no need to include peak factor and the assumption of equal peak factor will provide accurate enough response. Fig. 4.27 shows that the method can also be applied equally well for generation of spectra for high damping values.

4.7 SUMMARY AND CONCLUSIONS

An alternative approach based on the mode acceleration method of structural dynamics is developed for direct generation of floor spectra for classically damped systems. The seismic input in this approach are required in terms of relative acceleration and velocity spectra. The approach is especially very effective for the generation of floor spectra for the structural systems which have predominant high frequency modes, and also for floors close to the base. Only a first few modes need to be utilized in the analysis. The approach can also be used with computational advantage to obtain accurate results even for the cases which are not affected by high frequency modes. A good comparison of the results obtained by proposed approach and the simulation study validates the approach.

Chapter 5

NONCLASSICALLY DAMPED SYSTEMS: MODE ACCELERATION METHOD

5.1 INTRODUCTION

In Chapters 2 and 3, direct methods based on the, so called, mode displacement formulation were described for proportionally damped structural systems. Whereas in Chapter 4, a method based on mode acceleration formulation was proposed to alleviate certain problems associated with high frequency modes in proportionally damped structural systems. To alleviate similar problems with high frequency modes in nonproportionally damped systems an alternative method based on mode acceleration formulation is proposed in this chapter.

As in Chapter 4, the input, in this approach is required to be prescribed in terms of relative acceleration and relative velocity spectra. Maximum ground acceleration value is also required. The results showing comparison of mode acceleration approach with mode displacement approach for nonproportional system as well as the results of the numerical simulation study are presented.

5.2 FLOOR ACCELERATION RESPONSE

In this formulation, the vector of absolute acceleration of $\{\ddot{X}_a\}$ is expressed in a different manner. Using the lower half of response vector $\{y\}$, the relative displacement vector $\{x\}$ can be written as follows:

$$\{x\} = \sum_{j=1}^{2n} \{\phi_j\}_\ell \, z_j \tag{5.1}$$

in which $\{\phi_j\}_\ell$ is the lower half of modal matrix $[\phi]$. Using Eq. 5.1 in Eq. 3.12, the absolute acceleration vector can be written as

$$\{\ddot{X}_a\} = \sum_{j=1}^{2n} \{\phi_j\}_\ell \, \ddot{z}_j + \{r\} \, \ddot{X}_g(t) \tag{5.2}$$

and the absolute acceleration of, say, the mth floor is given by

$$\ddot{X}_{am} = \sum_{j=1}^{2n} \phi_j(m) \, \ddot{z}_j + r_m \, \ddot{X}_g \tag{5.3}$$

in which $\phi_j(m)$ is the mth element of the lower complex mode $\{\phi_j\}$, and r_m is the mth element of displacement influence vector $\{r\}$.

Eq. 5.3 forms the basis of the mode acceleration method of generation of floor spectra for nonclassically damped

structural systems. In order to define the floor spectra, the spectral density function of floor acceleration will be obtained using this equation. This spectral density function will be used as an input to an oscillator on the floor to calculate the floor response spectrum value.

5.3 AUTOCORRELATION AND SPECTRAL DENSITY FUNCTIONS OF FLOOR ACCELERATION

Eq. 5.3 can be rewritten as a summation over n terms by pairing complex conjugate terms as follows:

$$\ddot{X}_a(t) = \sum_{j=1}^{n} \phi_j \ddot{z}_j(t) + \sum_{j=1}^{n} \phi_j^* \ddot{z}_j^*(t) + \ddot{X}_g(t) \qquad (5.4)$$

where for brevity $\ddot{X}_{am}(t)$ has been replaced by $\ddot{X}_a(t)$ and $\phi_j(m)$ by ϕ_j, and r will be taken equal to 1 for generation of floor spectra in the direction of excitation. Note that ϕ_j here denotes an element of the lower part of the eigenvector whereas in Chapter 3, it denoted the upper part. Hereafter this notation will be used in this chapter.

For zero mean random process, $\ddot{X}_g(t)$, the mean of absolute acceleration of floor, $\ddot{X}_a(t)$, will be zero and its autocorrelation function can be obtained as

$$E[\ddot{X}_a(t_1)\ \ddot{X}_a(t_2)] = E[\ddot{X}_g(t_1)\ \ddot{X}_g(t_2)]$$

$$+ \sum_{k=1}^{n} \phi_k\, E[\ddot{X}_g(t_1)\ \ddot{z}_k(t_2)] + \sum_{k=1}^{n} \phi_k^*\, E[\ddot{X}_g(t_1)$$

$$\ddot{z}_k^*(t_2)] + \sum_{j=1}^{n} \phi_j\, E[\ddot{X}_g(t_2)\ \ddot{z}_j(t_1)]$$

$$+ \sum_{j=1}^{n} \phi_j^*\, E[\ddot{X}_g(t_2)\ \ddot{z}_j(t_1)]$$

$$+ \sum_{j=1}^{n} \sum_{k=1}^{n} \{\phi_j\, \phi_k\, E[\ddot{z}_j(t_1)\ \ddot{z}_k(t_2)]$$

$$+ \phi_j^*\, \phi_k^*\, E[\ddot{z}_j^*(t_1)\ \ddot{z}_k(t_2)] + \phi_j\, \phi_k^*\, E[\ddot{z}_j(t_1)$$

$$\ddot{z}_k^*(t_2)] + \phi_j^*\, \phi_k\, E[\ddot{z}_j(t_1)\ \ddot{z}_k(t_2)] \qquad (5.5)$$

in which $z_j(t)$ is defined by Eq. 3.11. Various expected values required in Eq. 5.5 can be obtained in terms of auto-correlation function or spectral density function of ground acceleration using Eq. 3.11. These are defined in Appendix IV-A. The expected value of 1st term is defined in Appendix III-A.

Single Summation Terms

In Eq. 5.5, the single summation terms and terms with $j=k$ and the cross-terms with $j \neq k$ will be evaluated separately to simplify the algebraic manipulations.

The single summation terms denoted by, R_s', can be written as

$$R_s' = \sum_{j=1}^{n} \{\phi_j \, E[\ddot{X}_g(t_1) \, \ddot{z}_j(t_2)] + \phi_j^* \, E[\ddot{X}_g(t_1) \, \ddot{z}_j^*(t_2)] + \phi_j \, E[\ddot{X}_g(t_2) \, \ddot{z}_j(t_1)] + \phi_j^* \, E[\ddot{X}_g(t_2) \, \ddot{z}_j(t_1)]\} \tag{5.6}$$

Substituting for the expected values from Appendix IV-A, Eq. 5.6 can be rewritten as

$$R_s' = - \sum_{j=1}^{n} \int_{-\infty}^{\infty} \omega^2 \, \Phi_g(\omega) e^{i\omega\tau} \left[\frac{q_j}{(p_j + i\omega)} + \frac{q_j^*}{(p_j^* + i\omega)} + \frac{q_j}{(p_j - i\omega)} + \frac{q_j^*}{(p_j^* - i\omega)} \right] d\omega \tag{5.7}$$

where, q_j is defined in Eq. 3.30 and 3.31. With appropriate combination of the 1st with 3rd term and the 2nd with 4th term, Eq. 5.7 can be written as

$$R_s' = - 4 \int_{-\infty}^{\infty} \omega^2 \, \Phi_g(\omega) e^{i\omega\tau} \, (\omega^2 \, t_1 + t_3) \, |H_j|^2 \, d\omega \tag{5.8}$$

in which coefficients t_1 and t_3 are defined as follows

$$t_1 = - \omega_j \, (a_j \, \beta_j + b_j \sqrt{1 - \beta_j^2}) \tag{5.9a}$$

$$t_3 = - \omega_j^2 \, (1 - 2 \, \beta_j^2) \, t_1 - 2 \, \omega_j^2 \, \beta_j \sqrt{1 - \beta_j^2} \, t_2 \tag{5.9b}$$

$$t_2 = \omega_j \ (a_j\sqrt{1 - \beta_j^2} - b_j \ \beta_j) \tag{5.9c}$$

Now consider the terms with j=k in the double summation terms in Eq. 5.5. Denoting them as R_s'', they can be written as follows:

$$R_s'' = \sum_{j=1}^{n} \{\phi_j^2 \ E[\ddot{z}_j(t_1) \ \ddot{z}_j(t_2)] + \phi_j^{*2} \ E[\ddot{z}_j^*(t_1) \ \ddot{z}_j^*(t_2)] + \phi_j \ \phi_j^* \ (E[\ddot{z}_j(t_1) \ \ddot{z}_j^*(t_2)] + E[\ddot{z}_j^*(t_1) \ \ddot{z}_j(t_2)])\} \tag{5.10}$$

Substituting for the expected values from Appendix IV-A, and combining the 1st term with 2nd term and the 3rd with 4th, and after some algebraic manipulations, Eq. 5.10 can be written as

$$R_s'' = 4 \sum_{j=1}^{n} \int_{-\infty}^{\infty} \omega^4 \ \Phi_g(\omega) \ e^{i\omega\tau} \ (a_j^2 \ \omega^2 + A_j') \ |H_j|^2 \ d\omega \tag{5.11}$$

where

$$A_j' = \omega_j^2 \ \{b_j^2 + (a_j^2 - b_j^2) \ \beta_j^2 - 2 \ a_j \ b_j \ \beta_j\sqrt{1 - \beta_j^2}\} \tag{5.12}$$

Double Summation Terms

The double summation terms with j≠k in Eq. 5.5, herein denoted as R_d, are also evaluated similarly. Substituting

for the expected values from Appendix IV-A, these terms can be written as:

$$R_d = \sum_{j=1}^{n} \sum_{k=j+1}^{n} \int_{-\infty}^{\infty} \omega^4 \Phi_g(\omega) e^{i\omega\tau} \left[\frac{1}{(-p_j+i\omega)(-p_k-i\omega)} + \frac{1}{(-p_j^*+i\omega)(-p_k^*-i\omega)} + \frac{1}{(-p_j+i\omega)(-p_k^*-i\omega)} + \frac{1}{(-p_j^*+i\omega)(-p_k-i\omega)} \right] d\omega \tag{5.13}$$

Substituting p_j and p_k in terms of their real and imaginary parts and after some algebraic manipulations, Eq. 5.13 can be written as

$$R_d = \sum_{j\neq k}^{n} \sum_{}^{n} \int_{-\infty}^{\infty} \Phi_g(\omega) e^{i\omega\tau} \left[X'_{jk}(\omega) + i\, Y'_{jk}(\omega) \right] H_j\, H_k^*\, d\omega \tag{5.14}$$

in which

$$X'_{jk} = 4\, a_j\, a_k\, (\omega^2 + \omega_j\, \omega_k\, \beta_j\, \beta_k) + 4\, \beta_j\, \beta_k\, \omega_j\, \omega_k \cdot \sqrt{1-\beta_j^2}\, \sqrt{1-\beta_k^2} - 4\, \omega_j\, \omega_k\, (a_j\, b_k\, \beta_j \sqrt{1-\beta_k^2} + a_k\, b_j\, \beta_k \sqrt{1-\beta_j^2}) \tag{5.15}$$

$$Y'_{jk} = 4\omega \{ a_j\, a_k\, (\omega_k\, \beta_k - \omega_j\, \beta_j) - (a_j\, b_k\, \omega_k \sqrt{1-\beta_k^2} - a_k\, b_j\, \omega_j \sqrt{1-\beta_j^2}) \tag{5.16}$$

Eq. 5.14 can also be rewritten in terms of absolute values of H_j and H_k^* as

$$R_d = \int_{-\infty}^{\infty} \phi_g(\omega)\ e^{i\omega\tau}\ [X_{jk}(\omega) + i\ Y_{jk}(\omega)]\ |H_j|^2\ |H_k|^2\ d\omega \tag{5.17}$$

in which $X_{jk}(\omega)$ and $Y_{jk}(\omega)$ are the same as in Eq. 3.42. Since $X_{jk} = X_{kj}$ and $Y_{jk} = -Y_{kj}$, Y_{jk} will be eliminated from the final expression when the cross terms with $j \neq k$ are combined together. Using Eqs. 5.5, 5.8, 5.11, and 5.17, complete autocorrelation function of the stationary response of the floor acceleration is given by the following expression:

$$E[\ddot{X}_a(t_1)\ \ddot{X}_a(t_2)] = \int_{-\infty}^{\infty} \phi_g(\omega)\ e^{i\omega\tau} \left[1 - \sum_{j=1}^{n} 4\ \omega^2 \cdot (\omega^2\ t_1 + t_3)\ |H_j|^2 + \sum_{j=1}^{n} 4\ \omega^4\ (a_j^2\ \omega^2 + A_j')\ |H_j|^2 + 2 \sum_{j\neq k}^{n}\sum^{n} X_{jk}(\omega)\ |H_j|^2\ |H_k|^2\right] d\omega \tag{5.18}$$

For $\tau = 0$, this equation also defines the mean square acceleration response of floor. From Eq. 5.18 the PSDF of the floor acceleration response can be written as

$$\Phi_m(\omega) = \Phi_g(\omega) - 4 \sum_{j=1}^{n} \omega^2 \Phi_g(\omega) (\omega^2 t_1 + t_3) |H_j|^2$$

$$+ 4 \sum_{j=1}^{n} \omega^4 \Phi_g(\omega) (a_j^2 \omega^2 + A_j') |H_j|^2$$

$$+ 2 \sum_{j=1}^{n} \sum_{k=j+1}^{n} \Phi_g(\omega) X_{jk}(\omega) |H_j|^2 |H_k|^2 \quad (5.19)$$

5.4 FLOOR RESPONSE SPECTRUM

Using the PSDF defined by Eq. 5.19, and employing Eq. 2.15, the floor response spectrum can be obtained as follows:

$$R_a^2(\omega_o, \beta_o) = P_F^2(\omega_o) \left[\int_{-\infty}^{\infty} \left\{ 1 - 4 \sum_{j=1}^{n} \omega^2(\omega^2 t_1 + t_3) |H_j|^2 \right.\right.$$

$$+ 4 \sum_{j=1}^{n} \omega^4 (a_j^2 \omega^2 + A_j') |H_j|^2 + 2 \sum_{j=1}^{n} \sum_{k=j+1}^{n}$$

$$\left.\left. \cdot X_{jk} |H_j|^2 |H_k|^2 \right\} \Phi_g(\omega) (\omega_o^4 + 4 \beta_o^2 \omega_o^2 \omega^2) \right.$$

$$\cdot |H_o|^2 \, d\omega \quad (5.20)$$

in which $P_F(\omega_o)$ is the peak factor by which the root mean square value is amplified to obtain floor response.

Eq. 5.20 defines the floor spectrum value at a frequency, ω_o and damping, β_o. To define the response

spectrum value in terms of ground response spectra, each term under single or double summation is resolved into partial fractions as was done in previous chapters. Once again, the cases with $\omega_j \neq \omega_o$ and $\omega_j = \omega_o$ with $\beta_j = \beta_o$ will be treated separately and referred to as nonresonance and resonance cases respectively.

5.4.1 Floor Spectrum for the Nonresonance Case

The first term in Eq. 5.20 is the same as the term defined by Eq. 4.9 and can be obtained in terms of maximum ground acceleration, relative acceleration and relative velocity spectrum values at oscillator frequencies.

Single Summation Terms

The integrand of the first part of the single summation term in Eq. 5.20 can be resolved into partial fractions as follows:

$$\omega^2 \Phi_g(\omega) (\omega^2 t_1 + t_3) (\omega_o^4 + 4 \beta_o^2 \omega_o^2 \omega^2) |H_j|^2 |H_o|^2$$
$$= \omega^2 \Phi_g(\omega) \omega_o \{(A_1 \omega_o^2 + A_2 \omega^2) |H_j|^2$$
$$+ (A_3 \omega_o^2 + A_4 \omega^2) |H_o|^2\} \qquad (5.21)$$

in which the factors A_1, A_2, etc. are defined in Appendix IV-B, Eq. IV.11. Integrating over the frequency domain and

by virtue of Eqs. 2.25 and 4.11, the above equation can be written as

$$I_s' = \omega_o \{A_1 \omega_o^2 I_2(\omega_j) + A_2 I_3(\omega_j) + A_3 \omega_o^2 I_2(\omega_o) + A_4 I_3(\omega_o)\} \quad (5.22)$$

where I_s' denotes the first part of the single summation term.

Similarly, the integrand of the second part the single summation term can also be split into partial fractions as follows:

$$\omega^4 \Phi_g(\omega) (a_j^2 \omega^2 + A_j') (\omega_o^4 + 4 \beta_o^2 \omega_o^2 \omega^2) |H_j|^2 |H_o|^2 = \omega_o^2 \omega^2 \Phi_g(\omega) \{(B_1 \omega_o^2 + B_2 \omega^2) |H_j|^2 + (B_3 \omega_o^2 + B_4 \omega^2) |H_o|^2\} \quad (5.23)$$

Integrating Eq. 5.23 over its frequency domain and denoting it by I_s'', the following is obtained

$$I_s'' = \omega_o^2 \{B_1 \omega_o^2 I_2(\omega_j) + B_2 I_3(\omega_j) + B_3 \omega_o^2 I_2(\omega_o) + B_4 I_3(\omega_o)\} \quad (5.24)$$

in which $I_2(\omega_j)$ and $I_3(\omega_j)$ are the frequency integrals defined by Eqs. 2.25 and 4.11 respectively and the coefficients B_1, B_2, ..., etc. are defined in Appendix IV-B, Eq. IV.14.

Double Summation Terms

After some algebraic manipulations, the complete double summation term in Eq. 5.20, here denoted by I_{dd}, can be written as follows:

$$I_{dd} = 2 \sum_{j=1}^{n} \sum_{k=j+1}^{n} \int_{-\infty}^{\infty} \omega^4 \, \Phi_g(\omega) \, N(\omega) \, (\omega_o^4 + 4 \, \beta_o^2 \, \omega_o^2 \, \omega^2) \, |H_j|^2 \, |H_k|^2 \, |H_o|^2 \, d\omega \qquad (5.25)$$

where

$$N(\omega) = D_1 \, \omega^6 + (C_1 \, D_1 + D_2 + E_2)\omega^4 + (C_1 \, D_2 + C_2 \, D_1 + E_3)\omega^2 + C_2 \, D_2 \qquad (5.26)$$

in which the coefficients C_1, C_2, D_1, D_2, ..., etc. are defined in Appendix IV-B, Eq. IV.22.

Resolving a part of the integrand of Eq. 5.25 into partial fractions and denoting it by I_d', the following is obtained

$$I_d' = \int_{-\infty}^{\infty} \omega^4 \, \Phi_g(\omega) \, (\omega_o^4 + 4 \, \beta_o^2 \, \omega_o^2 \, \omega^2) \, |H_o|^2 \cdot \{(F_1 \, \omega_o^4 + F_2 \, \omega_o^2 \, \omega^2) \, |H_j|^2 + (F_3 \, \omega_o^4 + F_4 \, \omega_o^2 \, \omega^2) \, |H_k|^2\} d\omega \qquad (5.27)$$

where F_1, F_2, ..., etc. are the coefficients of partial fractions as defined in Appendix IV-B, Eq. IV.19.

For nonresonance case when $\omega_j \neq \omega_o$ and $\omega_k \neq \omega_o$, the integrand of Eq. 5.27 can be further split into partial fractions as

$$I_d' = \int_{-\infty}^{\infty} \omega^2 \, \Phi_g(\omega) \, [(A_j \, \omega_o^4 + B_j \, \omega_o^2 \, \omega^2) \, |H_j|^2 + (C_j \, \omega_o^4 + D_j \, \omega_o^2 \, \omega^2) \, |H_o|^2 + (A_k \, \omega_o^4 + B_k \, \omega_o^2 \, \omega^2) \, |H_k|^2 + (C_k \, \omega_o^4 + D_k \, \omega_o^2 \, \omega^2) \, |H_o|^2] d\omega \tag{5.28}$$

in which factors A_j, B_j, A_k, B_k, ..., etc. are defined by Eq. IV.16 in Appendix IV-B. Using Eqs. 2.25 and 4.11, Eq. 5.28 can be written as

$$I_d = \omega_o^2 \{A_j \, \omega_o^2 \, I_2(\omega_j) + B_j \, I_3(\omega_j) + C_j \, \omega_o^2 \, I_2(\omega_o) + D_j \, I_3(\omega_o) + A_k \, \omega_o^2 \, I_2(\omega_k) + B_k \, I_3(\omega_k) + C_k \, \omega_o^2 \, I_2(\omega_o) + D_k \, I_3(\omega_o) \tag{5.29}$$

By substituting Eqs. 4.9, 5.22, 5.24 and 5.29 in Eq. 5.20, the response spectrum value at oscillator frequency ω_o and damping β_o can be obtained from the following equation

$$R_a^2(\omega_o, \beta_o) = P_F^2(\omega_o) \left[I_g - I_3(\omega_o) + 2\ \omega_o^2\ I_2(\omega_o) \right.$$

$$- 4\ \omega_o \sum_{j=1}^{n} \{A_1\ \omega_o^2\ I_2(\omega_j) + A_2\ I_3(\omega_j)$$

$$+ A_3\ \omega_o^2\ I_2(\omega_o) + A_4\ I_3(\omega_o)\} + 4\ \omega_o^2 \sum_{j=1}^{n} \{B_1\ \omega_o^2$$

$$\cdot\ I_2(\omega_j) + B_2\ I_3(\omega_j) + B_3\ \omega_o^2\ I_2(\omega_o)$$

$$+ B_4\ I_3(\omega_o)\} + 2\ \omega_o^2 \sum_{j=1}^{n} \sum_{k=j+1}^{n} \{A_j\ \omega_o^2\ I_2(\omega_j)$$

$$+ B_j\ I_3(\omega_j) + A_k\ \omega_o^2\ I_2(\omega_k) + B_k\ I_3(\omega_k)$$

$$\left. + (C_j + C_k)\ \omega_o^2\ I_2(\omega_o) + (D_j + D_k)\ I_3(\omega_o)\} \right] \quad (5.30)$$

where I_g is the variance of maximum ground acceleration as defined by Eq. 4.8.

The integrals $I_2(\omega_j)$ and $I_3(\omega_j)$ can be substituted in terms of response spectrum value and peak factors as done in previous chapters. This allows the incorporation of peak factors in the generation of floor spectra. However, if it is assumed that all peak factors are the same, Eq. 5.30 can be written in terms of ground response spectrum as:

$$R_a^2(\omega_o,\beta_o) = A_g^2 - R_r^2(\omega_o) + 2\ \omega_o^2\ R_v^2(\omega_o)$$

$$- 4\ \omega_o \sum_{j=1}^{n} \{A_1\ \omega_o^2\ R_v^2(\omega_j) + A_2\ R_r^2(\omega_j)$$

$$+ A_3\ \omega_o^2\ R_v^2(\omega_o) + A_4\ R_r^2(\omega_o)\} + 4\ \omega_o^2 \sum_{j=1}^{n}$$

$$\cdot \{B_1\ \omega_o^2\ R_v^2(\omega_j) + B_2\ R_r^2(\omega_j) + B_3\ \omega_o^2\ R_v^2(\omega_o)$$

$$+ B_4\ R_r^2(\omega_o)\} + 2\ \omega_o^2 \sum_{j=1}^{n} \sum_{k=j+1}^{n} \{A_j\ \omega_o^2\ R_v^2(\omega_j)$$

$$+ B_j\ R_r^2(\omega_j) + A_k\ \omega_o^2\ R_v^2(\omega_k) + B_k\ R_r^2(\omega_k)$$

$$+ (C_j + C_k)\ \omega_o^2\ R_v^2(\omega_o) + (D_j + D_k)\ R_r^2(\omega_o)\} \quad (5.31)$$

Eq. 5.31 defines the floor response spectrum independent of peak factors. This expression has been used to obtain numerical results for the same nonproportionally damped structural systems.

5.4.2 Floor Spectrum Value for the Resonance Case

In the special resonance case when $\omega_j = \omega_o$ and $\beta_j = \beta_o$ the coefficients of partial fractions A_1, B_1, A_2, etc. are undefined. In such a situation, the single and double summation terms in Eq. 5.20 can be treated in the same way as was done in the previous chapters.

Single Summation Terms

A term with $\omega_j = \omega_o$ and $\beta_j = \beta_o$, of the first single summation term, in Eq. 5.20 denoted as I_{s1}, can be written as

$$I_{s1} = \int_{-\infty}^{\infty} \Phi_g(\omega)\ \omega^2(\omega^2\ t_1 + t_3) \cdot (\omega_o^4 + 4\ \beta_o^2\ \omega_o^2\ \omega^2)\ |H_o|^4\ d\omega \qquad (5.32)$$

which because of peakedness of $|H_o|^4$ can be approximated as [52]

$$I_{s1} \simeq \Phi_g(\omega_o) \int_{-\omega_c}^{\omega_c} \omega^2\ (\omega^2\ t_1 + t_3)\ (\omega_o^4 + 4\ \beta_o^2\ \omega_o^2\ \omega^2)\ |H_o|^4\ d\omega - \frac{2}{3}\ t_3\ \Phi_g(\omega_o)/\omega_o + t_3/\omega_o^4 \int_{-\omega_o}^{\omega_o} \omega^2\ \Phi_g(\omega)\ d\omega \qquad (5.33)$$

The second integral in Eq. 5.33 is very small so it is neglected. The first integral is of the same form as integral in Eq. I.22 in Appendix I-C. Thus, Eq. 5.33 may be written as

$$I_{s1} = \Phi_g(\omega_o)\ \omega_c\ \{A_m - 2\ t_3/3\ \omega_o\ \omega_c\} \qquad (5.34)$$

in which A_m is defined in Appendix IV-C, Eq. IV.23. Using Eq. 4.28 and 2.24 and after some algebraic manipulations the following is obtained

$$I_{s1} = \frac{\omega_o^2 \, R_v^2(\omega_o)}{V_m} \left\{ A_m - \frac{2 \, t_3}{2 \, \omega_o \, \omega_c} \right\} \tag{5.35a}$$

or

$$I_{s1} = A_m' \, R_v^2(\omega_o) \tag{5.35b}$$

in which A_m' is defined as

$$A_m' = \frac{\omega_o^2}{V_m} \left\{ A_m - \frac{2 \, t_3}{2 \, \omega_o \, \omega_c} \right\} \tag{5.36}$$

A typical term with $\omega_j = \omega_o$ and $\beta_j = \beta_o$ of the second single summation in Eq. 5.20 at resonance, denoted as I_{s2}, can be written as

$$I_{s2} = \int_{-\omega_c}^{\omega_c} \omega^4 \, \Phi_g(\omega) \, (a_j^2 \, \omega^2 + A_j') \cdot (\omega_o^4 + 4 \, \beta_o^2 \, \omega_o^2 \, \omega^2) \, |H_o|^2 \, d\omega \tag{5.37}$$

which can be written as

$$I_{s2} = 4\, a_j^2\, \beta_o^2\, \omega_o^2 \int_{-\omega_c}^{\omega_c} \Phi_g(\omega)\, d\omega$$

$$+ \omega_o^2 \int_{-\omega_c}^{\omega_c} \Phi_g(\omega)\, N_1(\omega)\, |H_o|^4\, d\omega \qquad (5.38)$$

where

$$N_1(\omega) = b_o\, \omega_o^2\, \omega^6 + b_1\, \omega_o^4\, \omega^4 + b_2\, \omega_o^6\, \omega^2 + b_3\, \omega_o^8 \qquad (5.39)$$

in which the constants b_o, b_1, b_2, and b_3 are defined in Eq. IV.24 in Appendix IV-C. Since function H_o^4 is highly peaked, the second integral can be approximated as

$$I_{s2} = 4\, a_j^2\, \beta_o^2\, \omega_o^2 \int_{-\omega_c}^{\omega_c} \Phi_g(\omega)\, d\omega + \omega_o^2 \left\{ \Phi_g(\omega_o) \right.$$

$$\cdot \int_{-\omega_c}^{\omega_c} N_1(\omega)\, |H_o|^4\, d\omega - 2\, b_3\, \Phi_g(\omega_o)\, \omega_o$$

$$+ b_3 \int_{-\omega_o}^{\omega_o} \Phi_g(\omega)\, d\omega \qquad (5.40)$$

In Eq. 5.40 1st and 3rd integrals cancel each other. The 2nd integral is of the same form as in Eq. I.22 in Appendix I-C. Eq. 5.40 can then be written as

$$I_{s2} = \omega_o^2\, \Phi_g(\omega_o)\, \omega_c \{B_m - 2\, b_3\, r\} \qquad (5.41)$$

in which B_m is defined in Appendix IV-C, Eq. IV.25. Using Eqs. 4.28 and 2.24 to substitute for $\Phi_g(\omega_o) \cdot \omega_c$ in Eq. 5.41,

the following is obtained

$$I_s'' = B_m' \cdot R_v^2(\omega_o) \tag{5.42}$$

in which B is defined as

$$B_m' = \frac{\omega_o^4}{V_m} \{B_m - 2\, b_3\, r\} \tag{5.43}$$

Double Summation Terms

A typical double summation term in Eq. 5.20 is first split into two terms as shown in Eq. 5.27. With $\omega_j = \omega_o$ and $\beta_j = \beta_o$, the first set of terms, denoted by I_d', can be written as

$$I_d' = \int_{-\omega_c}^{\omega_c} \omega^4\, \Phi_g(\omega)\, (F_1\, \omega_o^4 + F_2\, \omega_o^2\, \omega^2) \cdot (\omega_o^4 + 4\, \beta_o^2\, \omega_o^2\, \omega^2)\, |H_o|^4\, d\omega \tag{5.44}$$

which can be rewritten as

$$I_d' = 4\, \beta_o^2\, F_2 \int_{-\omega_c}^{\omega_c} \Phi_g(\omega)\, d\omega + \int_{-\omega_c}^{\omega_c} \Phi_g(\omega)\, N_2(\omega)\, |H_o|^4\, d\omega \tag{5.45}$$

where

$$N_2(\omega) = C_o\, \omega_o^2\, \omega^6 + C_1\, \omega_o^4\, \omega^4 + C_2\, \omega_o^6\, \omega^2 + C_3\, \omega_o^8 \tag{5.46}$$

in which the coefficients C_o, C_1, C_2, and C_3 are defined in Appendix III-C, Eq. IV.28.

Since the function $|H_o|^4$ is highly peaked, Eq. 5.45 can be approximated as

$$I_d' \simeq 4\,\beta_o^2\,F_2 \int_{-\omega_c}^{\omega_c} \Phi_g(\omega)\,d\omega + \Phi_g(\omega_o) \int_{-\omega_c}^{\omega_c} N_2(\omega) \cdot |H_o|^4\,d\omega - 2\,\Phi_g(\omega_o)\cdot C_3\,\omega_o + C_3 \int_{-\omega_o}^{\omega_o} \Phi_g(\omega)\,d\omega \tag{5.47}$$

In Eq. 5.47, the 1st and 3rd integrals are small and they cancel each other. The 2nd integral is of the same form as the integral in Appendix I-C, Eq. I.22. Thus, Eq. 5.47 can be written as

$$I_d' = \Phi_g(\omega_o)\,\omega_c\,\{C_m - 2\,r\,C_3\} \tag{5.48}$$

in which C_m is defined in Appendix IV-C, Eq. IV.27. Using Eq. 4.29, Eq. 5.48 can be written as

$$I_d' = C_m'\,R_v^2(\omega_o) \tag{5.49}$$

where C_m' is defined as follows:

$$C_m' = \frac{\omega_o^2}{V_m}\,\{C_m - 2\,r\,C_3\} \tag{5.50}$$

Thus using Eqs. 4.9, 5.35, 5.42, and 5.49 in Eq. 5.20, the floor response spectrum value at resonance can be obtained as follows:

$$R_a^2(\omega_o,\beta_o) = P_F^2(\omega_o) \Big[I_g - I_3(\omega_o) + 2\ \omega_o^2\ I_2(\omega_o) - 4\ \omega_o \sum_{j=1}^{n} I_{s1} + 4\ \omega_o^2 \sum_{j=1}^{n} I_{s2} + 2\ \omega_o^2 \sum_{j=1}^{n} \sum_{k=j+1}^{n} \{I_d' + A_k\ \omega_o^2\ I_2(\omega_k) + B_k\ I_3(\omega_k) + C_k\ \omega_o^2\ I_2(\omega_o) + D_k\ I_3(\omega_o)\} \Big] \qquad (5.51)$$

In Eq. 5.51 the frequency integrals I_g, $I_2(\omega_j)$ and $I_3(\omega_j)$ can be substituted in terms of ground response spectrum values and their associated peak factors. An expression independent of peak factors, however, can be obtained by assuming all the peak factors to be equal. This expression can be written as follows:

$$R_a^2(\omega_o,\beta_o) = A_g^2 - R_r^2(\omega_o) + 2\ \omega_o^2\ R_v^2(\omega_o) - 4\ \omega_o \sum_{j=1}^{n} I_{s1} + 4\ \omega_o^2 \sum_{j=1}^{n} I_{s2} + 2\ \omega_o^2 \sum_{j=1}^{n} \sum_{k=j+1}^{n} \{I_d' + A_k\ \omega_o^2\ R_v^2(\omega_k) + B_k\ R_r^2(\omega_k) + C_k\ \omega_o^2\ R_v^2(\omega_o) + D_k\ R_r^2(\omega_o)\}] \qquad (5.52)$$

5.5 NUMERICAL RESULTS

As discussed in Sec. 4.6, the mode acceleration approach developed here, both for classically and nonclassically damped systems, are mathematically consistent and equivalent. In addition, they, in general, have some specific advantages over the mode displacement approach especially for the systems and responses which have dominant effect from the high frequency modes. The results substantiating these claims for the approach developed in this chapter for nonclassically damped systems are presented in this section.

First to cross check the analytical correctness of the formulations, as well as the computer code written to obtain the numerical results, mean square floor spectra were obtained for a proportionally damped system by the four approaches presented in Chapters 2 to 5. The seismic input was defined by the PSDF of Eq. 2.105. When the complete set of modes were used in the analyses, exactly the same results were obtained by all the four approaches. This cross-checked the formulations in Chapters 2 to 5 with each other.

To show the effectiveness of the mode acceleration approach in giving accurate results even with a first few

modes, the mean square values of the floor spectral response were obtained for a 15 D.O.F. structural system shown in Fig. 3.1. The mass and stiffness properties were adjusted such that the natural frequencies were on the high side. The damping values in X- and Y-directions were adjusted to create a nonproportionally damped system. The dynamic properties of the undamped structure e.g. natural frequencies, participation factors and modal damping values as defined by Eq. 3.25 are given in Table 5.1. The seismic input was defined by the PSDF of Eq. 2.105 with a cut-off frequency of 30 cps.

Table 5.2 shows the numerical results for floors 1, 3 and 5. Floor 1 is lowest and 5 the roof top floor. The mean square floor response spectrum values obtained by considering all 15 modes in the analyses are given in columns (2), (5) and (8) for various floors. In other columns the response values obtained by mode displacement and mode acceleration approaches with only 3 modes used in the analysis are shown in terms of their ratios to the values obtained with exact mean square value (with all 15 modes). Hence, the closeness of the ratio to 1 means a more accurate result.

It is seen that the results obtained by mode displacement approach are grossly underestimated for the lower

floors and rather overestimated for the higher floors. As the lower floors are affected by the high frequency modes, the omission of these modes in mode displacement approach introduces unacceptable errors in the calculated response. It is also seen from Table 5.2 that the results obtained by mode acceleration approach, on the other hand, are consistently accurate for all the floors.

Table 5.3 shows similar results, but for the floor spectrum values (rather than the mean square values as in Table 5.2) for the input defined by the average spectra of 30-sec. time history set. Again, the same conclusions, as in the preceding paragraph, are drawn from these results.

In the development of the approach presented in this chapter, assumptions like stationarity of input and response have been made. Therefore numerical verification of the approach by simulation study is essential. For this, the floor spectra results obtained by the time history analysis for the 30-sec. time history set are compared with the results obtained by the direct approach presented here. For a proper comparison, the time history results were also obtained by the mode acceleration approach. Hence, Eq. 3.8 was solved using Eq. 3.11 to obtain $z_j(t)$ which in turn was used to obtain the floor acceleration time history, $\ddot{X}_a(t)$, from Eq. 5.3. This time history was used as an

input to the oscillator, Eq. 2.5, to obtain the floor spectrum value. The floor spectrum values obtained for the time history ensemble were statistically processed to obtain mean and mean + one standard deviation spectra for the 5 floors of the 15-D.O.F. structure used in Chapter 3.

Mean floor spectrum curves are compared in Figs. 5.1 - 5.8 and mean + one standard deviation curves in Figs. 5.9 - 5.12. It is seen that the results obtained by the direct approach compare very well with the time history results, thus validating Eqs. 5.31 and 5.52 in spite of the simplifying assumptions made in their development.

5.6 SUMMARY AND CONCLUSIONS

In this chapter, a direct mode acceleration approach is developed for generation of floor spectra for non-classically damped structural systems. The approach has similar attributes and advantages as the mode acceleration approach for classically damped system (Chapter 4). That is, with only a first few modes used in the analysis, this approach can be very effectively used to obtain accurate floor spectra for nonclassically damped stiff structural system and for floor close to base, where the higher modes have significant effect. For other cases also, i.e. where

high frequency modes are not necessarily dominant, this approach can be used with computational advantage. Numerical results substantiating these claims have been presented in this chapter.

Chapter 6

SUMMARY AND CONCLUSIONS

Several direct approaches for generation of floor spectra for classically and nonclassically damped structural systems are described in this thesis. Specifically, the mode displacement approaches which require pseudo-acceleration and relative velocity spectra as their seismic inputs are described in Chapters 2 and 3 for classically and nonclassically damped systems, respectively. The mode acceleration approaches, requiring relative acceleration and relative velocity spectra, are developed in Chapters 4 and 5 for the two types of structural systems. Since, several simplifying assumptions are made in the development of these direct approaches, a detailed numerical simulation study has been conducted to validate the proposed methodologies. In this simulation study, extensive numerical results covering a wide range of parameters, such as different structural systems, different floors of a structure, time histories of different durations, range of oscillator damping values, etc., have been obtained. Specific conclusions pertaining to an approach are given at the end of each chapter. Here, however, overall conclusions drawn from this study are given.

In general, the floor spectra results obtained by various direct approaches and time history ensemble analyses which are presented throughout this thesis, compare very well with each other. This corroboration validates the proposed approaches for their use in practice. In some cases, improvements in the results can be made by inclusion of unequal peak factors of the oscillators on ground and floor in the formulation if the frequency characteristic of the design input motion in terms of power spectral density function is known. However, if the right spectral density function is not known, the approximation of the frequency content distribution by the simple-to-use white noise spectral density function may not necessarily give correct results. Thus, such approximations should be avoided. In general, however, it has been observed from the results obtained in the study that the peak factor correction are not essential. That is, the formulation independent of peak factors will also provide very reasonable results of floor response spectra.

The mode acceleration approaches have been proposed as better alternatives to the mode displacement approaches, as the former consistently provide more accurate results than the latter with just a few modes used in the analysis. Especially, for generation of floor spectra of stiff

structural systems and for floors close to base where the higher frequency modes contribute significantly to the response, the use of the mode acceleration approach is strongly recommended. The only drawback associated with the use of the mode acceleration approach is that it requires relative acceleration spectra as input. Such spectra are not commonly used in practice currently. The pseudo-acceleration spectra are more widely used in practice and well accepted methods [9,34,35,36,39,43] to develop these for design purposes are also available to the profession. However, similar methods can also be developed to establish relative acceleration spectra for design. More research, involving several recorded earthquake accelerograms is required for this purpose. In this work, these relative spectra were developed for the synthetically generated ensembles of time histories for their use in this study.

REFERENCES

1. Ang, A. H-S. and Tang, W. H., "Probability Concepts in Engineering Planning and Design", Vol. I, John Wiley & Sons, Inc., New York, NY, 1975.

2. Atalik, T. S., "On Upperbound Instructure Response Spectra", Proceedings of SMiRT-5 Conference, Berlin, August 1979, paper K9/3.

3. Ayres, J. R., Sun Tseng-Yao and Brown, F. F., "Report on Damage to Building Mechanical Systems Due to the March 27, 1964, Alaska Earthquake", prepared for U.S. Army Engineer District-Anchorage, Alaska and Committee on the Alaska Earthquake Engineering Panel, National Academy of Sciences.

4. Benjamin, J. R. and Cornell, C. A., "Probability, Statistics and Decision for Civil Engineers", McGraw-Hill, Inc., New York, NY, 1970.

5. Biggs, J. M. and Rosset, J. M., "Seismic Analysis of Equipment Mounted on a Massive Structure", in Seismic Design for Nuclear Power Plants, edited by R.J. Hansen, MIT Press, Cambridge, Mass., 1970.

6. Biggs, J. M., "Seismic Response Spectra for Equipment Design in Nuclear Power Plants", Proceedings of SMiRT-1 Conference, Berlin, September 1971, paper K4/7.

7. Blume, J. A., Sharpe, R. L. and Dalal, J., "Recommendations for Shape of Earthquake Response Spectra", report prepared for the Directorate of Licensing, United States Atomic Energy Commission, Feb. 1973.

8. Caughey, T. K., "Classical Normal Modes in Damped Linear Dynamic Systems", Journal of Applied Mechanics, Vol. 27, June 1960, pp. 269-271.

9. Chakravorty, M. K. and Vanmarcke, E. H., "Probabilistic Seismic Analysis of Light Equipment within Buildings", Proceedings of 5th World Conference on Earthquake Engineering, Vol. II, Rome, Italy, 1973.

10. Clough, R. W. and Mojtahedi, S., "Earthquake Response Analysis Considering Non-Proportional Damping", Journal of Earthquake Engineering and Structural Dynamics, Vol. 4, 1976, pp. 489-496.

11. Clough, R. W. and Penzien, J., "Dynamics of Structures", McGraw Hill, Inc., New York, NY, 1975.

12. Collings, J. D. and Thomson, W. T., "The Eigenvalue Problem for Structural Systems with Statistical Properties", AIAA Journal, Vol. 7, No. 4, April 1969, pp. 642-648.

13. Crandall, S. H. and Mark, W. D., "Random Vibration in Mechanical Systems", Academic Press, Inc., New York, 1963.

14. Der Kiureghian, A., Sackman, J. L. and Nour-Omid, B., "Dynamic Response of Light Equipment in Structures", Report No. UCB/EERC-81/05, University of California, Berkeley, April 1981.

15. Foss, K. A., "Co-ordinates which Uncouple the Equations of Motion of Damped Linear Dynamic Systems", Journal of Applied Mechanics, Vol. 25, Spet. 1958, pp. 361-364.

16. Fox, R. L. and Kapoor, M. P., "Rates of Change of Eigenvalues and Eigenvectors", AIAA Journal, Vol. 6, No. 12, December 1968.

17. Gasparini, D., and Vanmarcke, E. H., "Simulated Earthquake Motions Compatible with Prescribed Response Spectra", Pub. No. R76-4, Dept. of Civil Eng., M.I.T., Jan. 1975.

18. Hadjian, A. H., "Probabilistic Frequency Variation of Concrete Structures", Proceedings of SMiRT-2 Conference, Berlin, September 1973.

19. Hou, S., Earthquake Simulation Models and Their Applications, Ph. D. Thesis, M.I.T., Dept. of Civil Eng., Res. Rep. R 68-17, 1968.

20. Housner, G., "Design Spectrum", Chapter 5, Earthquake Engineering, Ed. R. L. Weigel, Prentice Hall, Inc., Englewood Cliffs, NJ, 1970.

21. Hurty, W. C. and Rubinstein, M. F., "Dynamics of Structures", Prentice Hall, Inc., Englewood Cliffs, NJ, 1964.

22. "International Mathematics and Statistics Library", IMSL Library, IMSL LIB 0007, IMSL Inc., 1979.

23. Kapur, K. K. and Shao, L. C., "Generation of Seismic Floor Response Spectra for Equipment Design", Proceedings of Speciality Conference on Structural Design of Nuclear Power Plant Facilities, Chicago, IL., December 1973.

24. Kelly, J. M. and Sackman, J. L., "Response Spectra Design Methods for Tuned Equipment-Structure Systems", Journal of Sound and Vibration, Vol. 59, No. 2, pp. 171-179, 1978.

25. Kelly, J. M. and Sackman, J. L., "Conservation in Summation Rules for Closely Spaced Modes", Earthquake Engineering and Structural Dynamics, Vol. 8, pp. 63-74, 1980.

26. Lin, Y. K., "Probabilistic Theory of Structural Dynamics", McGraw Hill, Inc., New York, 1967.

27. Liu, L. K., Child, C. G. and Nowotny, B., "Effect of Parameter Variations on Floor Spectra", ASCE Proceedings, Structural Division of Nuclear Plant Facilities, Vol. II, Chicago, IL., Dec. 1973, p. 435.

28. Liu, S. C., "Earthquake Protection of Communication Facilities", Proceedings of 6th World Conference on Earthquake Engineering, New Delhi, India, Jan., 1977.

29. Meirovitch, L., "Computational Methods in Structural Dynamics", Sijthoff & Noordoff, The Netherlands, 1980.

30. Newmark, N. M., "Earthquake Response Analysis of Reactor Structures", Proceedings of SMiRT-1 Conference, Berlin, September 1971.

31. Newmark, N. M. and Hall, W. J., "Seismic Design Criteria for Nuclear Reactor Facilities", Proceedings of 4th World Conference on Earthquake Engineering, Santiago, Chile, 1969.

32. Newmark, N. M., Blume, J. A. and Kapur, K. K., "Seismic Design Spectra for Nuclear Power Plants", ASCE Journal of Power Division, Vol. 99, Nov. 1973.

33. Penzien, J. and Chopra, A. K., "Earthquake Response of Appendage on Multi-story Building", Proceedings of 3rd World Conference on Earthquake Engineering, Vol. II, New Zealand, 1965.

34. Peters, K. A., Schmitz, D. and Wagner, U., "Determination of Floor Response Spectra on the Basis of Response Spectrum Method", Nuclear Engineering and Design, Vol. 44, 1977, pp. 255-262.

35. Sackman, J. L. and Kelly, J. M., "Equipment Response Spectra for Nuclear Power Plant Systems", Proceedings of SMiRT-5 Conference, Berlin, August 1979, paper K9/1.

36. Scanlan, R. H. and Sachs, K., "Development of Compatible Secondary Spectra Without Time Histories", Proceedings of SMiRT-4 Conference, San Francisco, CA., August 1977, paper K4/13.

37. Scanlan, R. H. and Sachs, K., "Floor Response Spectra for Multi-Degree-of-Freedom Systems by Fourier Transforms", Proceedings of SMiRT-3 Conference, London, September 1975, paper K5/5.

38. Schmidt, D. and Peters, K., "Direct Evaluation of Floor Response Spectra from a Given Ground Response Spectrum", Proceedings of SMiRT-4 Conference, San Francisco, CA., August 1977, paper K4/10.

39. Singh, M. P., "Generation of Seismic Floor Spectra", ASCE Journal of the Engineering Mechanics Division, Vol. 101, No. EM5, Proc. paper 11651, Oct. 1975, pp. 593-607.

40. Singh, M. P. and Chu, S. L., "Stochastic Considerations in Seismic Analysis of Structures", Journal of Earthquake Engineering and Structural Dyanmics, Vol. 4, 1976, pp. 295-307.

41. Singh, M. P. and Wen, Y. K., "Nonstationary Seismic Response of Light Equipment", ASCE Journal of Engineering Mechanics Division, No. EM6, Dec. 1977.

42. Singh, M. P., Singh, S. and Ang, A. H-S., "Extended Applications of Response Spectra Curves in Seismic Design of Structures", Proceedings of 6th World Conference on Earthquake Engineering, New Delhi, India, Jan. 1977.

43. Singh, M. P., "Seismic Design Input for Secondary Systems", ASCE Journal of the Structural Division, Vol. 106, No. ST2, Proc. paper 15207, February 1980, pp. 505-517.

44. Singh, M. P., "Peak Seismic Response Characteristics of Secondary Systems", Proceedings of 7th World Conference on Earthquake Engineering, Istanbul, Turkey, September 1980.

45. Singh, M. P., "Seismic Response of Structures with Random Parameters", Proceedings of 7th World Conference on Earthquake Engineering, Istanbul, Turkey, Sept. 1980.

46. Singh, M. P., "Seismic Response by SRSS for Nonproportional Damping", Journal of the Engineering Mechanics Division, ASCE, Vol. 106, No. EM6, Proc. paper 15948, December 1980, pp. 1405-1419.

47. Singh, M. P. and Ashtiany, M. G., "Seismic Stability Evaluation of Earth Structures", College of Engineering, Virginia Polytechnic Institute and State University, Report No. VPI-E-80.30, Nov. 1980.

48. Singh, M. P., "Seismic Response Combination of High Frequency Modes", Proceedings of 7th European Conference on Earthquake Engineering, Athens, Greece, Sept. 1982.

49. Suzaki, K., "Analysis of Uncertainty in Seismic Response of Secondary Appendage System", Proceedings of SMiRT-4 Conference, San Francisco, CA, August 1977, paper K6/2.

50. Tsai, N. C., "Spectrum-Compatible Motions for Design Purpose", Journal of Engineering Mechanics Division, ASCE, EM2, April 1972.

51. U. S. Nuclear Regulatory Commission, "Design Response Spectra for Nuclear Power Plants", Nuclear Regulatory Guide No. 1.60, Washington, D.C., 1975.

52. Vanmarcke, E. H., "Seismic Structural Response", Chapter 8 in Seismic Risk and Engineering Decisions, Ed. C. Lomnitz and E. Rosenblueth, Elsevier Scientific Publishing Co., New York, 1976.

53. Vanmarcke, E. H., "A Simple Procedure for Predicting Amplified Response Spectra and Equipment Response", Proceedings of 6th World Conference on Earthquake Engineering, New Delhi, India, January 1977.

54. Villaverde, R. and Newmark, N. M., "Seismic Response of Light Attachments to Buildings", Structural Research Series No. 469, UILU-ENG 80-2006, Dept. of Civil Engineering, University of Illinois, Urbana, IL, February 1980.

Table 2.1 Parameters of Spectral Density Function, $\Phi_g(\omega)$, Eq. 2.105

j	S_j ft^2-sec/rad	ω_j rad/sec.	β_j
1	0.0015	13.5	0.3925
2	0.000495	23.5	0.3600
3	0.000375	39.0	0.3350

Table 2.2 Dynamic Properties of 11-FRQ Structure

Mode No.	Frequency Cps	Modal Damping	Participation Factor
1	3.6659	0.0500	-10.2168
2	4.5203	0.0500	0.7984
3	5.6356	0.0500	-59.6307
4	6.2336	0.0500	-7.4238
5	7.2047	0.0500	4.3600
6	11.8574	0.0500	16.7521
7	12.0161	0.0500	48.9363
8	13.1243	0.0500	6.4819
9	13.5679	0.0500	-19.0773
10	14.7744	0.0500	-29.3388
11	16.4835	0.0500	-7.9668

Displacement Mode Shapes for Floor No. 3-X

-.267 E-3	.555 E-4	-.366 E-2	.374 E-3	.396 E-3	.431 E-2
.103 E-1	.181 E-2	-.774 E-2	-.628 E-2	-.811 E-3	

Displacement Mode Shapes for Floor No. 6-X

-.213 E-2	.260 E-3	-.223 E-1	-.305 E-2	.124 E-2	-.305 E-2
-.212 E-2	-.130 E-2	.990 E-2	.364 E-3	.600 E-2	

Table 2.3 Dynamic Properties of 10-Story Structure

Mode No.	Frequency Cps	Modal Damping	Participation Factor
1	1.0638	0.050	318.9844
2	3.1676	0.050	-104.7328
3	5.2007	0.050	60.9079
4	7.1176	0.050	41.4039
5	8.8755	0.050	29.9754
6	10.4352	0.050	22.1802
7	11.7617	0.050	16.2979
8	12.8255	0.050	11.5118
9	13.6028	0.050	7.3736
10	14.0763	0.050	3.6030

Displacement Mode Shapes for Floor No. 4-X

.224 E-2 -.388 E-2 .593 E-3 -.345 E-2 -.311 E-2 .117 E-2
.397 E-2 .172 E-2 -.270 E-2 -.370 E-2

Displacement Mode Shapes for Floor No. 6-X

.311 E-2 -.172 E-2 -.388 E-2 .142 E-17 .388 E-2 -.172 E-2
-.311 E-2 .311 E-2 .172 E-2 -.388 E-2

Displacement Mode Shapes for Floor No. 10-X

.397 E-2 .388 E-2 .370 E-2 -.345 E-2 .311 E-2 -.270 E-2
.224 E-2 -.172 E-2 .117 E-2 -.593 E-3

Table 3.1 Dynamic Properties of a 15-D.O.F. Structure Used in Simulation Study

Mode No.	Frequency Cps	Modal Damping	Participation Factor
1	3.0043	0.0289	-1.4180
2	3.0044	0.0289	1.4180
3	5.9020	0.0214	-0.0103
4	7.5637	0.0918	-0.5506
5	7.5640	0.0918	-0.5507
6	11.7745	0.1427	-0.3211
7	11.7755	0.1427	-0.3211
8	13.0685	0.0711	-0.0029
9	15.6633	0.1599	0.2273
10	15.6640	0.1599	-0.2273
11	19.9848	0.1717	-0.1769
12	19.9854	0.1717	0.1769
13	21.0994	0.0798	0.0012
14	30.9933	0.0776	0.0009
15	44.5844	0.0731	-0.0007

Table 3.2 Response Spectrum Value Obtained for Various Floors of 15-degree-of-freedom Non-proportionally Damped Structure by Normal Mode and Complex Mode Approaches Using PSDF (Eq. 2.105) as Input (Oscillator Damping = 1%, e/r = 0.01)

	Floor 1		Floor 3		Floor 5	
Oscillator Period sec.	Spectrum Value[1] ft/sec^2	Ratio[2]	Spectrum Value[1] ft/sec^2	Ratio[2]	Spectrum Value[1] ft/sec^2	Ratio[2]
.02	.67	1.09	1.31	1.23	2.10	1.25
.04	.69	1.09	1.31	1.23	2.12	1.25
.08	1.41	1.08	1.64	1.18	2.28	1.26
.10	2.35	1.03	2.12	1.15	2.60	1.25
.15	3.93	1.11	3.17	1.21	5.32	1.24
.20	2.86	1.01	2.08	1.18	5.45	1.11
.34	9.03	1.38	26.31	1.45	42.77	1.46
.40	5.34	1.01	9.93	1.04	14.06	1.05
1.00	1.85	1.00	1.99	1.00	2.10	1.00

[1]Value obtained using complex mode approach

[2]Ratio of values obtained by normal mode approach to complex mode approach

Table 3.3 Response Spectrum Values Obtained for Various Floors of a 15-degrees-of-freedom Non-proportionally Damped Structure by Normal Mode and Complex Mode Approaches Using Ground Spectra as Seismic Input (Oscillator Damping = 1%, e/r = 0.01)

Oscillator Period sec.	Floor 1		Floor 3		Floor 5	
	Spectrum Value[1] g-units	Ratio[2]	Spectrum Value[1] g-units	Ratio[2]	Spectrum Value[1] g-units	Ratio[2]
.020	.13	1.07	.24	1.19	.38	1.20
.040	.16	1.08	.24	1.19	.39	1.20
.080	.30	1.17	.32	1.13	.42	1.23
.085*	.30	1.18	.34	1.14	.44	1.23
.132*	.31	1.24	.42	1.41	.96	1.43
.200	.47	1.01	.38	1.15	.93	1.09
.340	1.36	1.37	3.85	1.45	6.23	1.47
.400	.77	1.02	1.41	1.05	2.00	1.06
1.000	.20	1.00	.22	1.00	.23	1.00

*Structural period

[1]Value obtained by complex mode approach

[2]Ratio of values obtained by normal mode to complex mode approach

Table 4.1 Dynamic Properties of 30-D.O.F. Structure (First 10 Modes)

Mode No.	Frequency Cps	Modal Damping	Participation Factor
1	12.3495	0.0500	1.9621
2	12.3612	0.0500	1.9632
3	23.0685	0.0500	-0.0815
4	30.8771	0.0500	-0.7656
5	30.9180	0.0500	-0.7695
6	44.6019	0.0500	0.1479
7	48.1747	0.0500	0.4763
8	48.3239	0.0500	-0.4554
9	65.5549	0.0500	-0.3544
10	65.7332	0.0500	0.3548

Table 4.2 Response Spectrum Value Obtained for Various Floors of a 30-D.O.F. Structure by Mode Displacement and Mode Acceleration Approaches with Only First 4 Modes (Oscillator Damping 2%)

	Floor 1			Floor 2			Floor 5			Floor 8			Floor 10		
		Ratio			Ratio			Ratio			Ratio			Ratio	
Oscillator Period sec. (1)	Spectrum Value* ft/sec^2 (2)	Mode Displ. Appr.[1] (3)	Mode Accl. Appr.[2] (4)	Spectrum Value* ft/sec^2 (5)	Mode Displ. Appr.[1] (6)	Mode Accl. Appr.[2] (7)	Spectrum Value* ft/sec^2 (8)	Mode Displ. Appr.[1] (9)	Mode Accl. Appr.[2] (10)	Spectrum Value* ft/sec^2 (11)	Mode Displ. Appr.* (12)	Mode Accl. Appr. (13)	Spectrum Value* ft/sec^2 (14)	Mode Displ. Appr.[1] (15)	Mode Accl. Appr. (16)
0.02	.56	.23	.99	.59	.46	.99	.75	.93	.99	.98	1.05	1.00	1.12	1.02	1.00
0.04	.59	.25	.99	.63	.48	.99	.83	.94	.99	1.13	1.04	1.00	1.33	1.01	.99
0.08	1.50	.68	.98	2.35	.90	.99	5.80	.99	.99	9.54	1.00	1.00	11.72	1.00	.99
0.10	1.69	.32	.98	2.01	.50	.98	3.05	.94	.99	4.11	1.05	1.00	4.71	1.03	1.00
0.15	2.30	.21	.98	2.42	.42	.98	2.80	.91	.99	3.14	1.11	1.00	3.33	1.06	1.00
0.20	2.35	.20	.99	2.42	.39	.99	2.61	.90	.99	2.78	1.13	1.00	2.87	1.07	1.00
0.40	2.37	.18	.99	2.38	.37	.99	2.43	.90	.99	2.47	1.15	1.00	2.49	1.08	1.00
1.00	1.26	.18	.99	1.26	.37	.99	1.27	.90	.99	1.27	1.15	1.00	1.27	1.08	1.00

*Value obtained with all modes

[1]Ratio of values obtained by mode displacement approach with 4 modes and with 30 modes

[2]Ratio of values obtained by mode acceleration approach with 4 modes and with 30 modes

Table 5.1 Dynamic Properties of 15-D.O.F. Stiff Structural System

Mode No.	Frequency Cps	Modal Damping	Participation Factor
1	18.0113	0.0288	1.4174
2	18.0265	0.0289	1.4180
3	35.4632	0.0216	-0.0517
4	45.3425	0.0915	-0.5491
5	45.3840	0.0918	-0.5507
6	70.5108	0.1412	0.3214
7	70.6530	0.1427	-0.3211
8	78.6324	0.0726	-0.0132
9	93.8843	0.1593	0.2277
10	93.9839	0.1599	-0.2273
11	119.8302	0.1713	0.1770
12	119.9124	0.1717	0.1769
13	126.8534	0.0805	0.0059
14	186.2789	0.0781	0.0045
15	267.9215	0.0735	-0.0037

Table 5.2 Response Spectrum Values for Various Floors of a 15-D.O.F. Nonproportionally Damped Structure by Mode Displacement and Mode Acceleration Approaches with Only First 3 Modes (Oscillator Damping 1%, e/r = 0.05)

	Floor 1			Floor 3			Floor 5		
		Ratio			Ratio			Ratio	
Oscillator Period sec. (1)	Spectrum Value* ft/sec^2 (2)	Mode Displ. Appr.[1] (3)	Mode Accl. Appr.[2] (4)	Spectrum Value* ft/sec^2 (5)	Mode Displ. Appr.[1] (6)	Mode Accl. Appr.[2] (7)	Spectrum Value* ft/sec^2 (8)	Mode Displ. Appr.[1] (9)	Mode Accl. Appr.[2] (10)
0.02	.58	.33	.99	.72	.88	.99	.93	1.14	1.00
0.04	.81	.42	.91	1.09	1.05	1.03	2.12	.90	.95
0.06	2.41	.65	.97	5.50	.95	.99	8.38	1.04	1.00
0.10	2.10	.30	.98	2.54	.84	.98	2.90	1.23	1.01
0.15	3.18	.26	.99	3.44	.82	.99	3.65	1.29	1.00
0.20	3.29	.25	.99	3.44	.81	.99	3.55	1.32	1.00
0.40	3.35	.24	.99	3.39	.81	.99	3.42	1.34	1.00
1.00	1.78	.24	.91	1.79	.81	.99	1.79	1.34	1.00

*Value obtained with all 15 modes.

[1]Ratio of values obtained by node displacement approach with 3 modes and with 15 modes.

[2]Ratio of values obtained by mode acceleration approach with 3 modes and with 15 modes.

Table 5.3 Response Spectrum Values for Various Floors of a 15-D.O.F. Nonproportionally Damped Structure by Mode Displacement and Mode Acceleration Approaches with Only First 3 Modes (Oscillator Damping 1%, e/r = 0.05).

	Floor 1			Floor 3			Floor 5		
		Ratio			Ratio			Ratio	
Oscillator Period sec. (1)	Spectrum Value[1] g-units (2)	Mode Displ. Appr.[2] (3)	Mode Accl. Appr.[3] (4)	Spectrum Value[1] g-units (5)	Mode Displ. Appr.[2] (6)	Mode Accl. Appr.[3] (7)	Spectrum (8)	Mode Displ. Appr.[2] (9)	Mode Accl. Appr.[3] (10)
0.014*	.12	.32	.99	.15	.87	.98	.19	1.17	1.00
0.020	.12	.33	.99	.15	.89	.99	.20	1.17	.99
0.028*	.13	.34	.98	.16	.89	.99	.22	1.13	.99
0.04	.17	.48	.92	.23	1.06	1.03	.45	.91	.96
0.055*	.58	.69	.98	1.63	.95	.99	2.62	1.04	1.00
0.100	.40	.29	.98	.47	.84	.98	.54	1.24	1.01
0.150	.57	.26	.99	.62	.82	.99	.66	1.30	1.00
0.200	.54	.25	.99	.57	.81	.99	.58	1.32	1.00
0.400	.48	.24	.99	.48	.81	.99	.49	1.34	1.00
1.00	.17	.24	.99	.17	.81	.99	.17	1.34	1.00

*Structural period

[1]Value obtained with all 15 modes

[2]Ratio of values obtained by mode displacement approach with 3 modes and with 15 modes

[3]Ratio of values obtained by mode acceleration approach with 3 modes and with 15 modes

FIGURES FOR CHAPTER 2

CLASSICALLY DAMPED SYSTEMS: MODE DISPLACEMENT METHOD

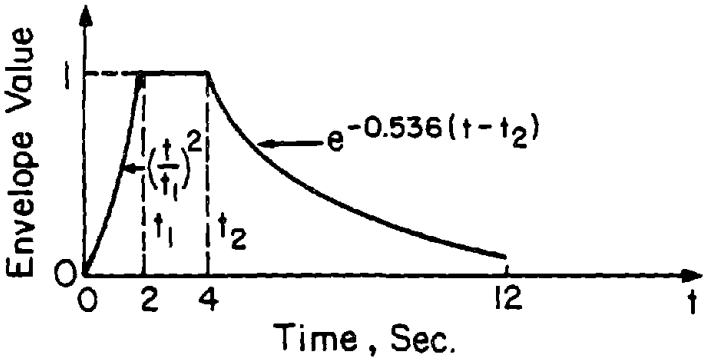

a) 12 Sec. Duration

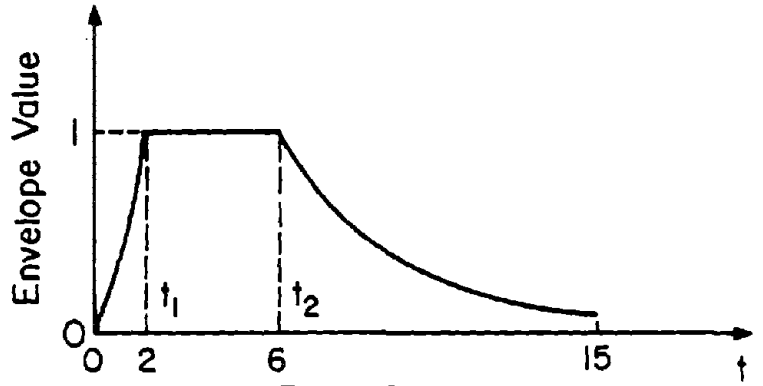

b) 15 Sec. Duration

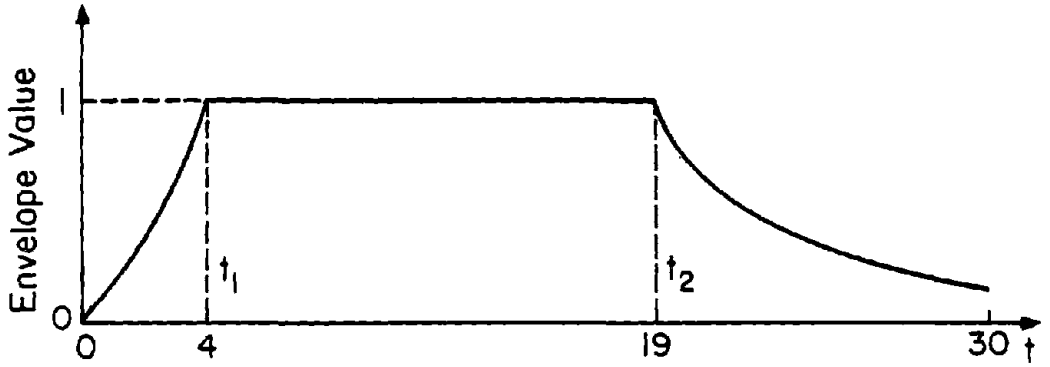

c) 30 Sec. Duration

Fig. 2.1 Intensity Modulation Functions Used in Generation of Acceleration Time Histories

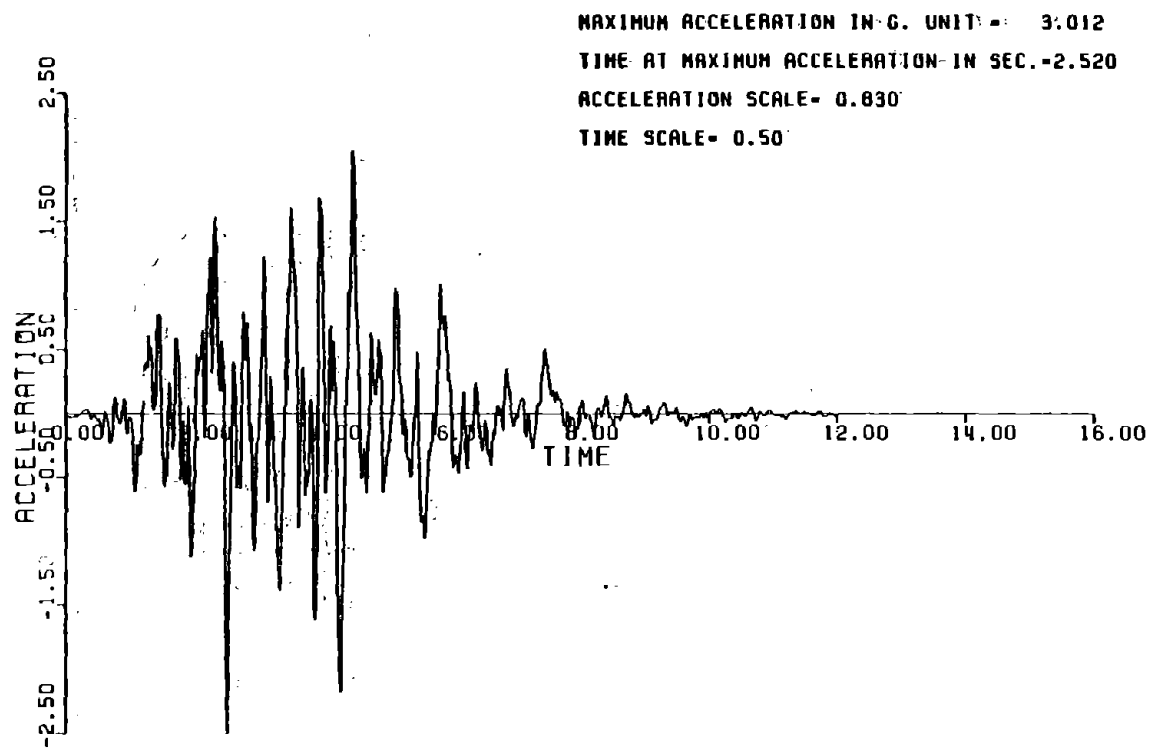

Fig. 2.2 A Sample Acceleration Time History of 12-sec. Duration

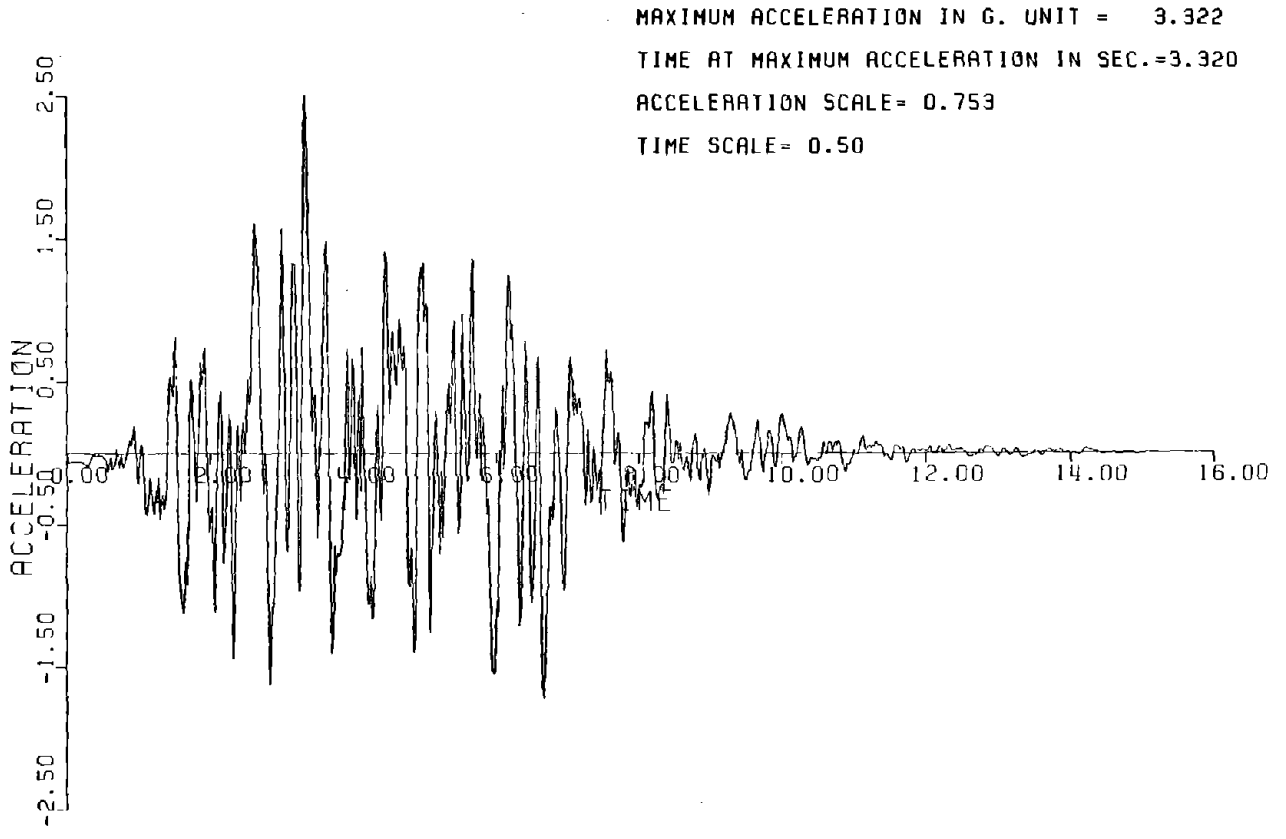

Fig. 2.3 A Sample Acceleration Time History of 15-sec. Duration

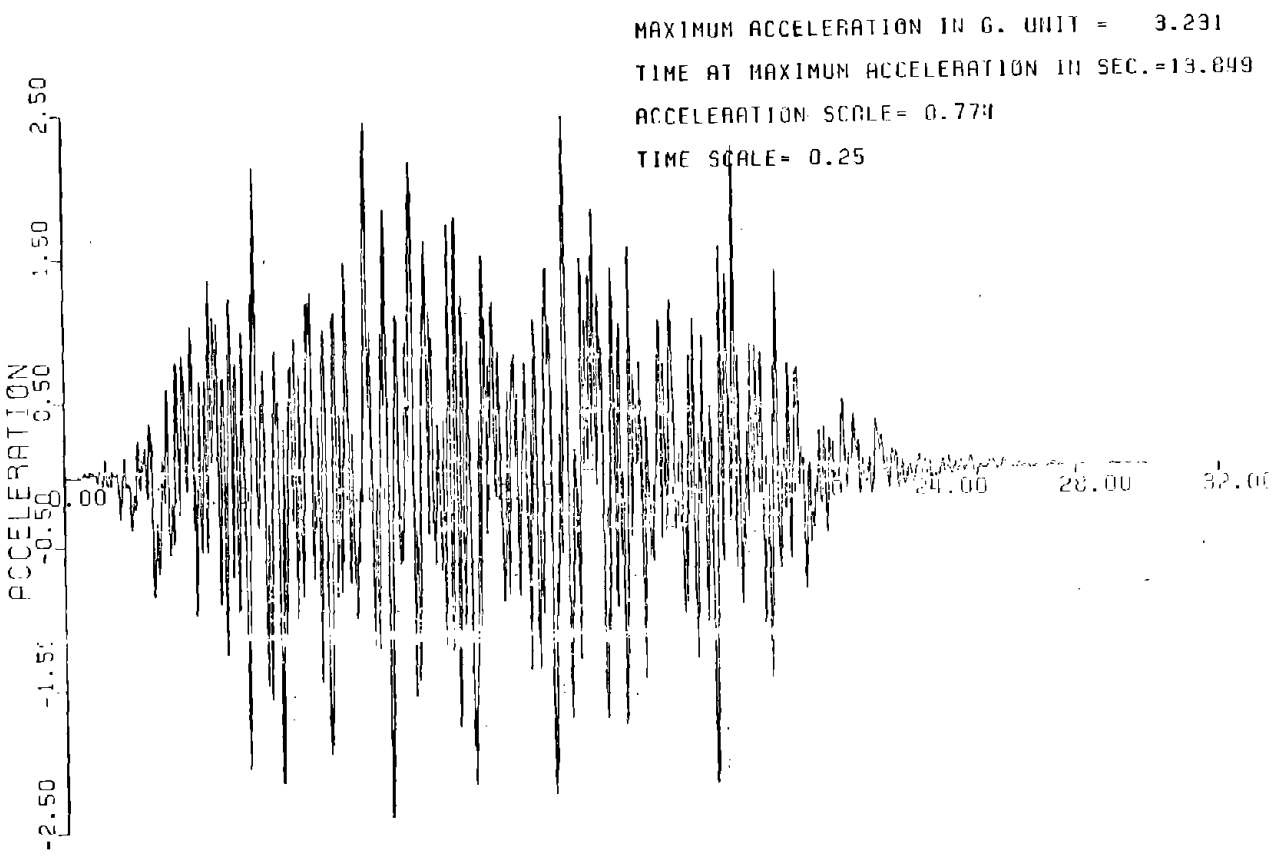

Fig. 2.4 A Sample Acceleration Time History of 30-sec Duration

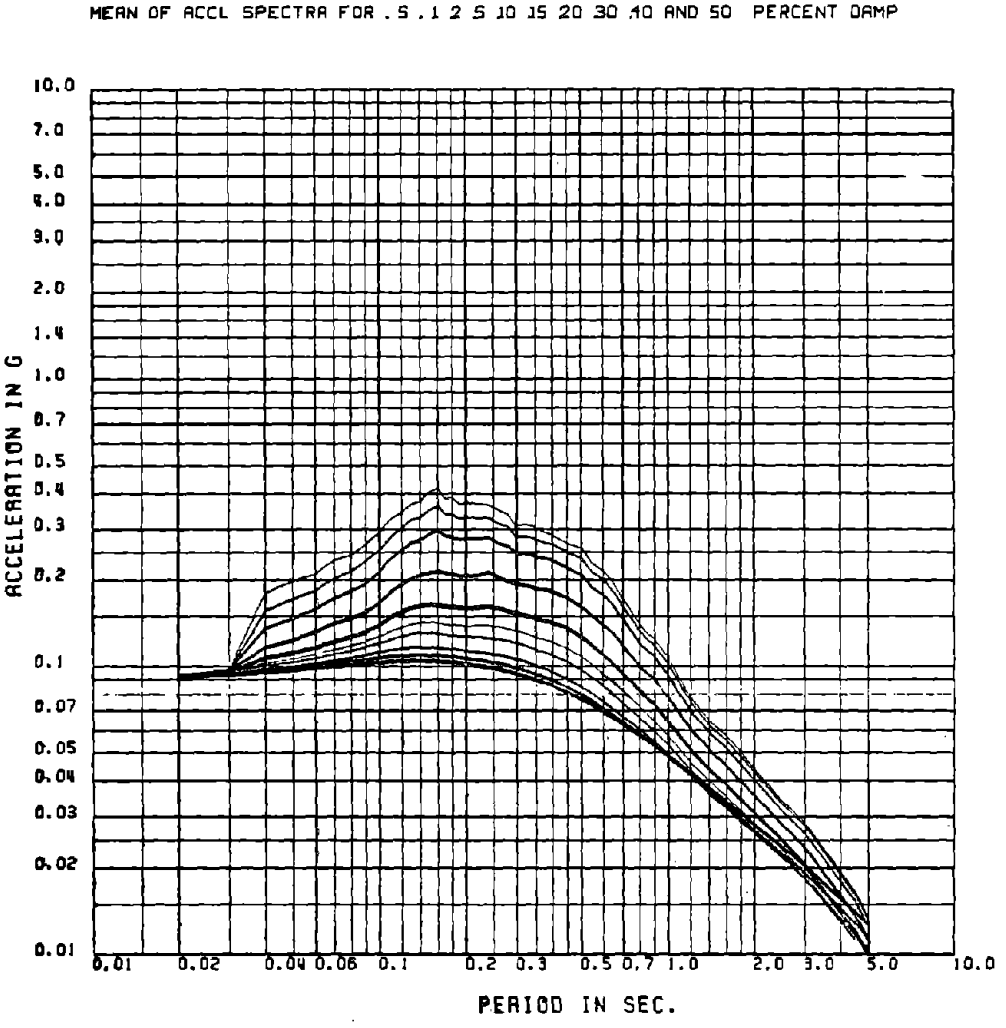

Fig. 2.5 Mean Pseudo Acceleration Spectra for the Ensemble of 12-sec Time Histories

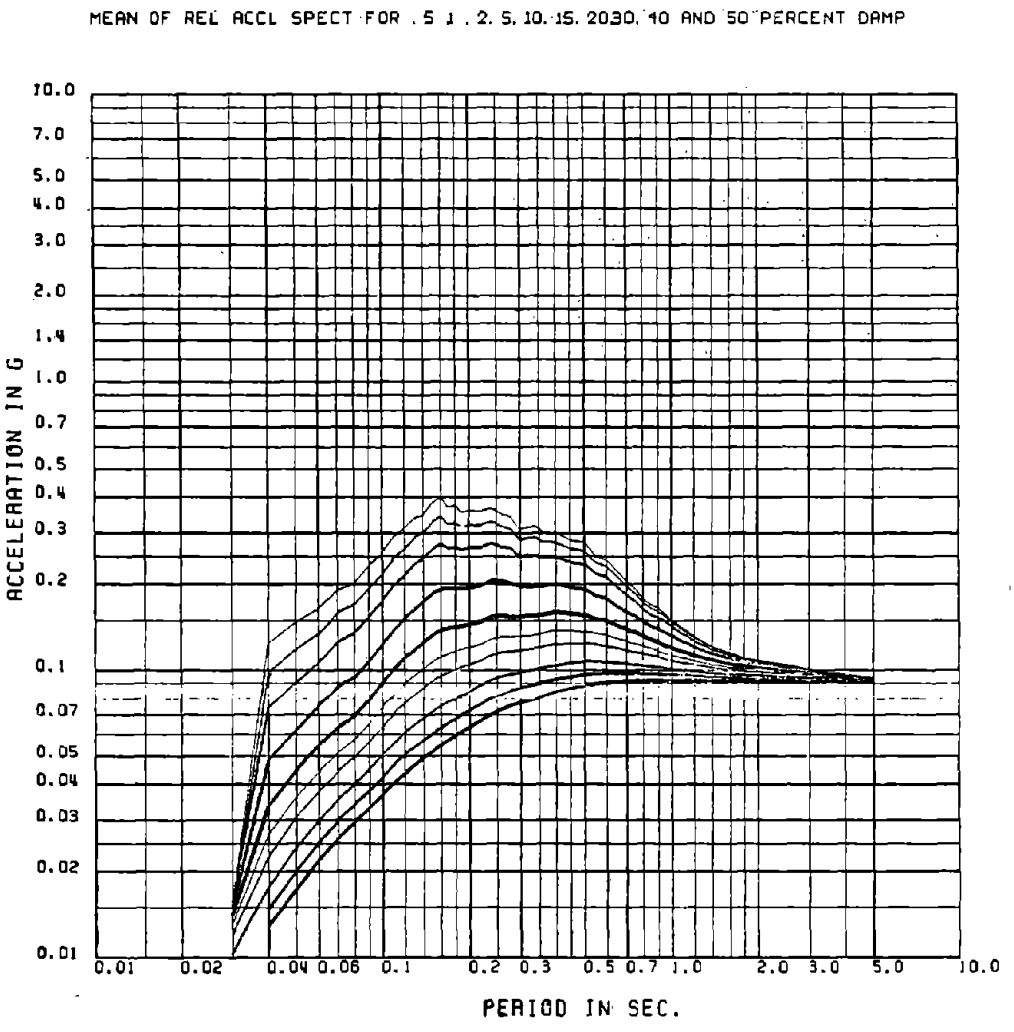

Fig. 2.6 Mean Relative Acceleration Spectra for the Ensemble of 12-sec Time Histories

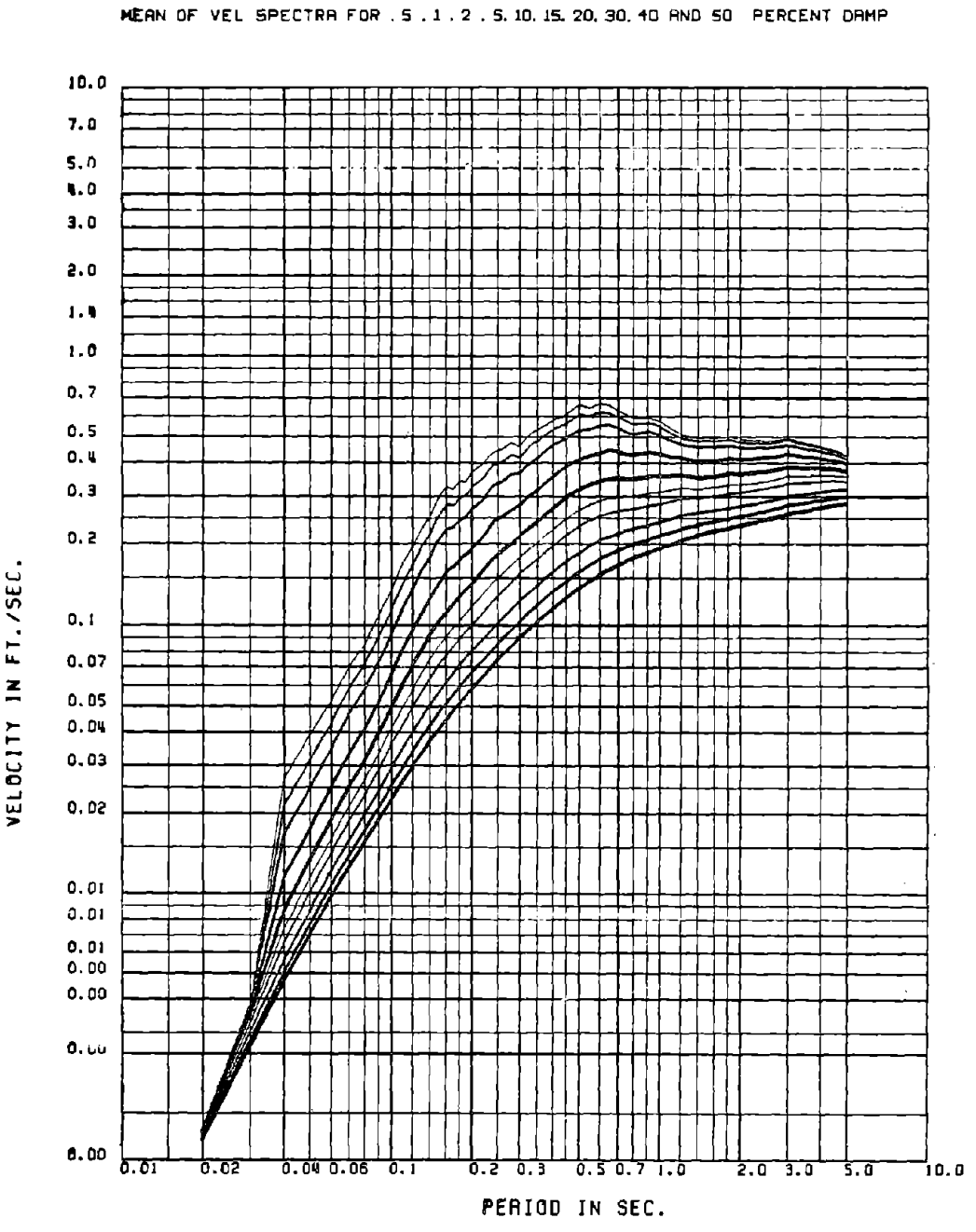

Fig. 2.7 Mean Relative Velocity Spectra for the Ensemble of 12-sec Time Histories

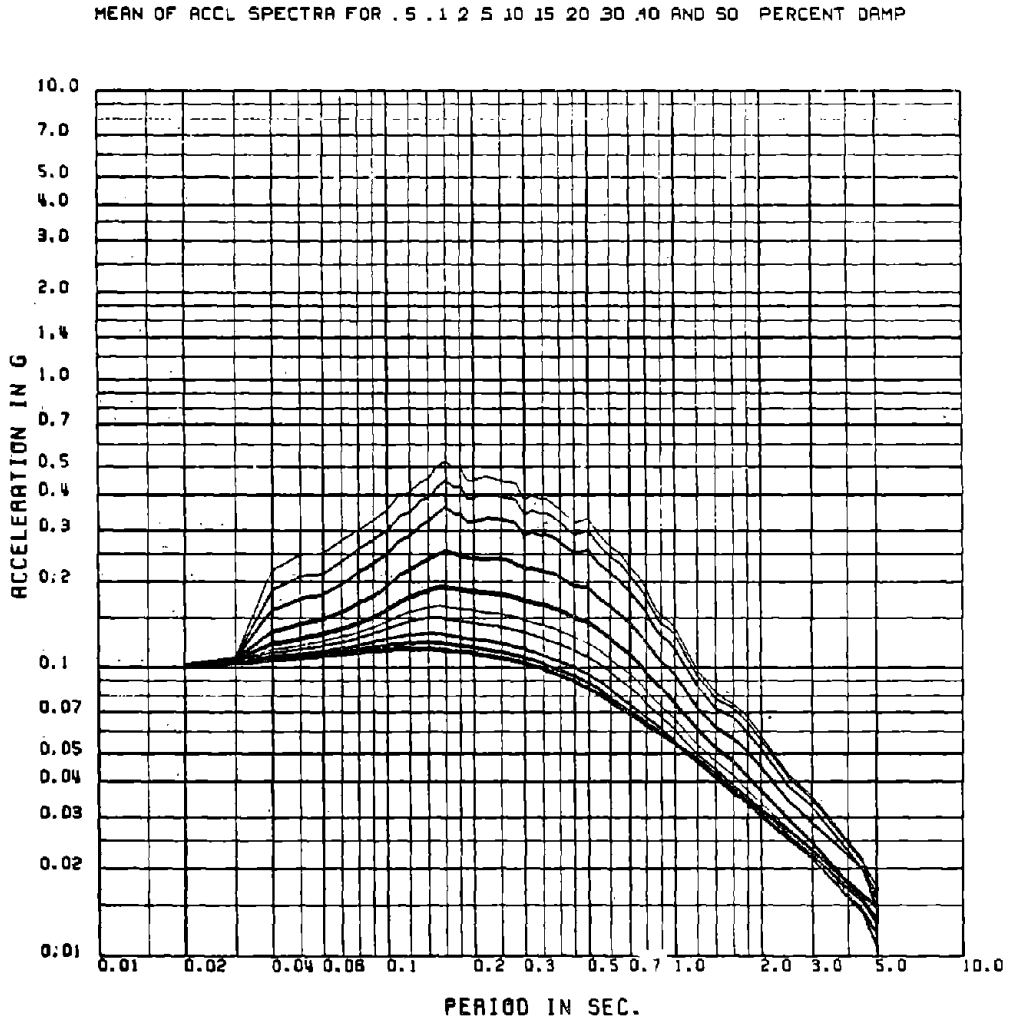

Fig. 2.8 Mean Pseudo Acceleration Spectra for the Ensemble of 15-sec Time Histories

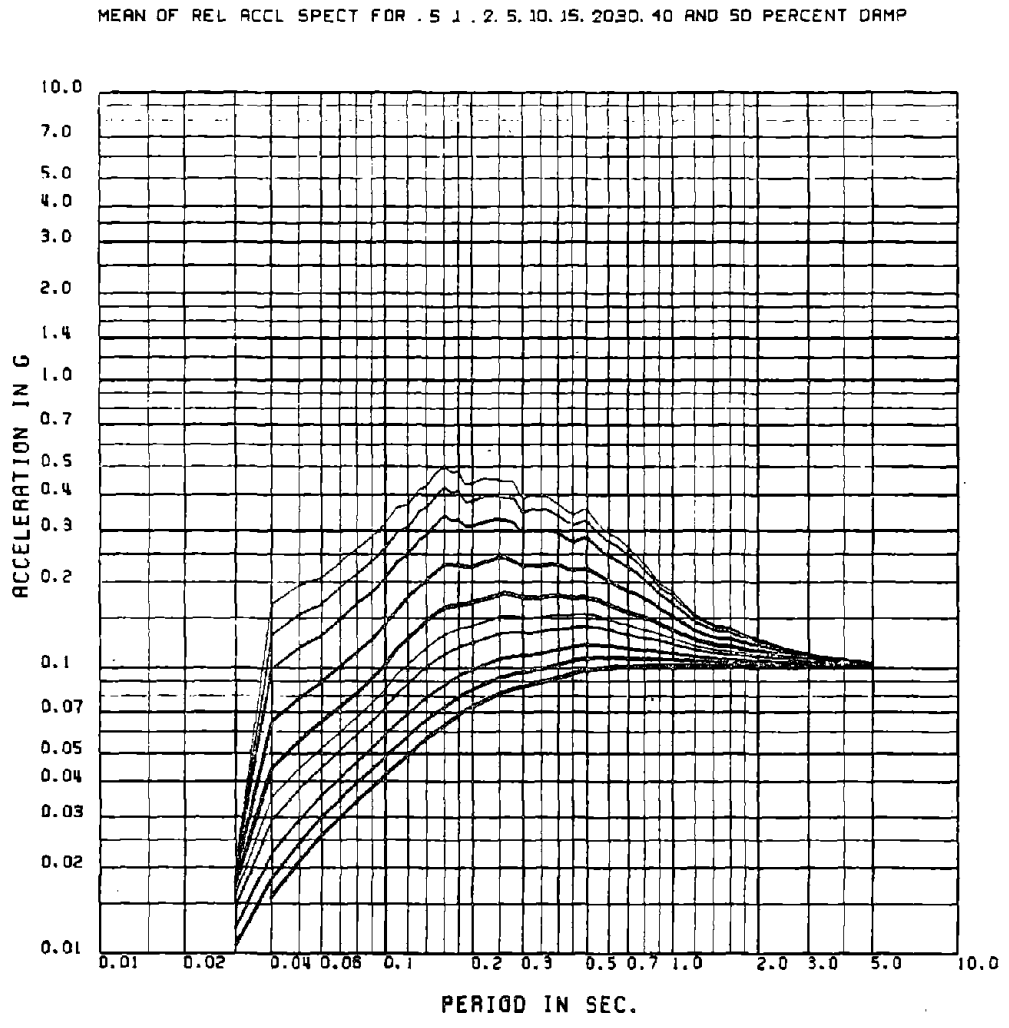

Fig. 2.9 Mean Relative Acceleration Spectra for the Ensemble of 15-sec Time Histories

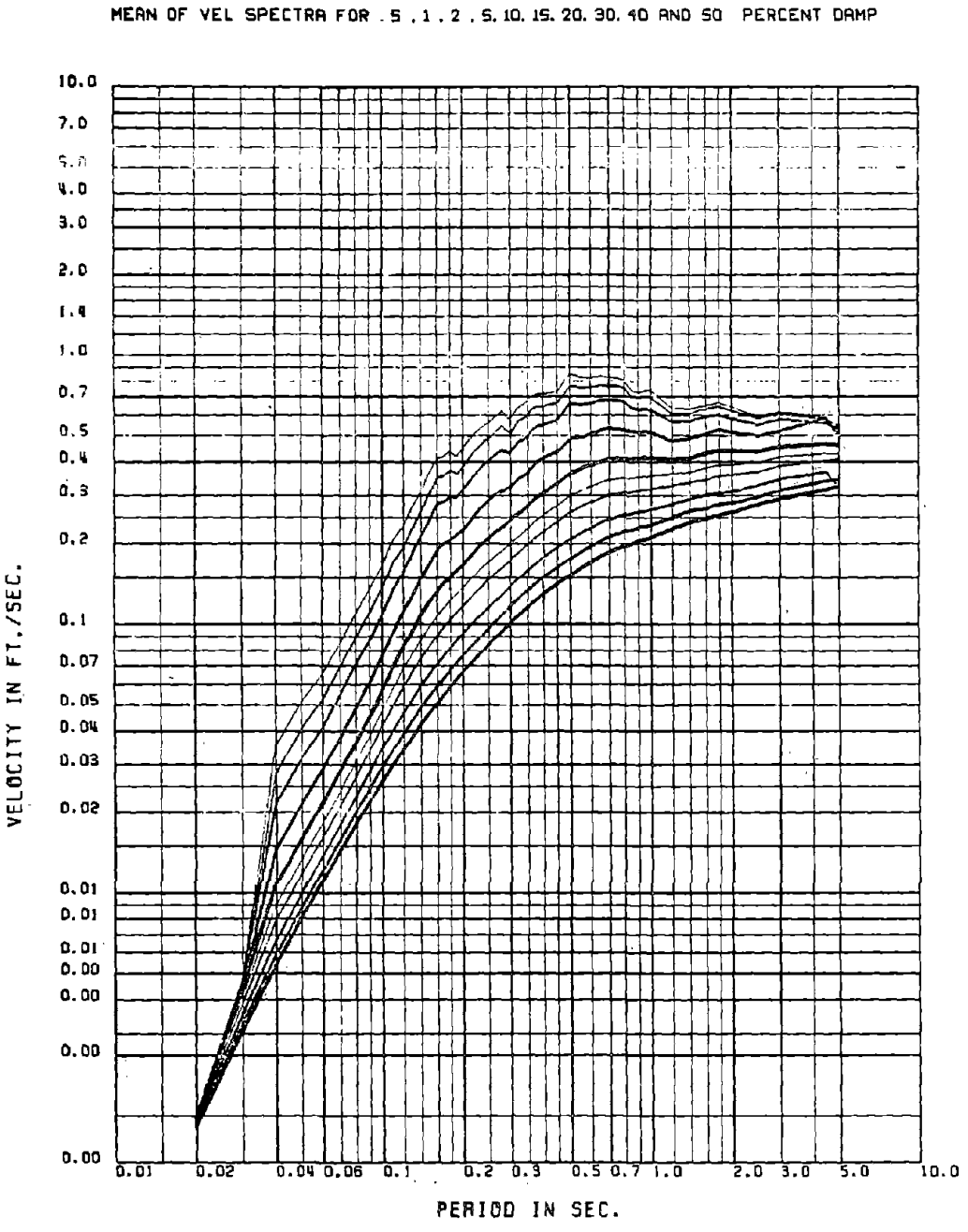

Fig. 2.10 Mean Relative Velocity Spectra for the Ensemble of 15-sec Time Histories

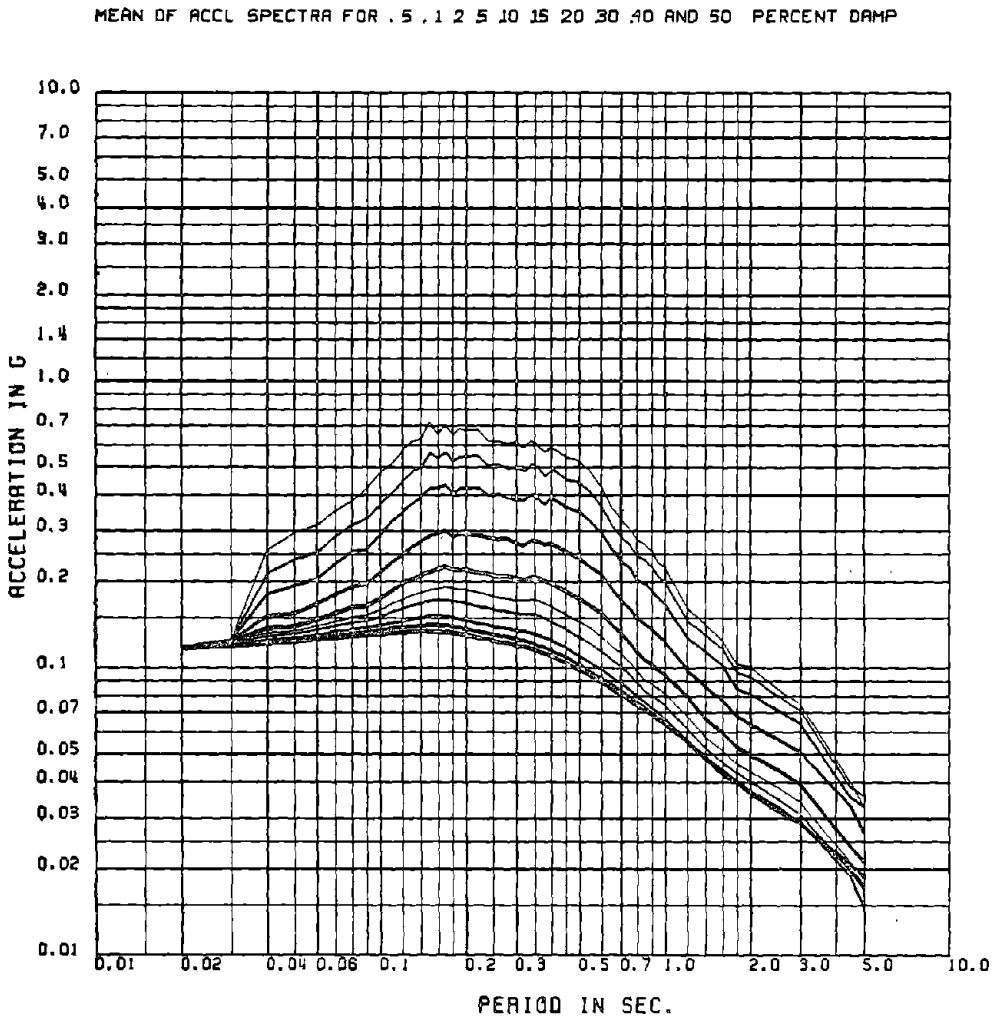

Fig. 2.11 Mean Pseudo Acceleration Spectra for the Ensemble of 30-sec Time Histories

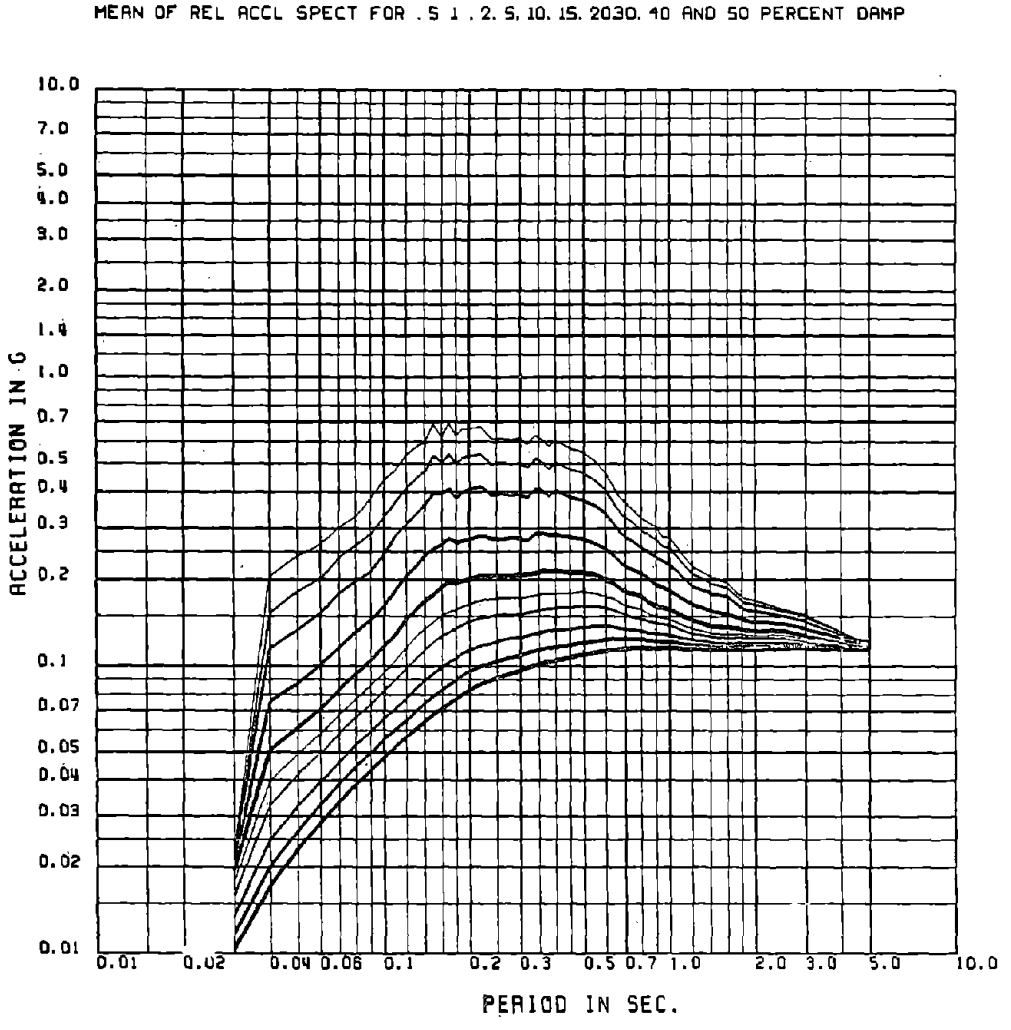

Fig. 2.12 Mean Relative Acceleration Spectra for the Ensemble of 30-sec Time Histories

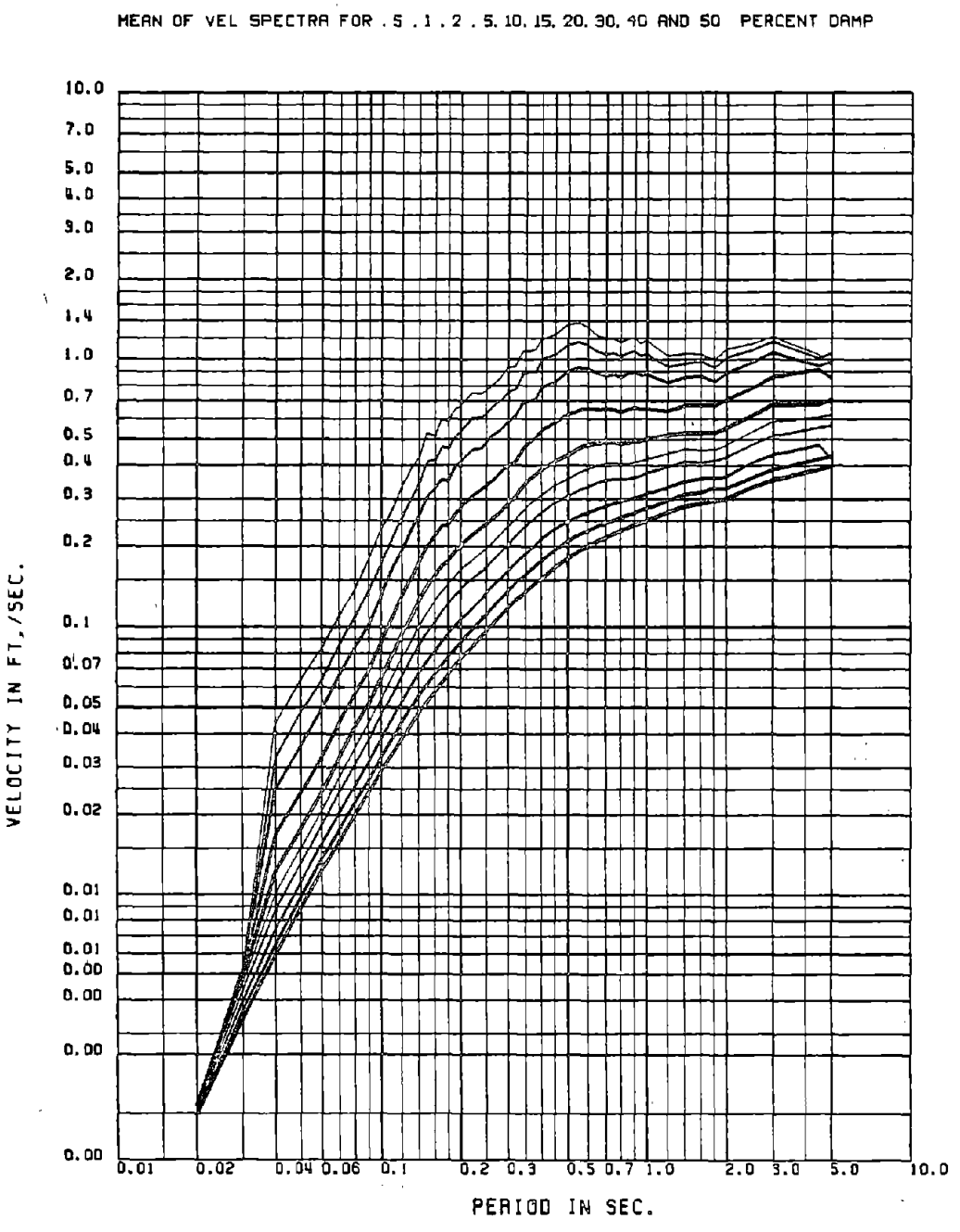

Fig. 2.13 Mean Relative Velocity Spectra for the Ensemble of 30-sec Time Histories

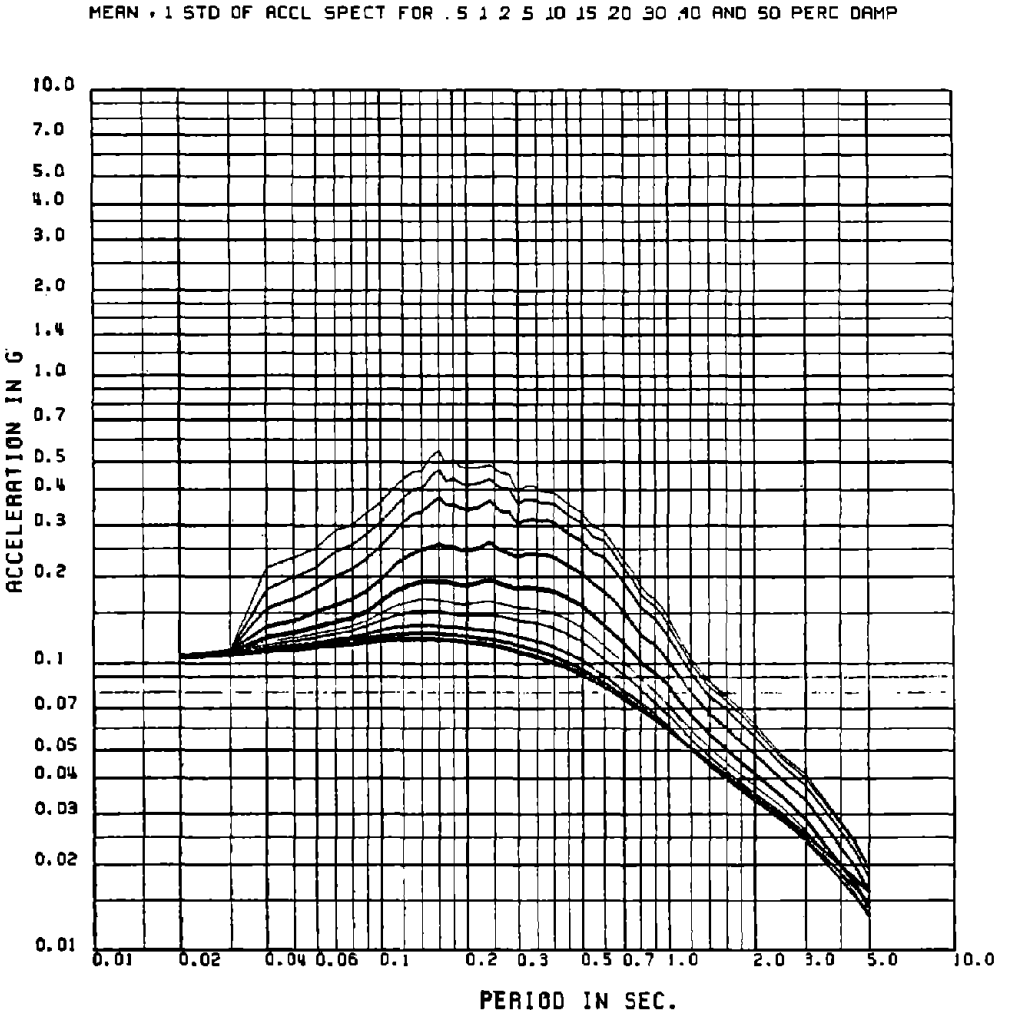

Fig. 2.14 Mean + One Standard Deviation Pseudo Acceleration Spectra for the Ensemble of 12-sec Time Histories

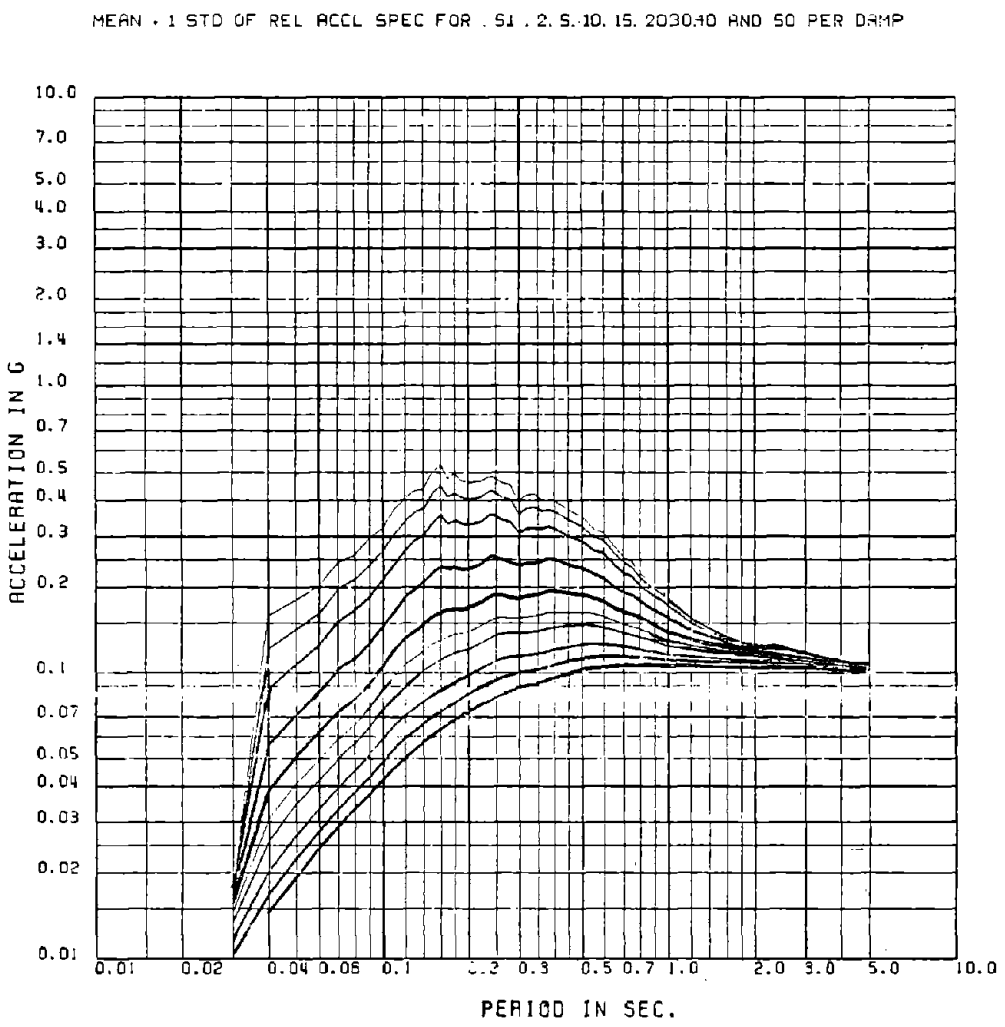

Fig. 2.15 Mean + One Standard Deviation Relative Acceleration Spectra for the Ensemble of 12-sec Time Histories

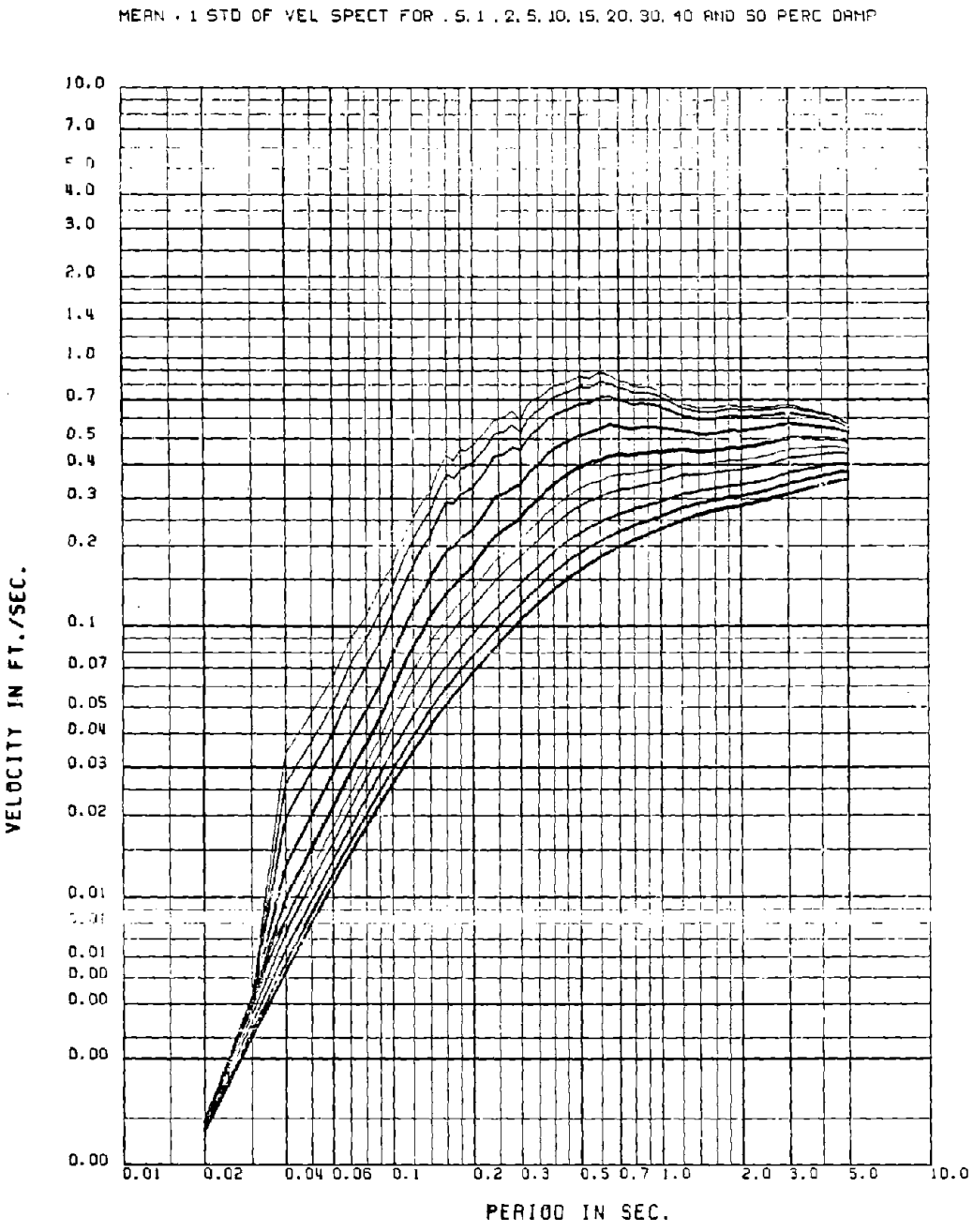

Fig. 2.16 Mean + One Standard Deviation Relative Velocity Spectra for the Ensemble of 12-sec Time Histories

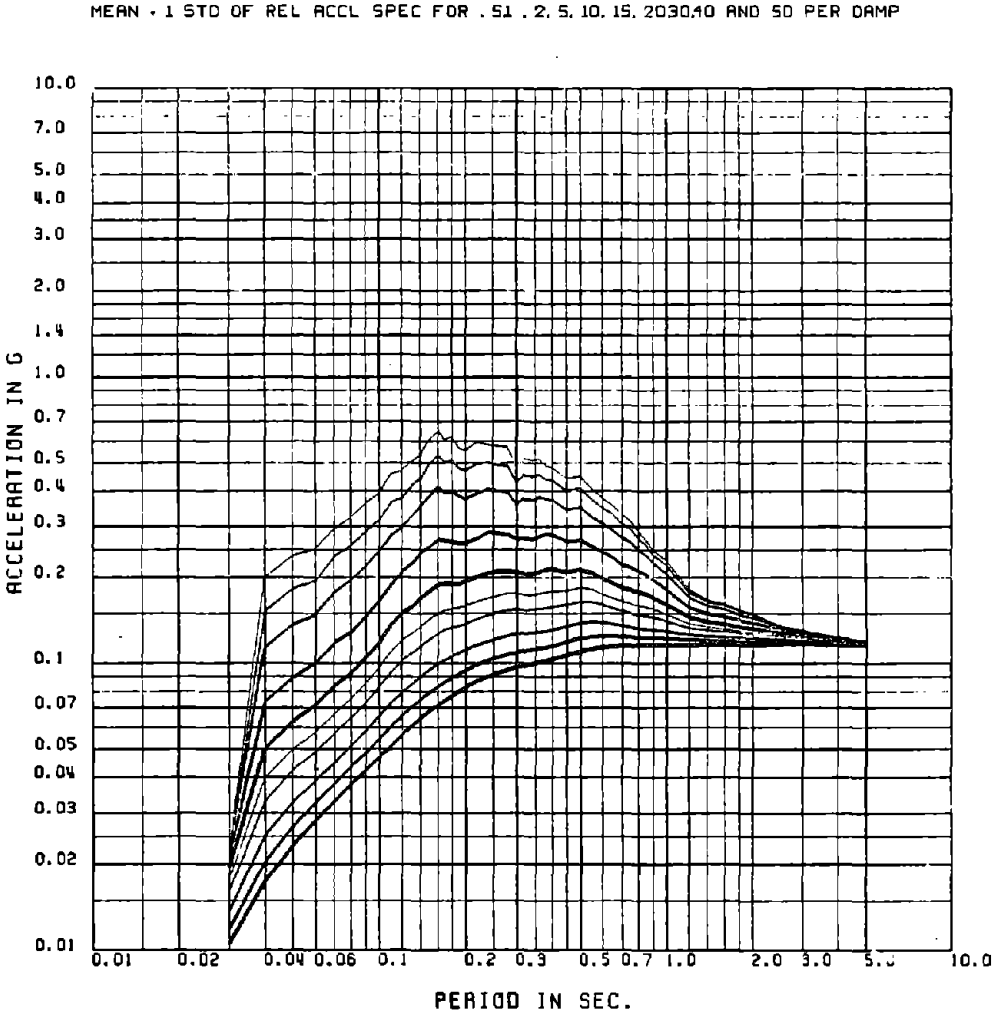

Fig. 2.17 Mean + One Standard Deviation Pseudo Acceleration Spectra for the Ensemble of 15-sec Time Histories

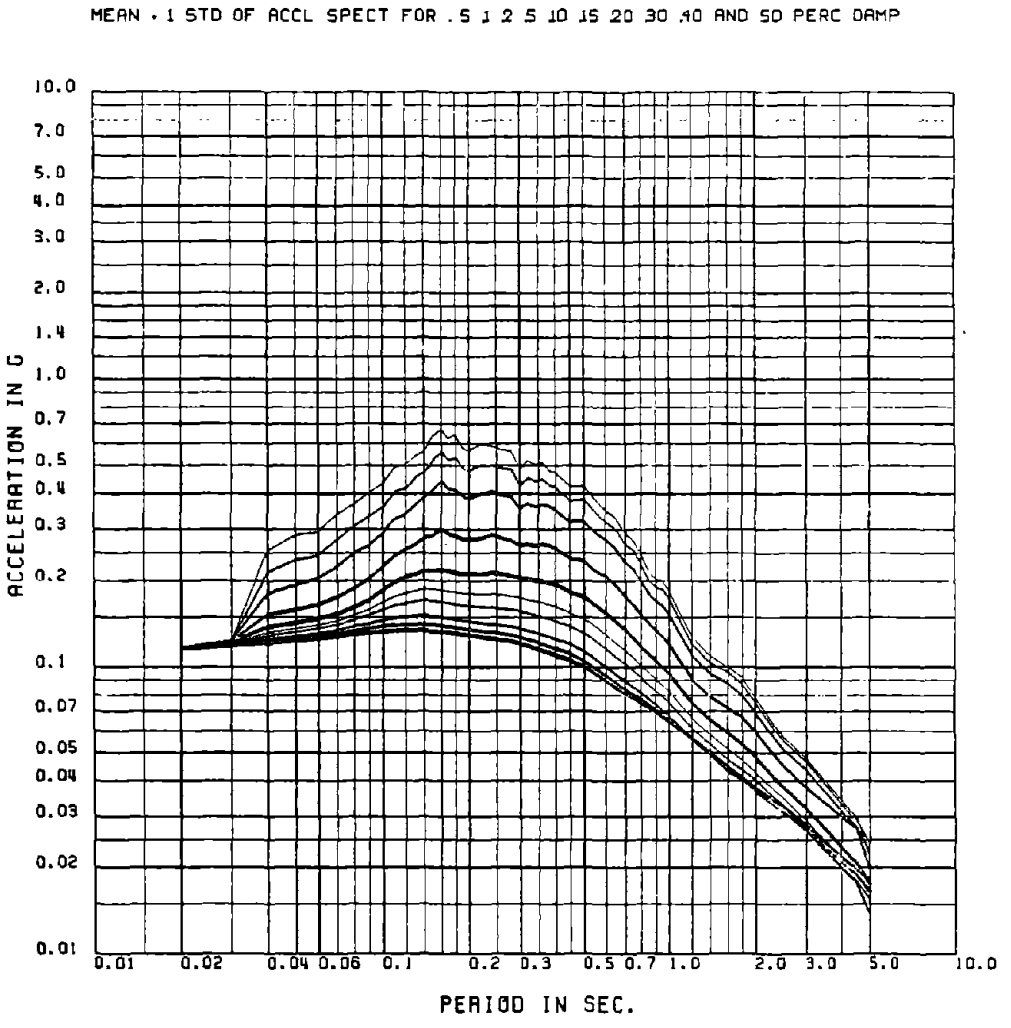

Fig. 2.18 Mean + One Standard Deviation Relative Acceleration Spectra for the Ensemble of 15-sec Time Histories

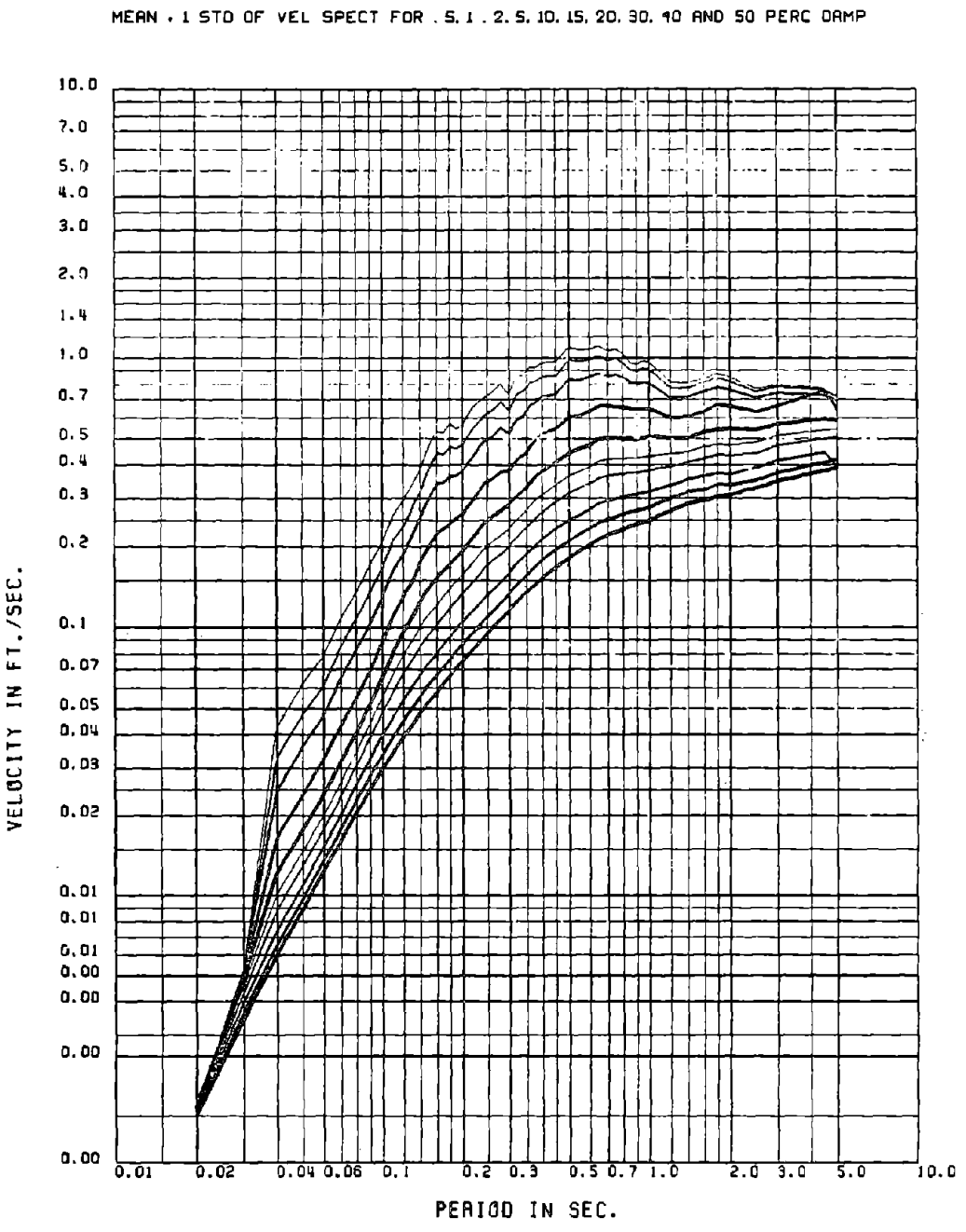

Fig. 2.19 Mean + One Standard Deviation Relative Velocity Spectra for the Ensemble of 15-sec Time Histories

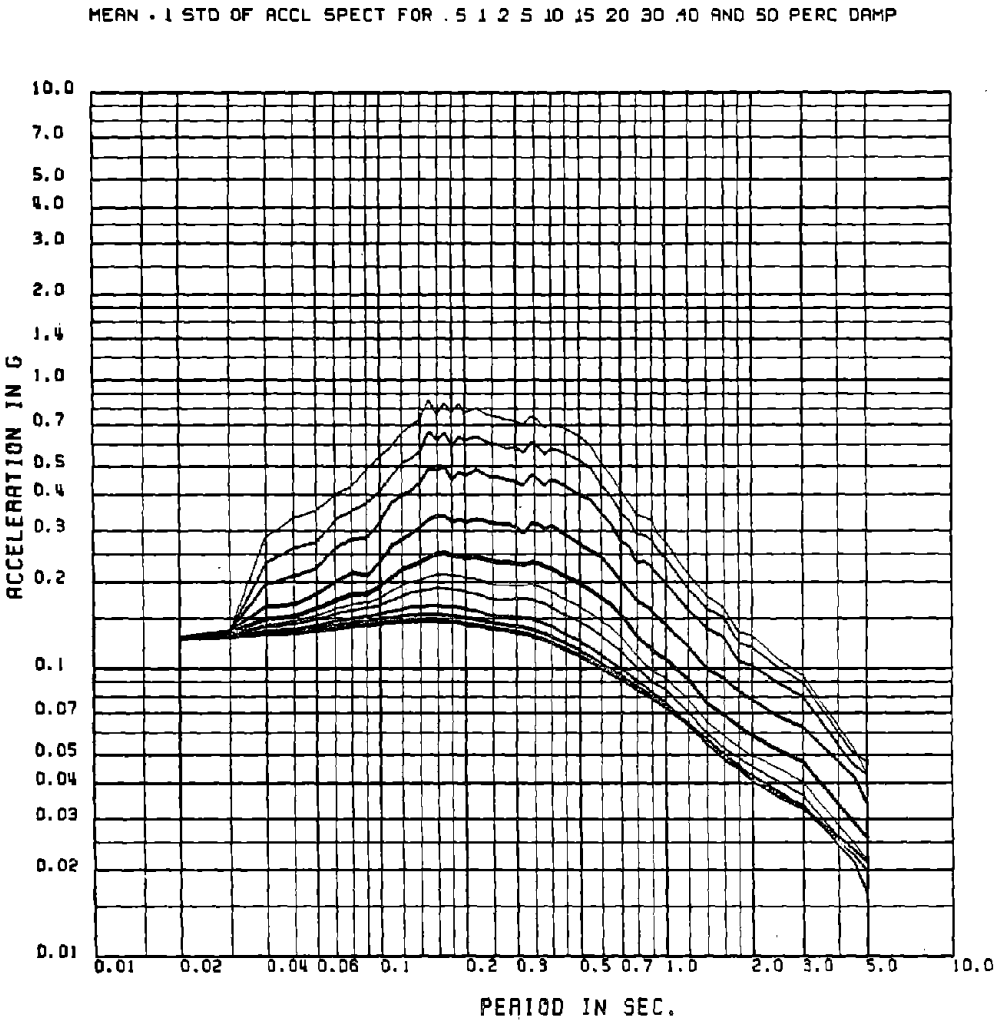

Fig. 2.20 Mean + One Standard Deviation Pseudo Acceleration Spectra for the Ensemble of 30-sec Time Histories

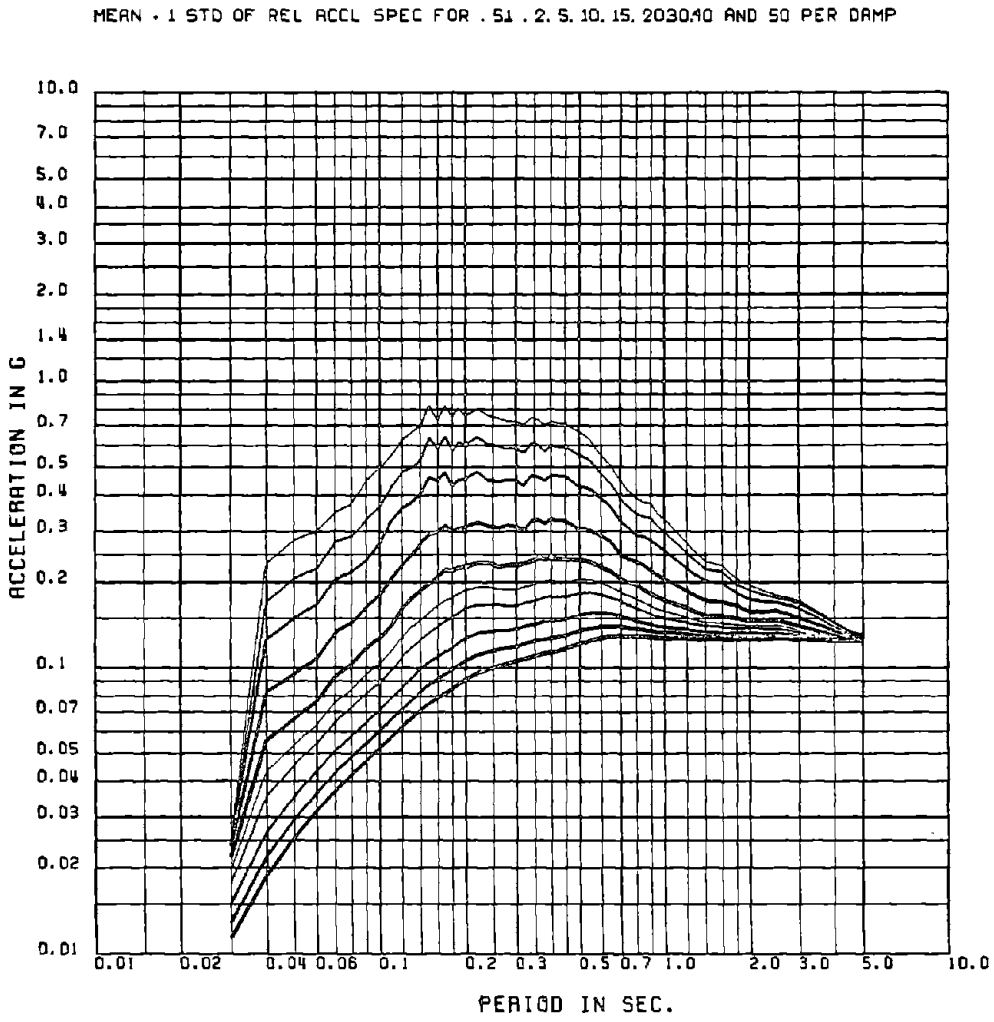

Fig. 2.21 Mean + One Standard Deviation Relative Acceleration Spectra for the Ensemble of 30-sec Time History

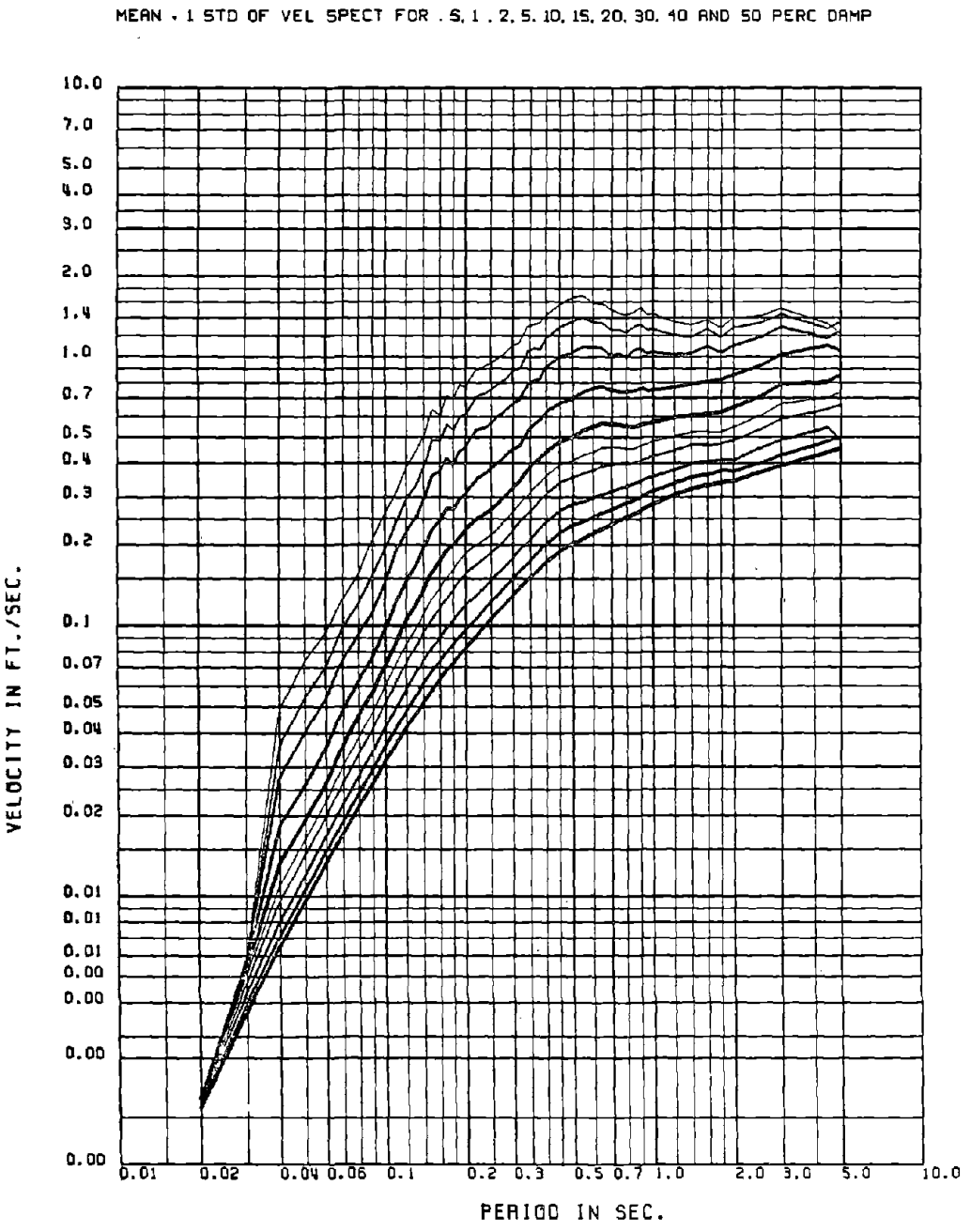

Fig. 2.22 Mean + One Standard Deviation Relative Velocity Spectra for the Ensemble of 30-sec Time History

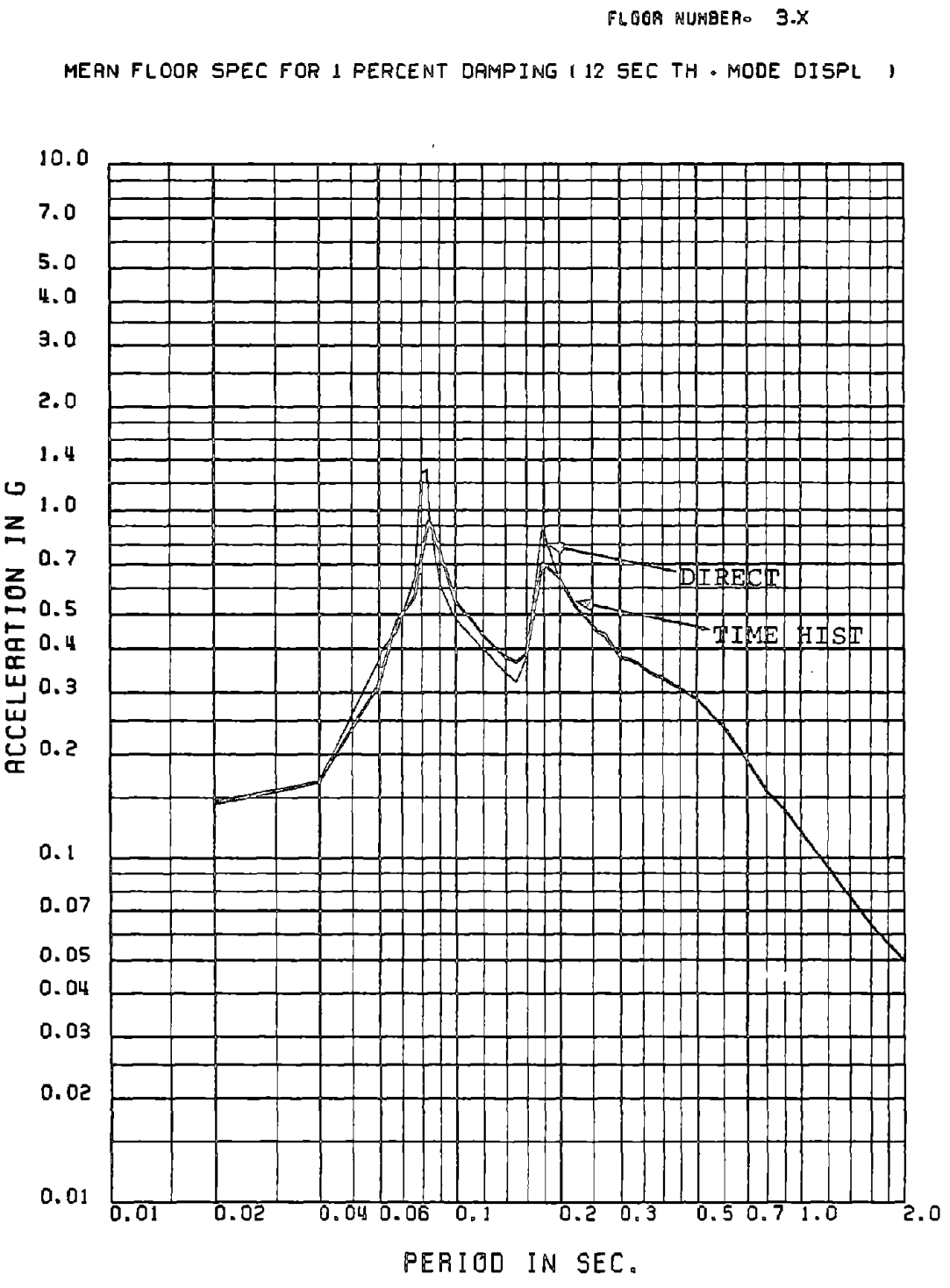

Fig. 2.23 Comparison of Floor Spectra Obtained by Mode Displacement Approach and Time History Analysis for 1% Damping: Mean Spectra, 12-sec TH, Floor No. 3-X, 11-FRQ Model

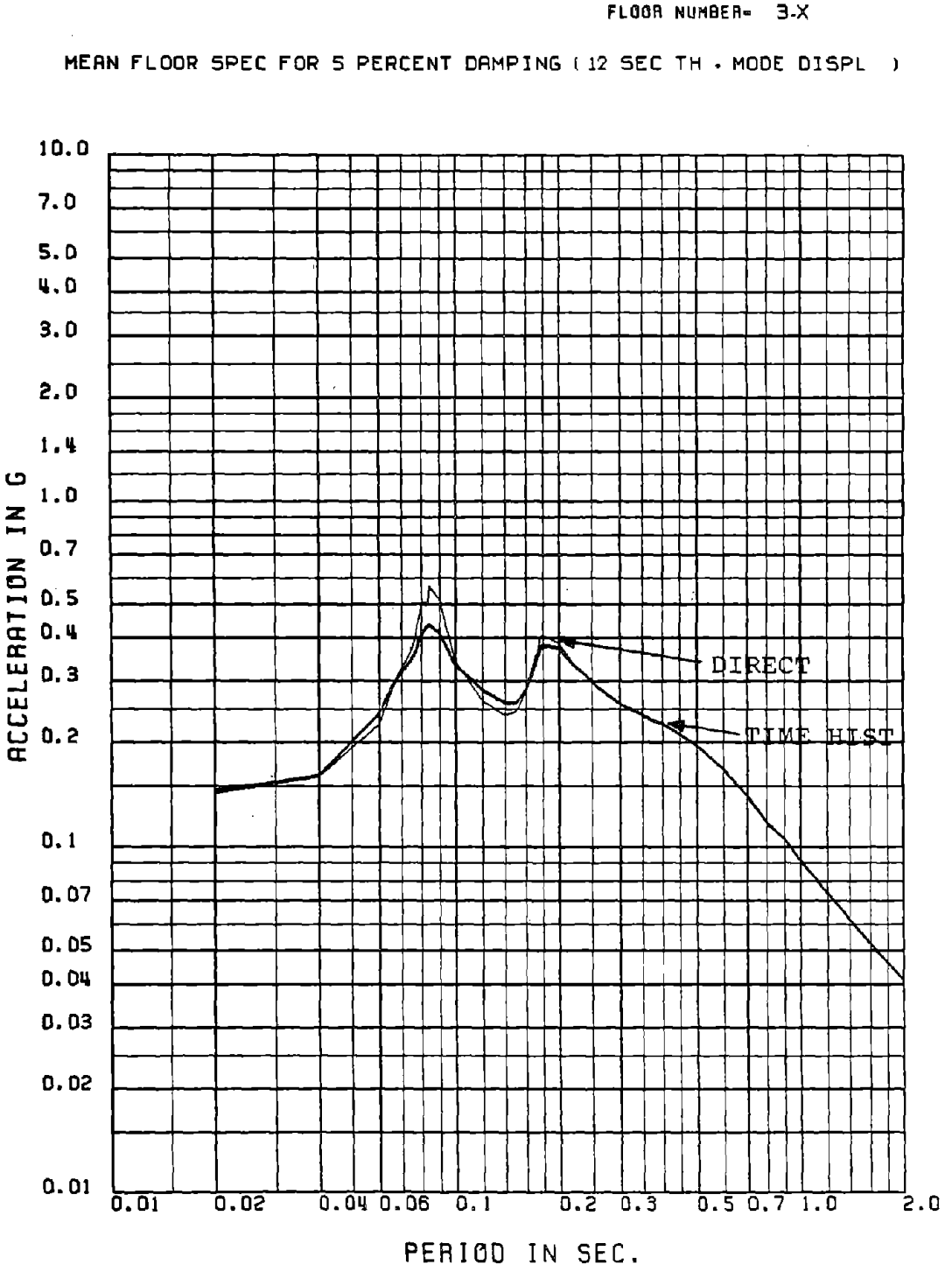

Fig. 2.24 Comparison of Floor Spectra Obtained by Mode Displacement Approach and Time History Analysis for 5% Damping: Mean Spectra, 12-sec TH, Floor No. 3-X, 11-FRQ Model

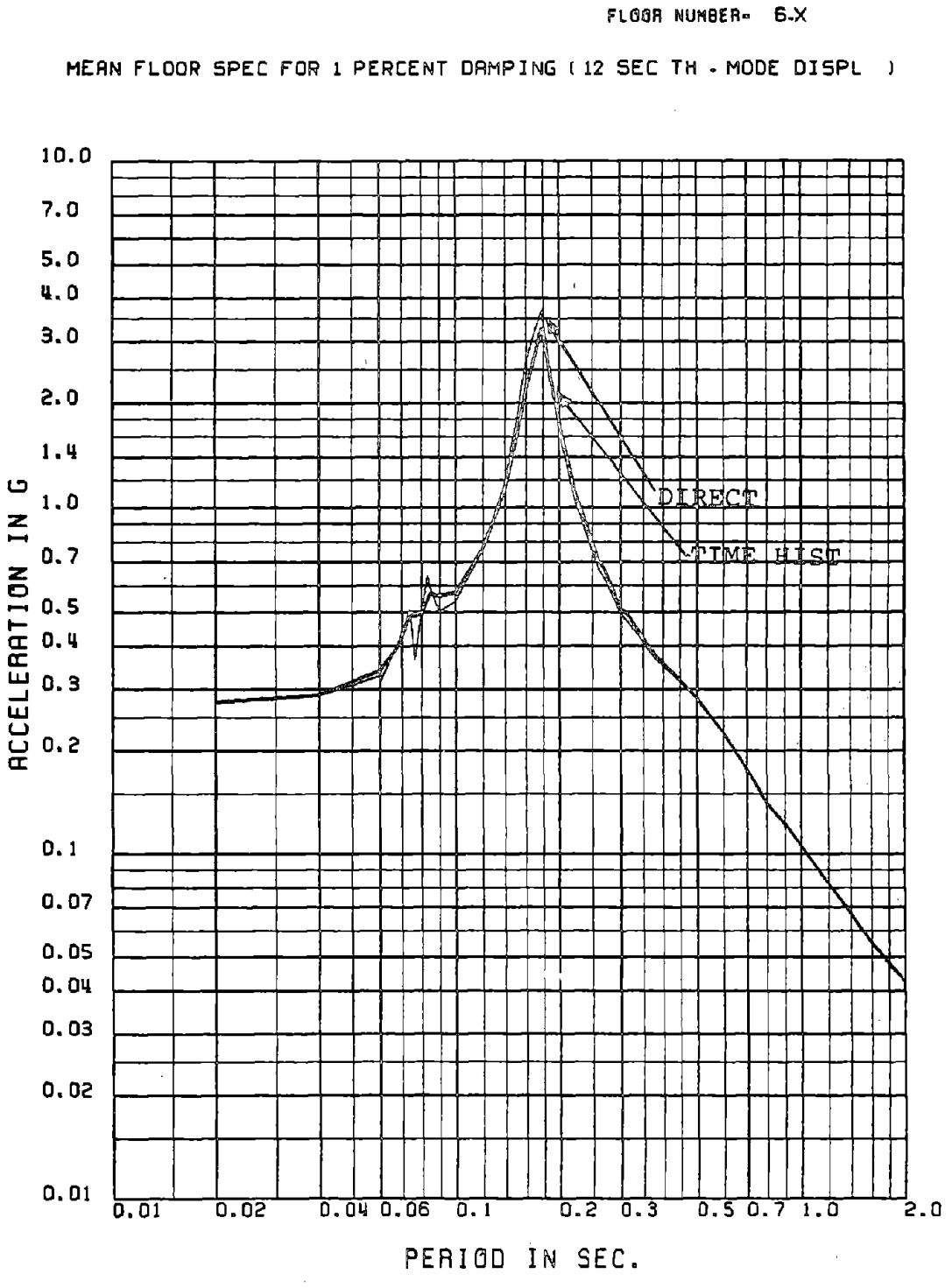

Fig. 2.25 Comparison of Floor Spectra Obtained by Mode Displacement Approach and Time History Analysis for 1% Damping: Mean Spectra, 12-sec TH, Floor No. 6-X, 11-FRQ Model

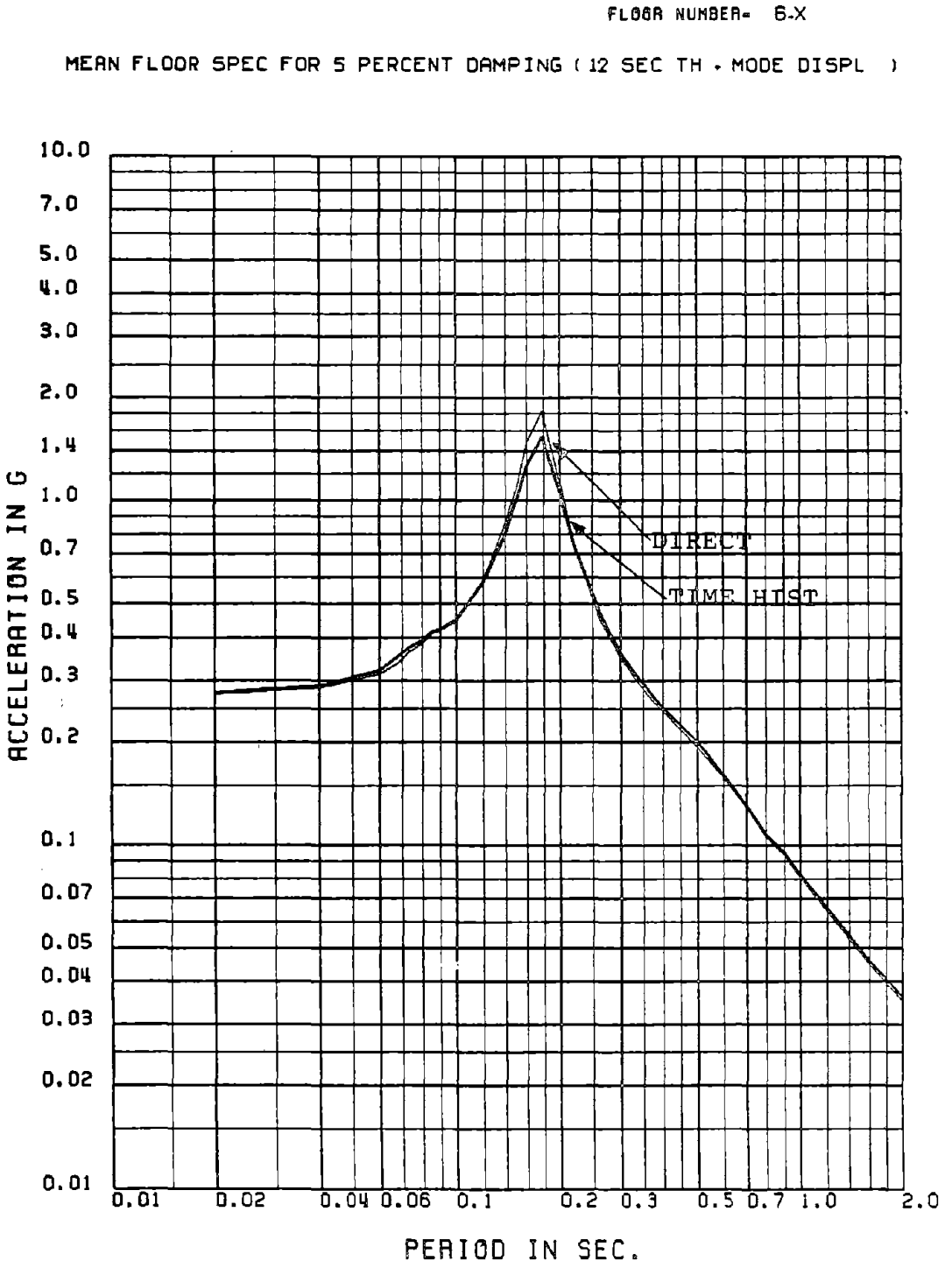

Fig. 2.26 Comparison of Floor Spectra Obtained by Mode Displacement Approach and Time History Analysis for 1% Damping: Mean Spectra, 15-sec TH, Floor No. 3-X, 11-FRQ Model

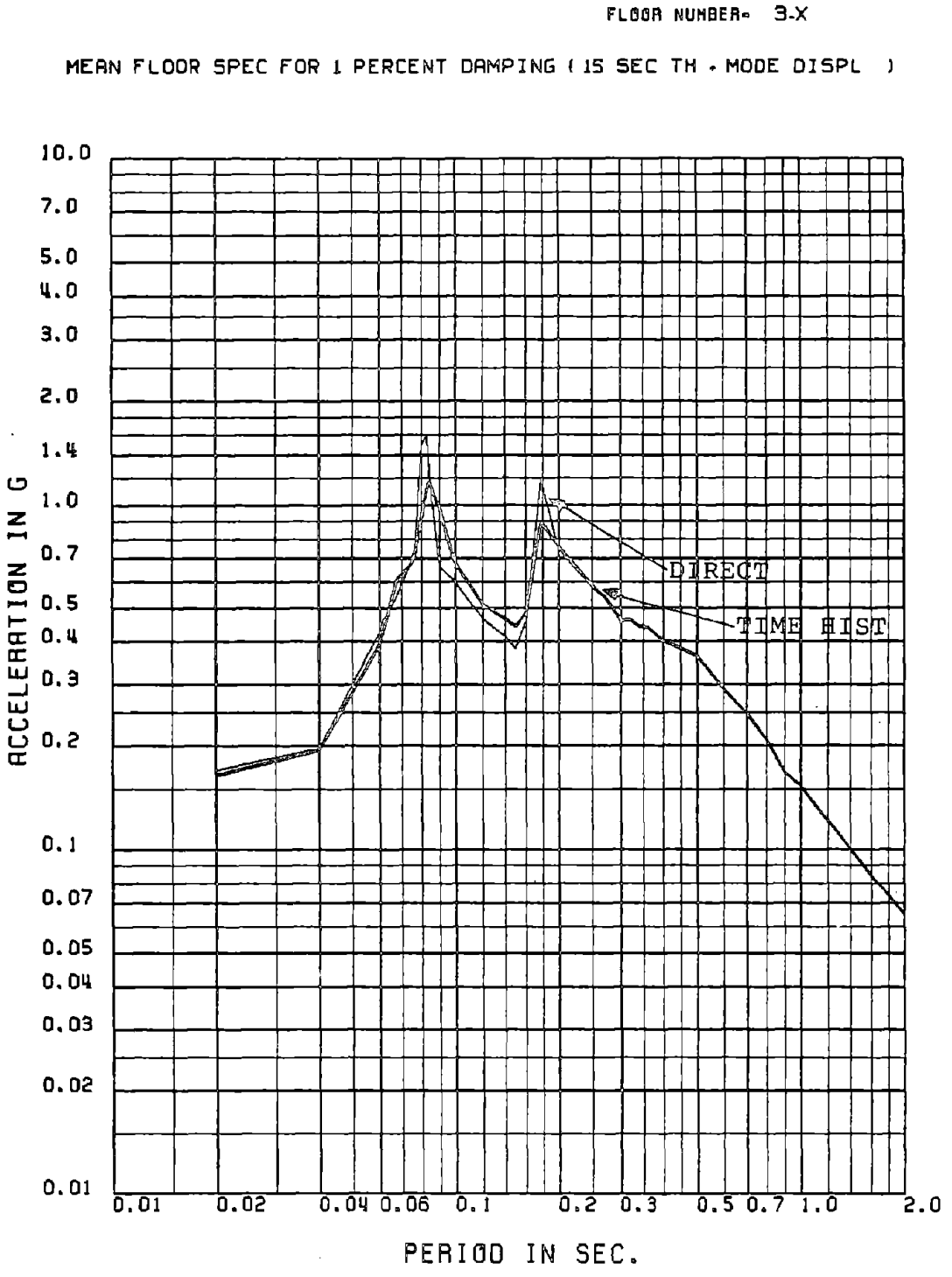

Fig. 2.27 Comparison of Floor Spectra Obtained by Mode Displacement Approach and Time History Analysis for 1% Damping: Mean Spectra, 15-sec TH, Floor No. 3-X, 11-FRQ Model

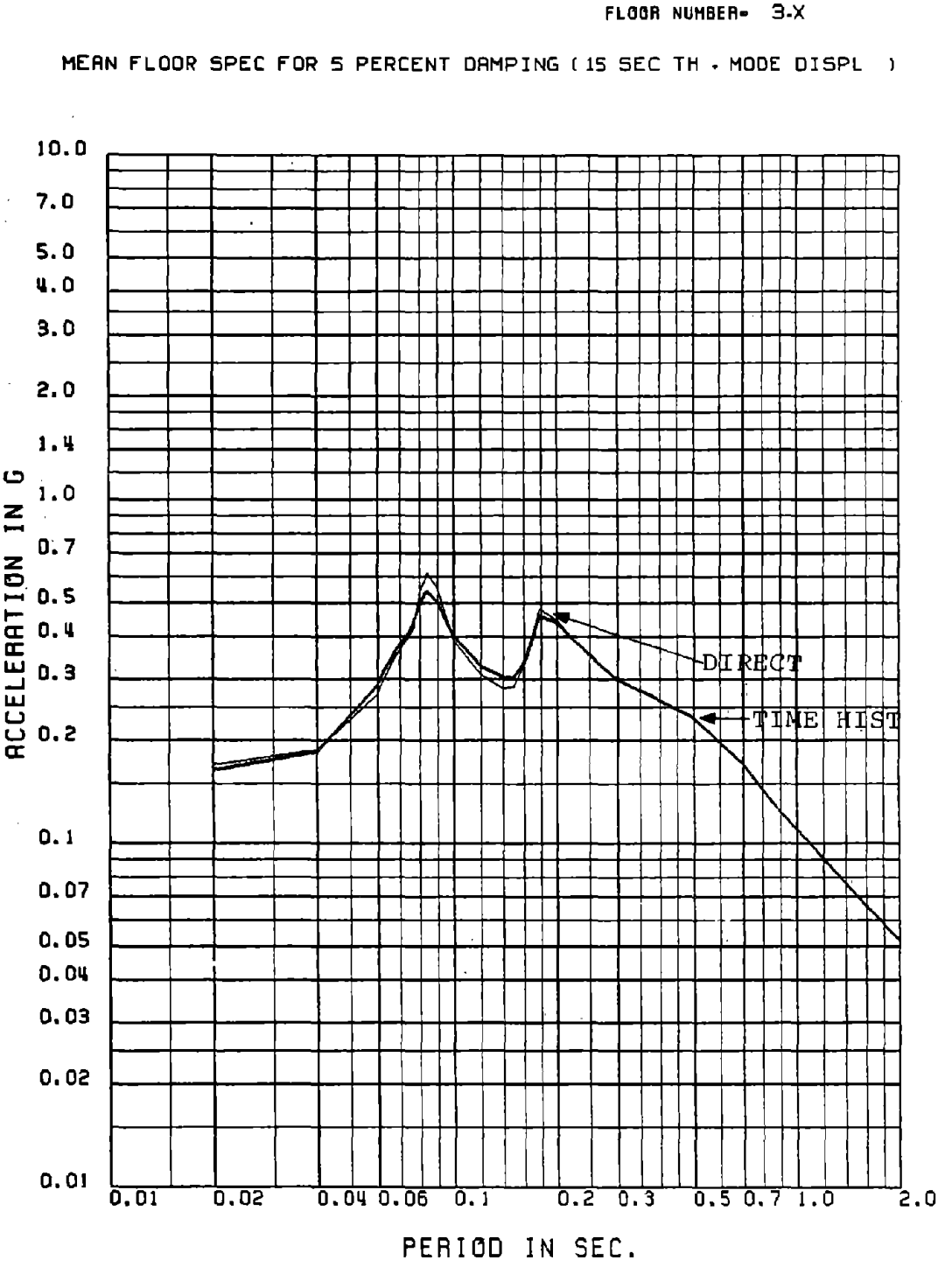

Fig 2.28 Comparison of Floor Spectra Obtained by Mode Displacement Approach and Time History Analysis for 5% Damping: Mean Spectra, 15-sec TH, Floor No. 3-X, 11-FRQ Model

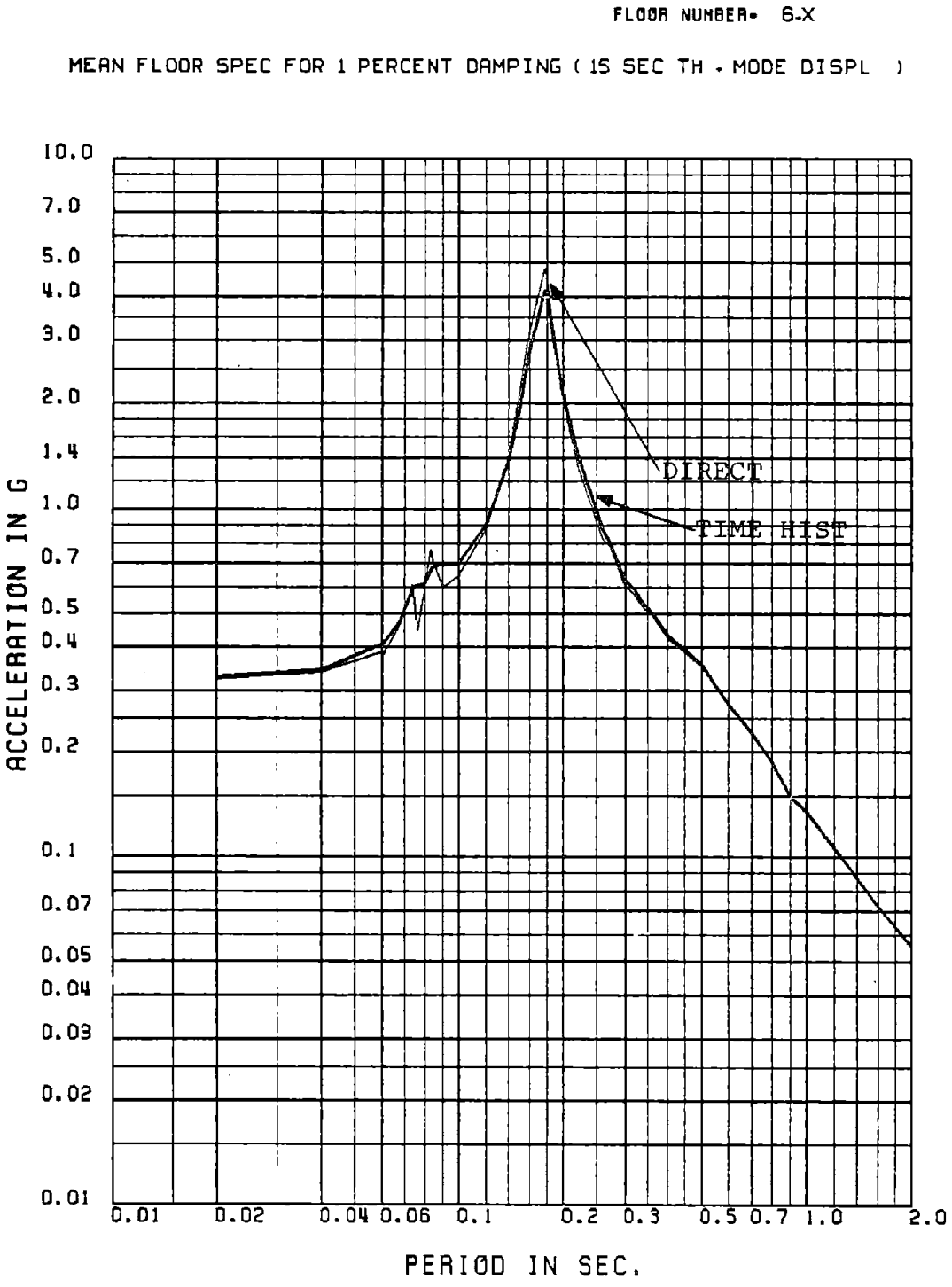

Fig. 2.29 Comparison of Floor Spectra Obtained by Mode Displacement Approach and Time History Analysis for 1% Damping: Mean Spectra, 15-sec TH, Floor No. 6-X, 11-FRQ Model

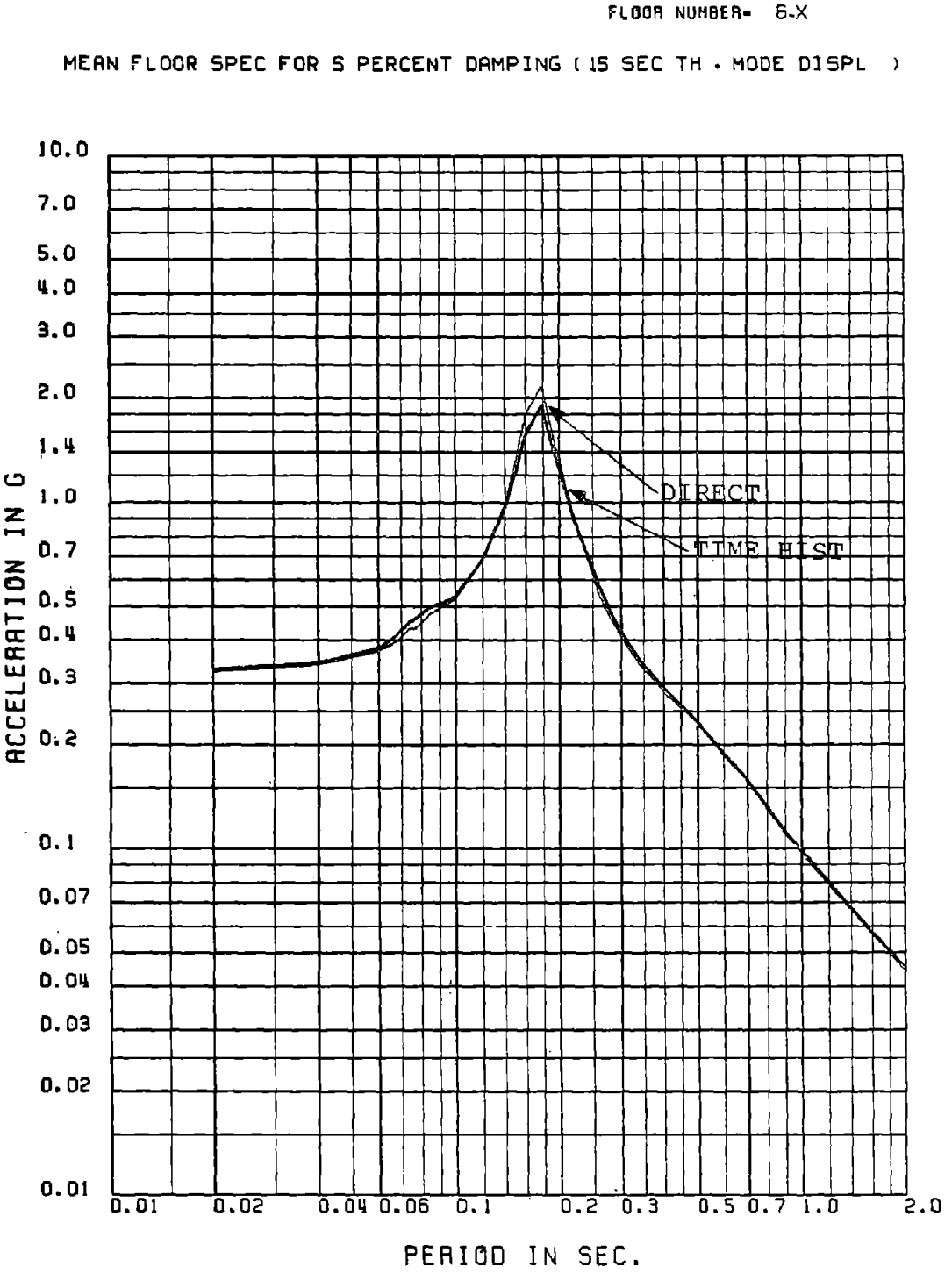

Fig. 2.30 Comparison of Floor Spectra Obtained by Mode Displacement Approach and Time History Analysis for 5% Damping: Mean Spectra, 15-sec TH, Floor No. 6-X, 11-FRQ Model

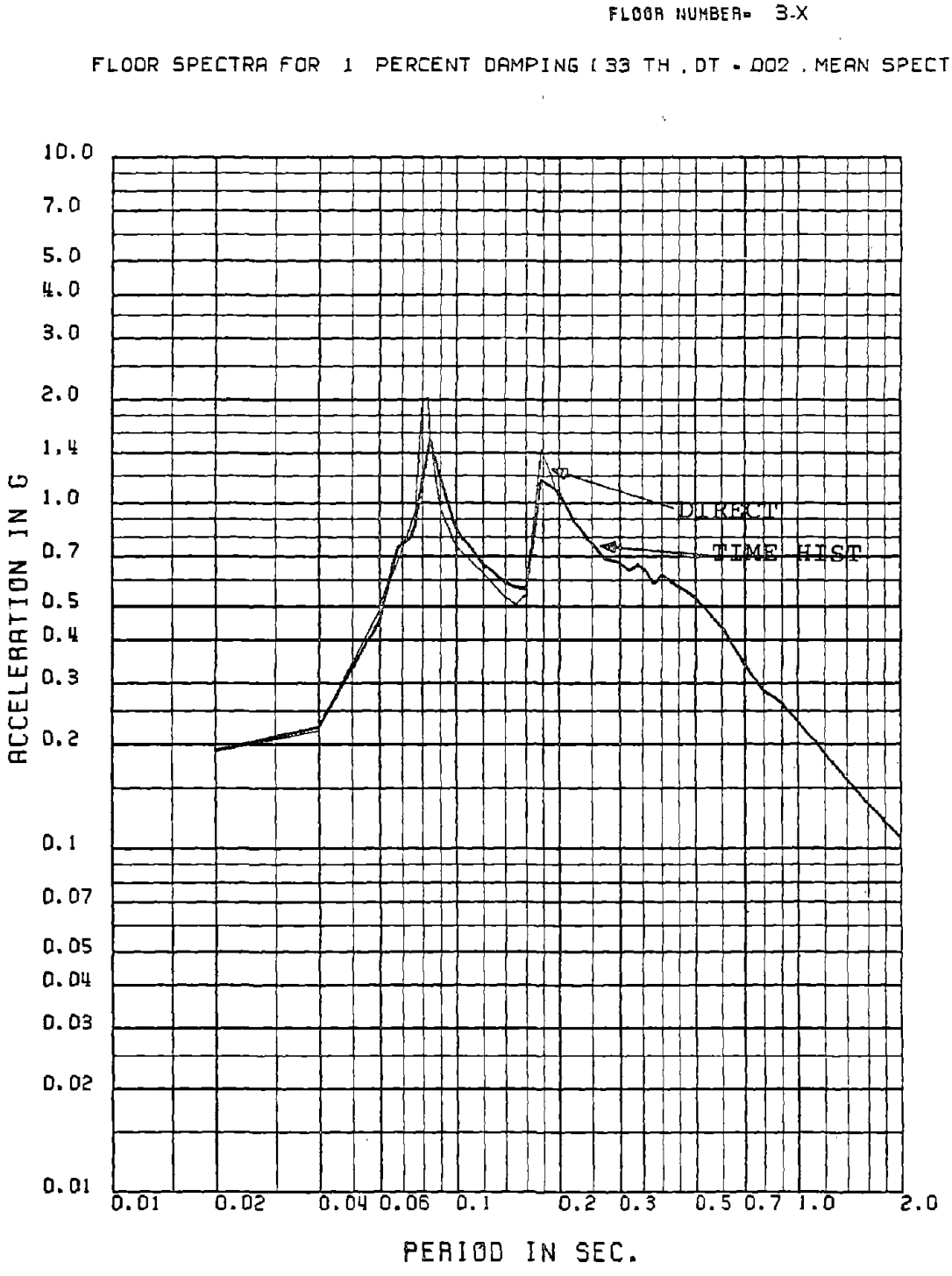

Fig. 2.31 Comparison of Floor Spectra Obtained by Mode Displacement Approach and Time History Analysis for 1% Damping: Mean Spectra, 30-sec TH, Floor No. 3-X, 11-FRQ Model

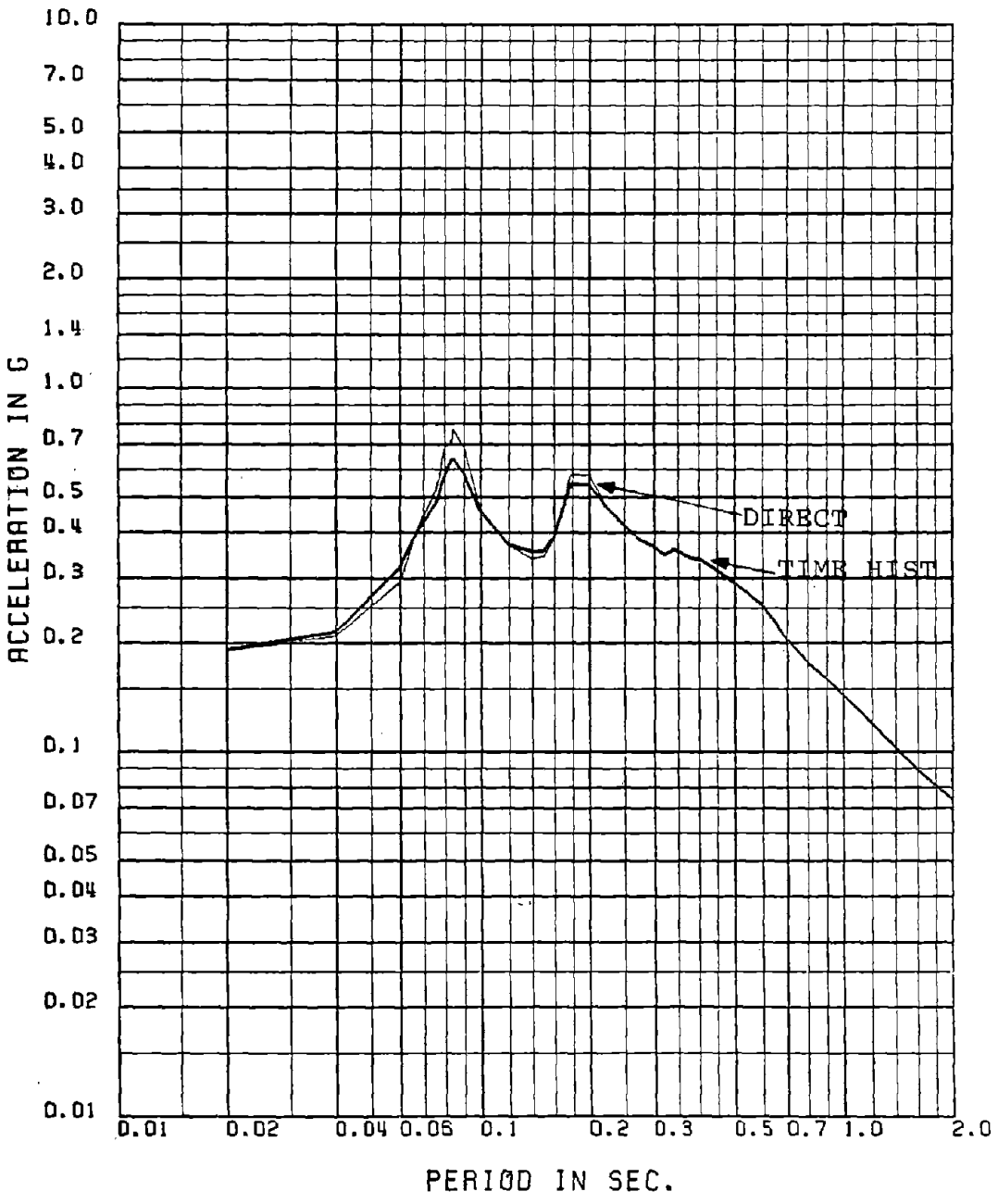

Fig. 2.32 Comparison of Floor Spectra Obtained by Mode Displacement Approach and Time History Analysis for 5% Damping: Mean Spectra, 30-sec TH, Floor No. 3-X, 11-FRQ Model

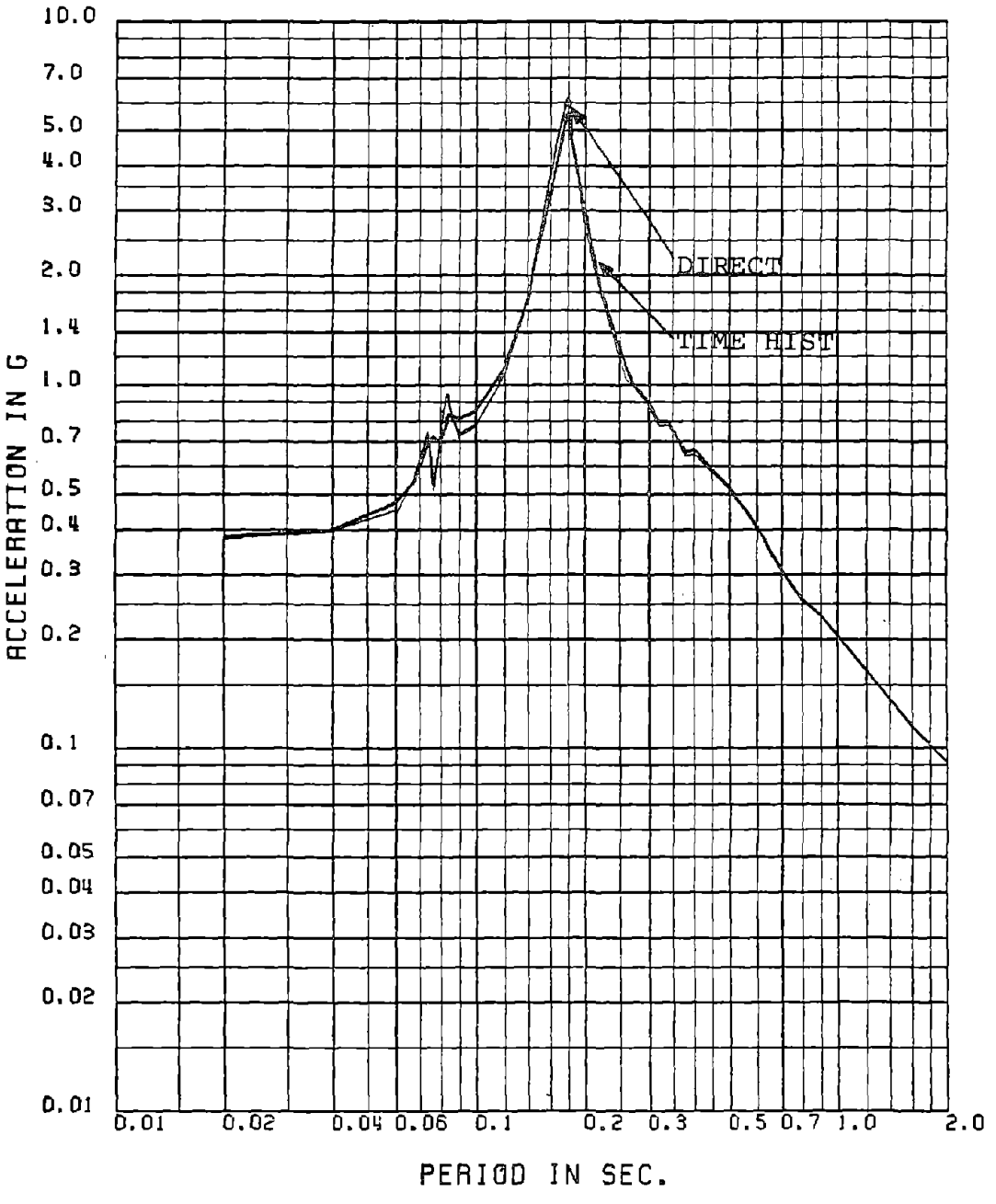

Fig. 2.33 Comparison of Floor Spectra Obtained by Mode Displacement Approach and Time History Analysis for 1% Damping: Mean Spectra, 30-sec TH, Floor No. 6-X, 11-FRQ Model

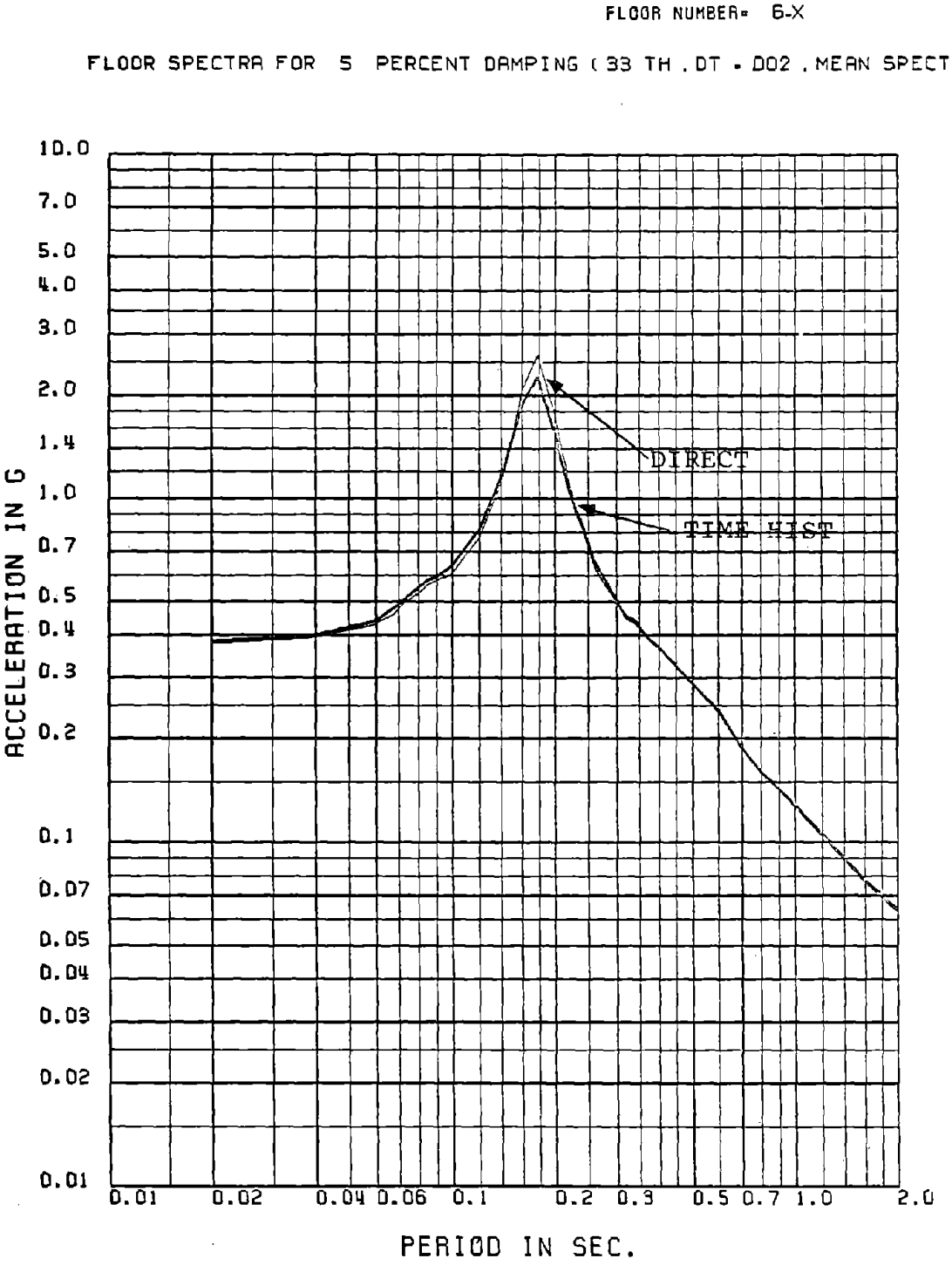

Fig. 2.34 Comparison of Floor Spectra Obtained by Mode Displacement Approach and Time History Analysis for 5% Damping: Mean Spectra, 30-sec TH, Floor No. 6-X, 11-FRQ Model

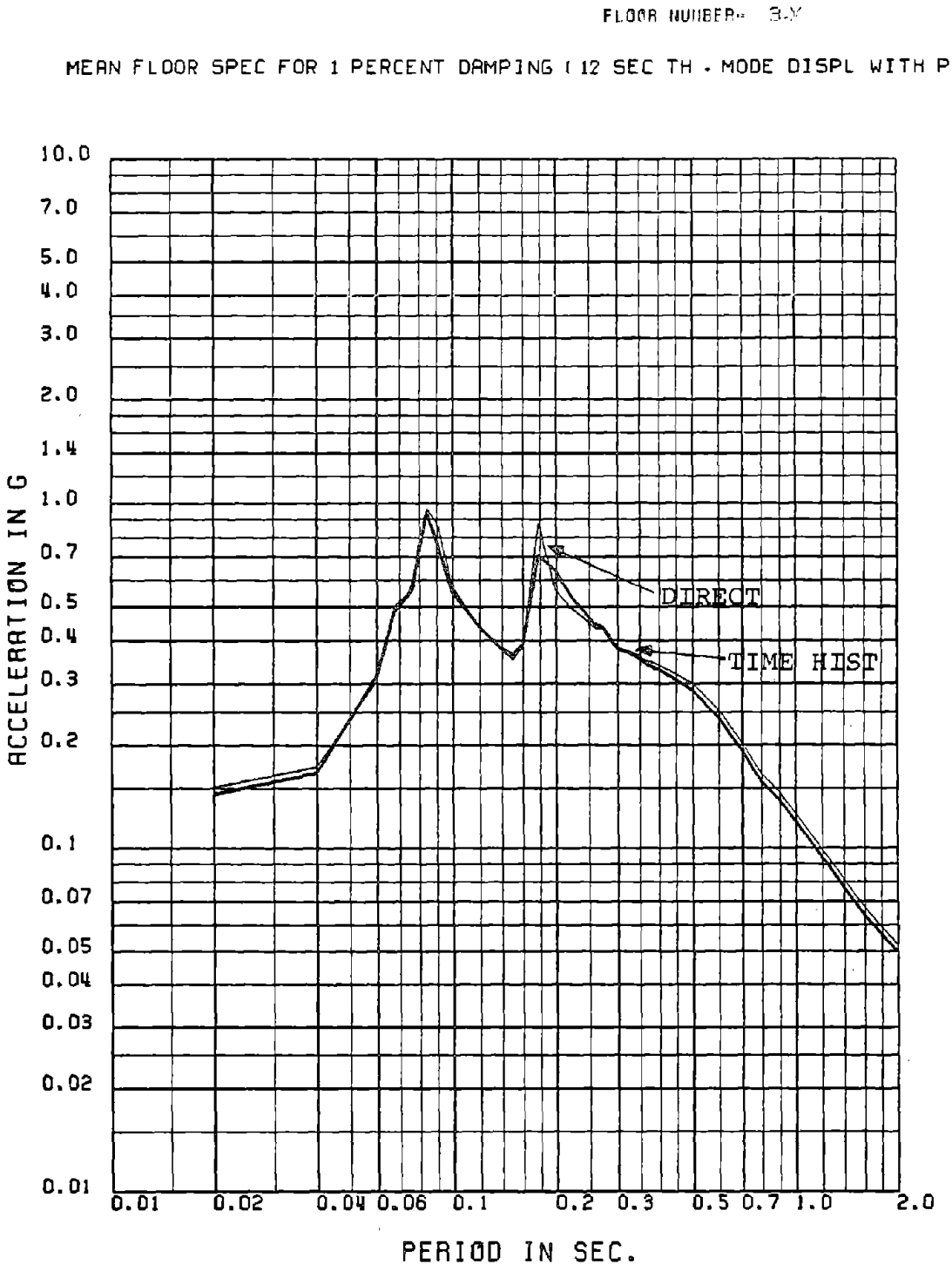

Fig. 2.35 Comparison of Floor Spectra Obtained by Mode Displacement Approach with Peak Factors (3-T, K-T PSDF) and Time History Analysis for 1% Damping: Mean Spectra, 12-sec TH, Floor No. 3-X, 11-FRQ Model

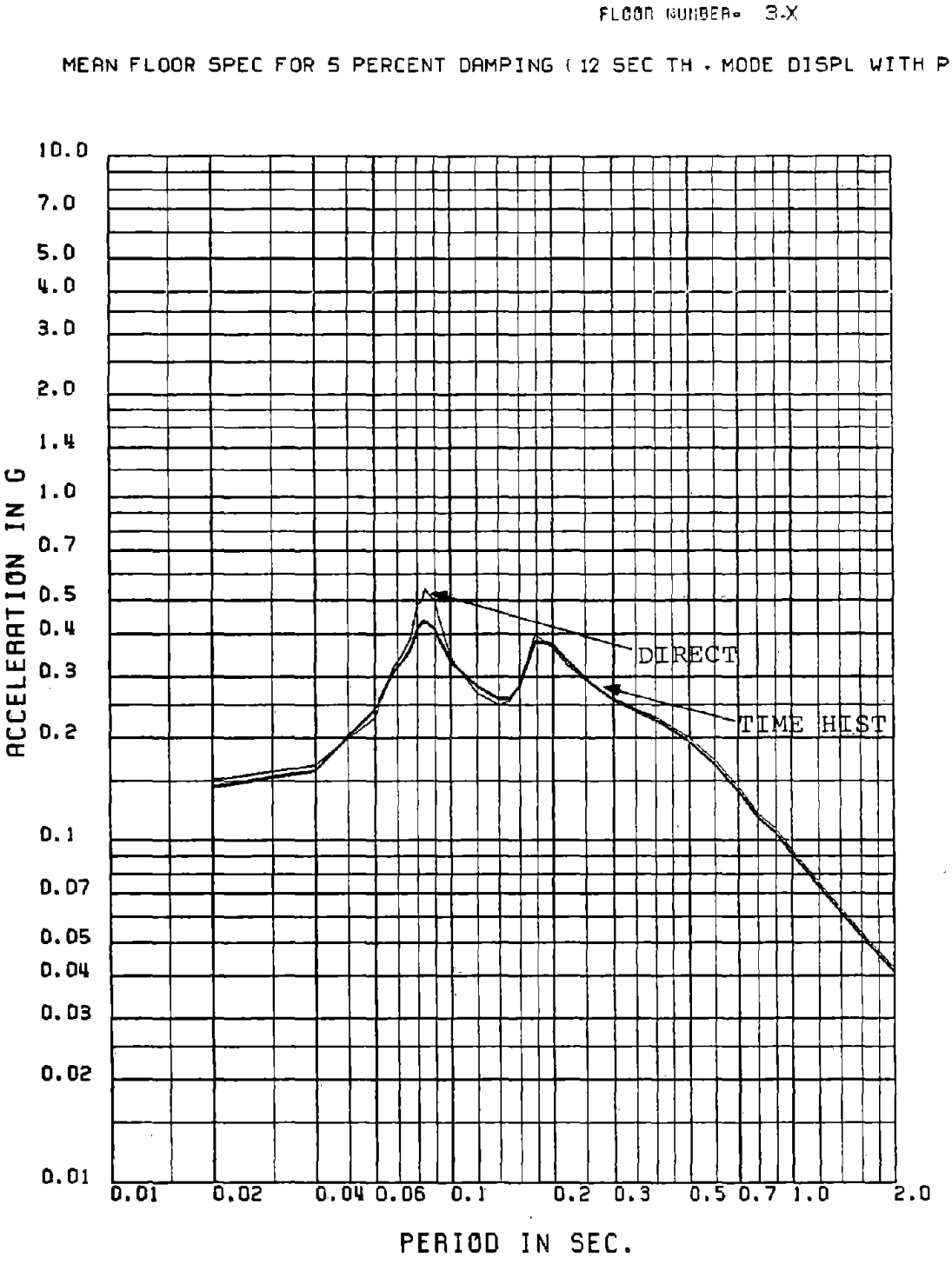

Fig. 2.36 Comparison of Floor Spectra Obtained by Mode Displacement Approach with Peak Factors (3-T, K-T PSDF) and Time History Analysis for 5% Damping: Mean Spectra, 12-sec TH, Floor No. 3-X, 11-FRQ Model

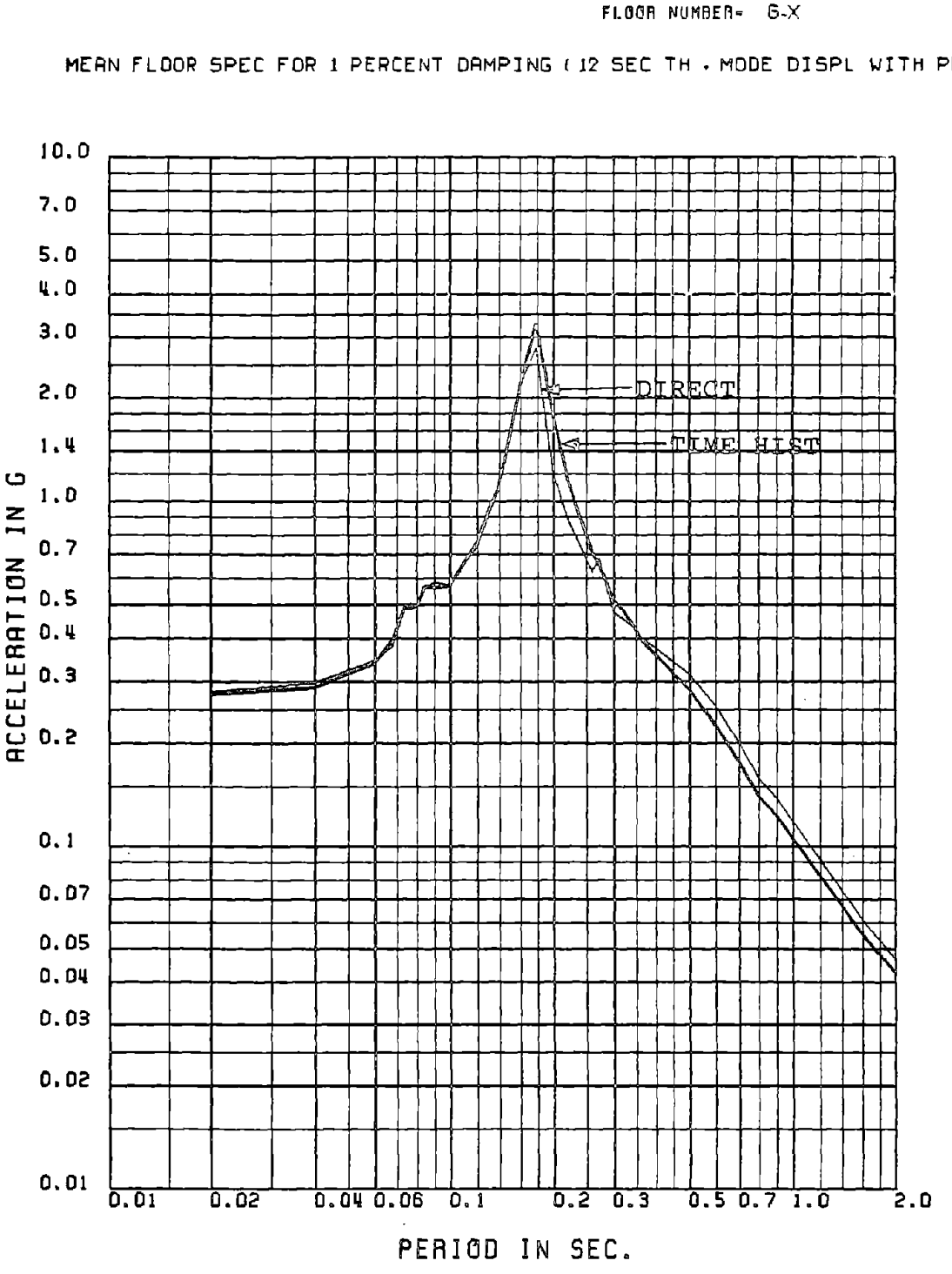

Fig. 2.37 Comparison of Floor Spectra Obtained by Mode Displacement Approach with Peak Factors (3-T, K-T PSDF) and Time History Analysis for 1% Damping: Mean Spectra, 12-sec TH, Floor No. 6-X, 11-FRQ Model

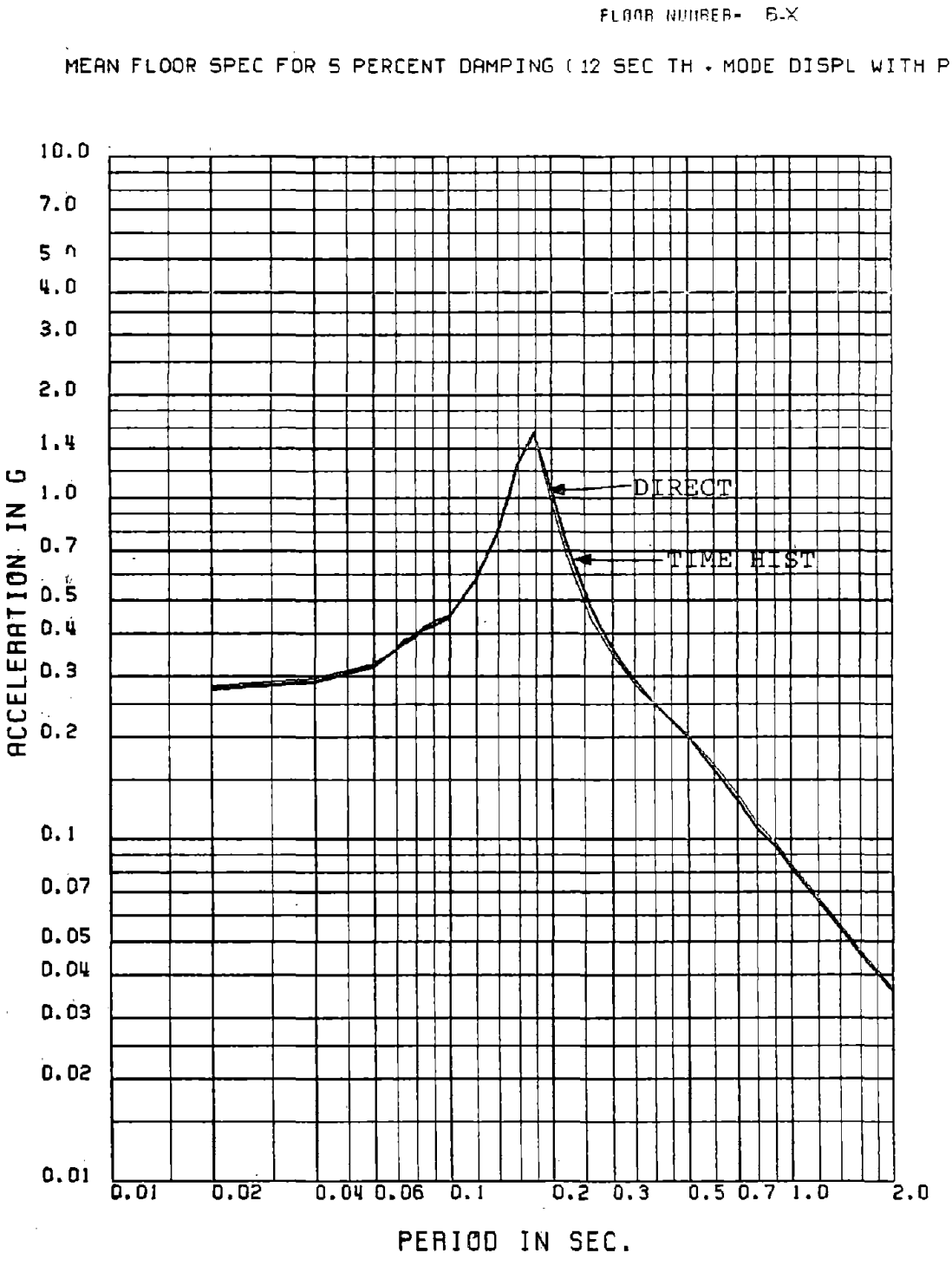

Fig. 2.38 Comparison of Floor Spectra Obtained by Mode Displacement Approach with Peak Factors (3-T, K-T PSDF) and Time History Analysis for 5% Damping: Mean Spectra, 12-sec TH, Floor No. 6-X, 11-FRQ Model

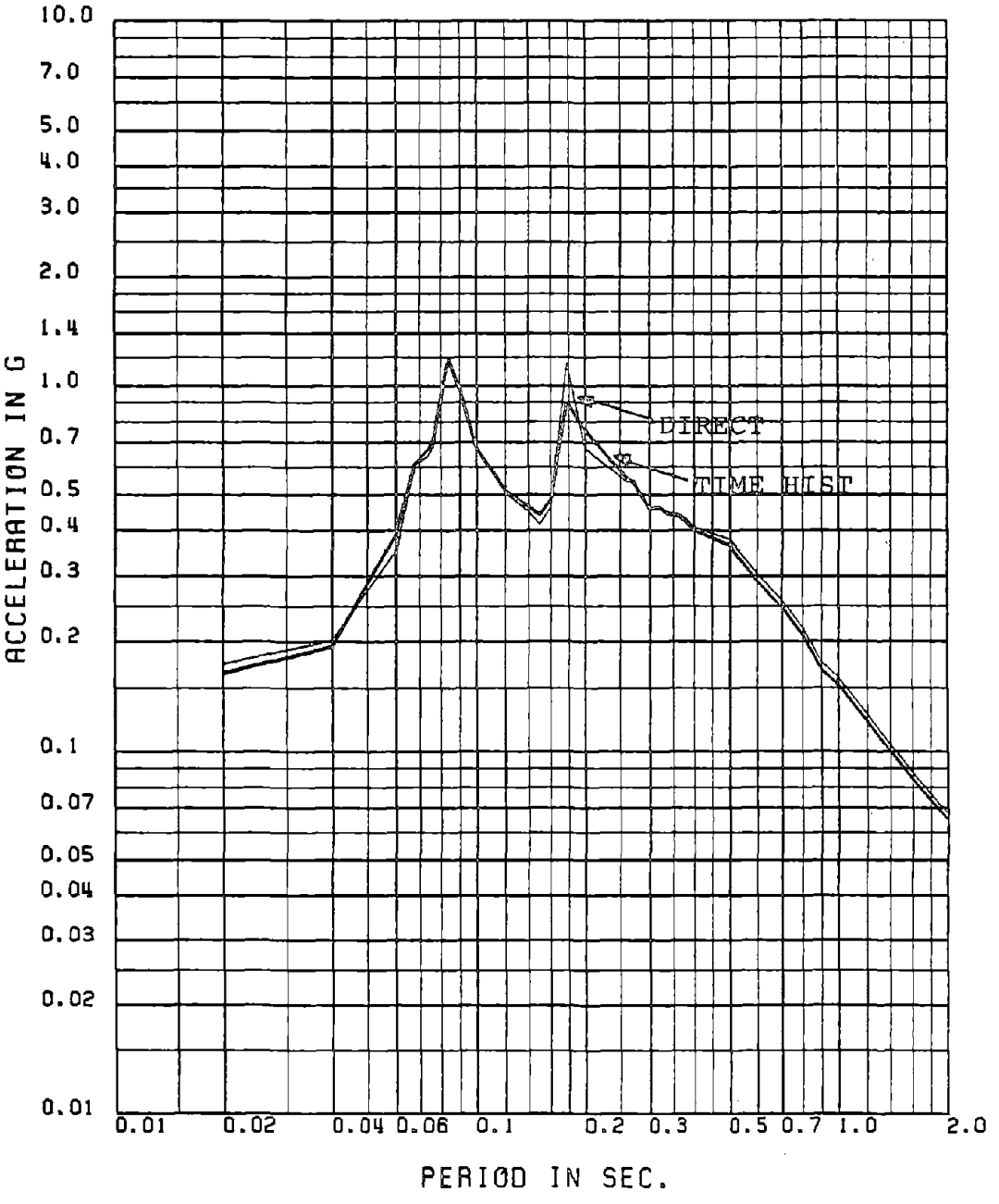

Fig. 2.39 Comparison of Floor Spectra Obtained by Mode Displacement Approach with Peak Factors (3-T, K-T PSDF) and Time History Analysis for 1% Damping: Mean Spectra, 15-sec TH, Floor No. 3-X, 11-FRQ Model

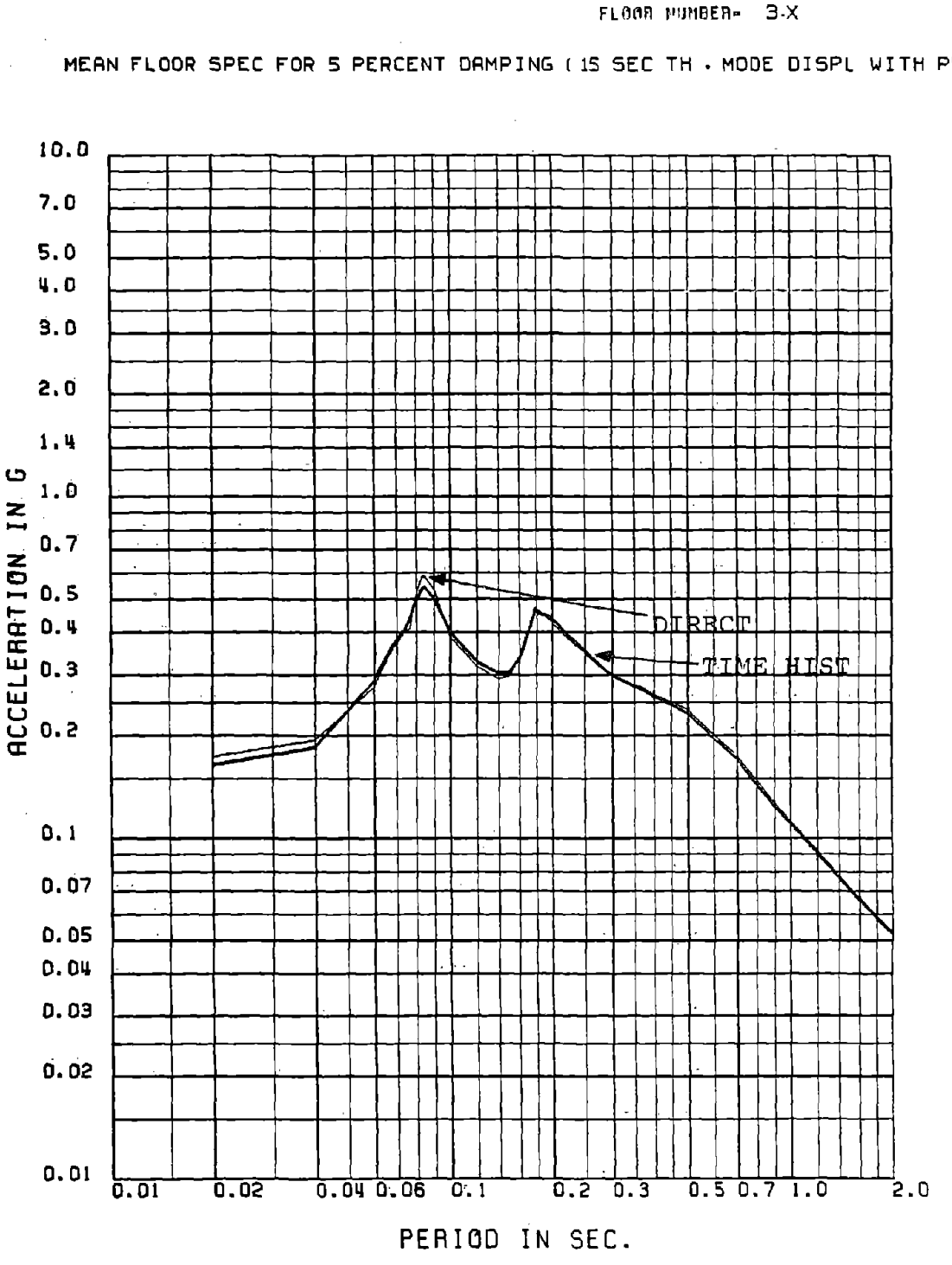

Fig. 2.40 Comparison of Floor Spectra Obtained by Mode Displacement Approach with Peak Factors (3-T, K-T PSDF) and Time History Analysis for 5% Damping: Mean Spectra, 15-sec TH, Floor No. 3-X, 11-FRQ Model

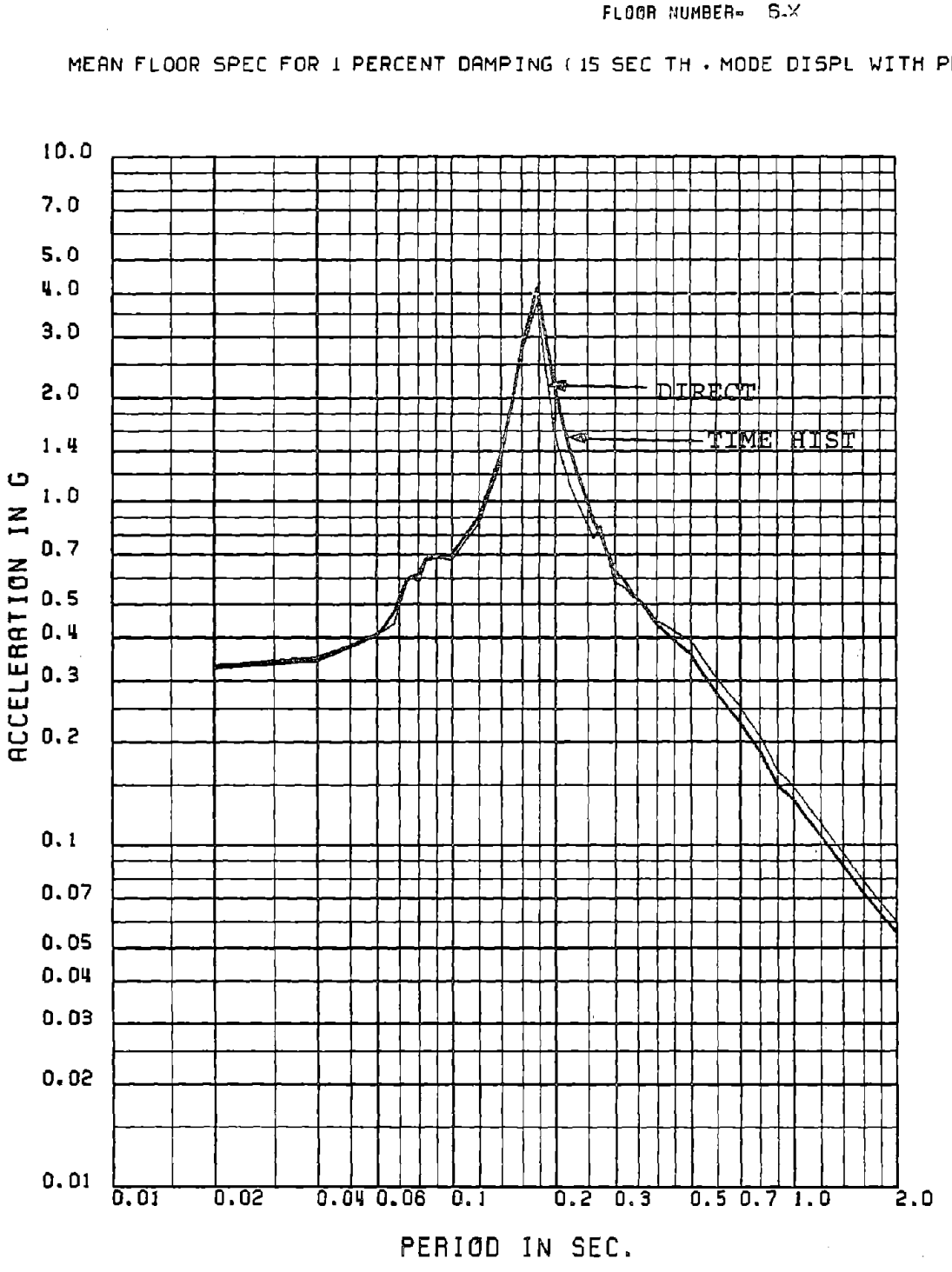

Fig. 2.41 Comparison of Floor Spectra Obtained by Mode Displacement Approach with Peak Factors (3-T, K-T PSDF) and Time History Analysis for 1% Damping: Mean Spectra, 15-sec TH, Floor No. 6-X, 11-FRQ Model

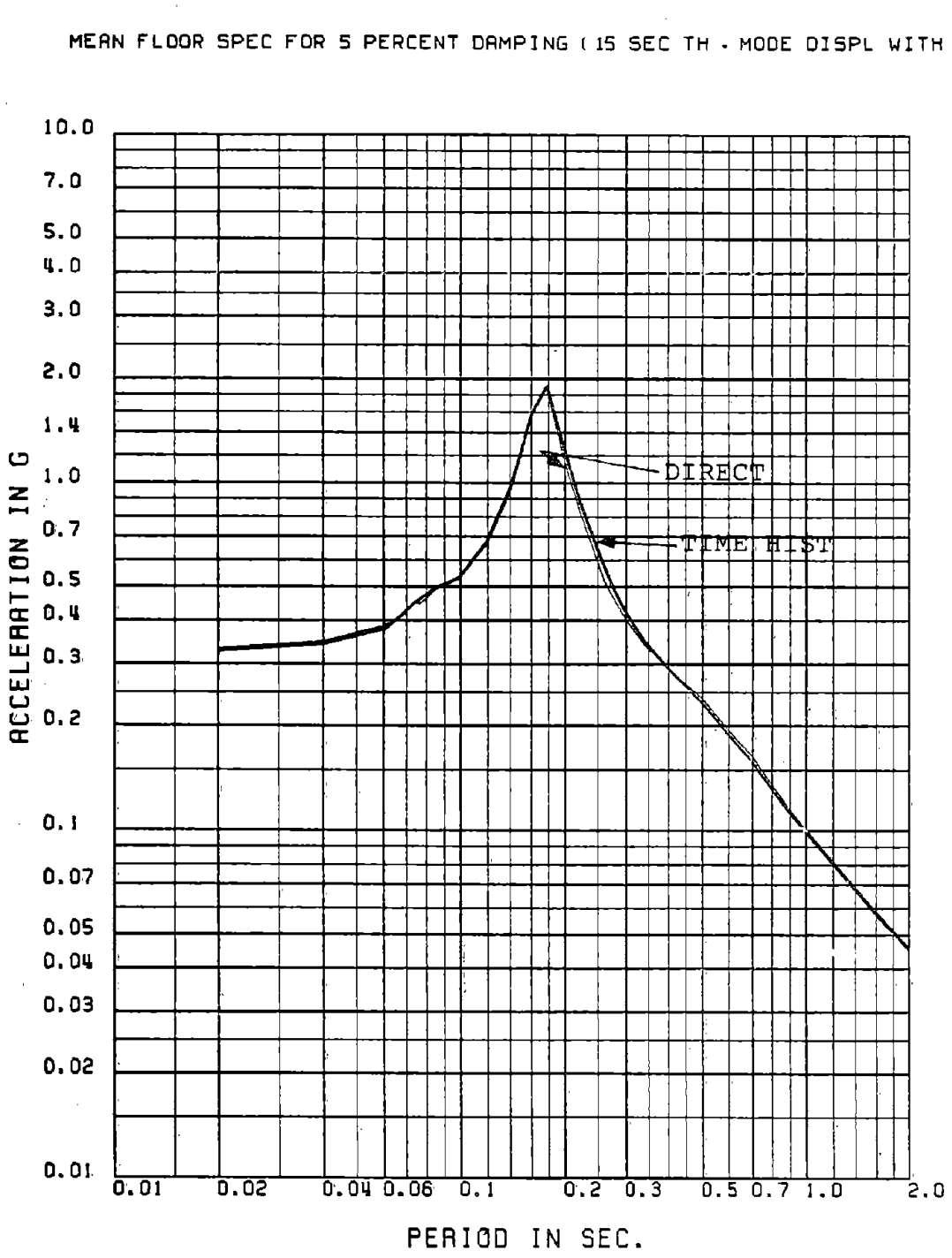

Fig. 2.42 Comparison of Floor Spectra Obtained by Mode Displacement Approach with Peak Factors (3-T, K-T PSDF) and Time History Analysis for 5% Damping: Mean Spectra, 15-sec TH, Floor No. 6-X, 11-FRQ Model

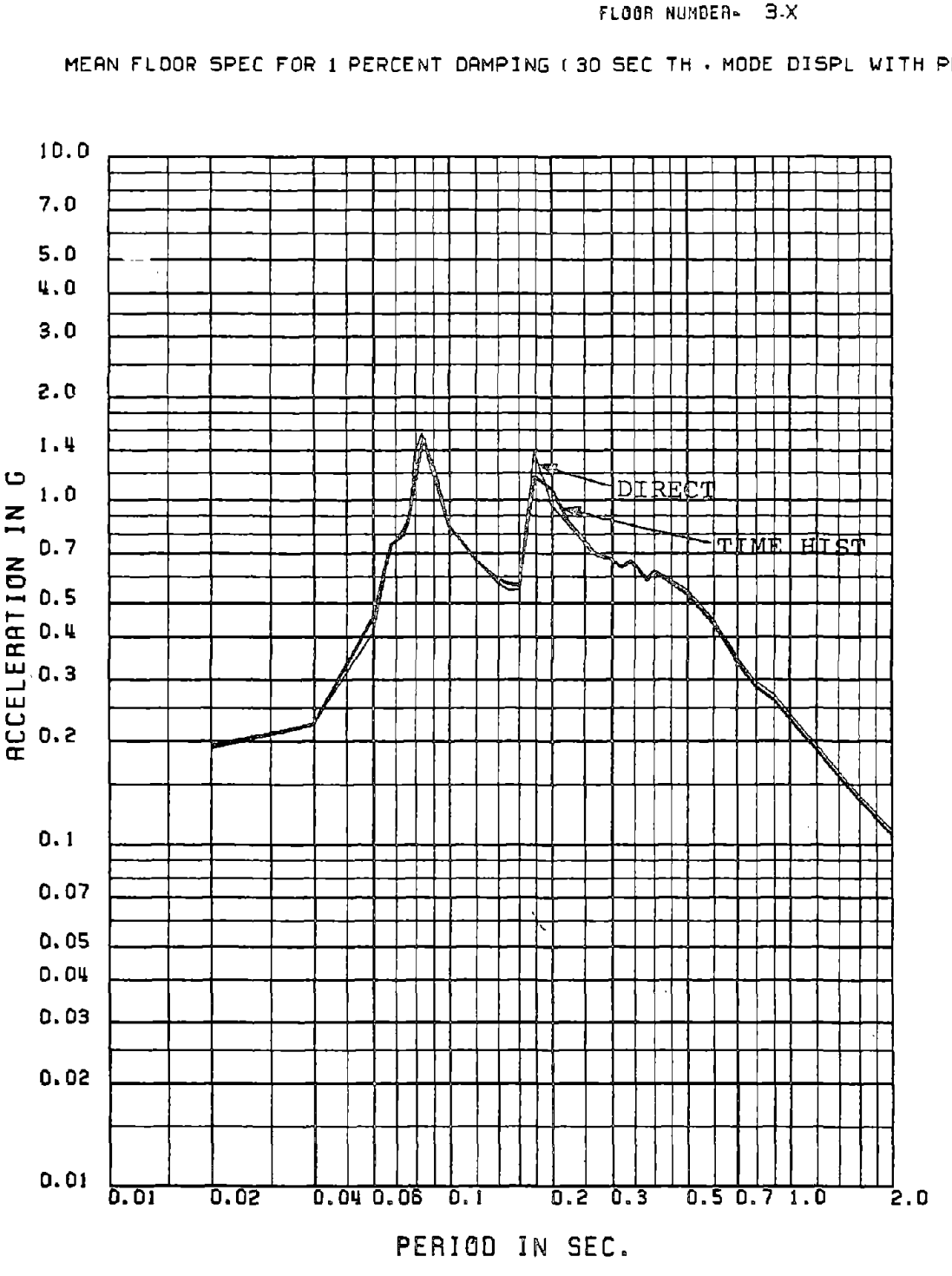

Fig. 2.43 Comparison of Floor Spectra Obtained by Mode Displacement Approach with Peak Factors (3-T, K-T PSDF) and Time History Analysis for 1% Damping: Mean Spectra, 30-sec TH, Floor No. 3-X, 11-FRQ Model

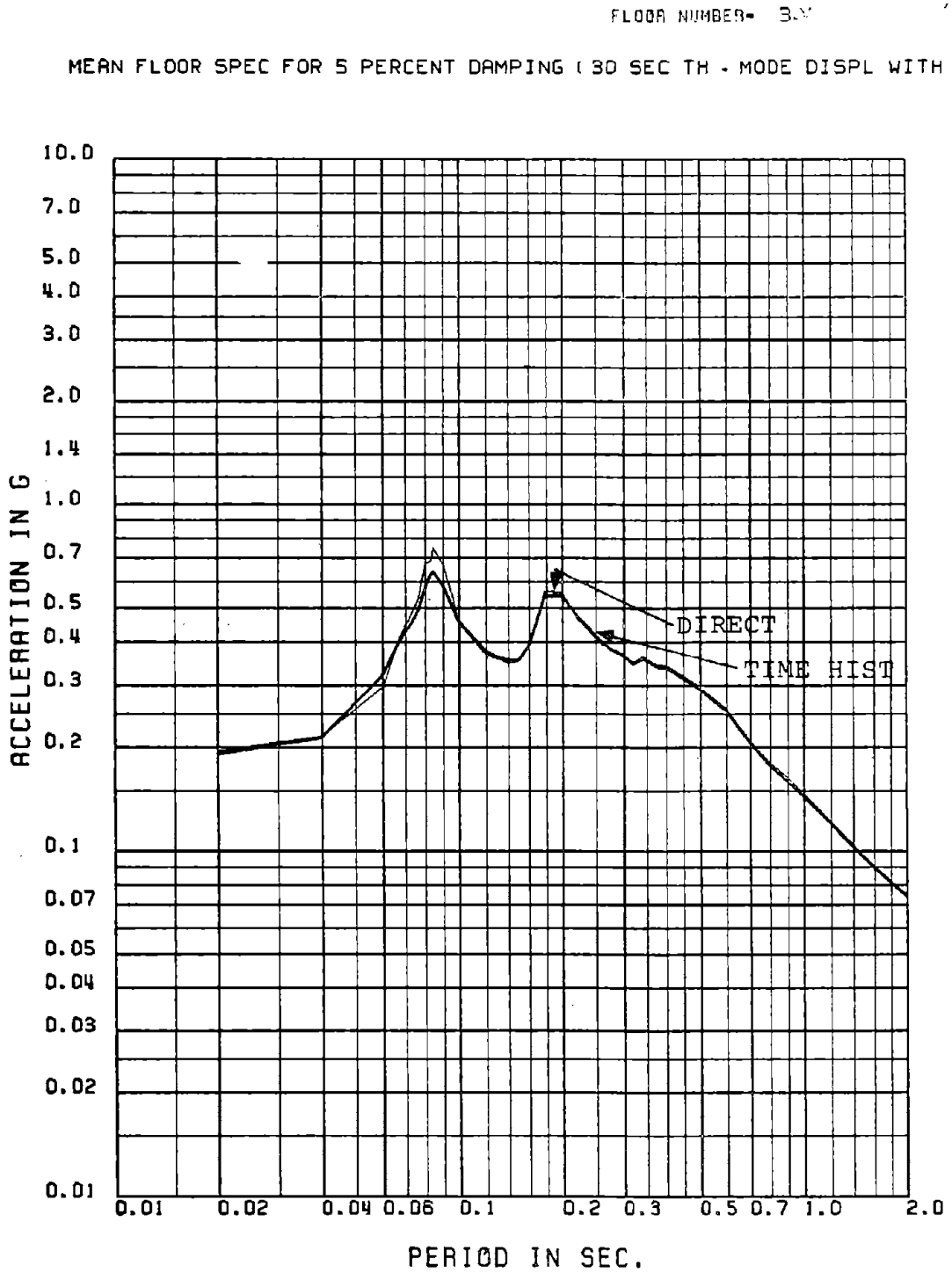

Fig. 2.44 Comparison of Floor Spectra Obtained by Mode Displacement Approach with Peak Factors (3-T, K-T PSDF) and Time History Analysis for 5% Damping: Mean Spectra, 30-sec TH, Floor No. 3-X, 11-FRQ Model

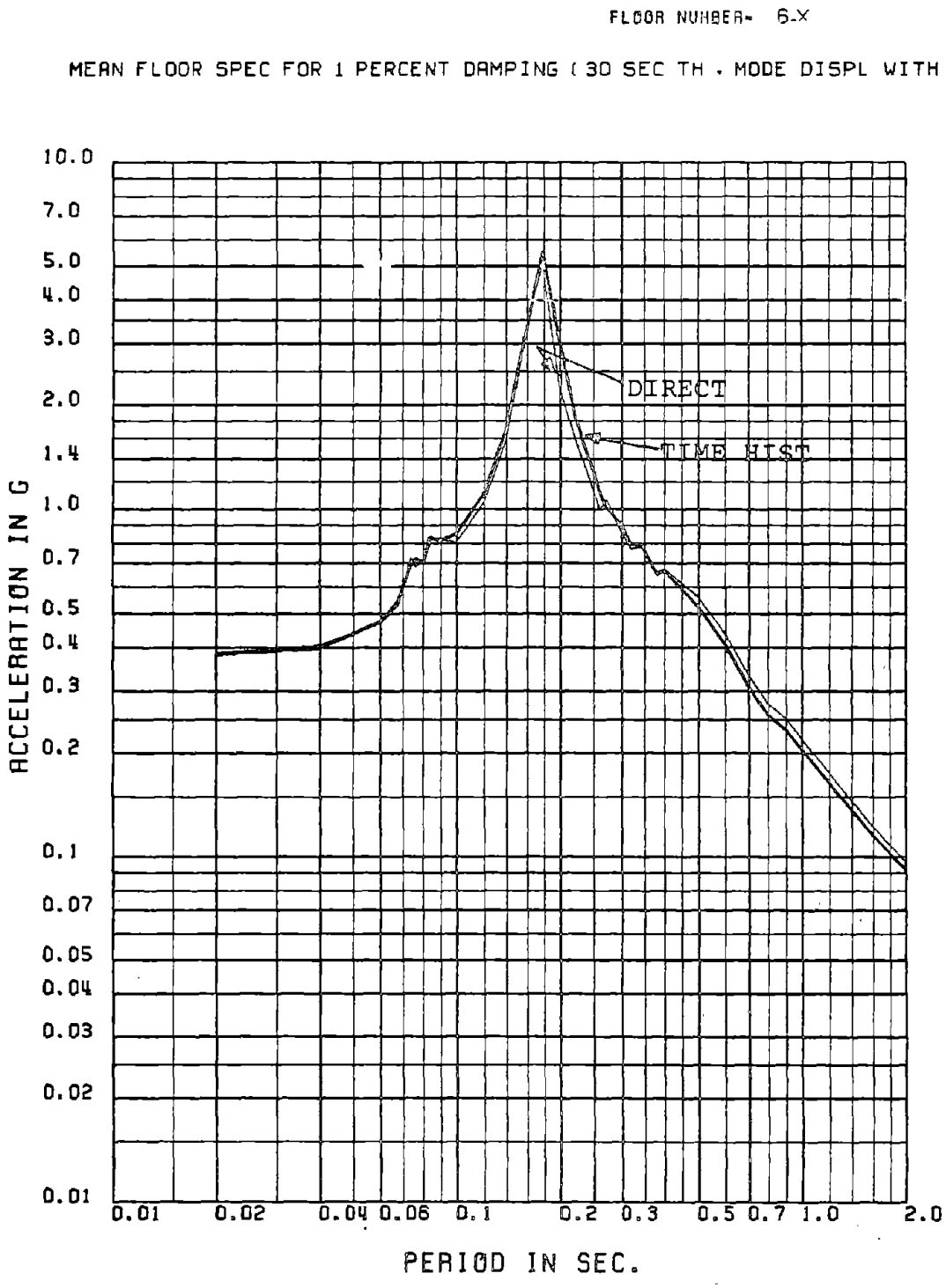

Fig. 2.45 Comparison of Floor Spectra Obtained by Mode Displacement Approach with Peak Factors (3-T, K-T PSDF) and Time History Analysis for 1% Damping: Mean Spectra, 30-sec TH, Floor No. 6-X, 11-FRQ Model

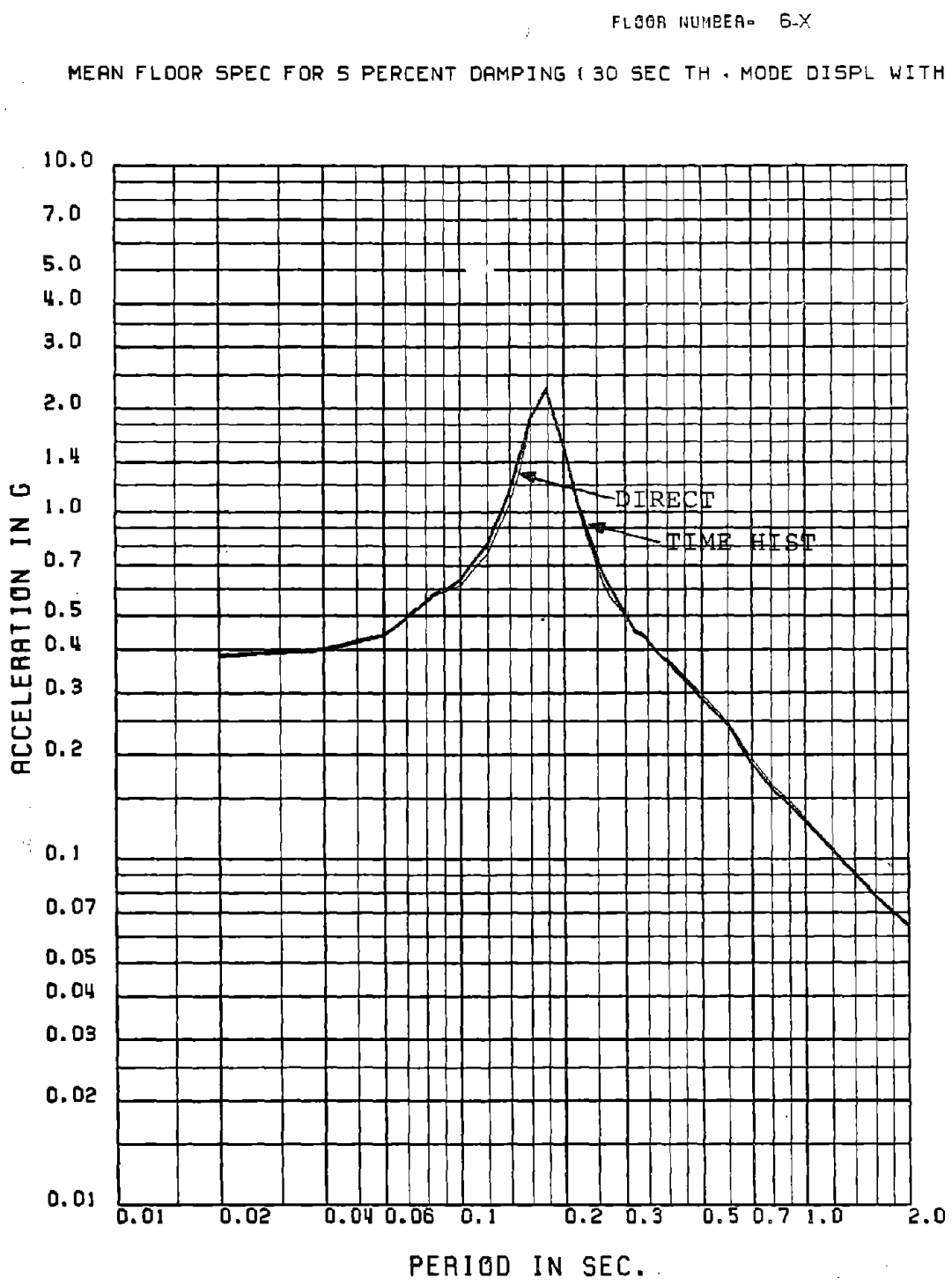

Fig. 2.46 Comparison of Floor Spectra Obtained by Mode Displacement Approach with Peak Factors (3-T, K-T PSDF) and Time History Analysis for 5% Damping: Mean Spectra, 30-sec TH, Floor No. 6-X, 11-FRQ Model

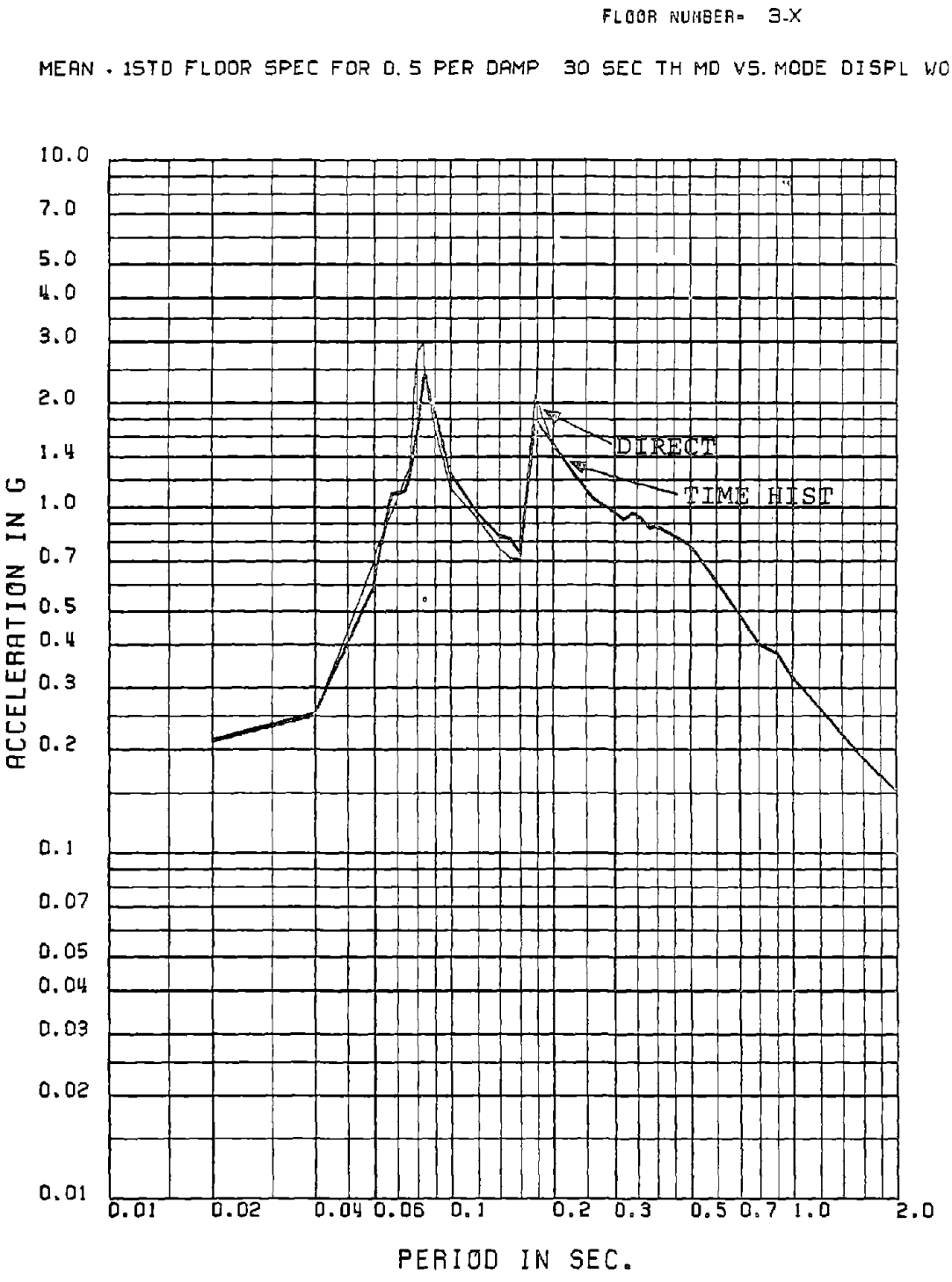

Fig. 2.47 Comparison of Floor Spectra Obtained by Mode Displacement Approach and Time History Analysis for 0.5% Damping: Mean + 1 Standard Deviation Spectra, 30-sec TH, Floor No. 3-X, 11-FRQ Model

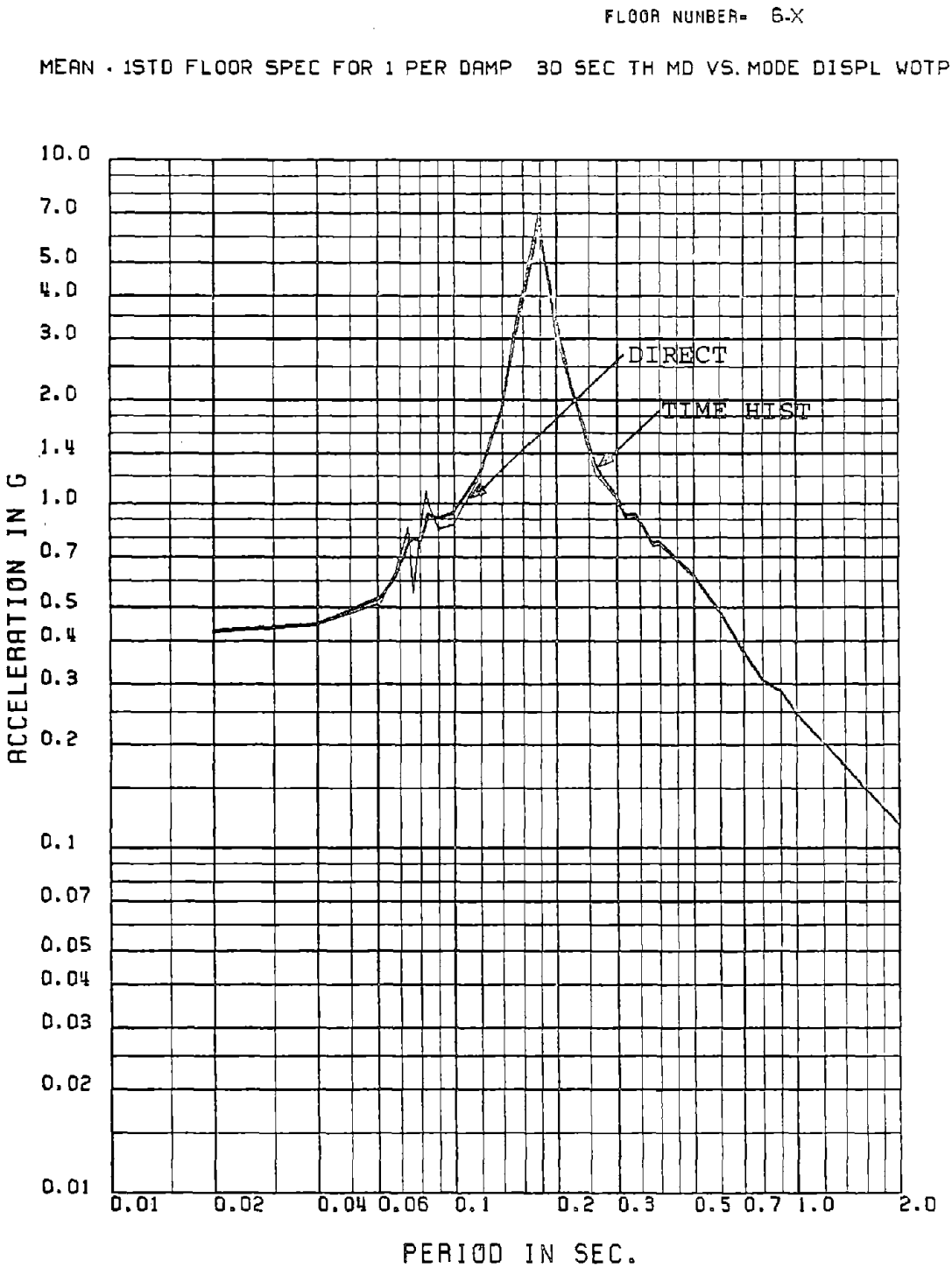

Fig. 2.48 Comparison of Floor Spectra Obtained by Mode Displacement Approach and Time History Analysis for 1% Damping: Mean + 1 Standard Deviation Spectra, 30-sec TH, Floor No. 6-X, 11-FRQ Model

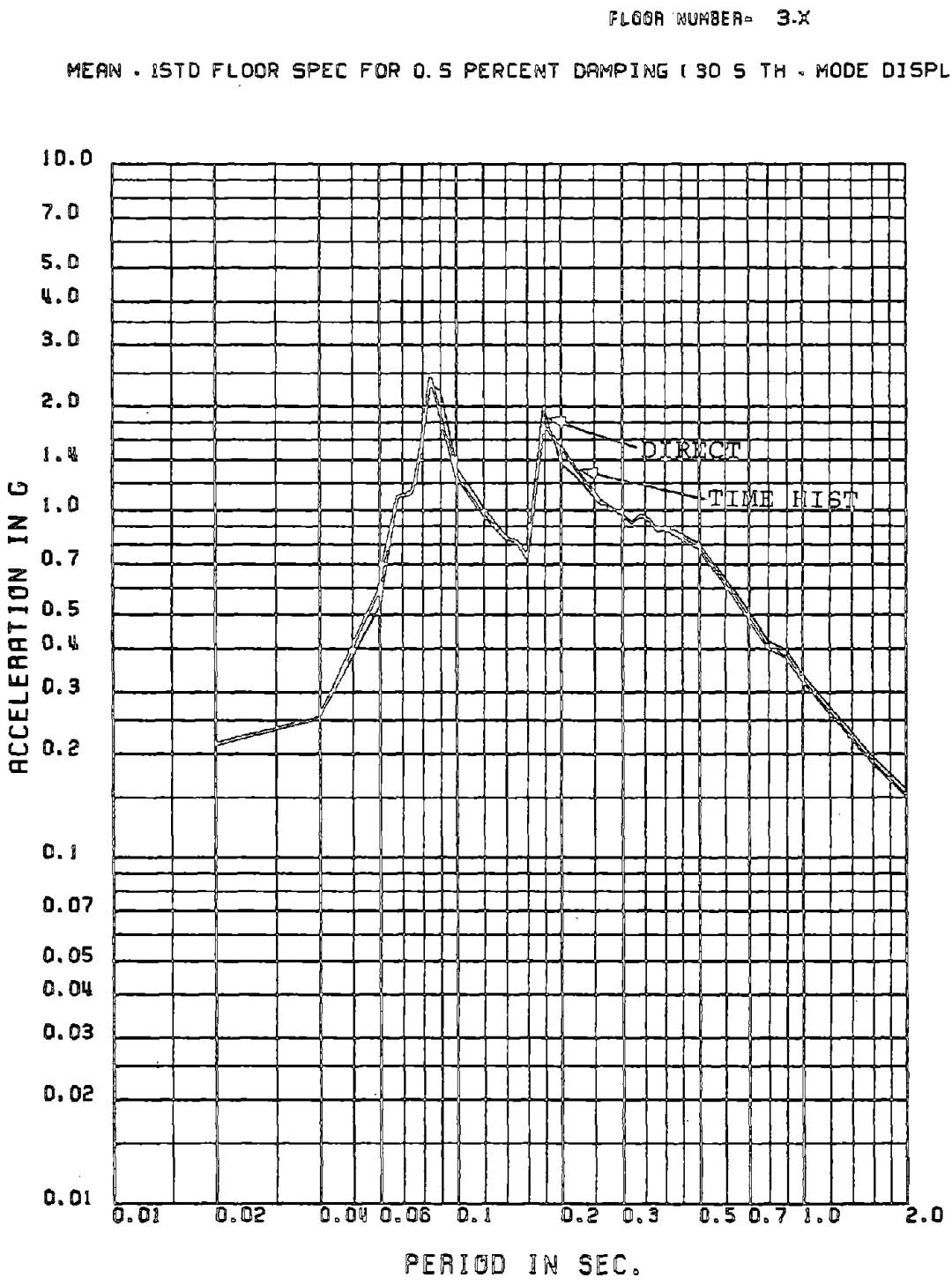

Fig. 2.49 Comparison of Floor Spectra Obtained by Mode Displacement Approach with Peak Factors (3-T, K-T PSDF) and Time History Analysis for 0.5% Damping: Mean + 1 Standard Deviation Spectra, 30-sec TH, Floor No. 3-X, 11-FRQ Model

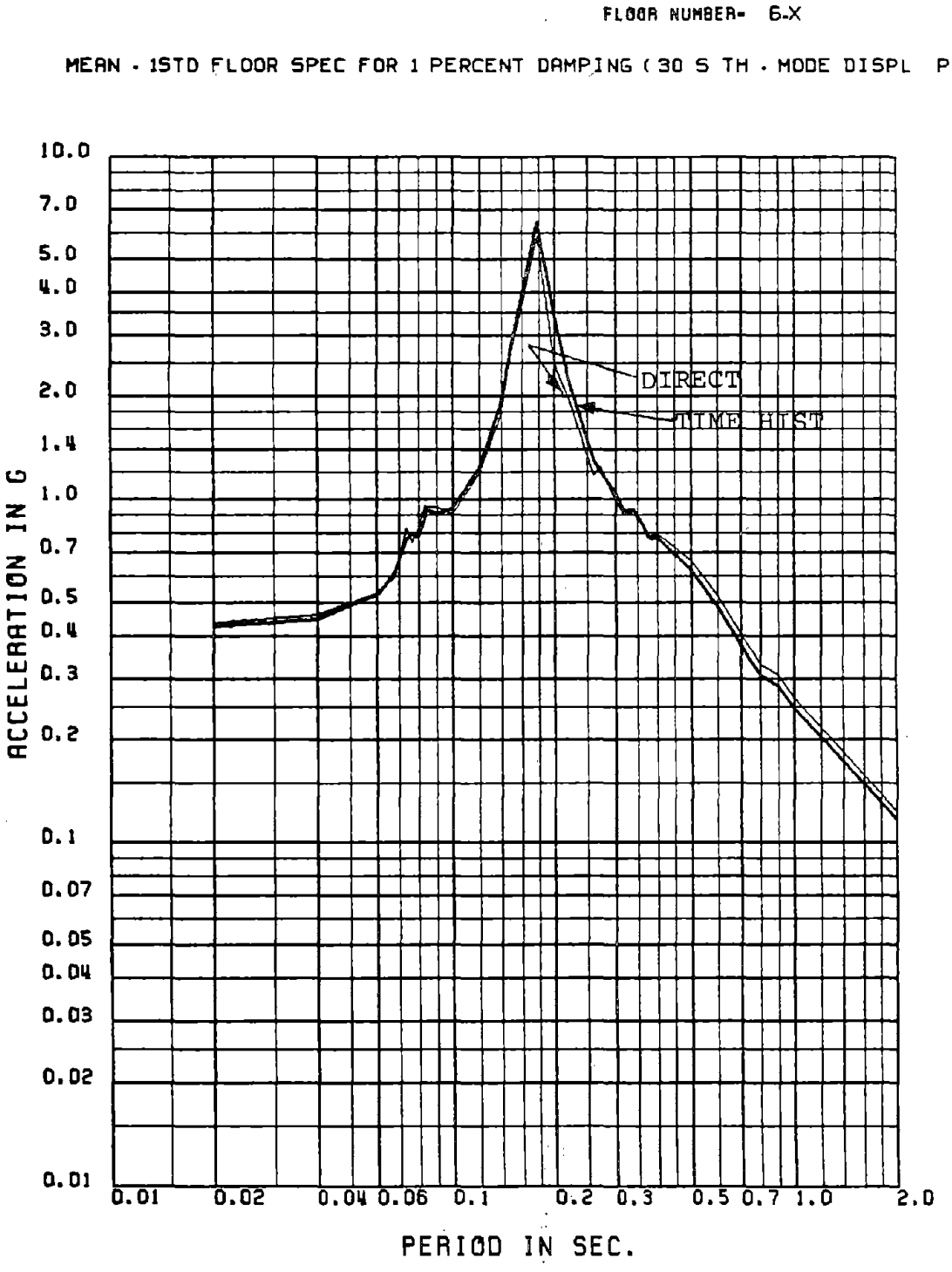

Fig. 2.50 Comparison of Floor Spectra Obtained by Mode Displacement Approach with Peak Factors (3-T, K-T PSDF) and Time History Analysis for 1% Damping: Mean + 1 Standard Deviation Spectra, 30-sec TH, Floor 6-X, 11-FRQ Model

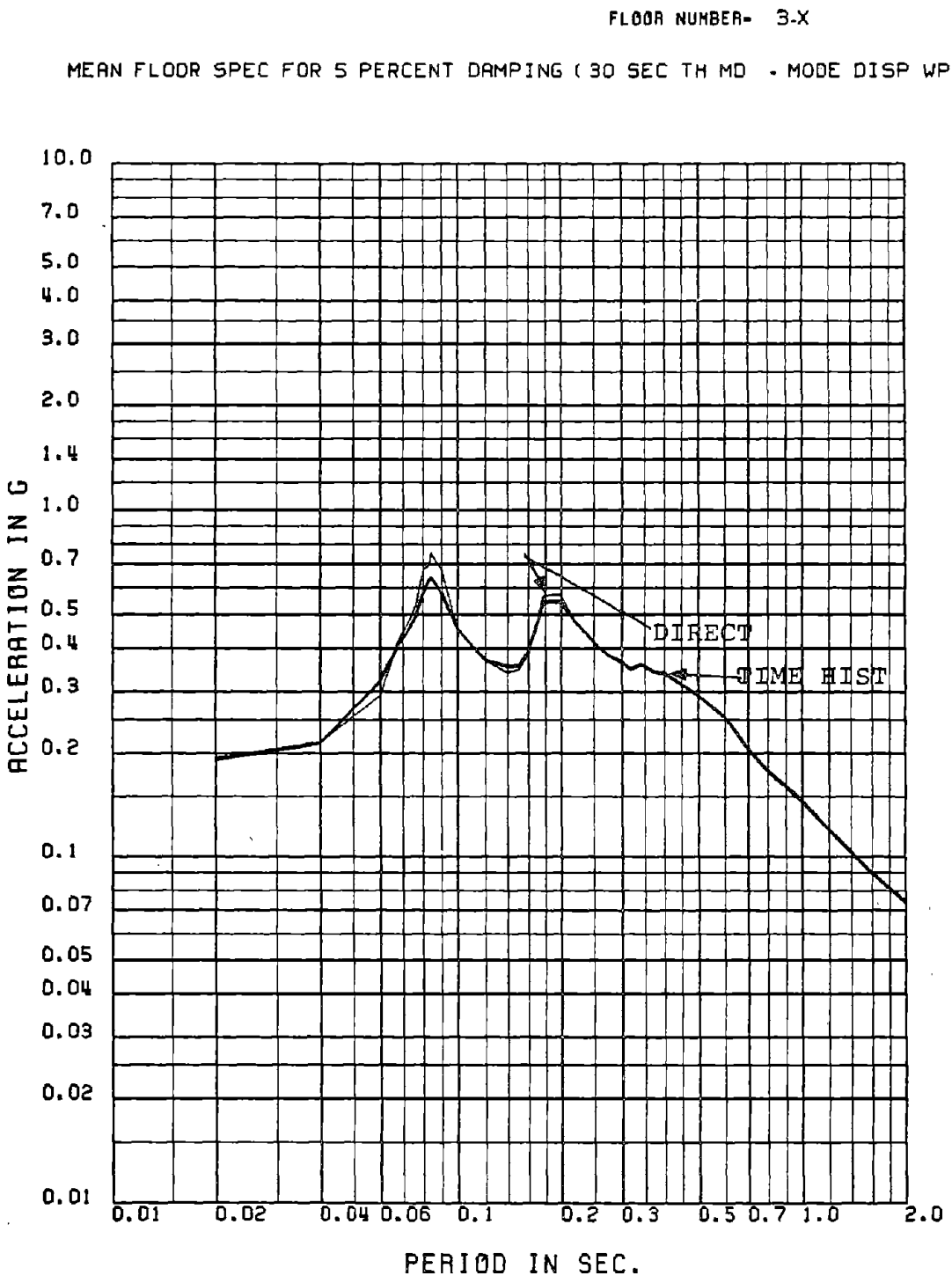

Fig. 2.52 Comparison of Floor Spectra Obtained by Mode Displacement Approach with Peak Factors (1-T, K-T PSDF) and Time History Analysis for 5% Damping: Mean Spectra, 30-sec TH, Floor No. 3-X, 11-FRQ Model

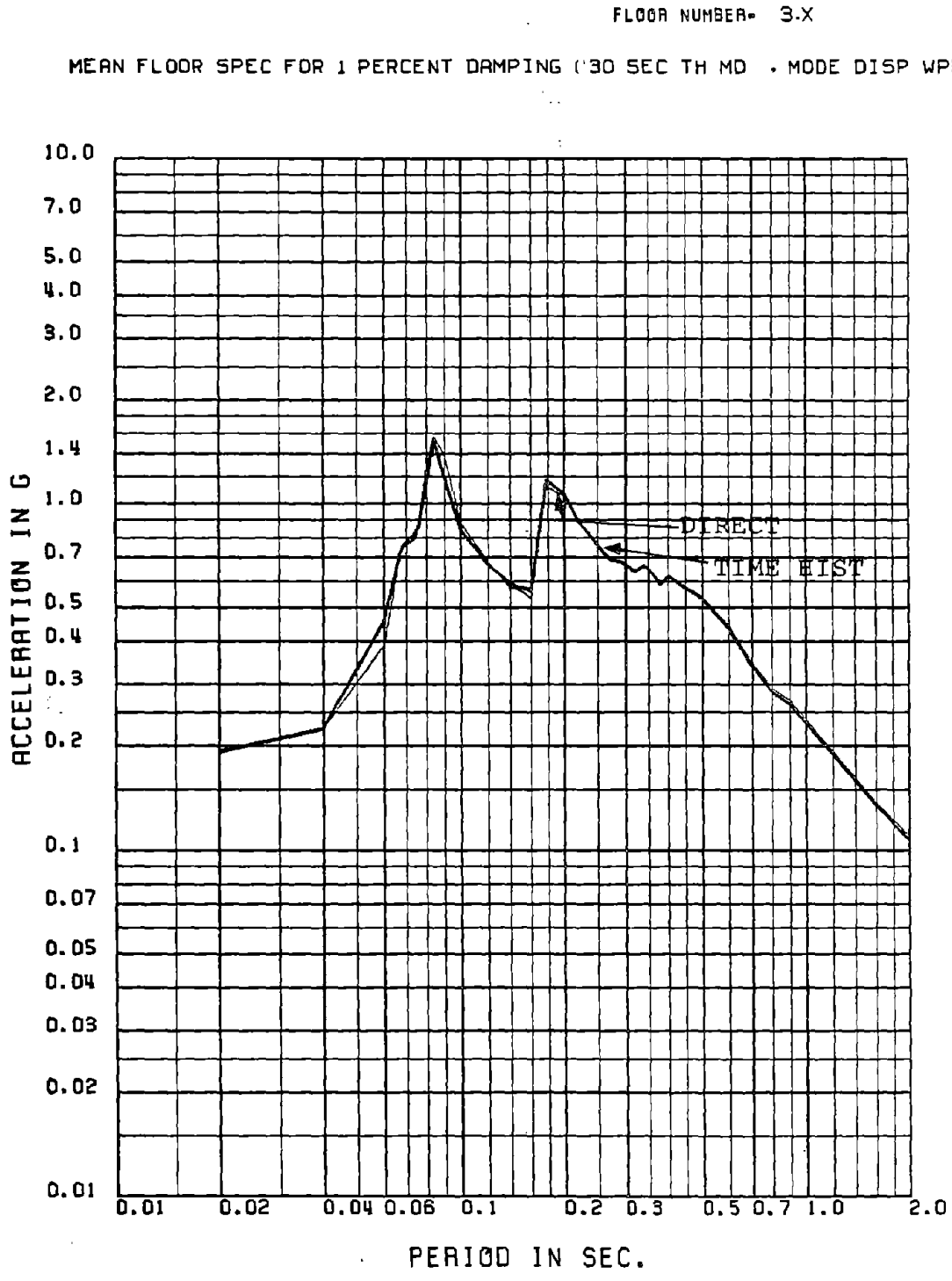

Fig. 2.51 Comparison of Floor Spectra Obtained by Mode Dispalcement Approach with Peak Factors (1-T, K-T PSDF) and Time History Analysis for 1% Damping: Mean Spectra, 30-sec TH, Floor No. 3-X, 11-FRQ Model

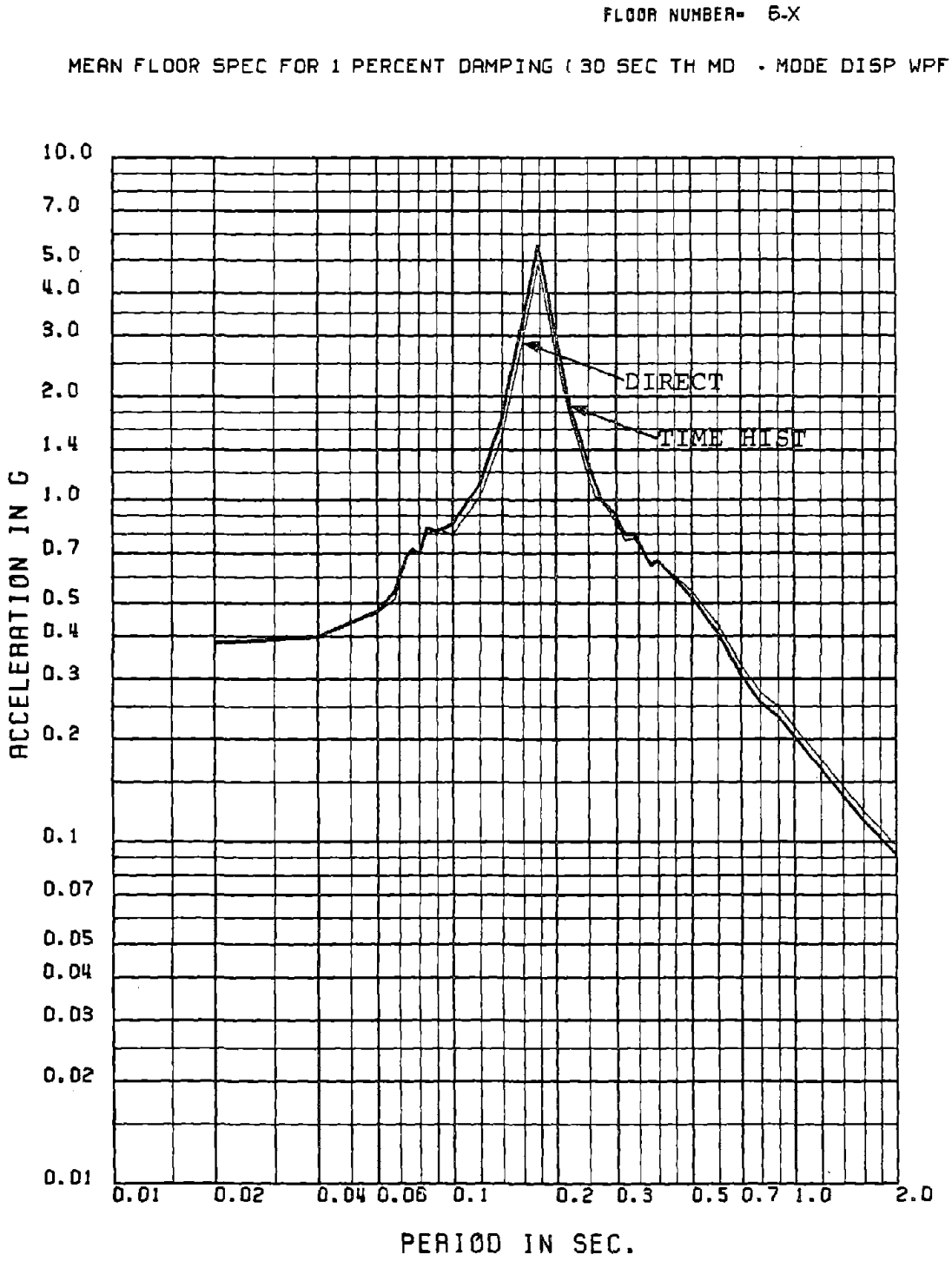

Fig. 2.53 Comparison of Floor Spectra Obtained by Mode Displacement Approach with Peak Factors (1-T, K-T PSDF) and Time History Analysis for 1% Damping: Mean Spectra, 30-sec TH, Floor No. 6-X, 11-FRQ Model

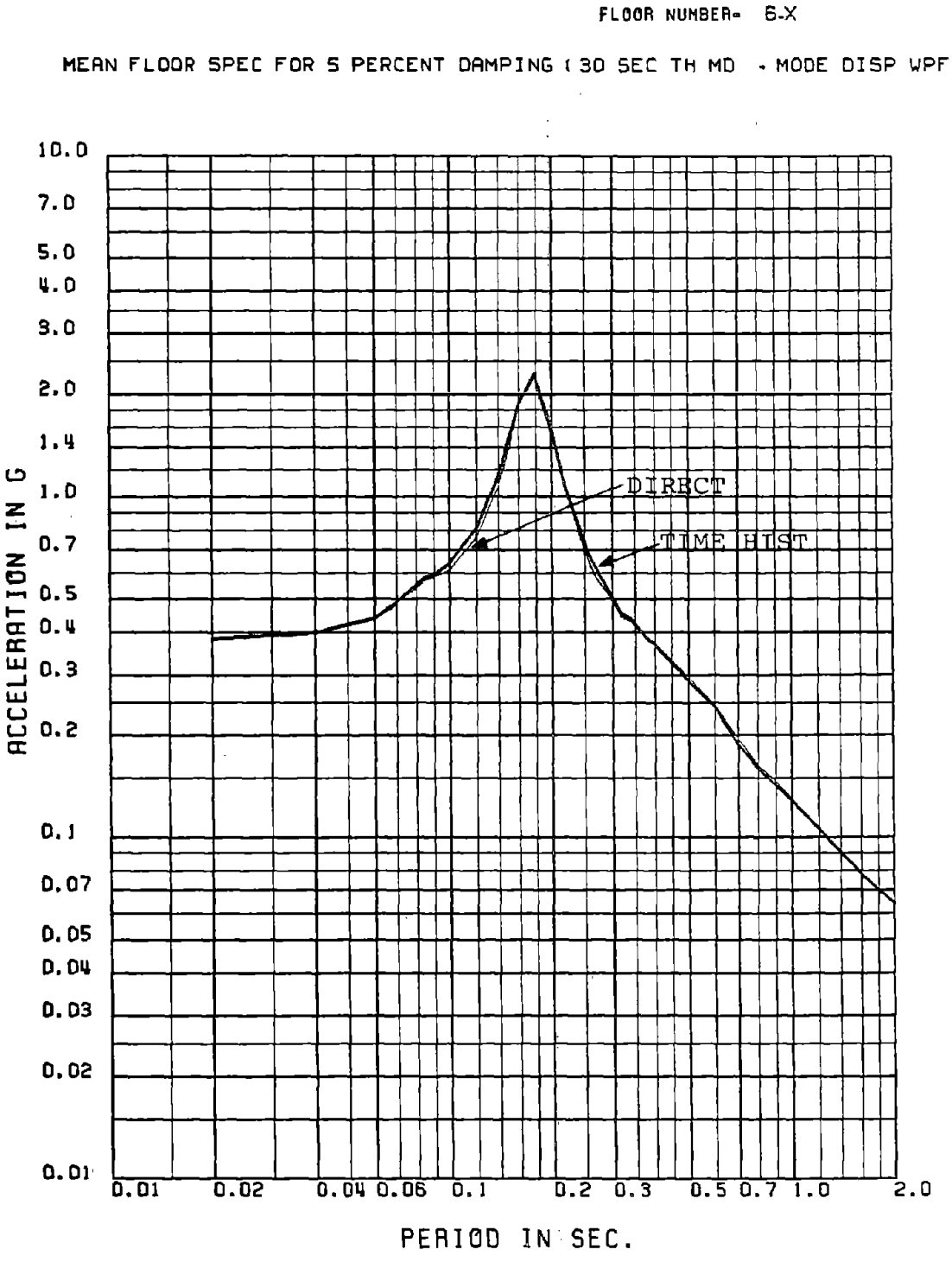

Fig. 2.54 Comparison of Floor Spectra Obtained by Mode Displacement Approach with Peak Factors (1-T, K-T PSDF) and Time History Analysis for 5% Damping: Mean Spectra, 30-sec TH, Floor No. 6-X, 11-FRQ Model

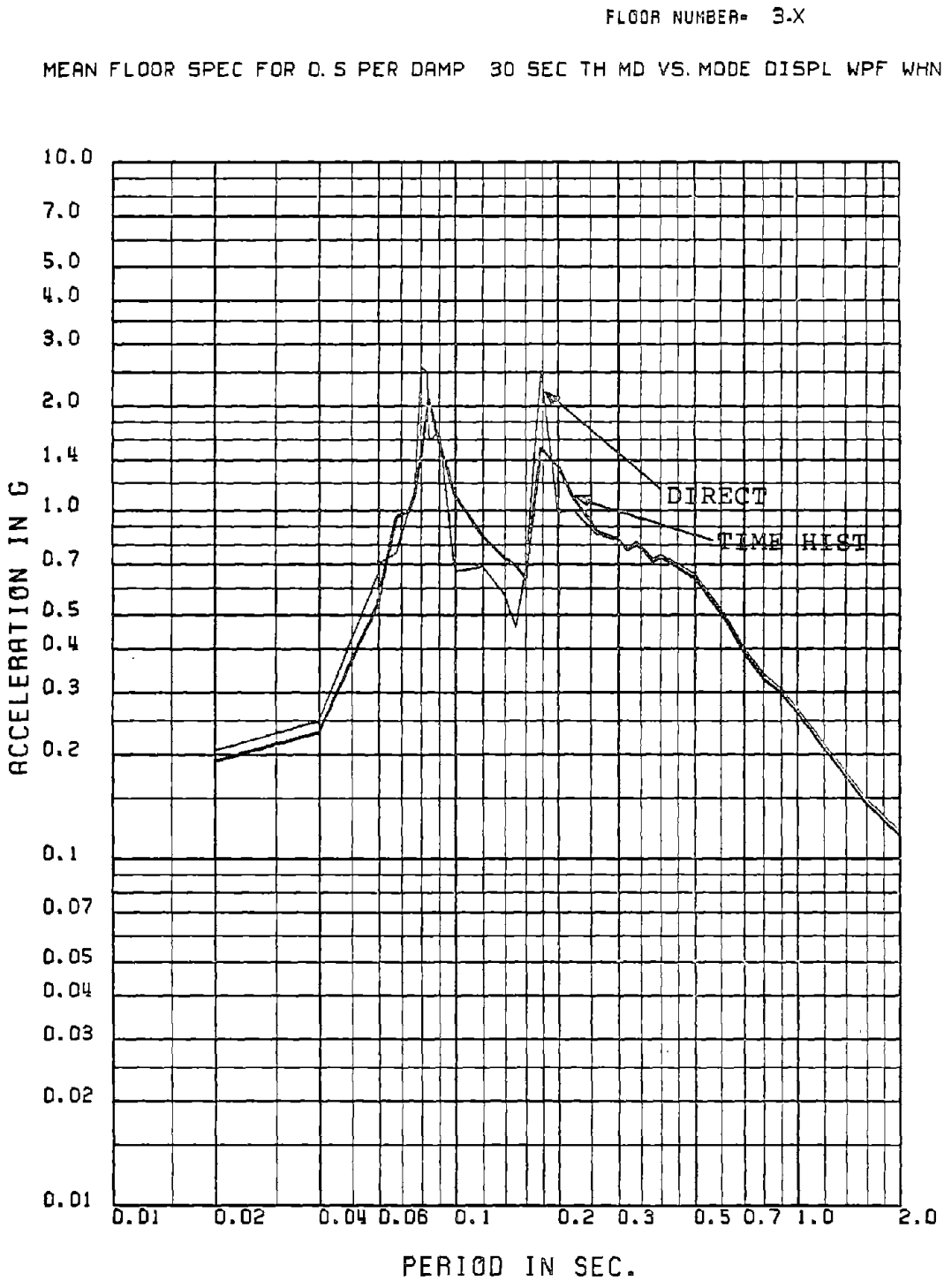

Fig. 2.55 Comparison of Floor Spectra Obtained by Mode Displacement Approach with Peak Factors (White Noise PSDF) and Time History Analysis for 0.5% Damping: Mean Spectra, 30-sec TH, Floor No. 3-X, 11-FRQ Model

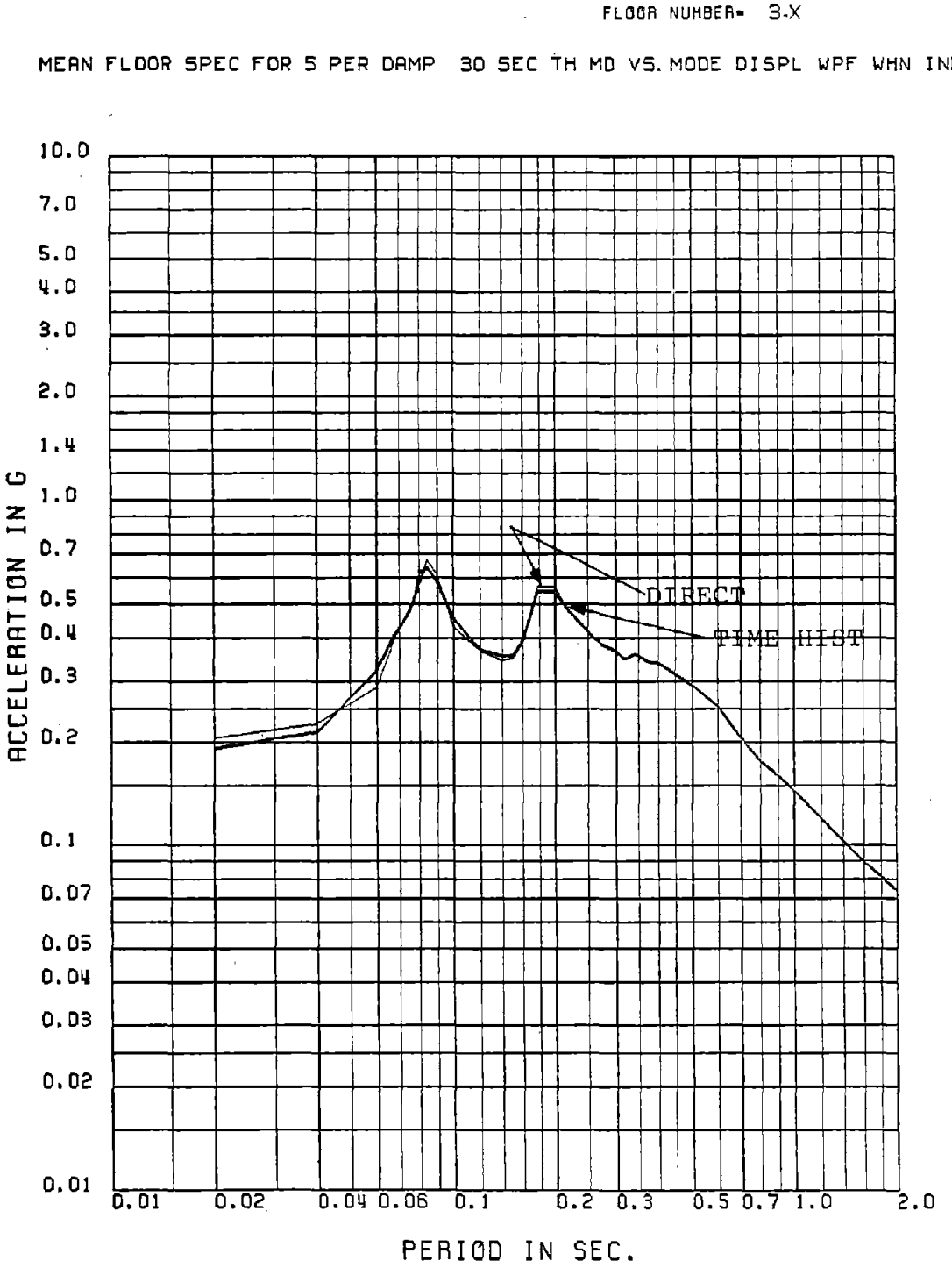

Fig. 2.56 Comparison of Floor Spectra Obtained by Mode Displacement Approach with Peak Factors (White Noise PSDF) and Time History Analysis for 5% Damping: Mean Spectra, 30-sec TH, Floor No. 3-X, 11-FRQ Model

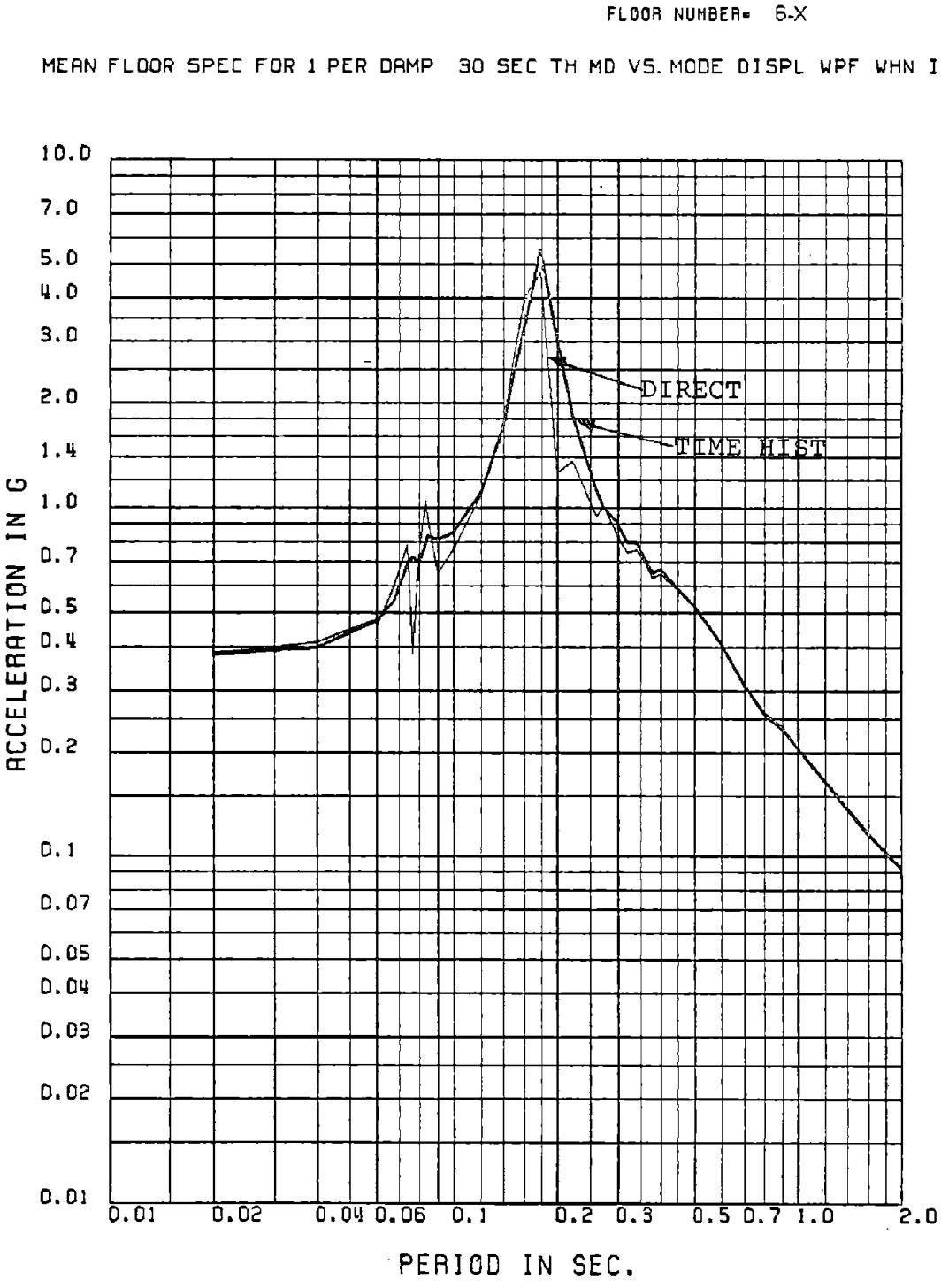

Fig. 2.57 Comparison of Floor Spectra Obtained by Mode Displacement Approach with Peak Factors (White Noise PSDF) and Time History Analysis for 1% Damping: Mean Spectra, 30-sec TH, Floor 6-X, 11-FRQ Model

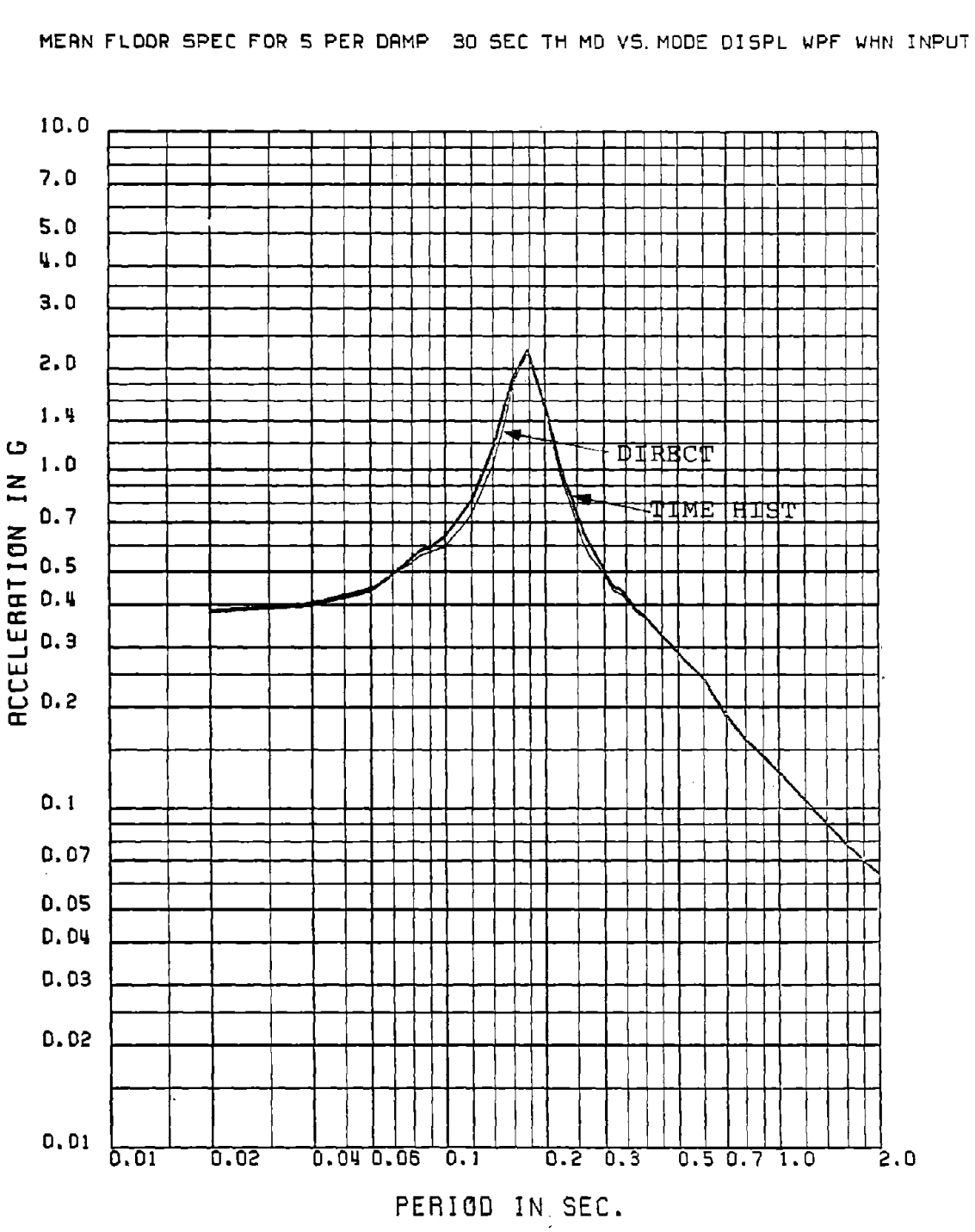

Fig. 2.58 Comparison of Floor Spectra Obtained by Mode Displacement Approach with Peak Factors (White Noise PSDF) and Time History Analysis for 5% Damping: Mean Spectra, 30-sec TH, Floor No. 6-X, 11-FRQ Model

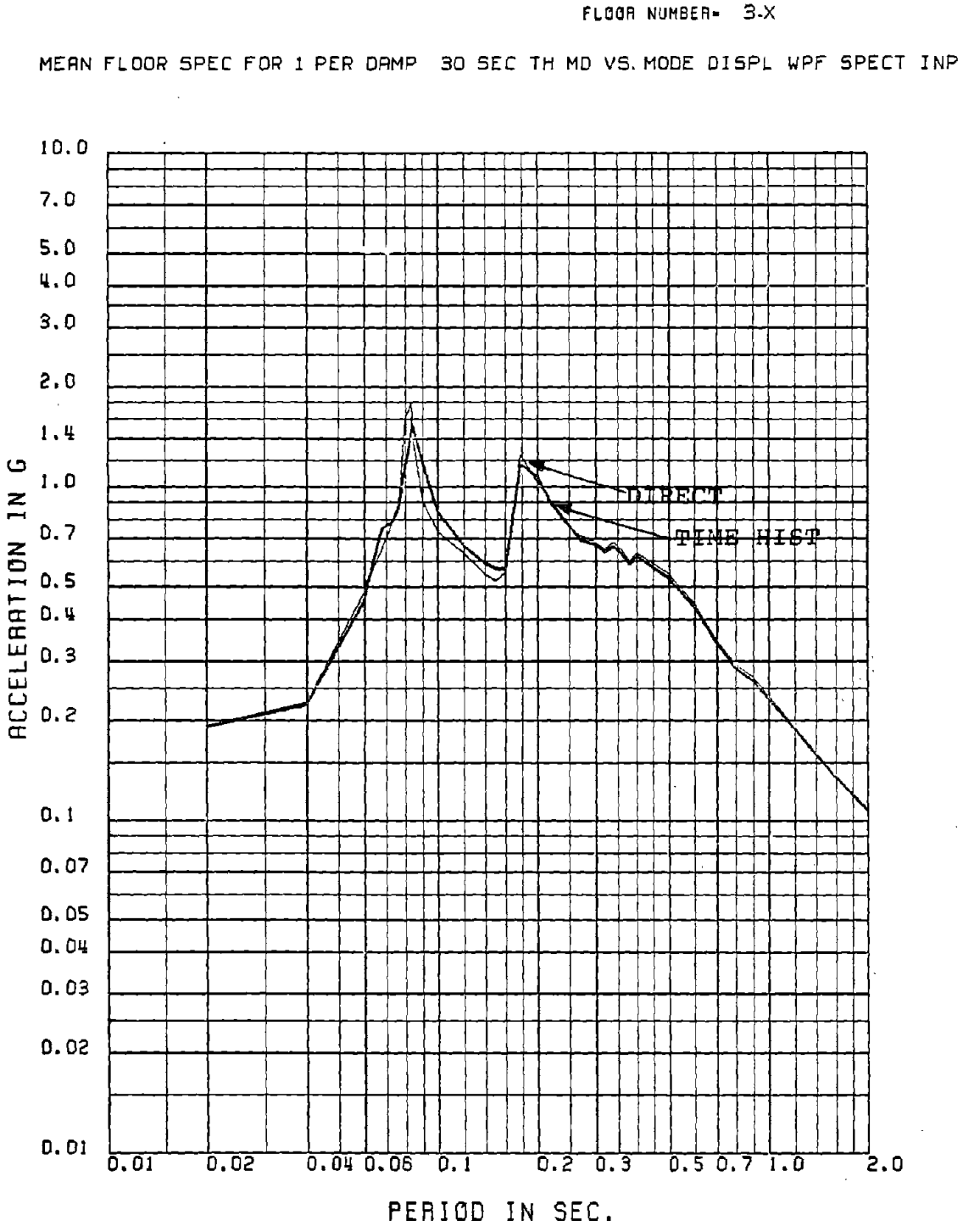

Fig. 2.59 Comparison of Floor Spectra Obtained by Mode Displacement Approach with Peak Factors (Ground Spectra) and Time History Analysis for 1% Damping: Mean Spectra, 30-sec TH, Floor No. 3-X, 11-FRQ Model

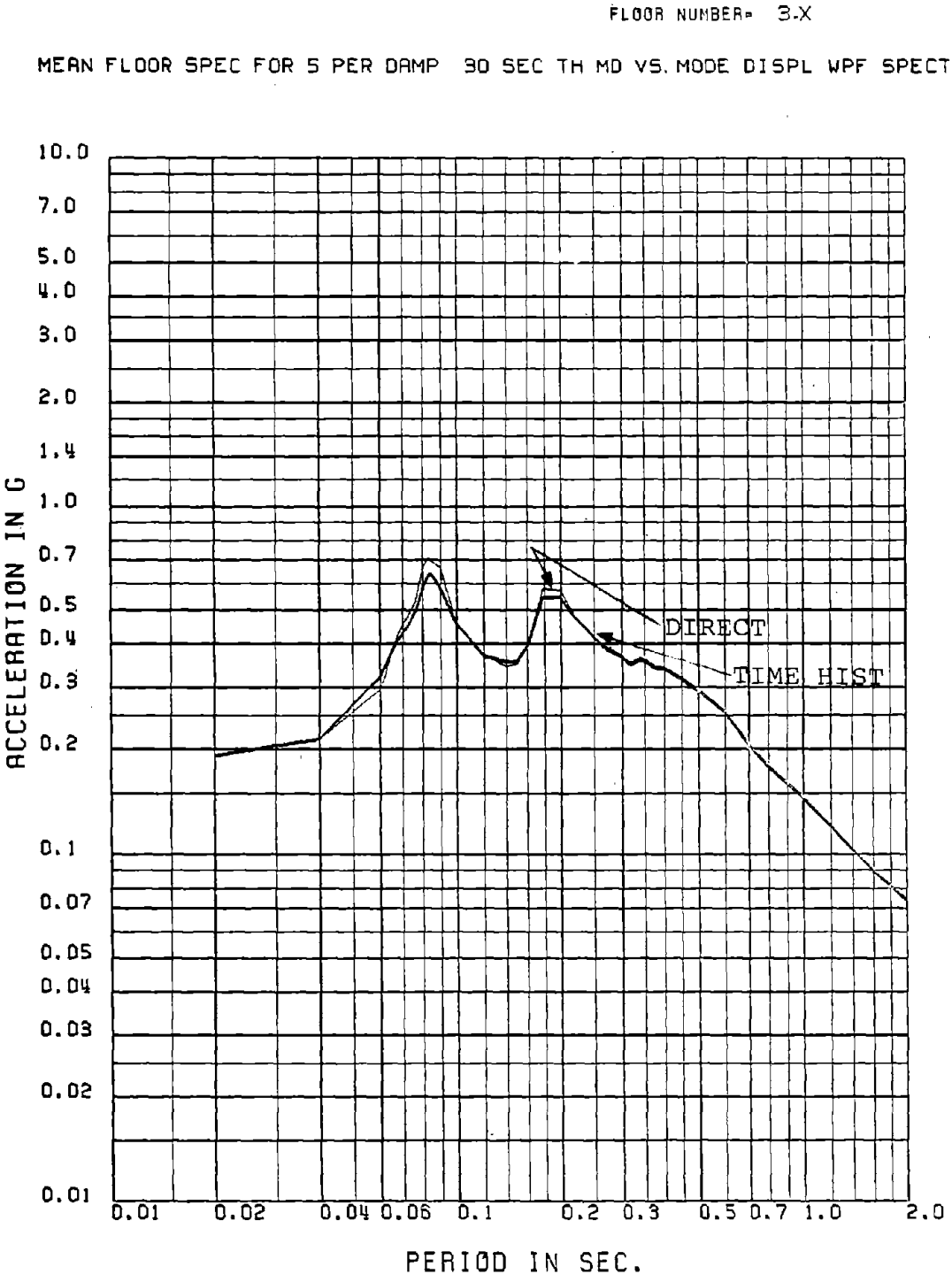

Fig. 2.60 Comparison of Floor Spectra Obtained by Mode Displacement Approach with Peak Factors (Ground Spectra) and Time History Analysis for 5% Damping: Mean Spectra, 30-sec TH, Floor No. 3-X, 11-FRQ Model

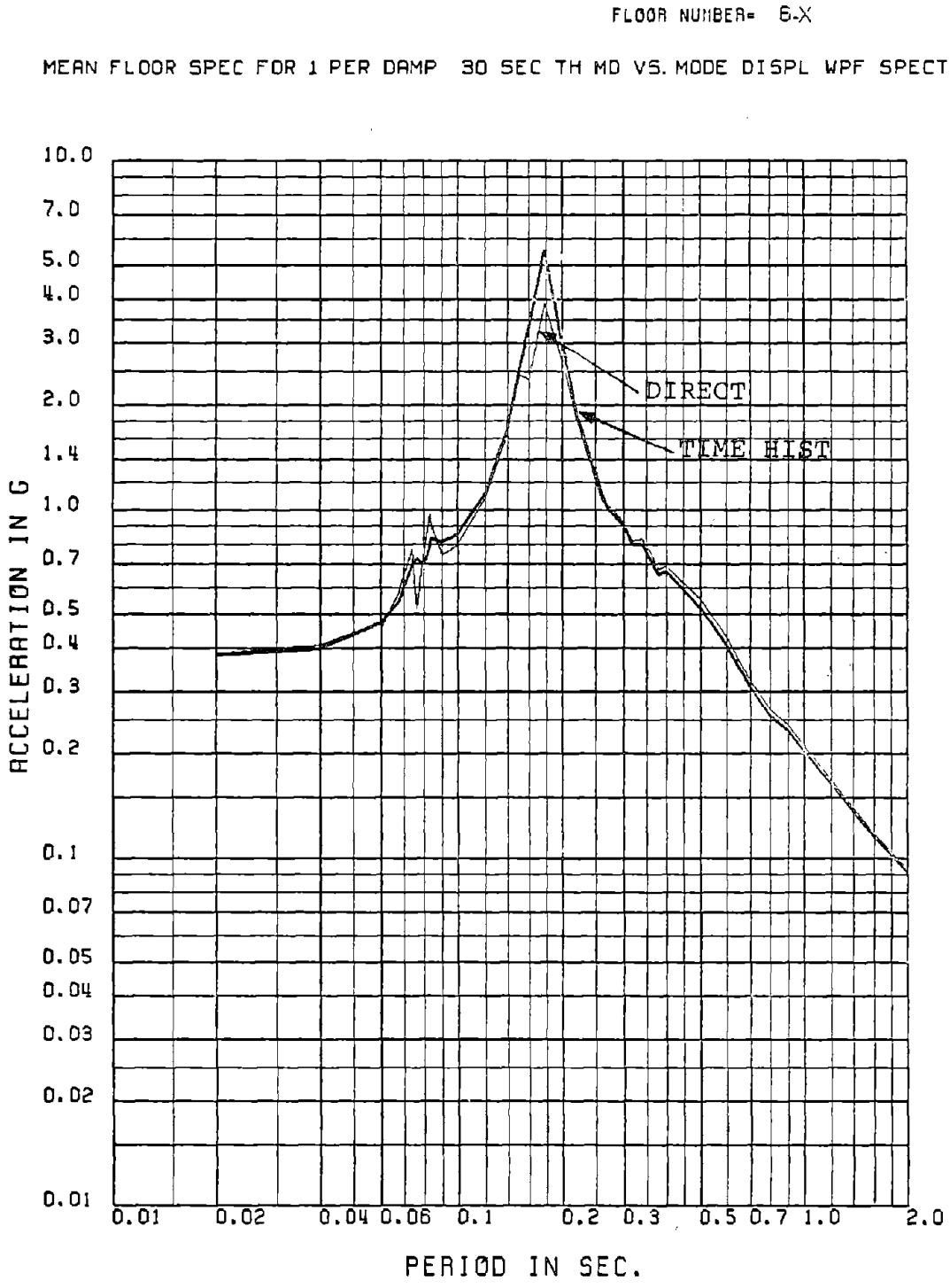

Fig. 2.61 Comparison of Floor Spectra Obtained by Mode Displacement Approach with Peak Factors (Ground Spectra) and Time History Analysis for 1% Damping: Mean Spectra, 30-sec TH, Floor No. 6-X, 11-FRQ Model

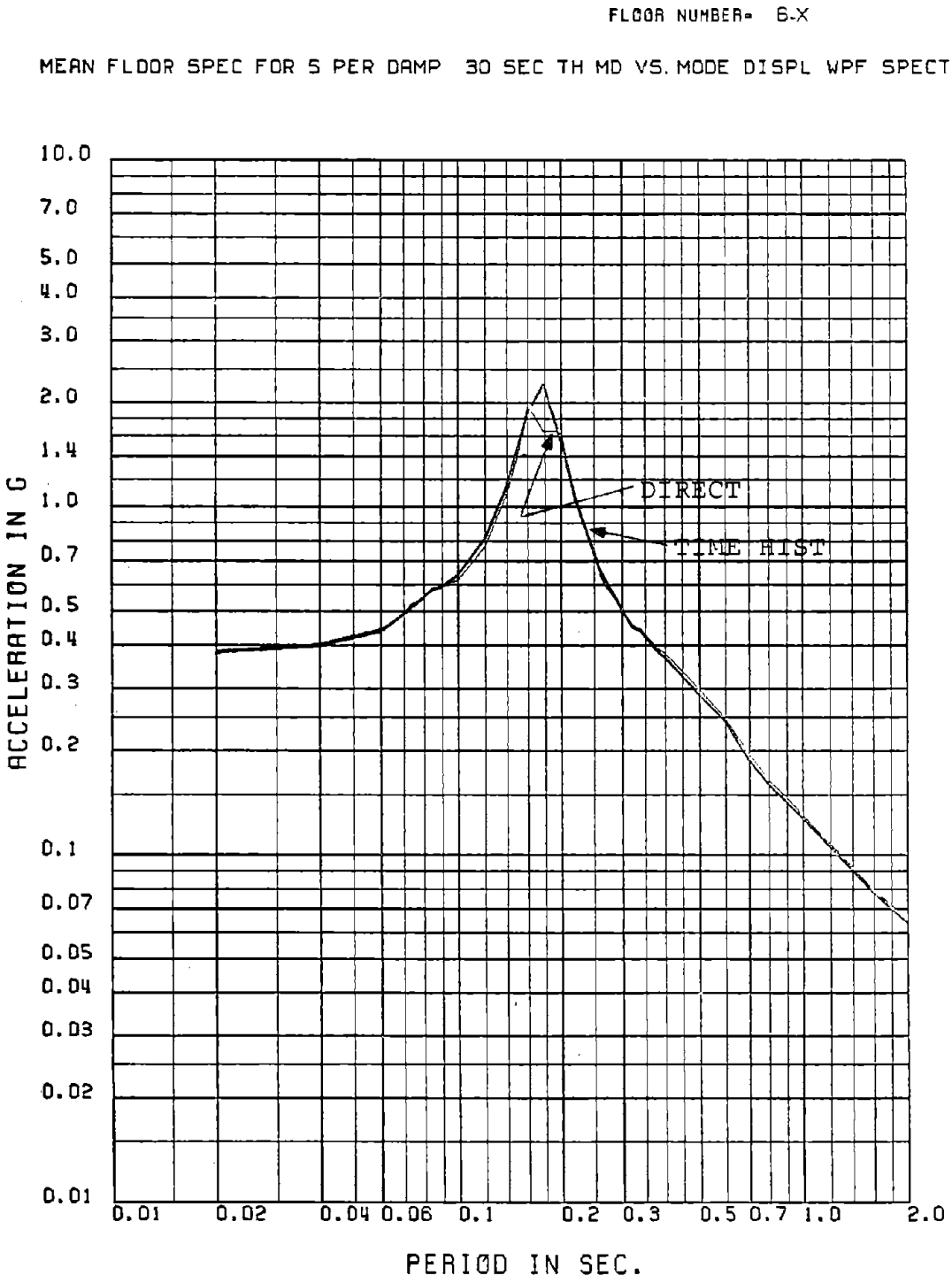

Fig. 2.62 Comparison of Floor Spectra Obtained by Mode Displacement Approach with Peak Factors (Ground Spectra) and Time History Analysis 5% Damping: Mean Spectra, 30-sec TH, Floor No. 6-X, 11-FRQ Model

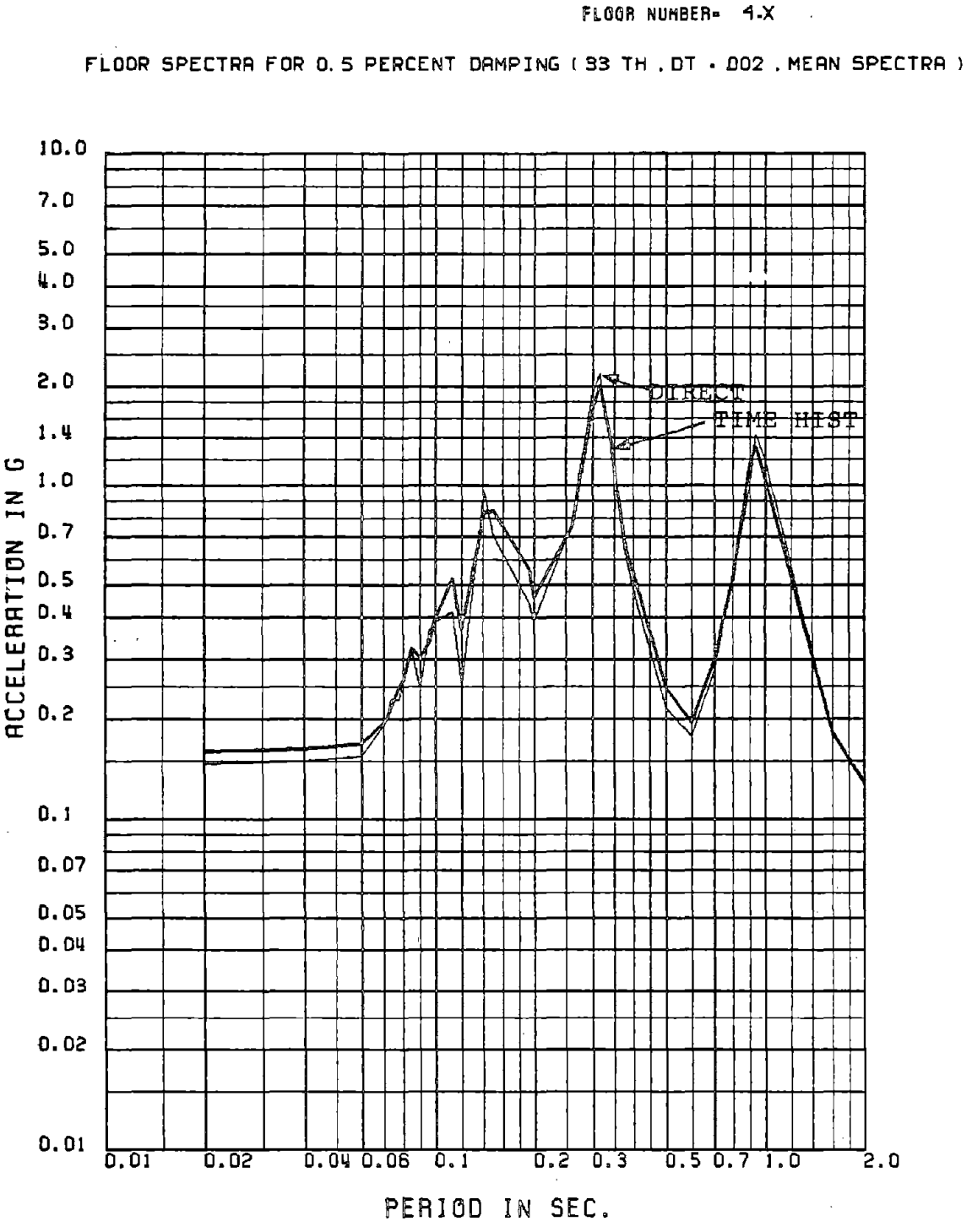

Fig. 2.63 Comparison of Floor Spectra Obtained by Mode Displacement Approach and Time History Analysis for 0.5% Damping: Mean Spectra, 30-sec TH, Floor No. 4-X, 10-Story Model

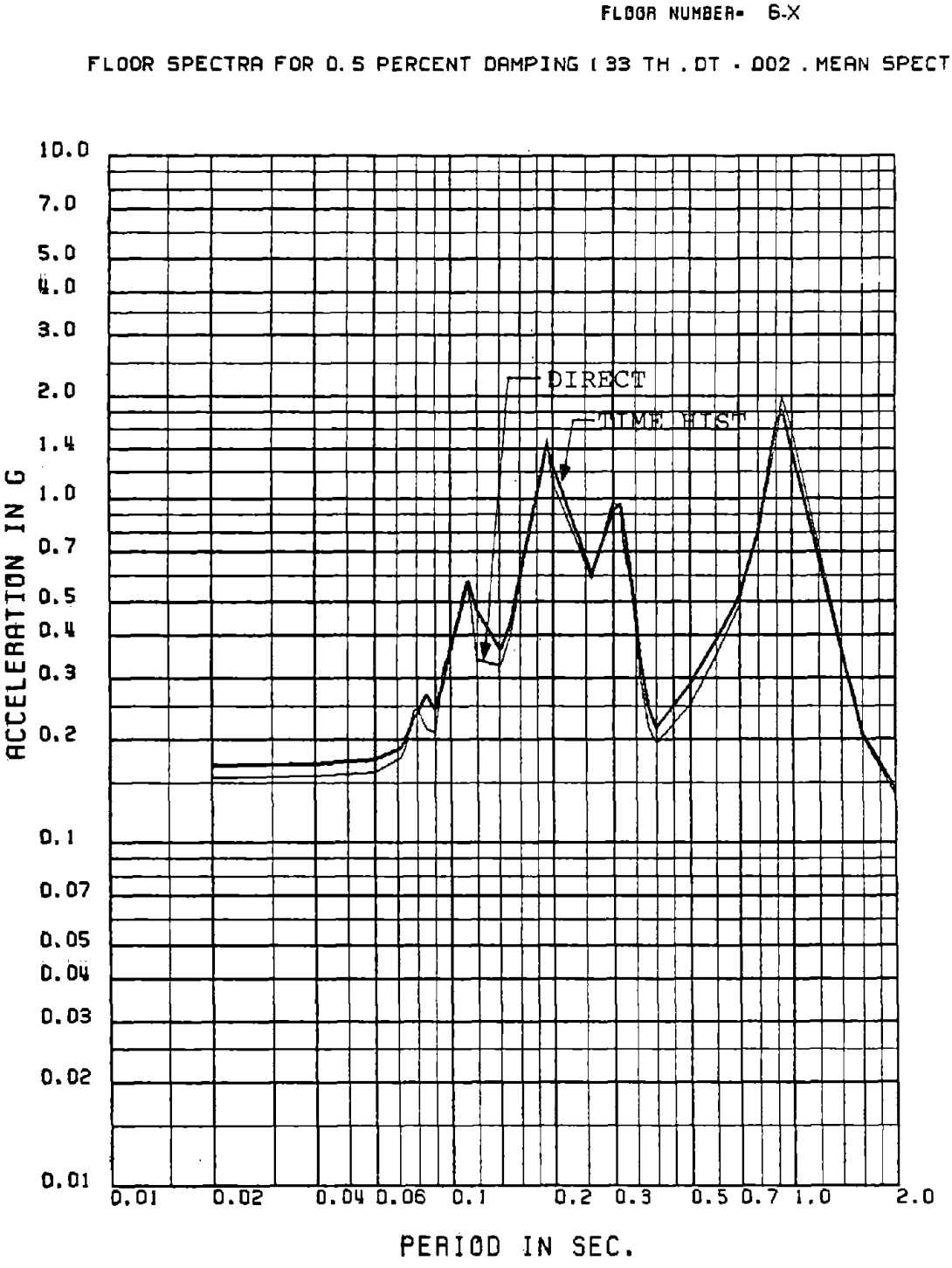

Fig. 2.64 Comparison of Floor Spectra Obtained by Mode Displacement Approach and Time History Analysis for 0.5% Damping: Mean Spectra, 30-sec TH, Floor No. 6-X, 10-Story Model

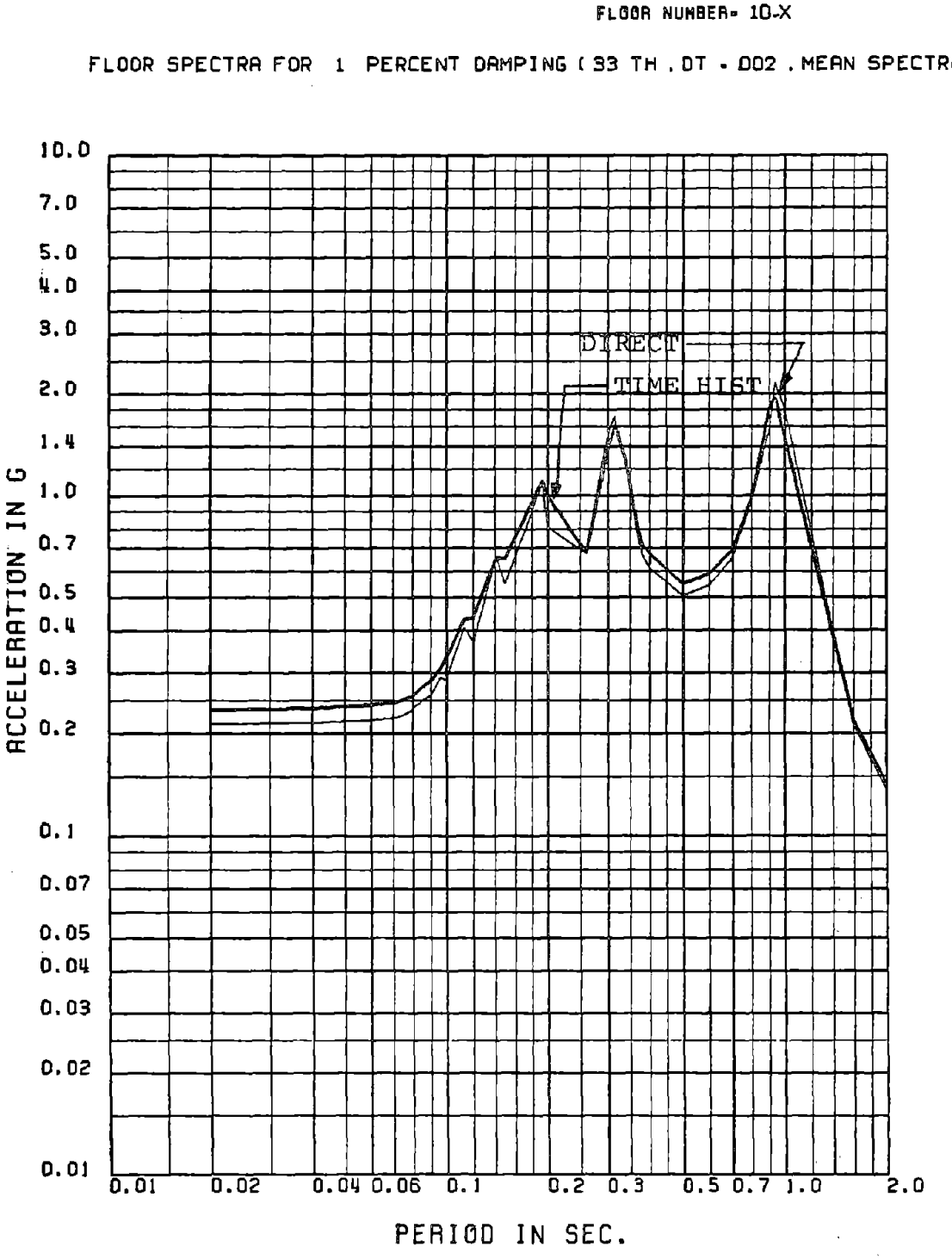

Fig. 2.65 Comparison of Floor Spectra Obtained by Mode Displacement Approach and Time History Analysis for 1% Damping: Mean Spectra, 30-sec TH, Floor No. 10-X, 10-Story Model

FIGURES FOR CHAPTER 3

NONCLASSICALLY DAMPED SYSTEMS: MODE DISPLACEMENT METHOD

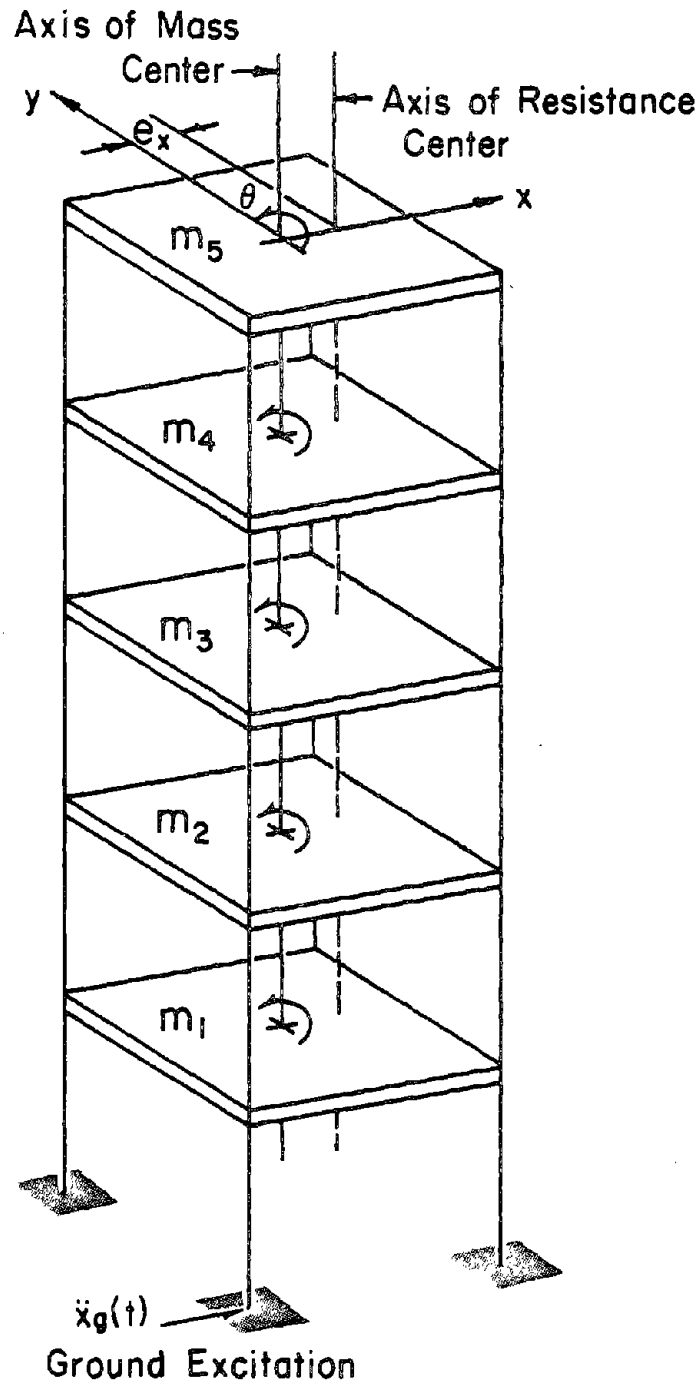

Fig. 3.1 A 5 Story 15-D.O.F. Torsional Structure Model

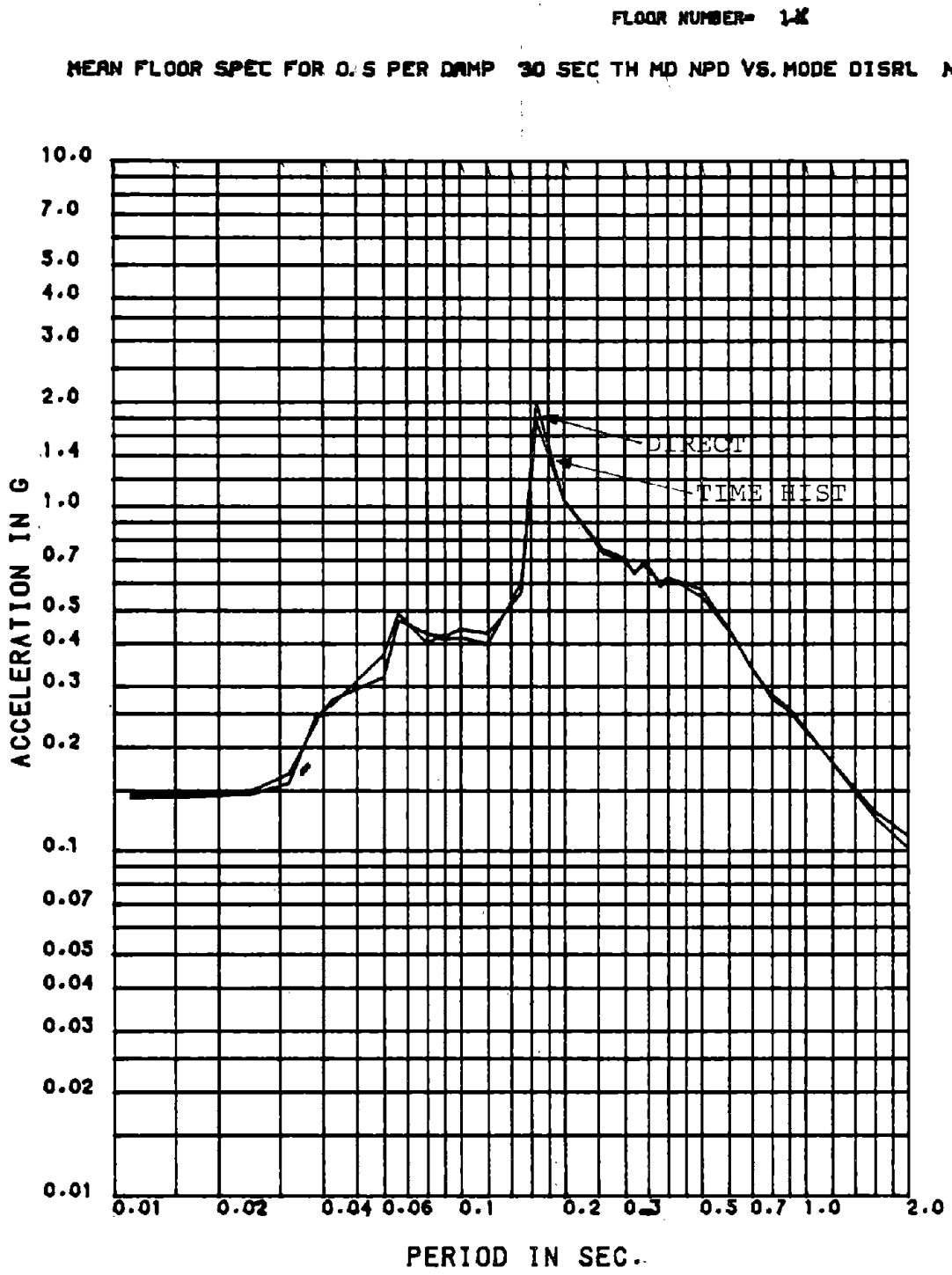

Fig. 3.2 Comparison of Floor Spectra Obtained by Mode Displacement Approach and Time History Analysis for 0.5% Damping: Mean Spectra, 30-sec TH, Floor No. 1-X, Nonproportionally Damped 15-D.O.F. Model

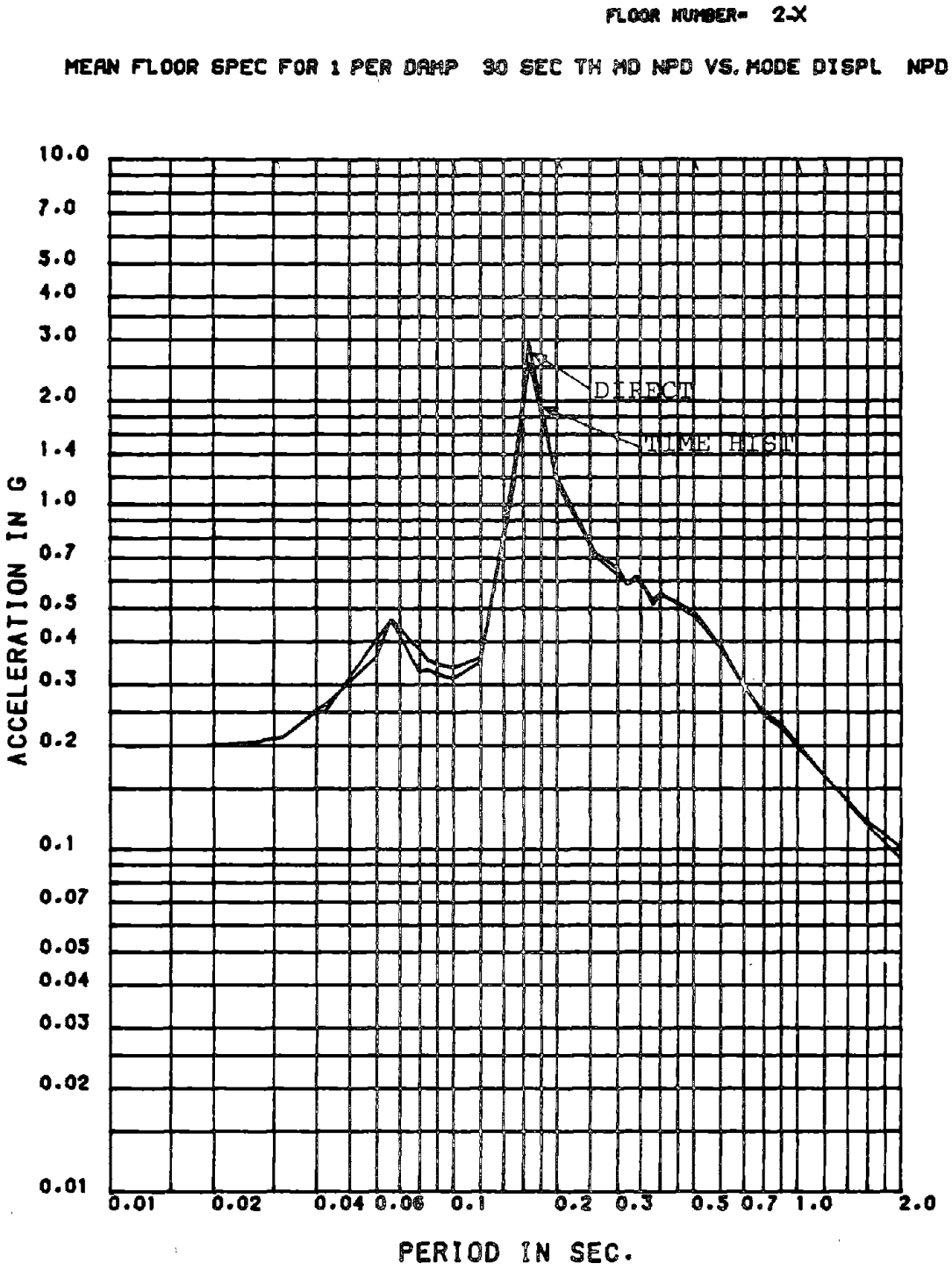

Fig. 3.3 Comparison of Floor Spectra Obtained by Mode Displacement Approach and Time History Analysis for 1% Damping: Mean Spectra, 30-sec TH, Floor No. 2-X, Nonproportionally Damped 15-D.O.F. Model

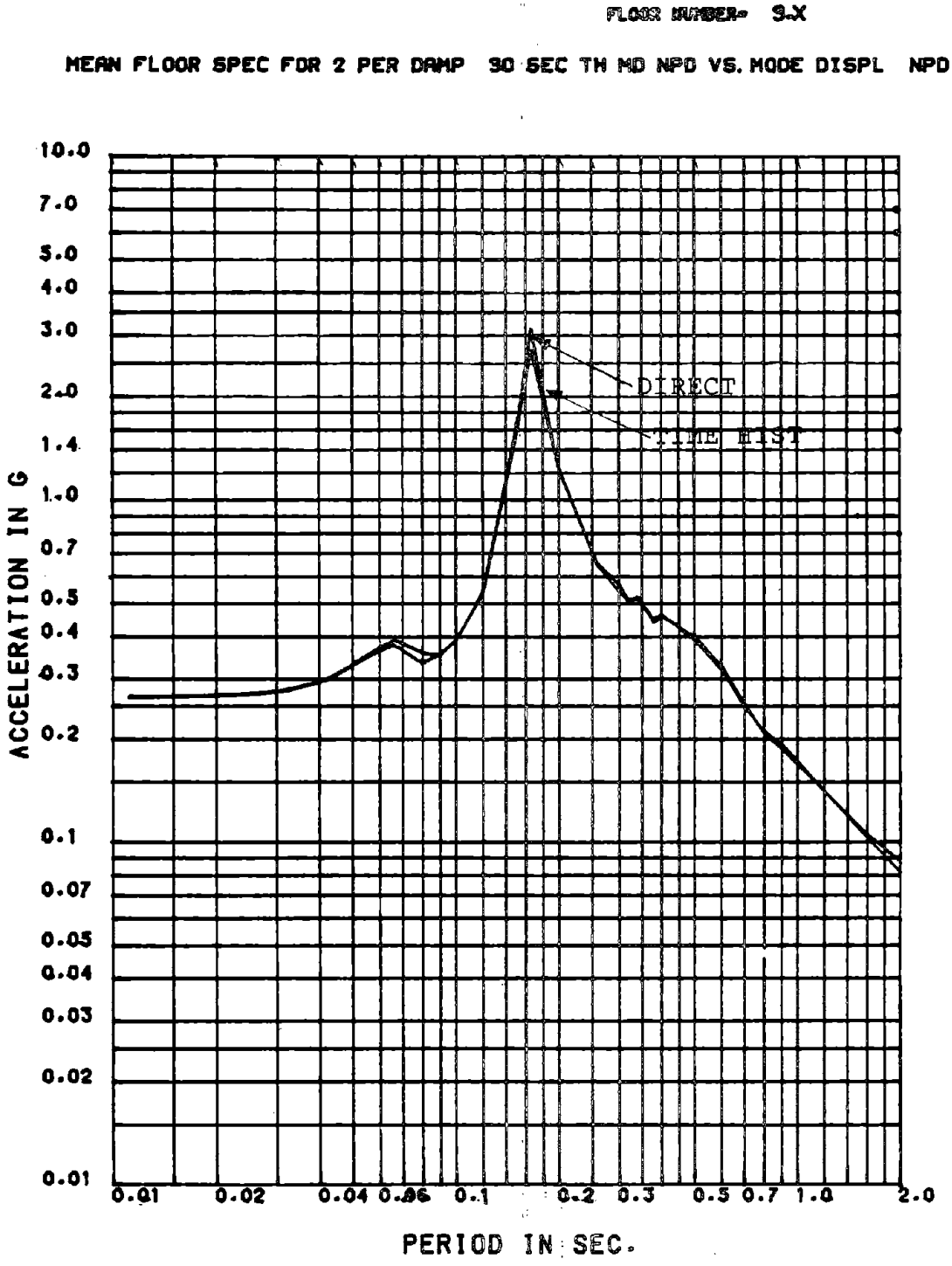

Fig. 3.4 Comparison of Floor Spectra Obtained by Mode Displacement Approach and Time History Analysis for 2% Damping: Mean Spectra, 30-sec TH, Floor No. 3-X, Nonproportionally Damped 15-D.O.F. Model

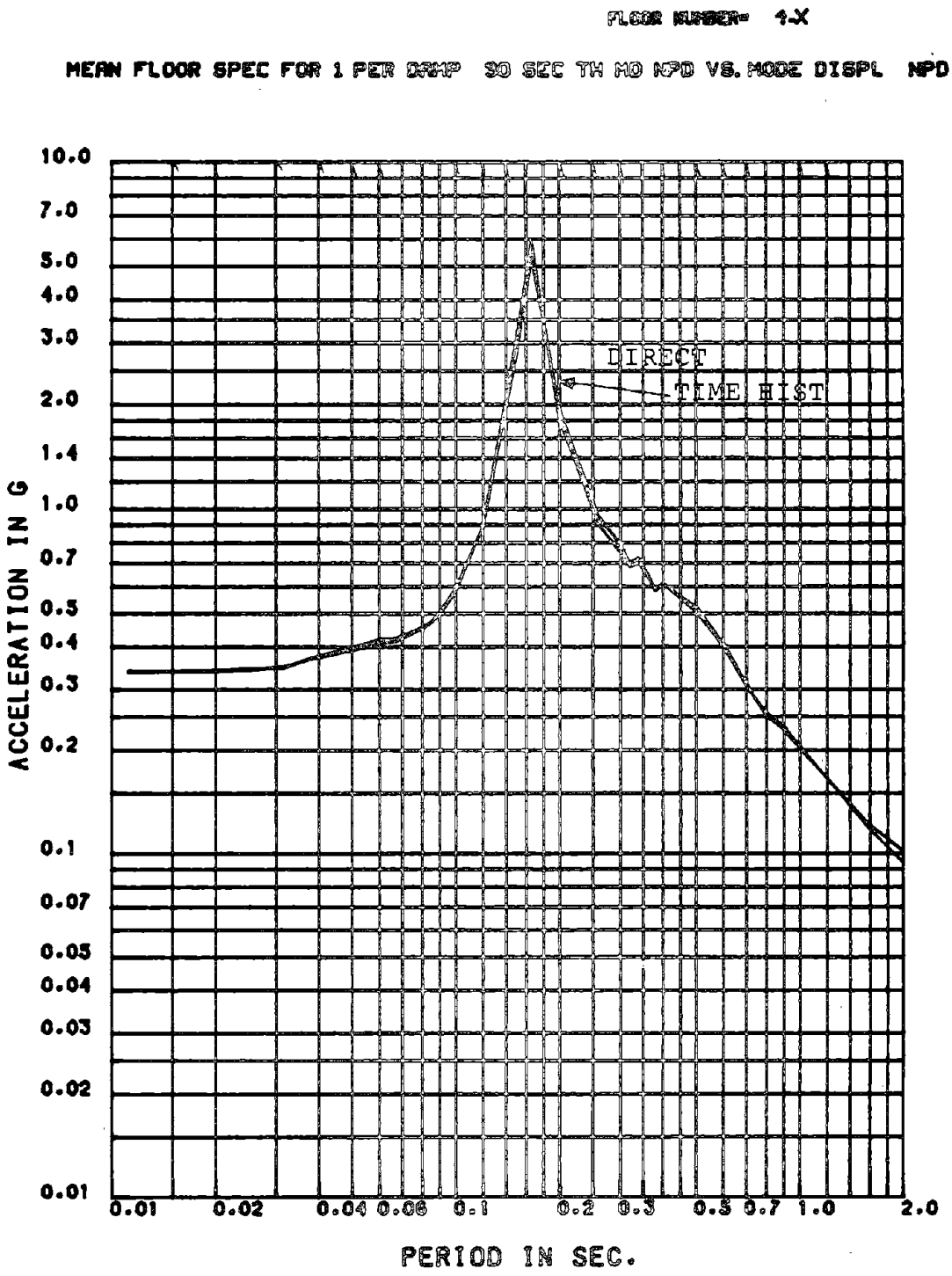

Fig. 3.5 Comparison of Floor Spectra Obtained by Mode Displacement Approach and Time History Analysis for 1% Damping: Mean Spectra, 30-sec TH, Floor No. 4-X, Nonproportionally Damped 15 D.O.F. Model

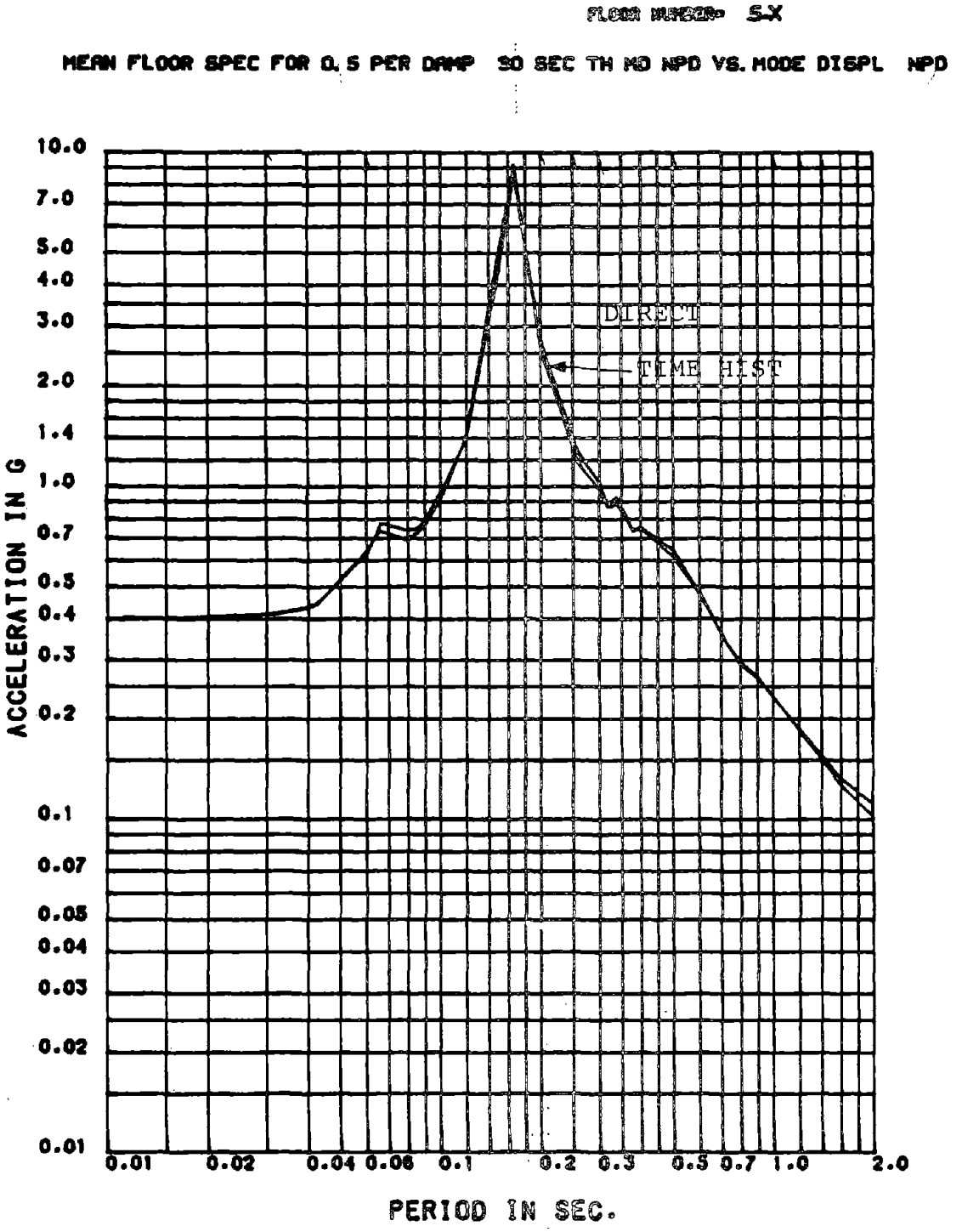

Fig. 3.6 Comparison of Floor Spectra Obtained by Mode Displacement Approach and Time History Analysis for 5% Damping: Mean Spectra, 30-sec TH, Floor No. 5-X, Nonproportionally Damped 15-D.O.F. Model

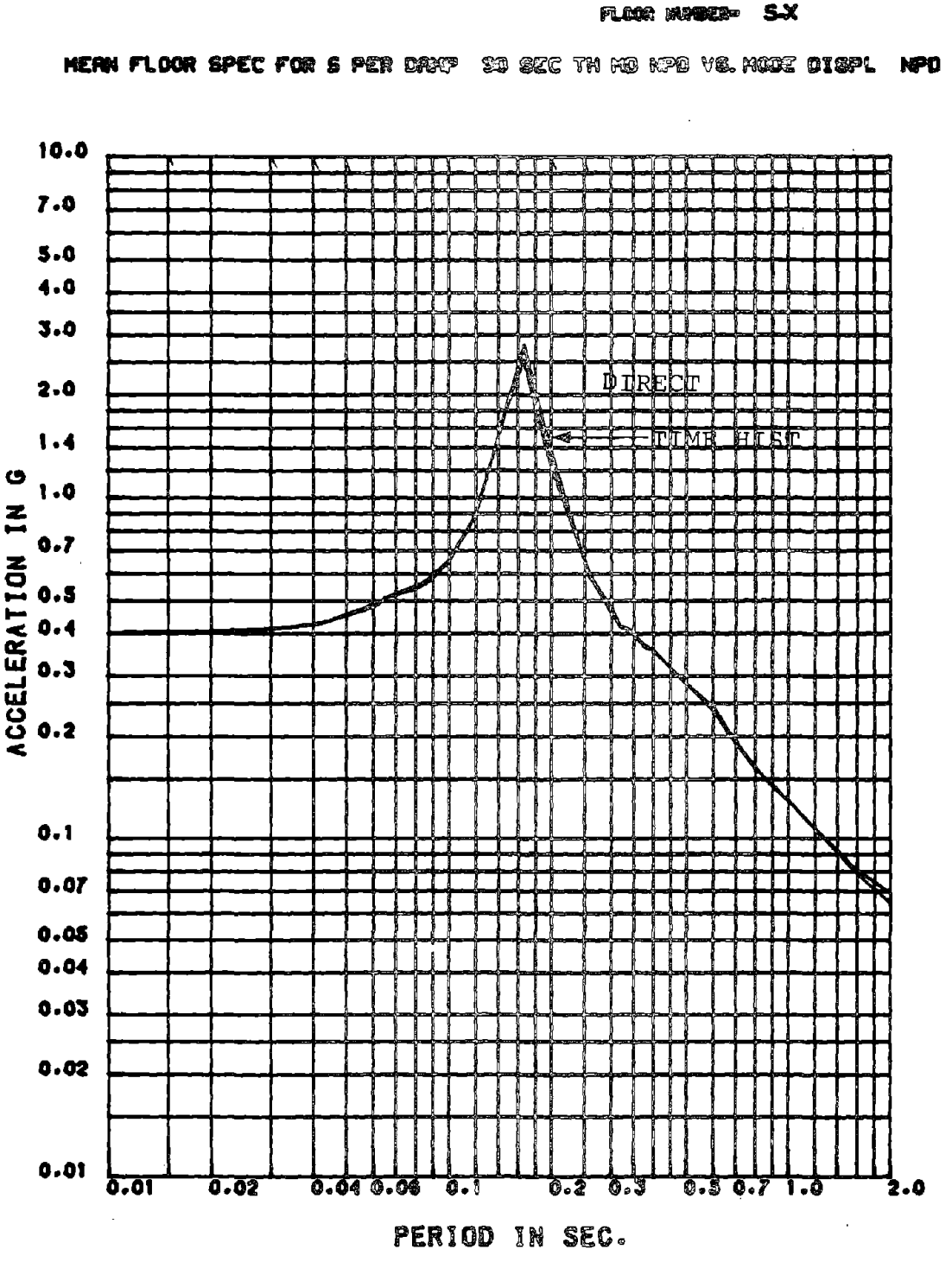

Fig. 3.7 Comparison of Floor Spectra Obtained by Mode Displacement Approach and Time History Analysis for 5% Damping: Mean Spectra, 30-sec TH, Floor No. 5-X, Nonproportionally Damped 15-D.O.F. Model

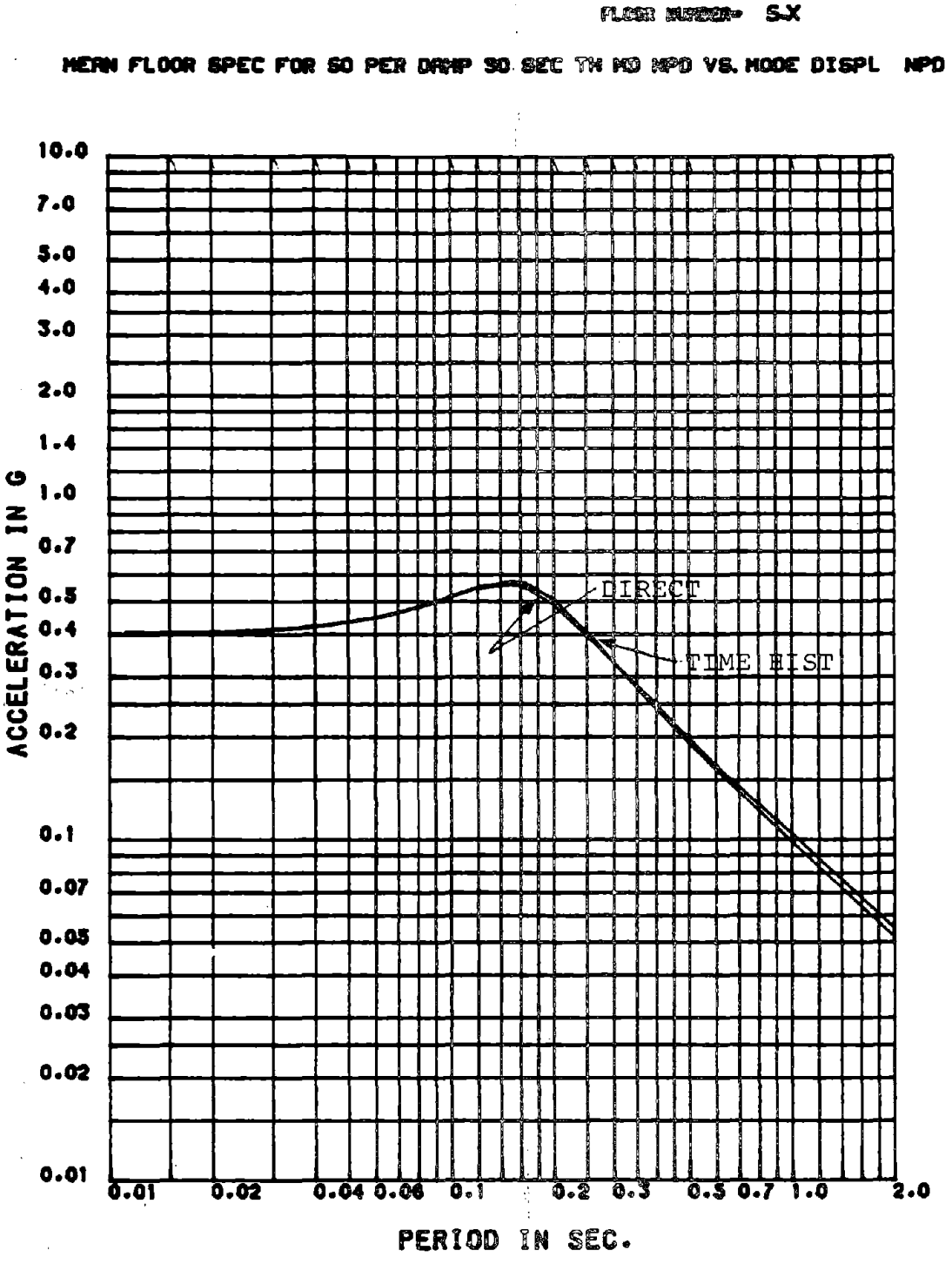

Fig. 3.8 Comparison of Floor Spectra Obtained by Mode Displacement Approach and Time History Analysis for 50% Damping: Mean Spectra, 30-sec TH, Floor No. 5-X, Nonproportionally Damped 15-D.O.F. Model

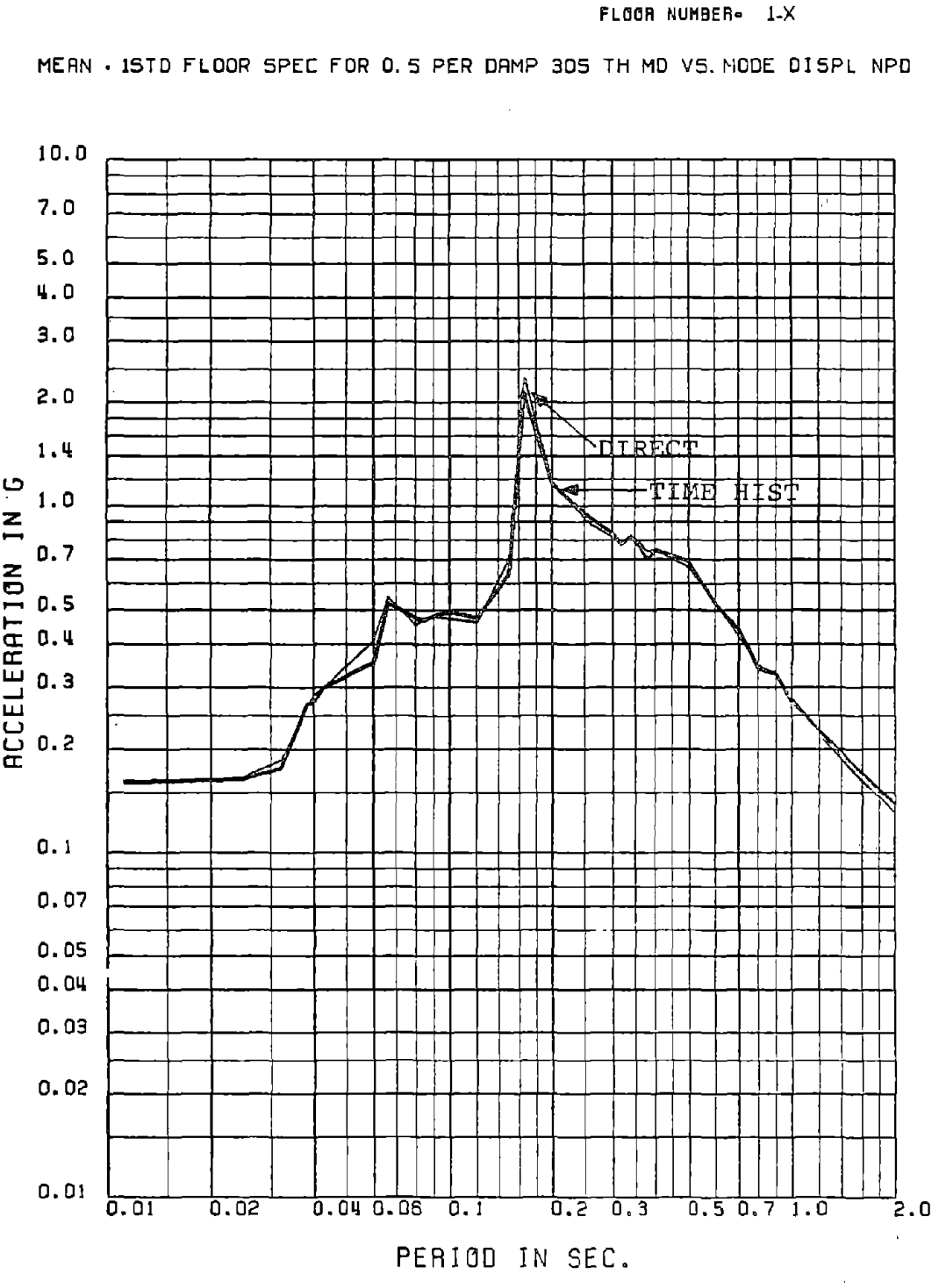

Fig. 3.9 Comparison of Floor Spectra Obtained by Mode Displacement Approach and Time History Analysis for 0.5% Damping: Mean + 1 Standard Deviation Spectra, 30-sec TH, Floor No. 1-X, Nonproportionally Damped 15-D.O.F. Model

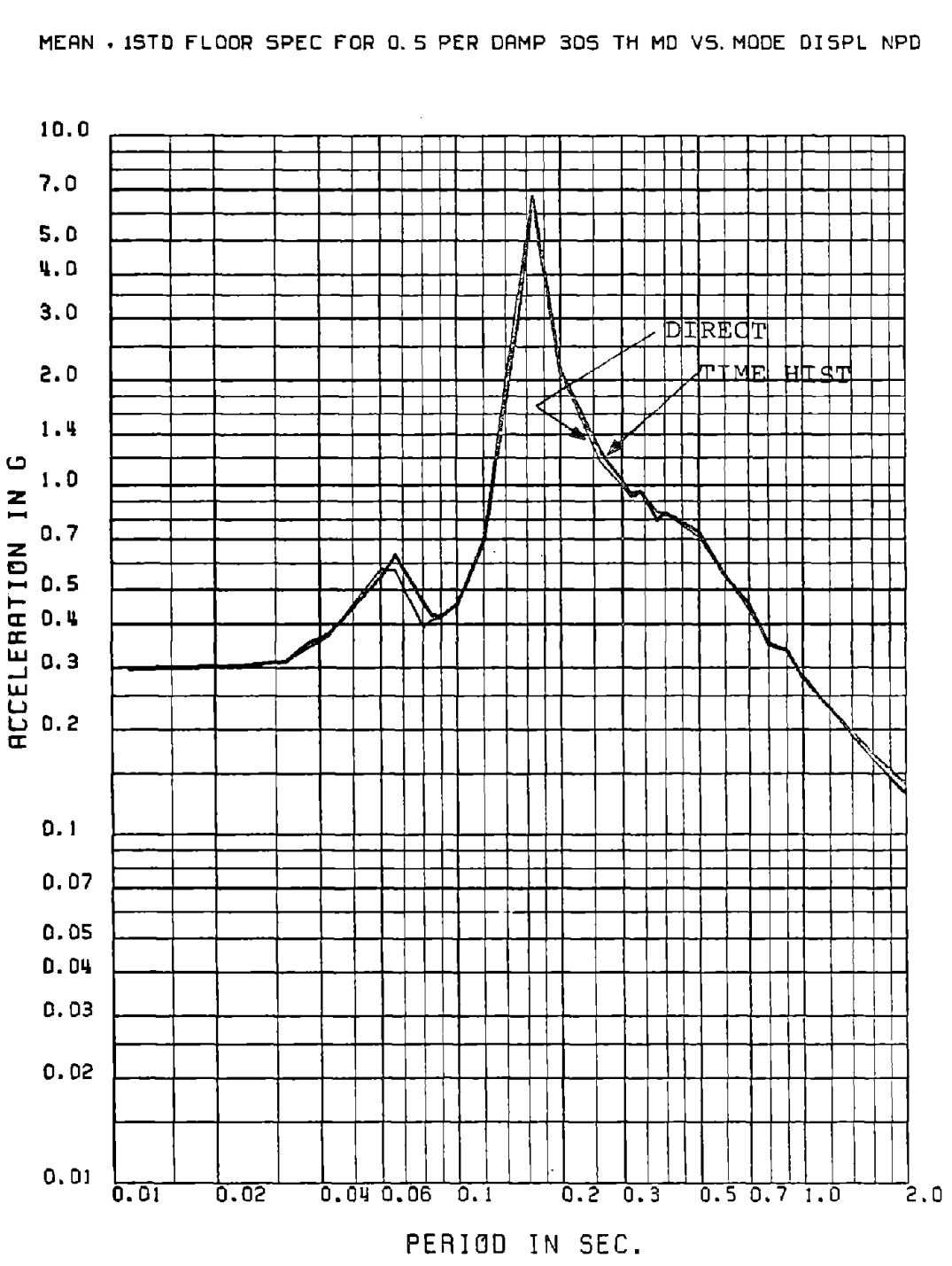

Fig. 3.10 Comparison of Floor Spectra Obtained by Mode Displacement Approach and Time History Analysis for 0.5% Damping: Mean + 1 Standard Deviation Spectra, 30-sec TH, Floor No. 3-X, Nonproportionally Damped 15-D.O.F. Model

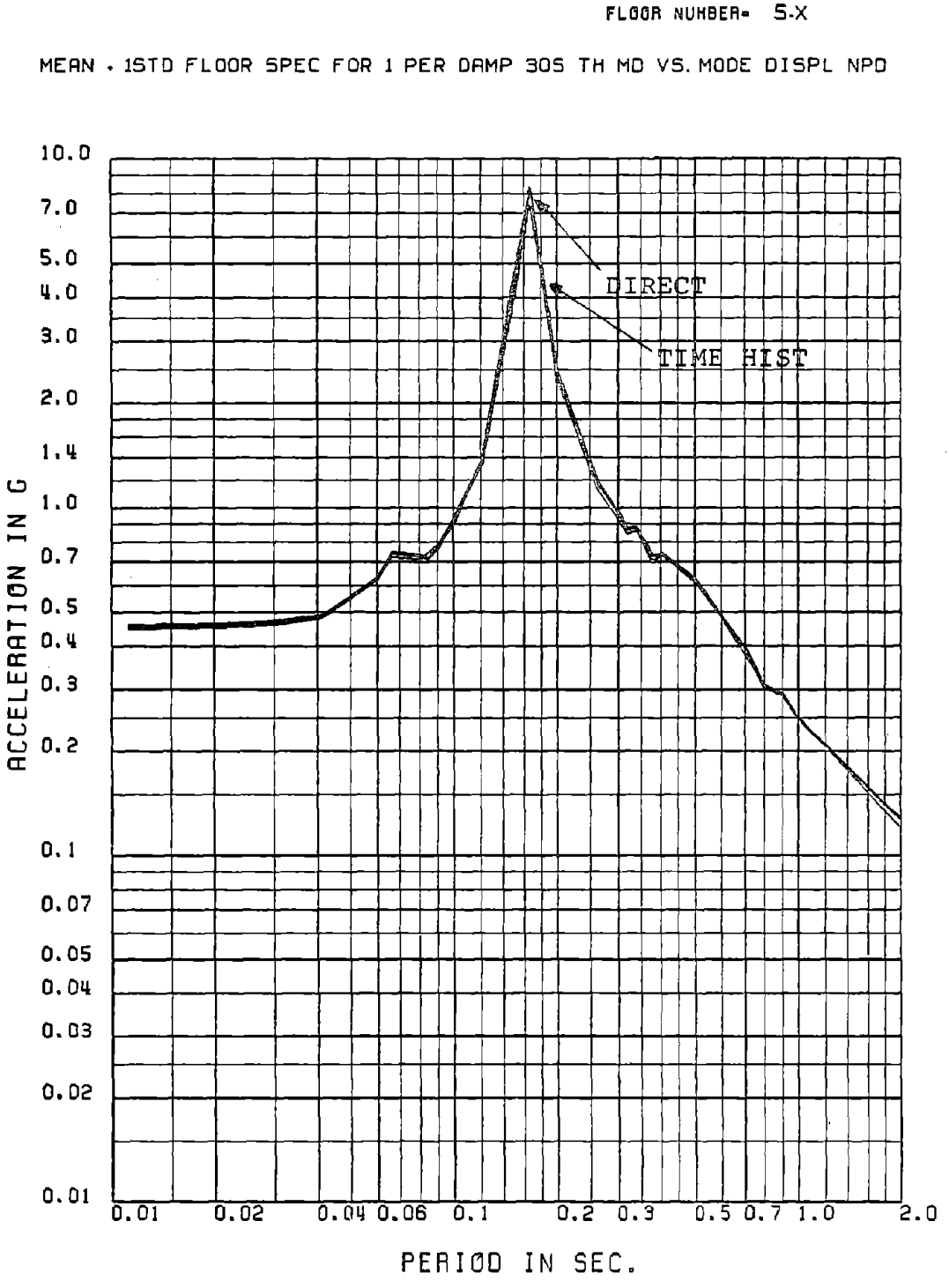

Fig. 3.11 Comparison of Floor Spectra Obtained by Mode Displacement Approach and Time History Analysis for 1% Damping: Mean + 1 Standard Deviation Spectra, 30-sec TH, Floor No. 5-X, Non-proportionally Damped 15-D.O.F. Model

FIGURES FOR CHAPTER 4

CLASSICALLY DAMPED SYSTEMS: MODE ACCELERATION METHOD

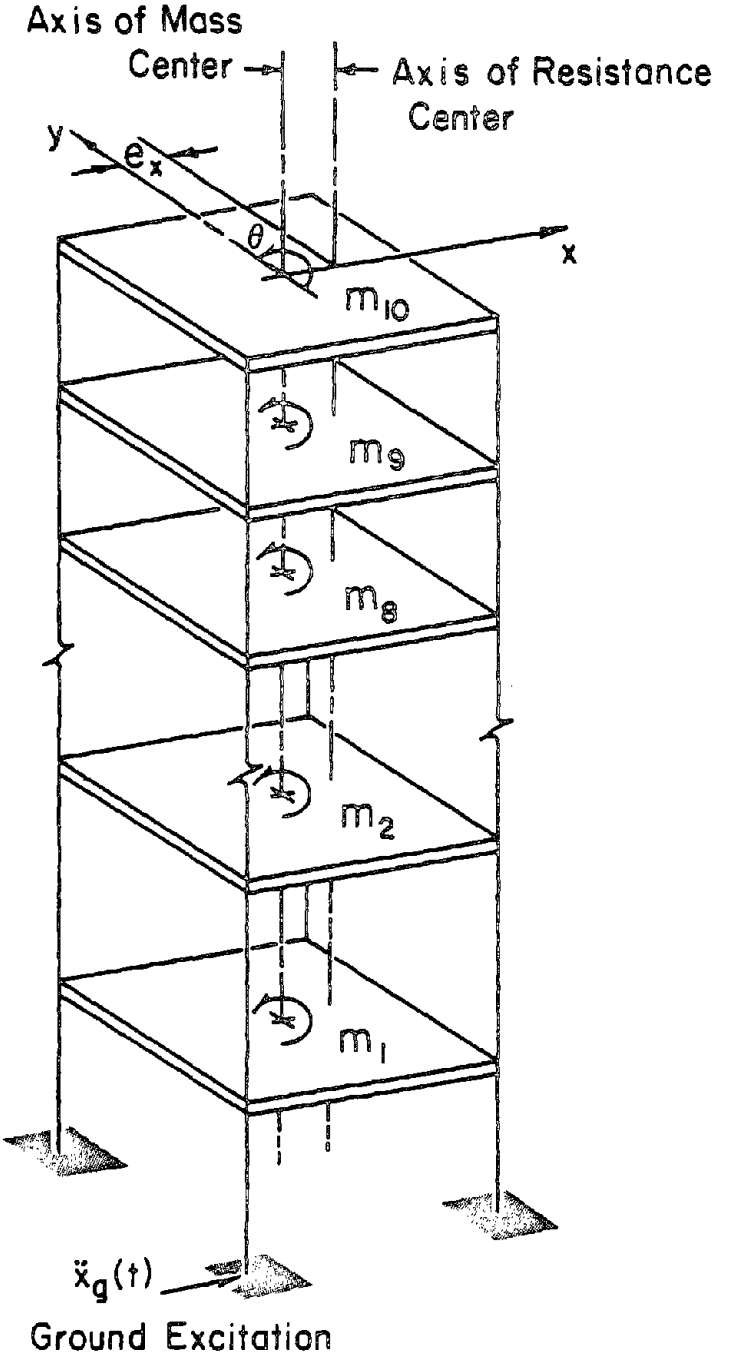

Fig. 4.1 A 10-Story 30-D.O.F. Torsional Structure Model

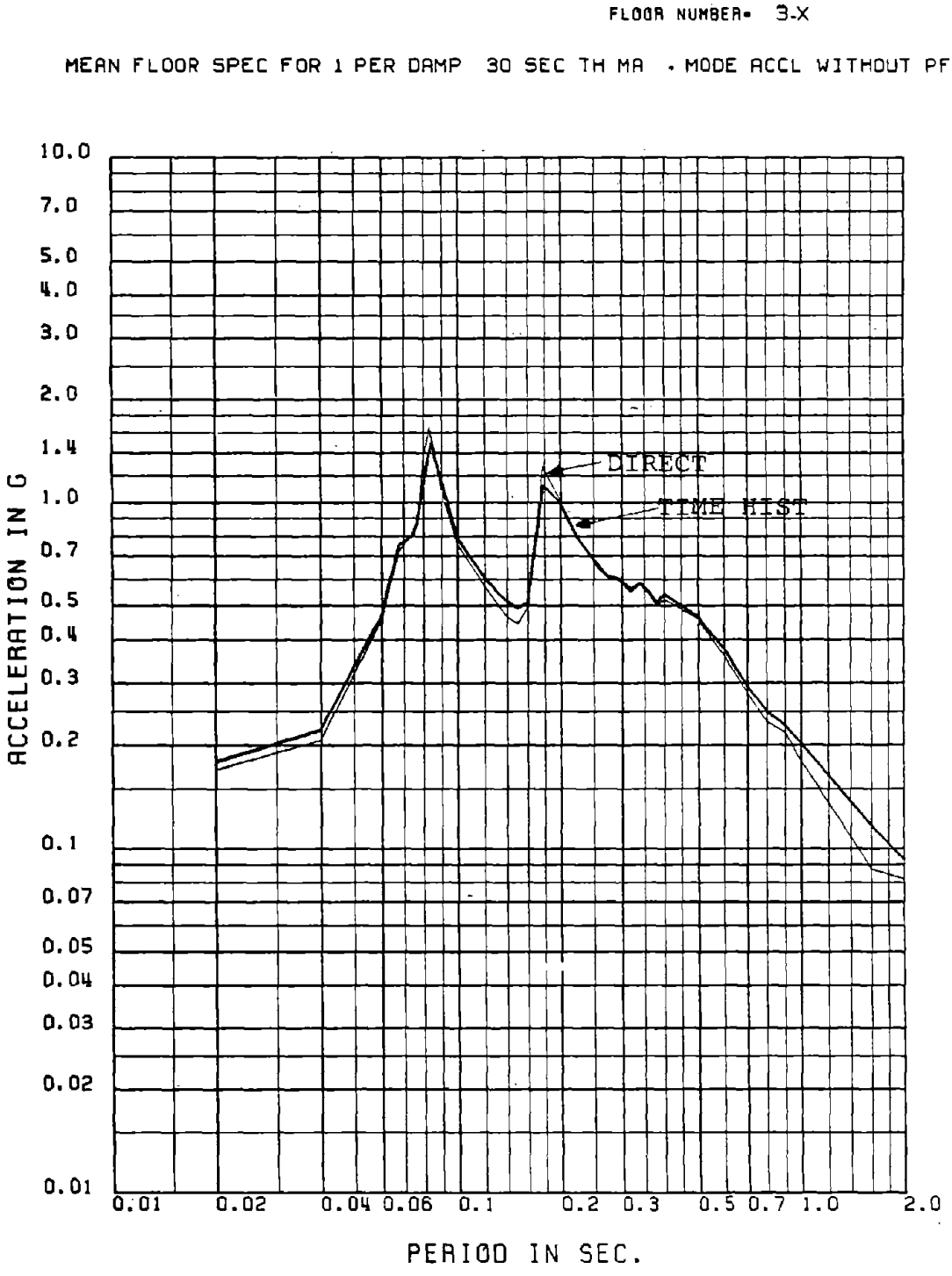

Fig. 4.2 Comparison of Floor Spectra Obtained by Mode Acceleration Approach and Time History Analysis for 1% Damping: Mean Spectra, 30-sec TH, Floor No. 3-X, 11-FRQ Model

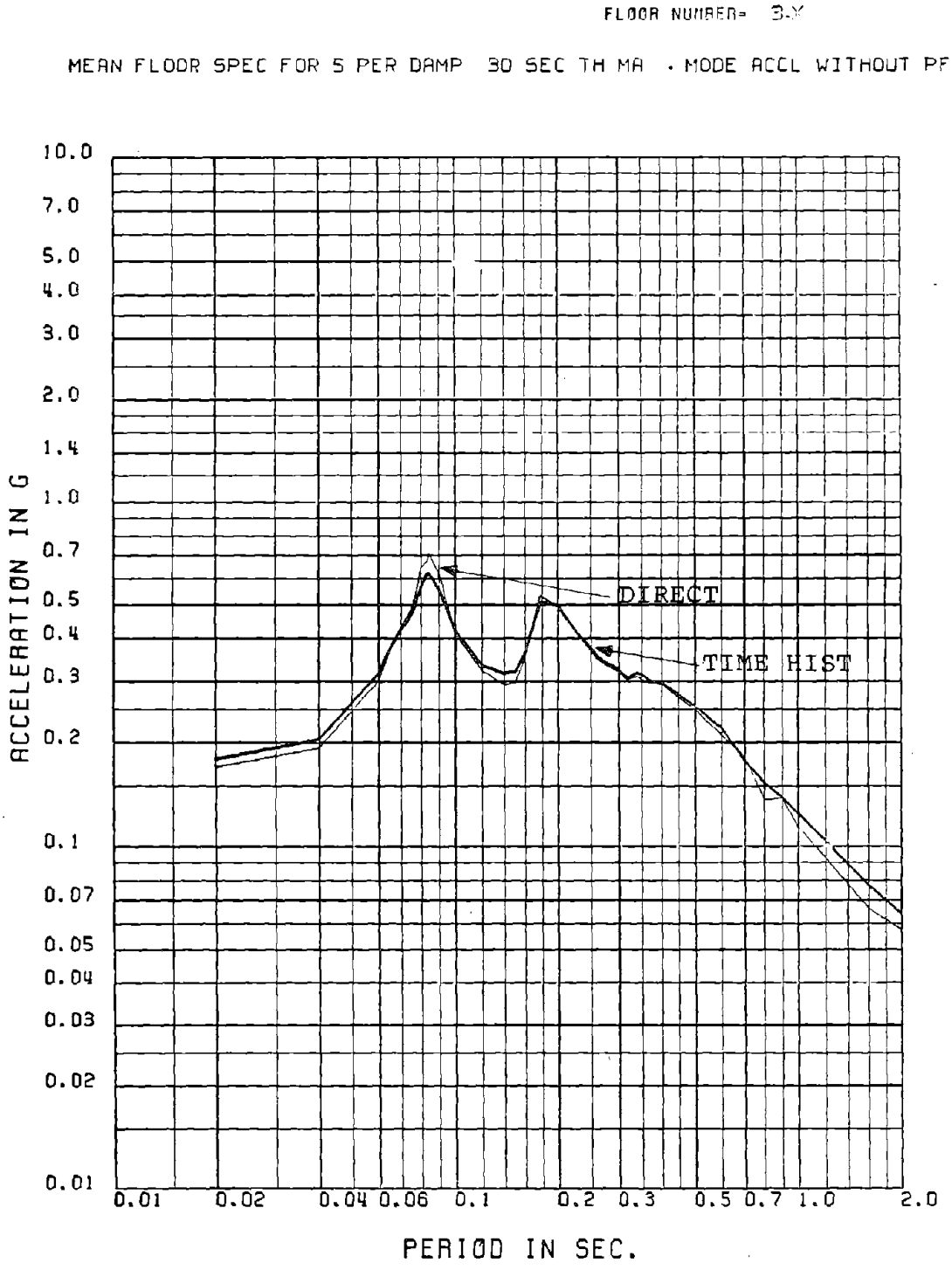

Fig. 4.3 Comparison of Floor Spectra Obtained by Mode Acceleration Approach and Time History Analysis for 5% Damping: Mean Spectra, 30-sec TH, Floor No. 3-X, 11-FRQ Model

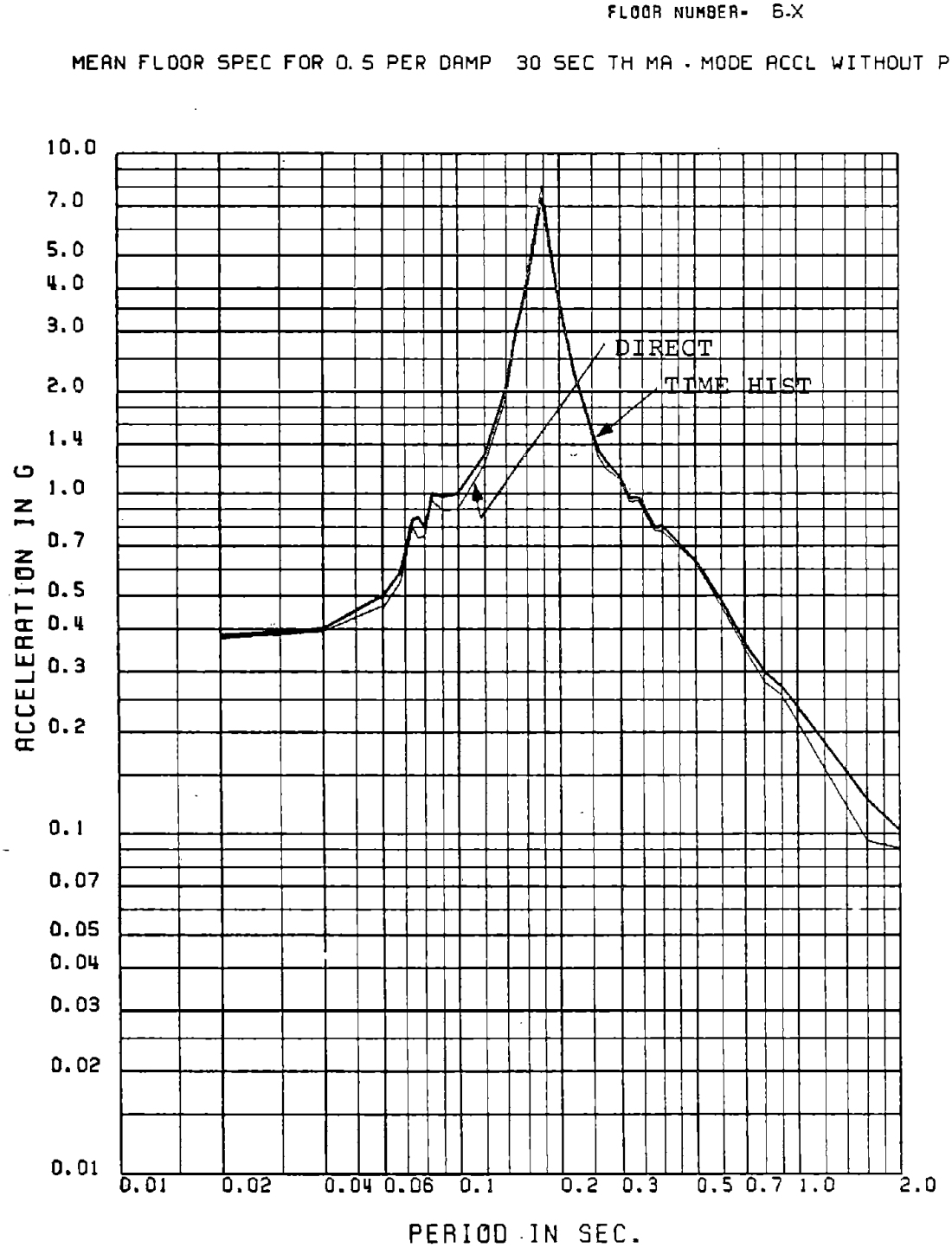

Fig. 4.4 Comparison of Floor Spectra Obtained by Mode Acceleration Approach and Time History Analysis for 0.5% Damping: Mean Spectra, 30-sec TH, Floor No. 6-X, 11-FRQ Model

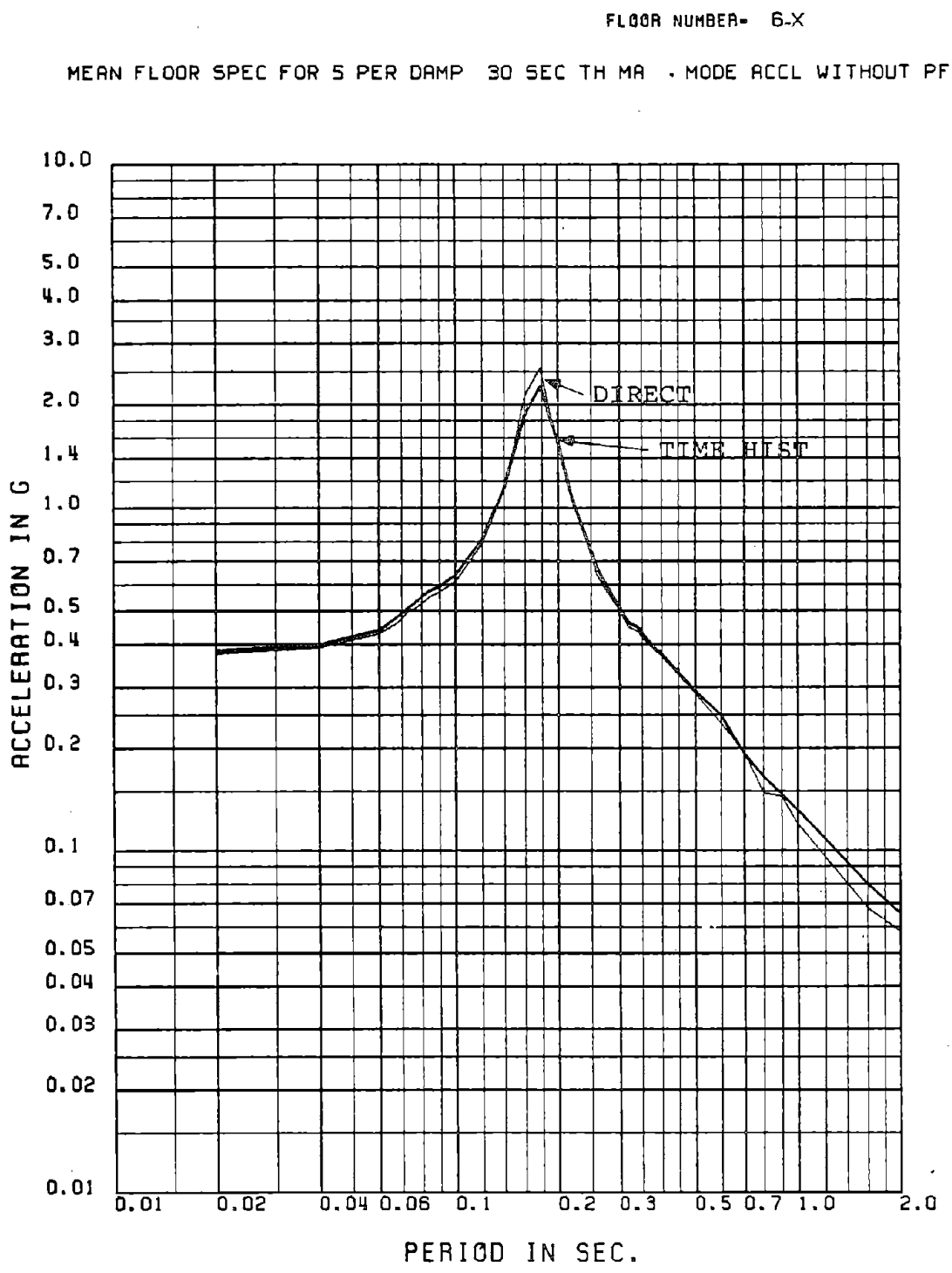

Fig. 4.5 Comparison of Floor Spectra Obtained by Mode Acceleration Approach and Time History Analysis for 5% Damping: Mean Spectra, 30-sec TH, Floor No. 6-X, 11-FRQ Model

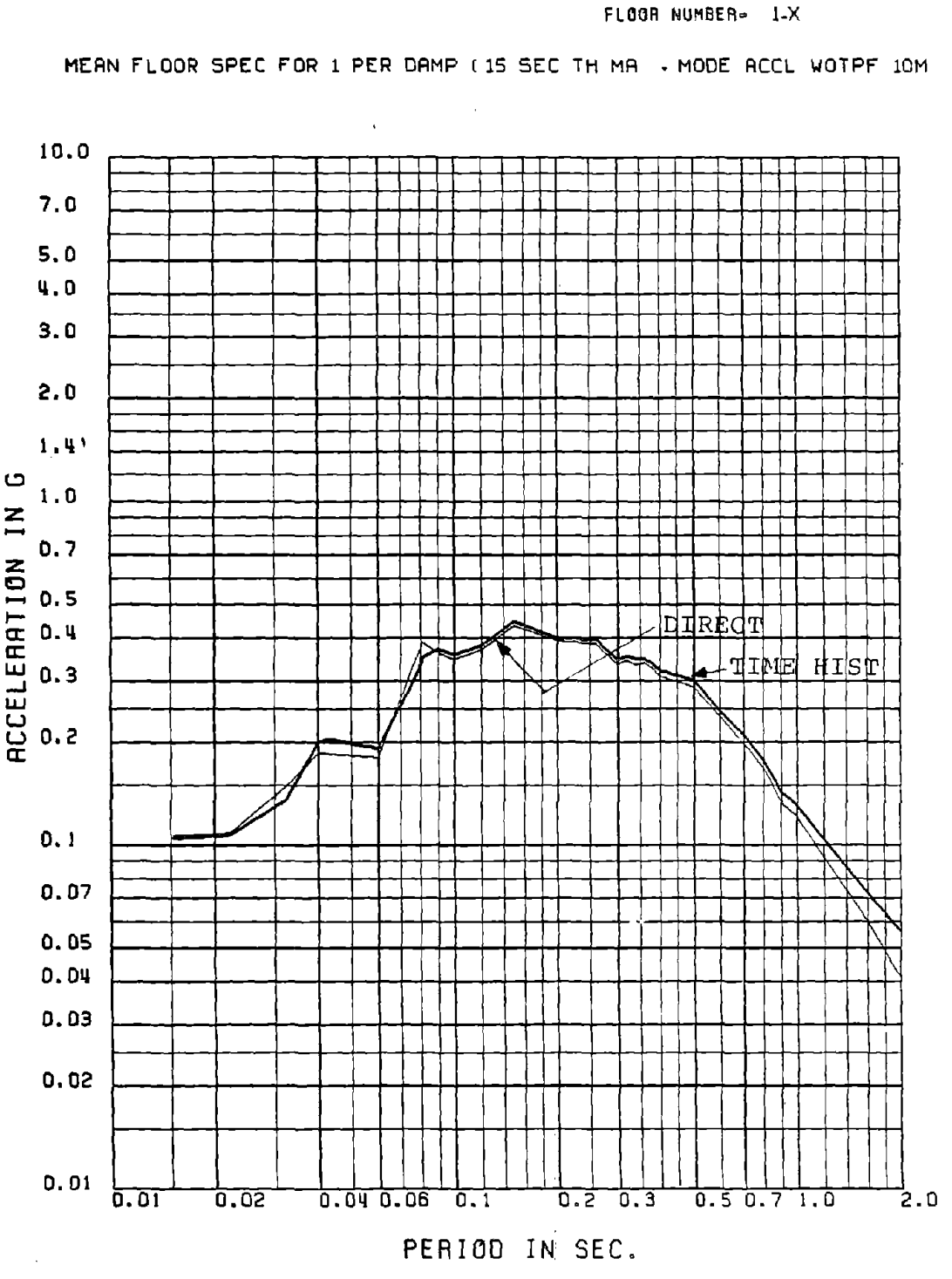

Fig. 4.6 Comparison of Floor Spectra Obtained by Mode Acceleration Approach with 10 Modes and by Time History Analysis for 1% Damping: Mean Spectra, 15-sec TH, Floor No. 1-X, 30-D.O.F. Model

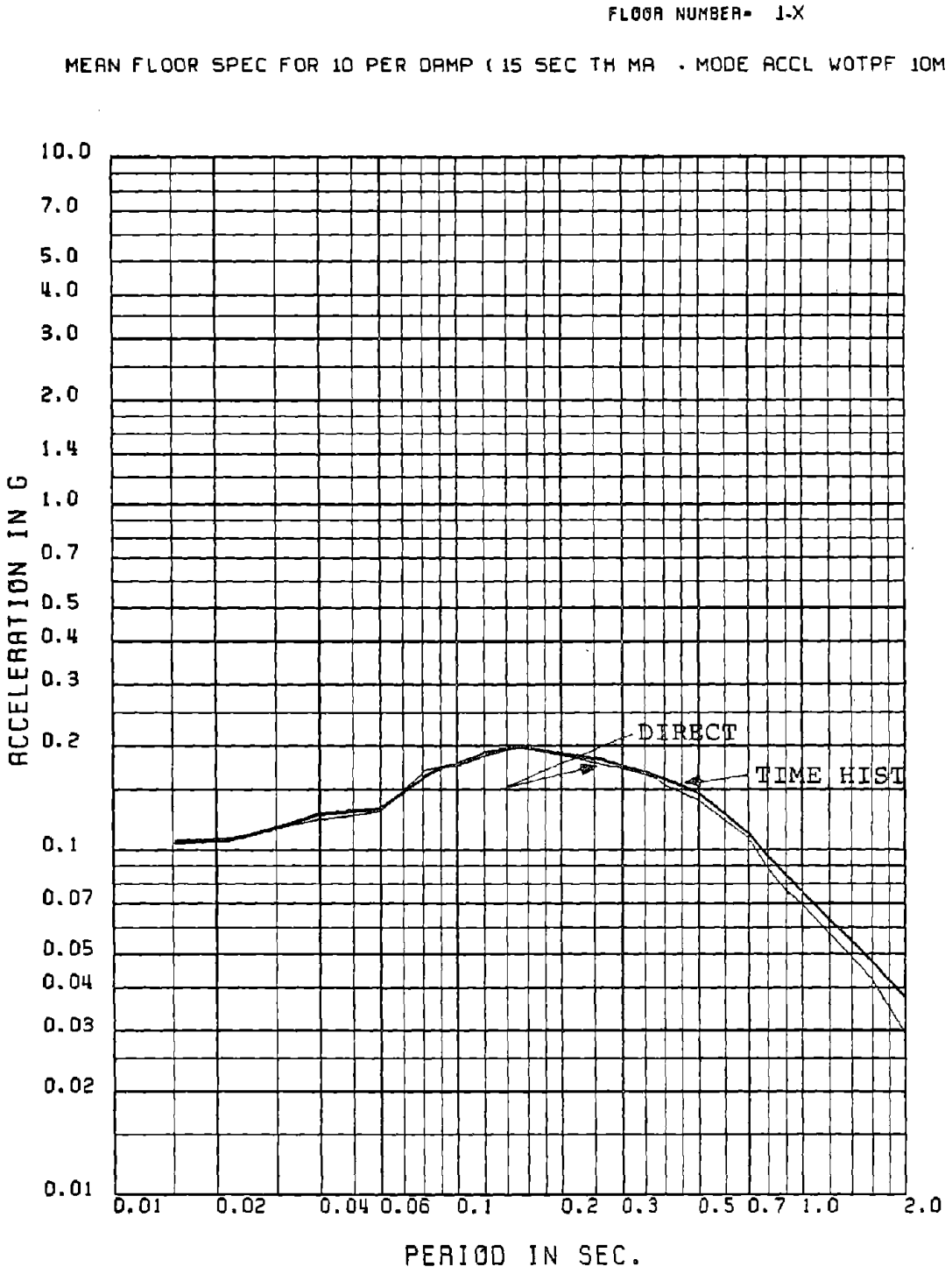

Fig. 4.7 Comparison of Floor Spectra Obtained by Mode Acceleration Approach with 10 Modes and by Time History Analysis for 10% Damping: Mean Spectra, 15-sec TH, Floor No. 1-X, 30-D.O.F. Model

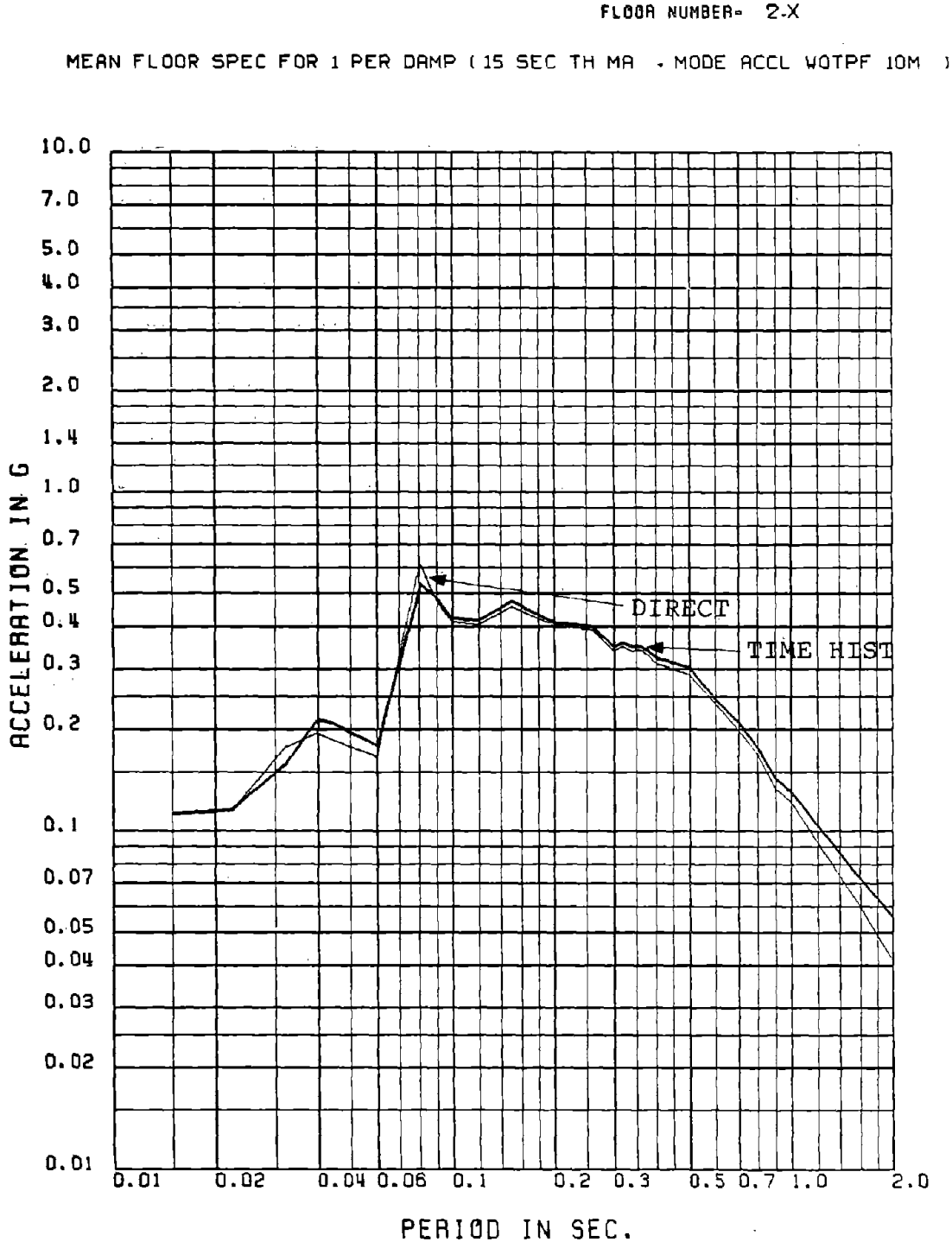

Fig. 4.8 Comparison of Floor Spectra Obtained by Mode Acceleration Approach with 10 Modes and by Time History Analysis for 1% Damping: Mean Spectra, 15-sec TH, Floor No. 2-X, 30-D.O.F. Model

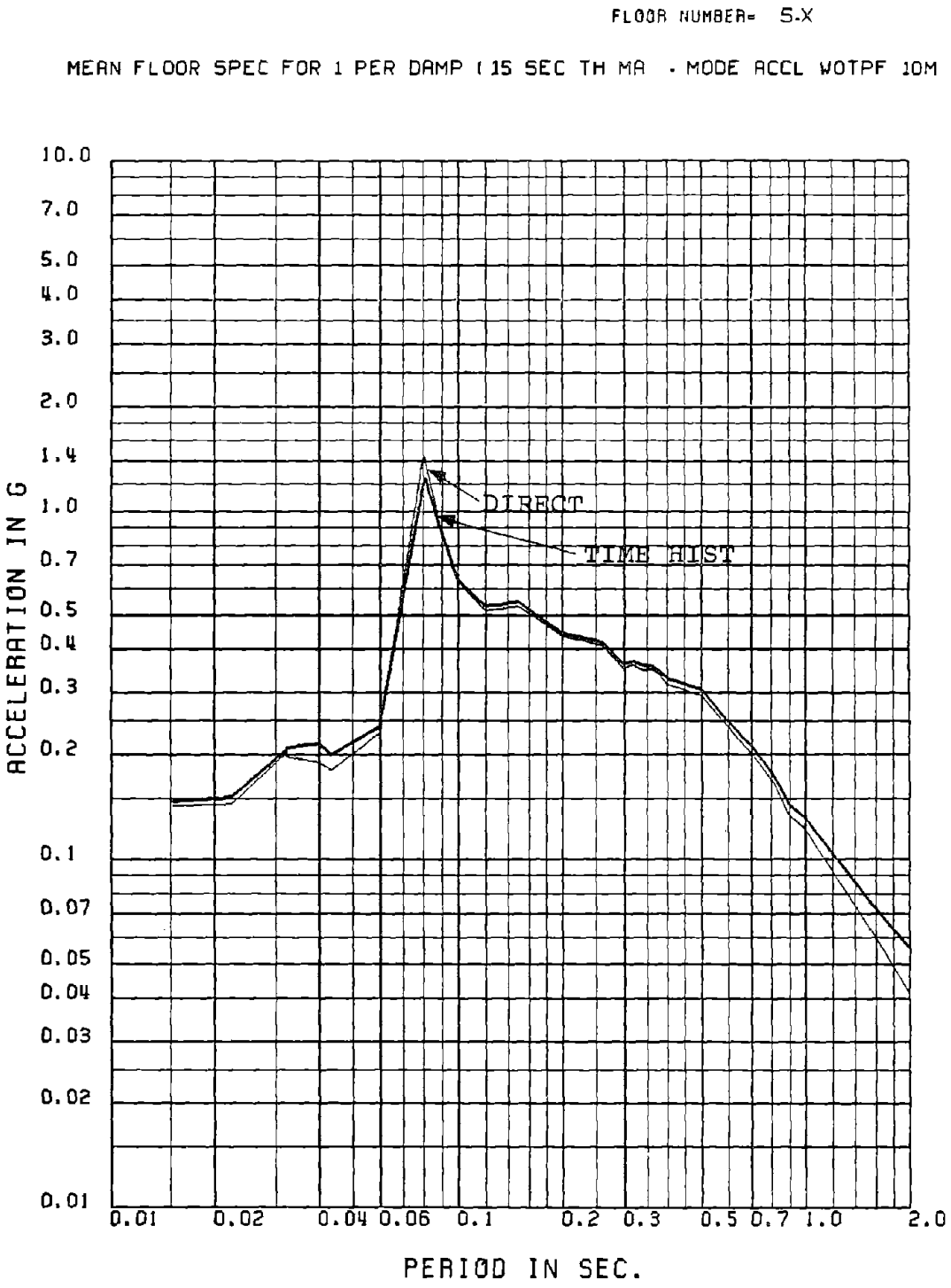

Fig. 4.9 Comparison of Floor Spectra Obtained by Mode Acceleration Approach with 10 Modes and by Time History Analysis for 1% Damping: Mean Spectra, 15-sec TH, Floor No. 5-X, 30-D.O.F. Model

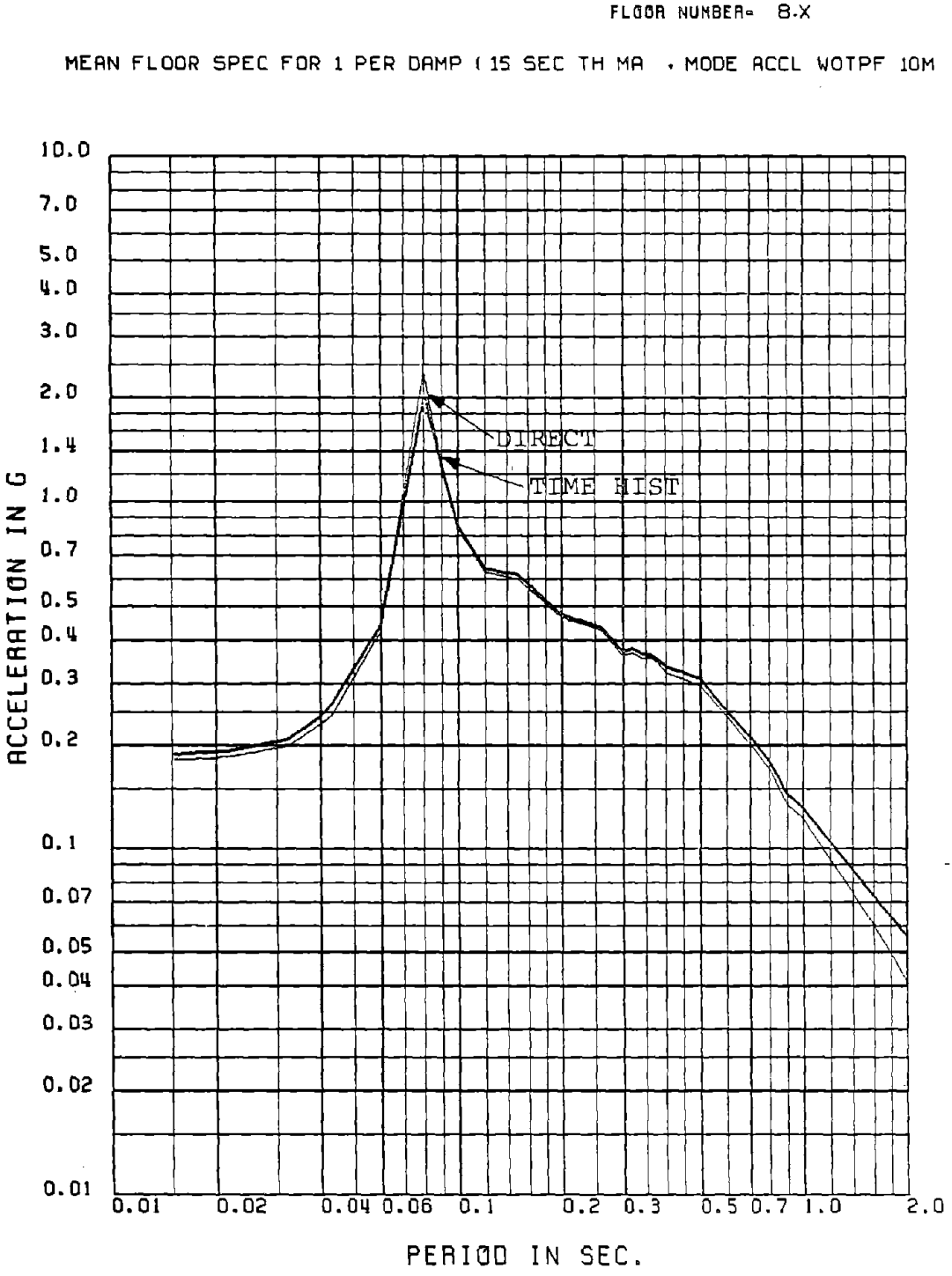

Fig. 4.10 Comparison of Floor Spectra Obtained by Mode Acceleration Approach with 10 Modes and by Time History Analysis for 1% Damping: Mean Spectra, 15-sec TH, Floor No. 8-X, 30-D.O.F. Model

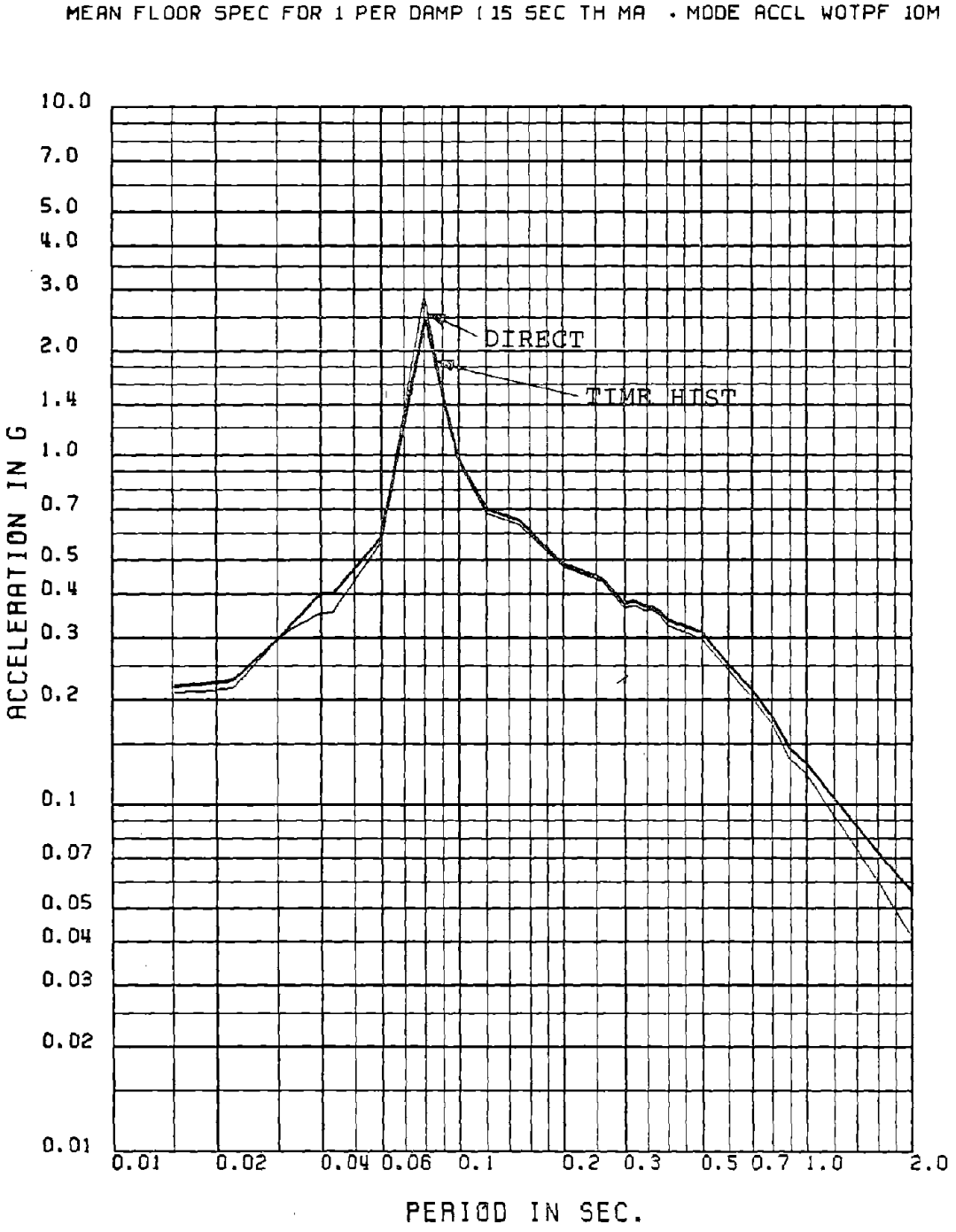

Fig. 4.11 Comparison of Floor Spectra Obtained by the Mode Acceleration Approach with 10 Modes and by Time History Analysis for 1% Damping: Mean Spectra, 15-sec TH, Floor No. 10-X, 30-D.O.F. Model

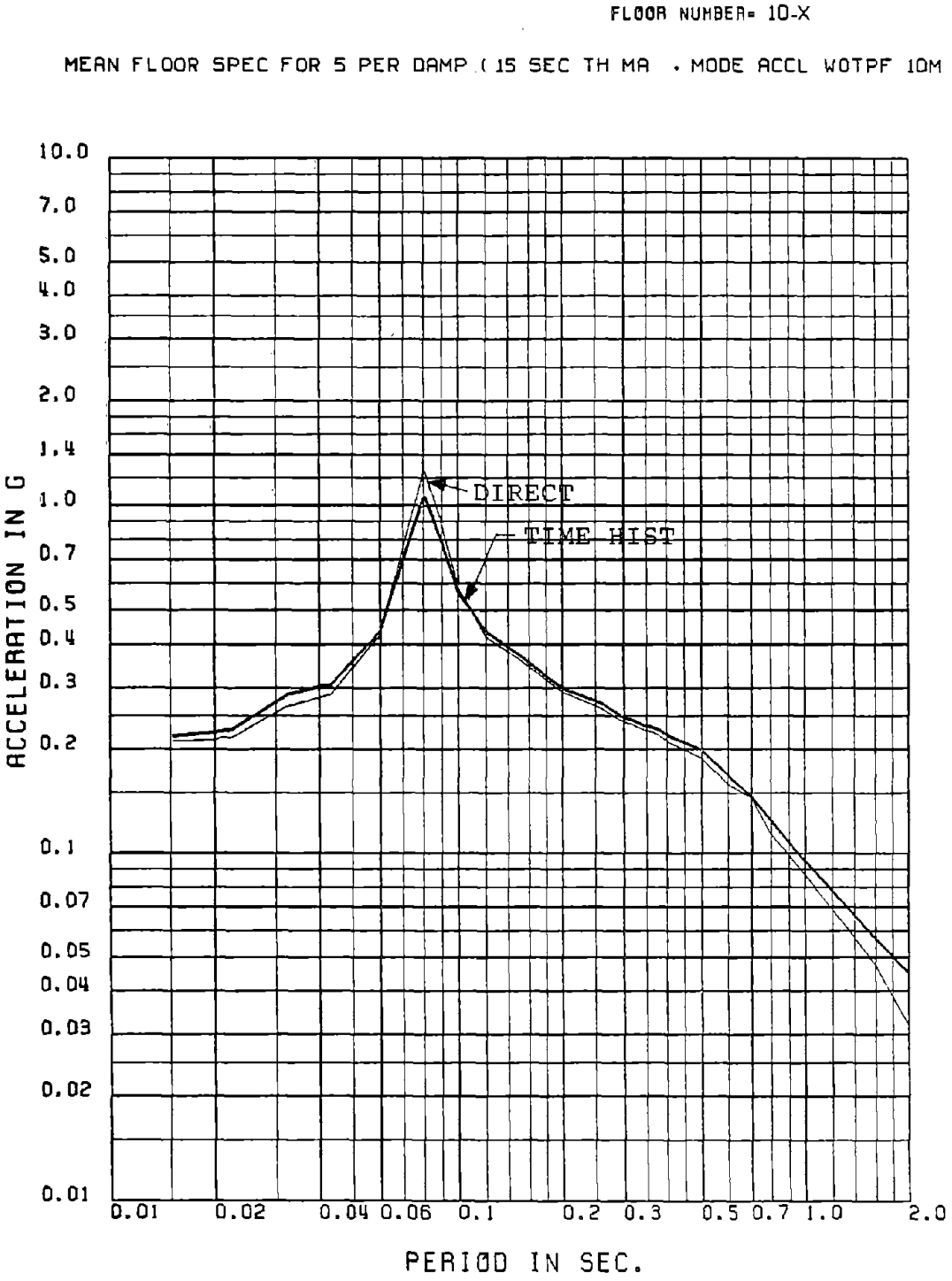

Fig. 4.12 Comparison of Floor Spectra Obtained by the Mode Acceleration Approach with 10 Moes and by Time History Analysis for 5% Damping: Mean Spectra, 15-sec TH, Floor No. 10-X, 30-D.O.F. Model

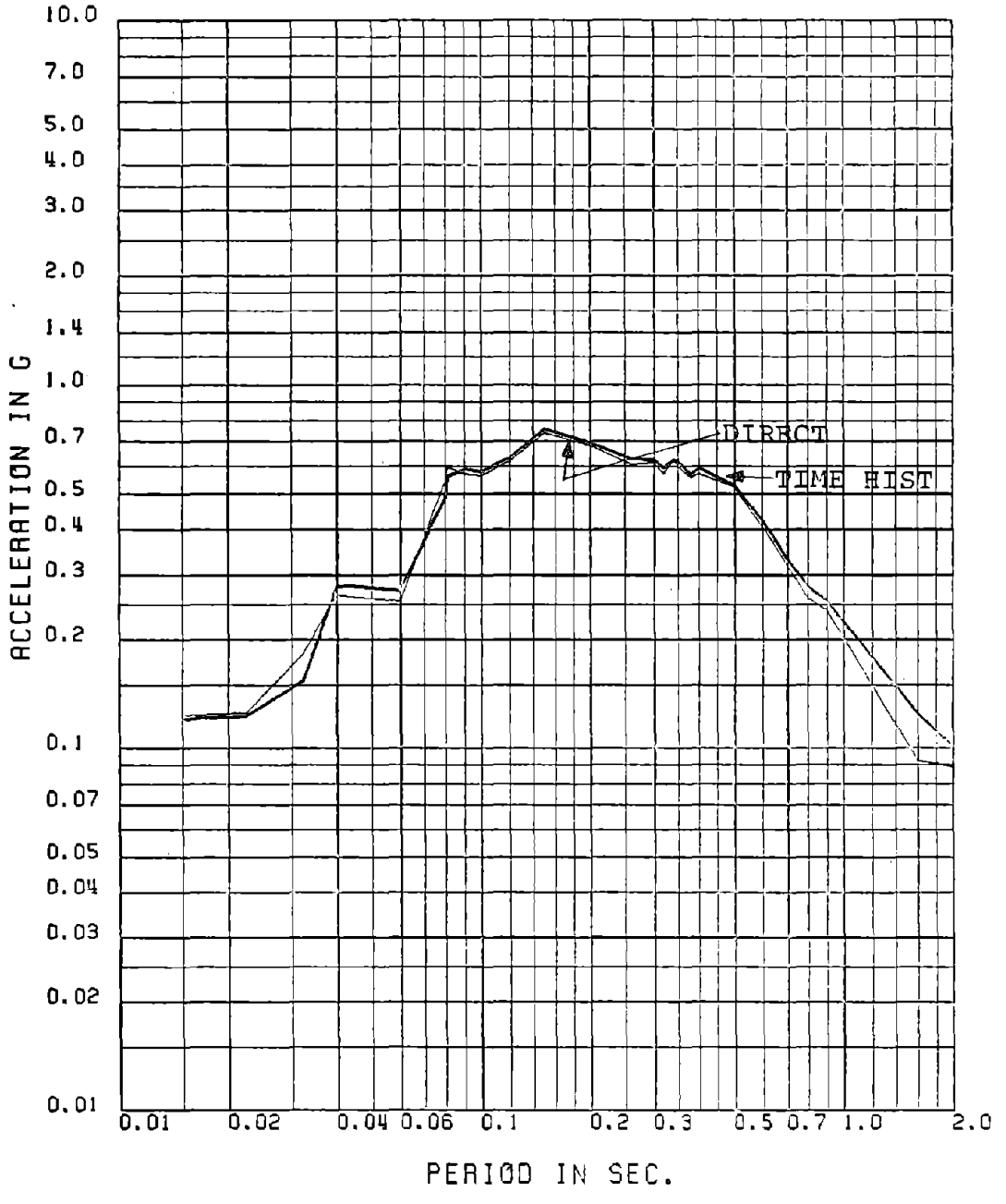

Fig. 4.13 Comparison of Floor Spectra Obtained by Mode Acceleration Approach with 10 Modes and by Time History Analysis for 0.5% Damping: Mean Spectra, 30-sec TH, Floor No. 1-X, 30-D.O.F. Model

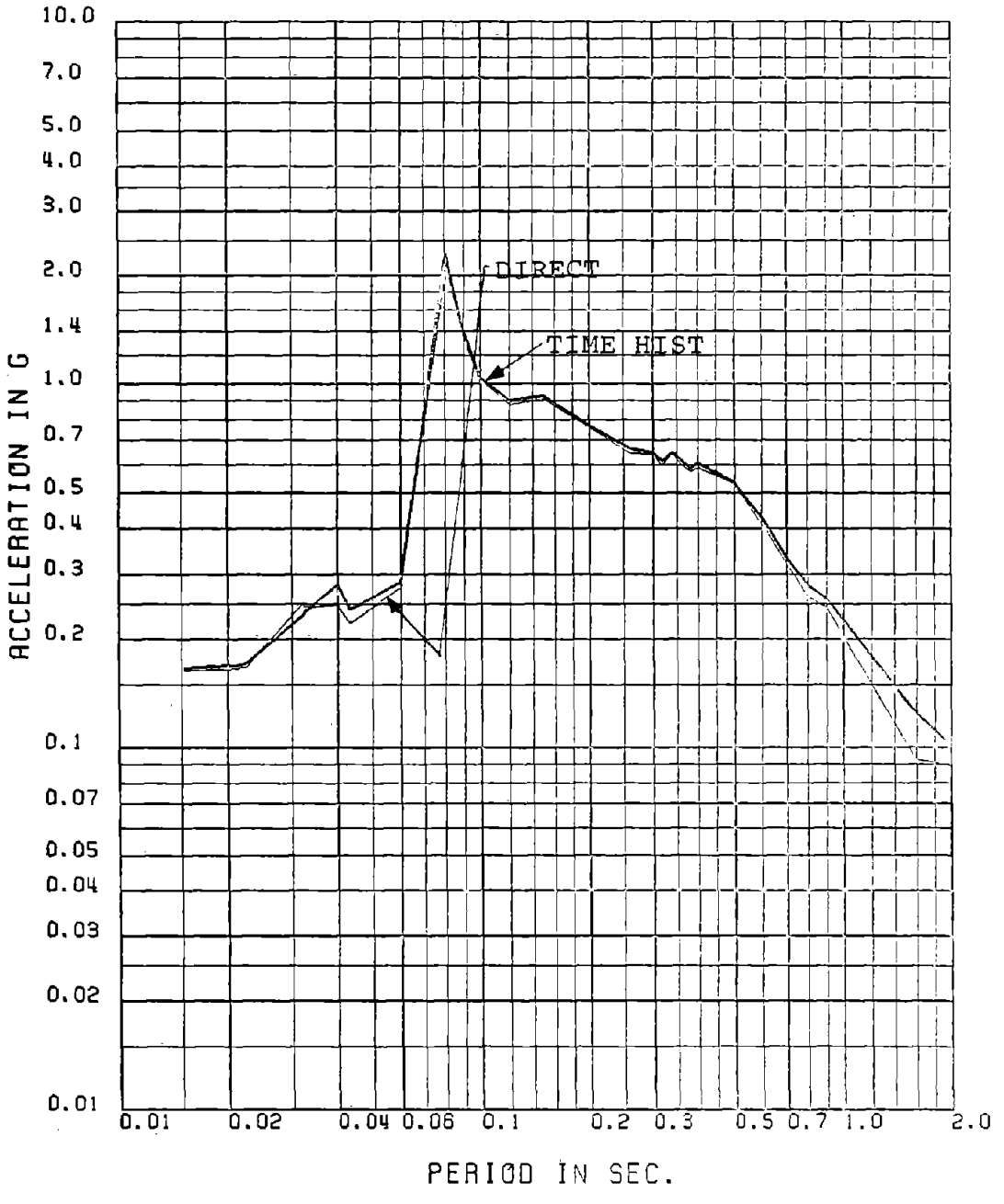

Fig. 4.14 Comparison of Floor Spectra Obtained by Mode Acceleration Approach with 10 Modes and by Time History Analysis for 0.5% Damping: Mean Spectra, 30-sec TH, Floor No. 5-X, 30-D.O.F. Model

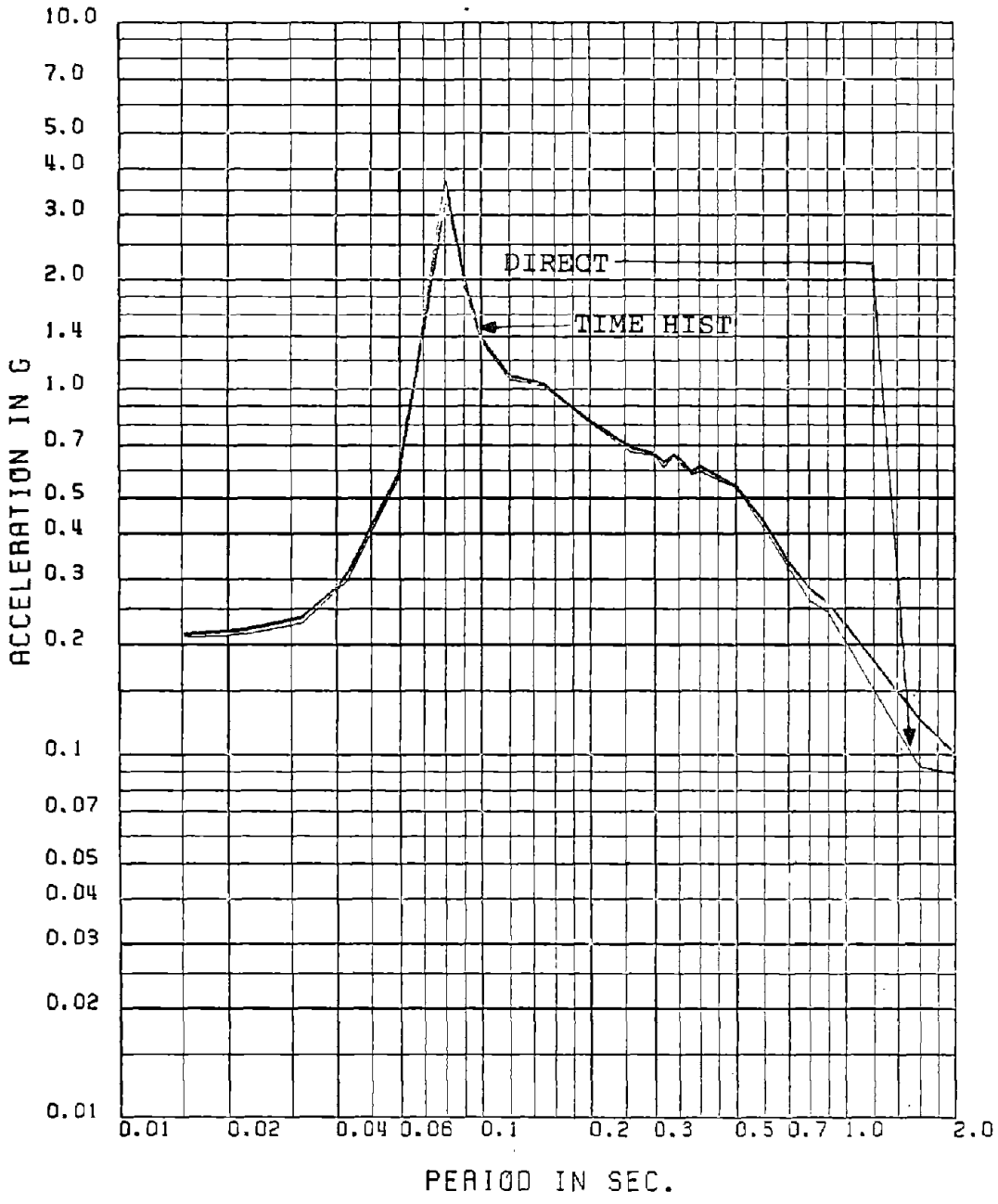

Fig. 4.15 Comparison of Floor Spectra Obtained by Mode Acceleration Approach with 10 Modes and by Time History Analysis for 0.5% Damping: Mean Spectra, 30-sec TH, Floor No. 8-X, 30-D.O.F. Model

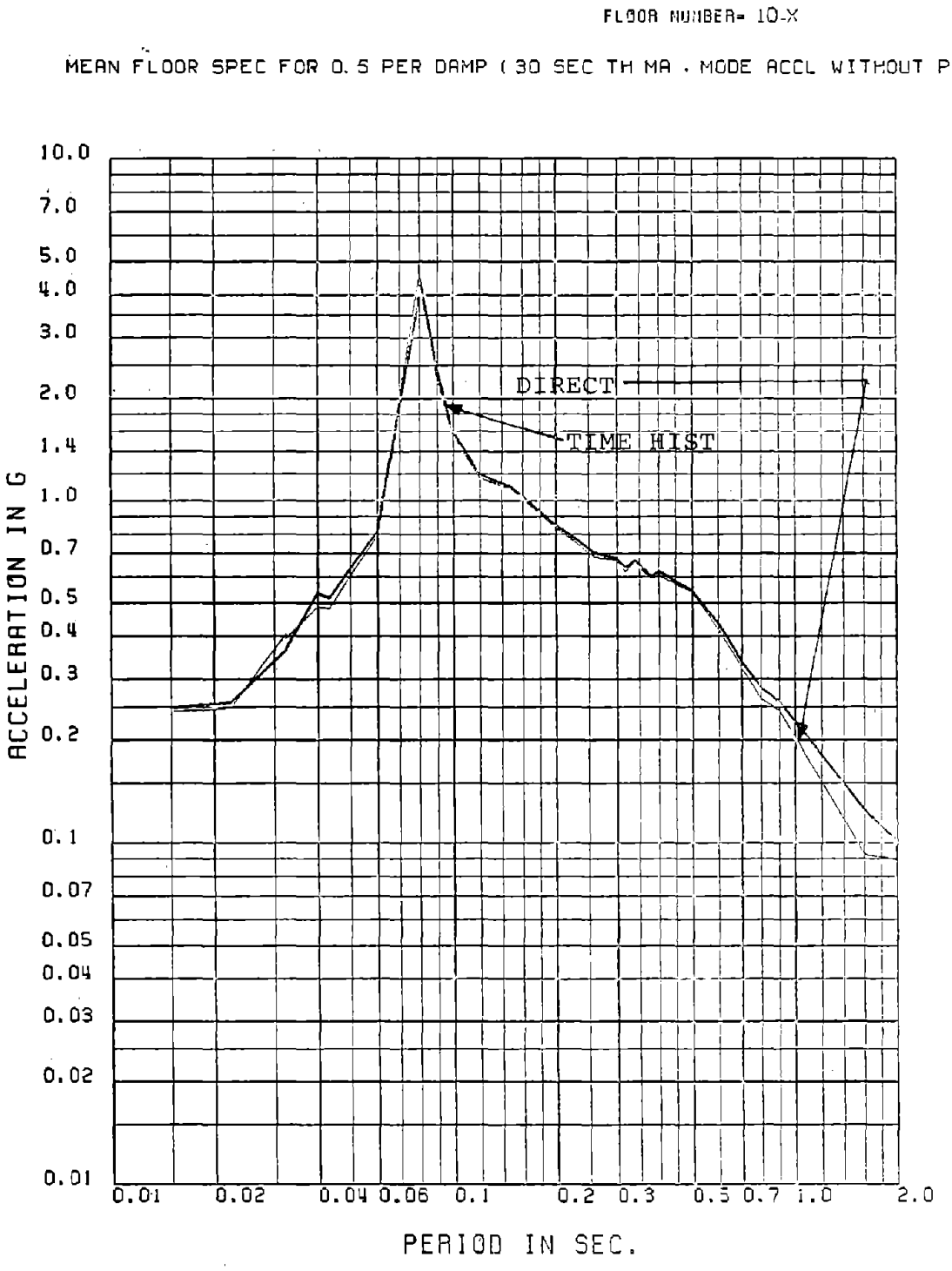

Fig. 4.16 Comparison of Floor Spectra Obtained by Mode Acceleration Approach with 10 Modes and by Time History Analysis for 0.5% Damping: Mean Spectra, 30-sec TH, Floor No. 10-X, 30-D.O.F. Model

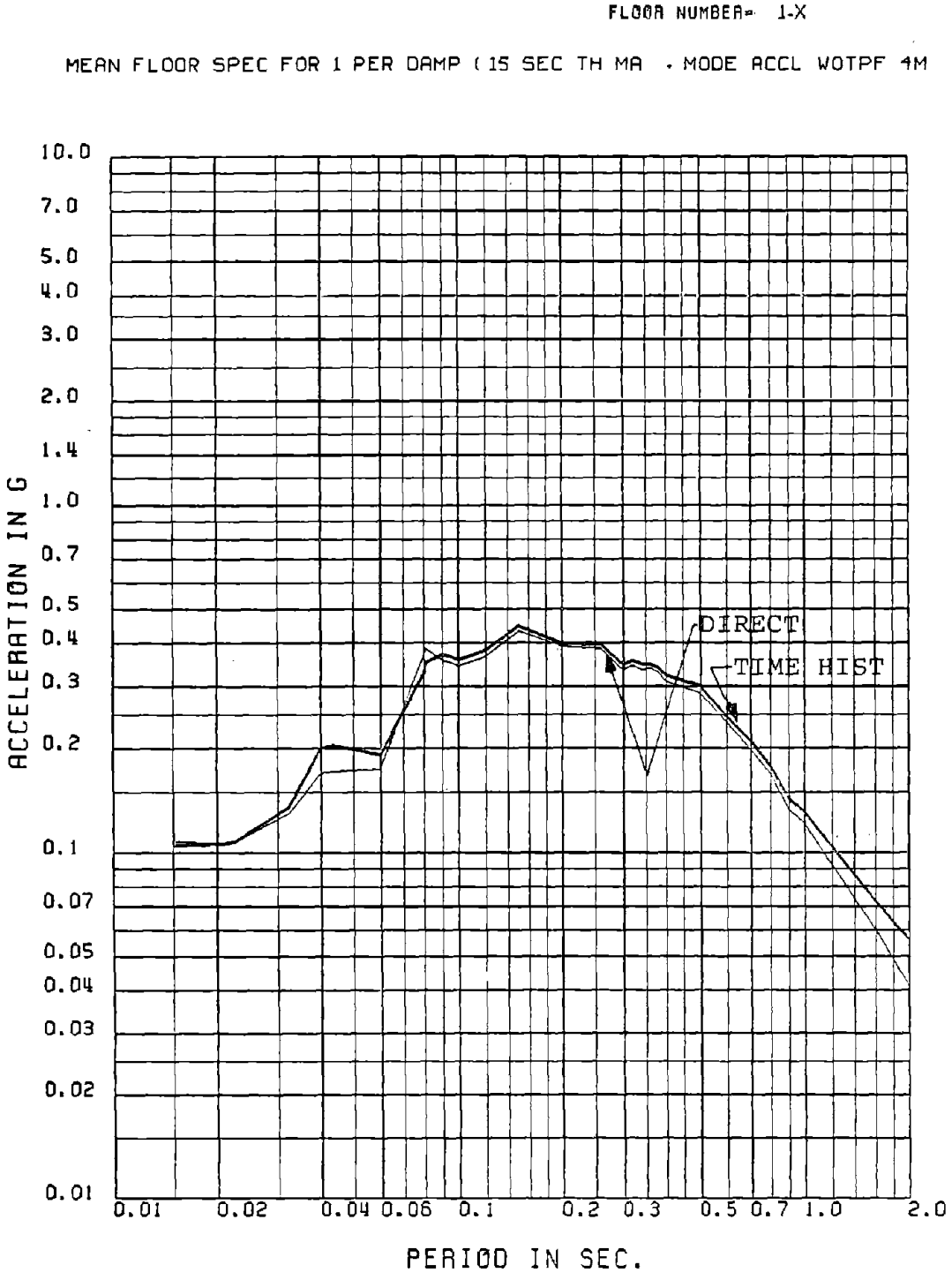

Fig. 4.17 Comparison of Floor Spectra Obtained by Mode Acceleration Approach with 4 Modes and by Time History Analysis for 1% Damping: Mean Spectra, 15-sec TH, Floor No. 1-X, 30-D.O.F. Model

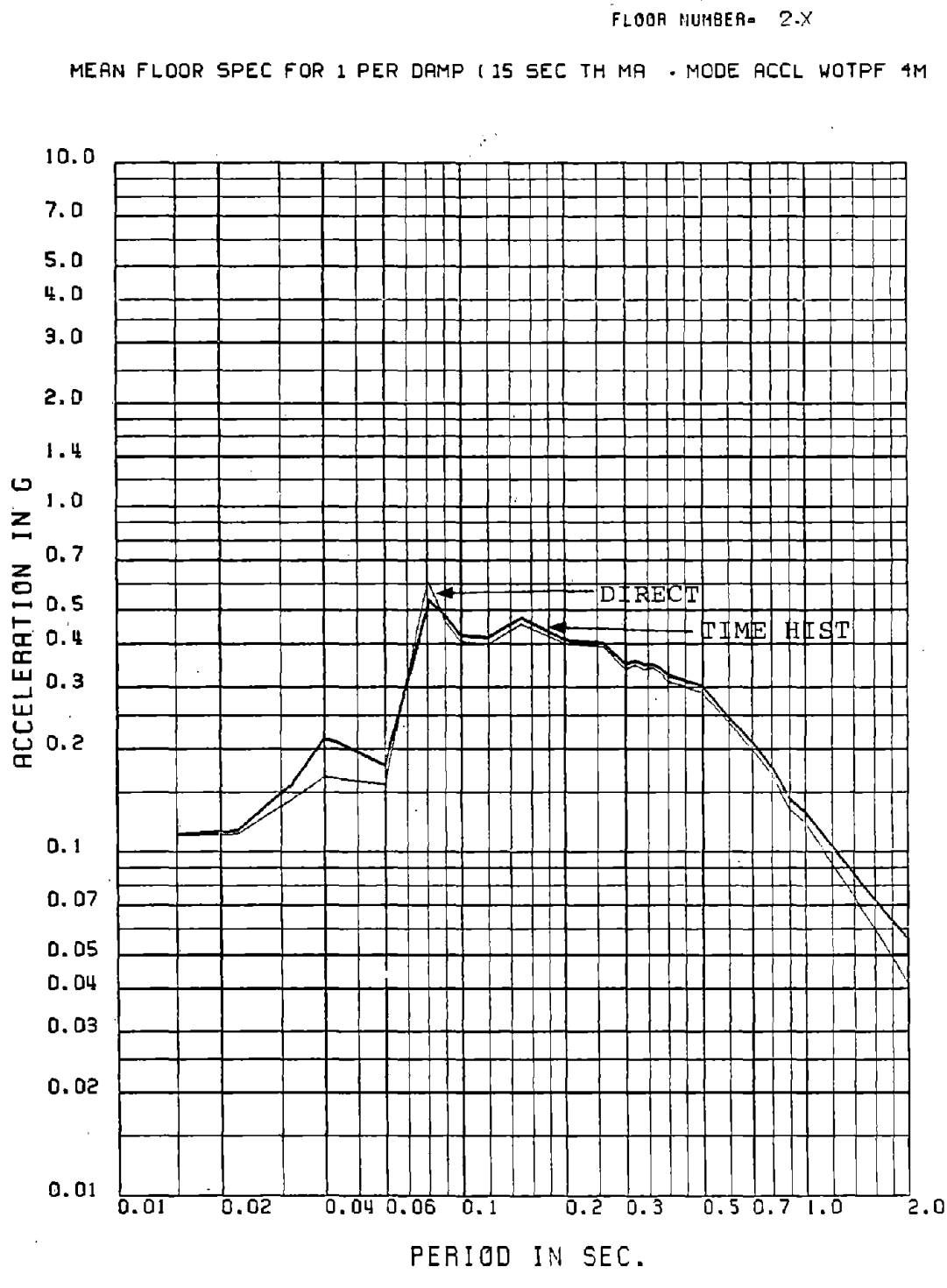

Fig. 4.18 Comparison of Floor Spectra Obtained by Mode Acceleration Approach with 4 Modes and by Time History Analysis for 1% Damping: Mean Spectra, 15-sec TH, Floor No. 2-X, 30-D.O.F. Model

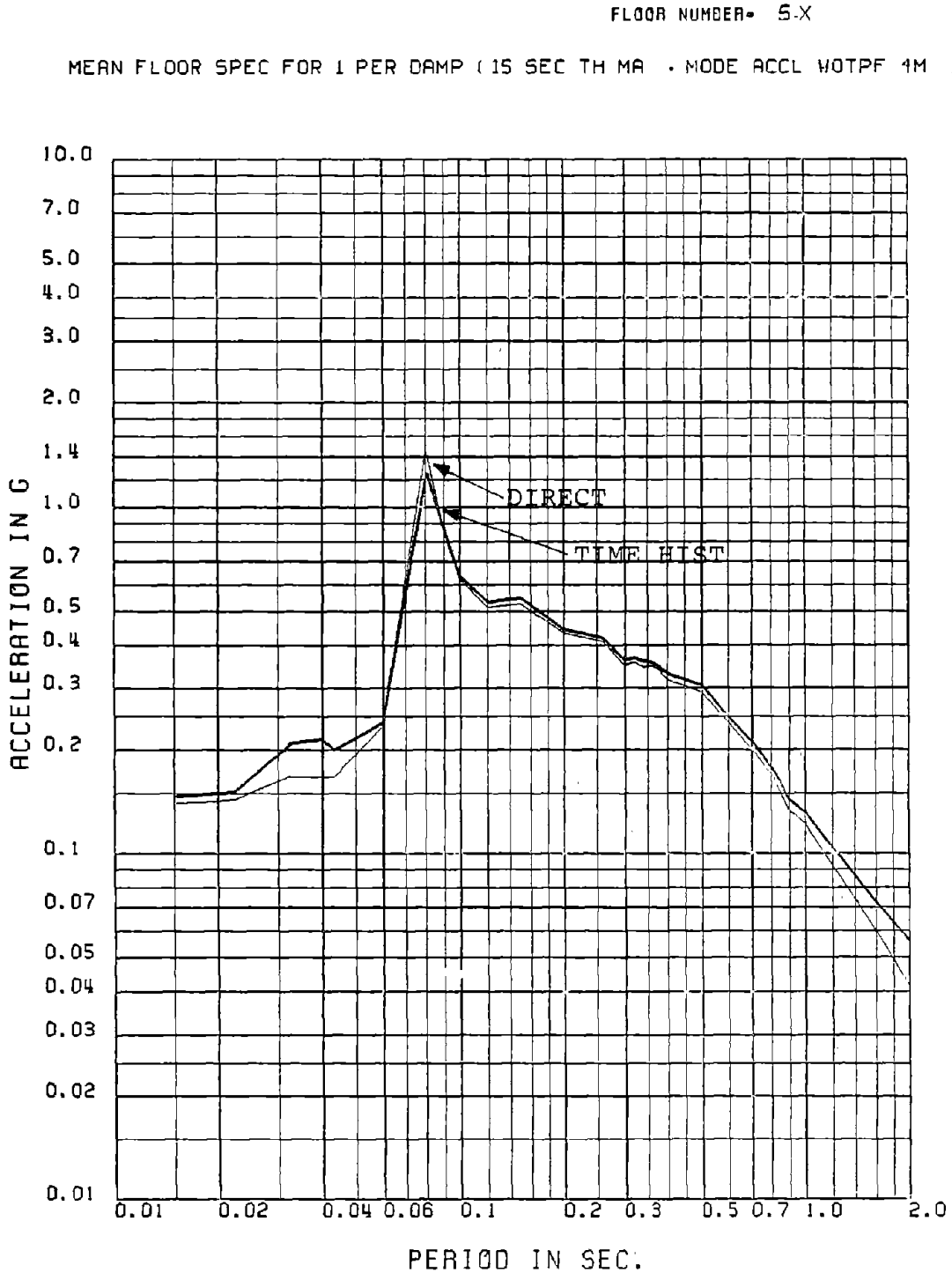

Fig. 4.19 Comparison of Floor Spectra Obtained by Mode Acceleration Approach with 4 Modes and by Time History Analysis for 1% Damping: Mean Spectra, 15-sec TH, Floor No. 5-X, 30-D.O.F. Model

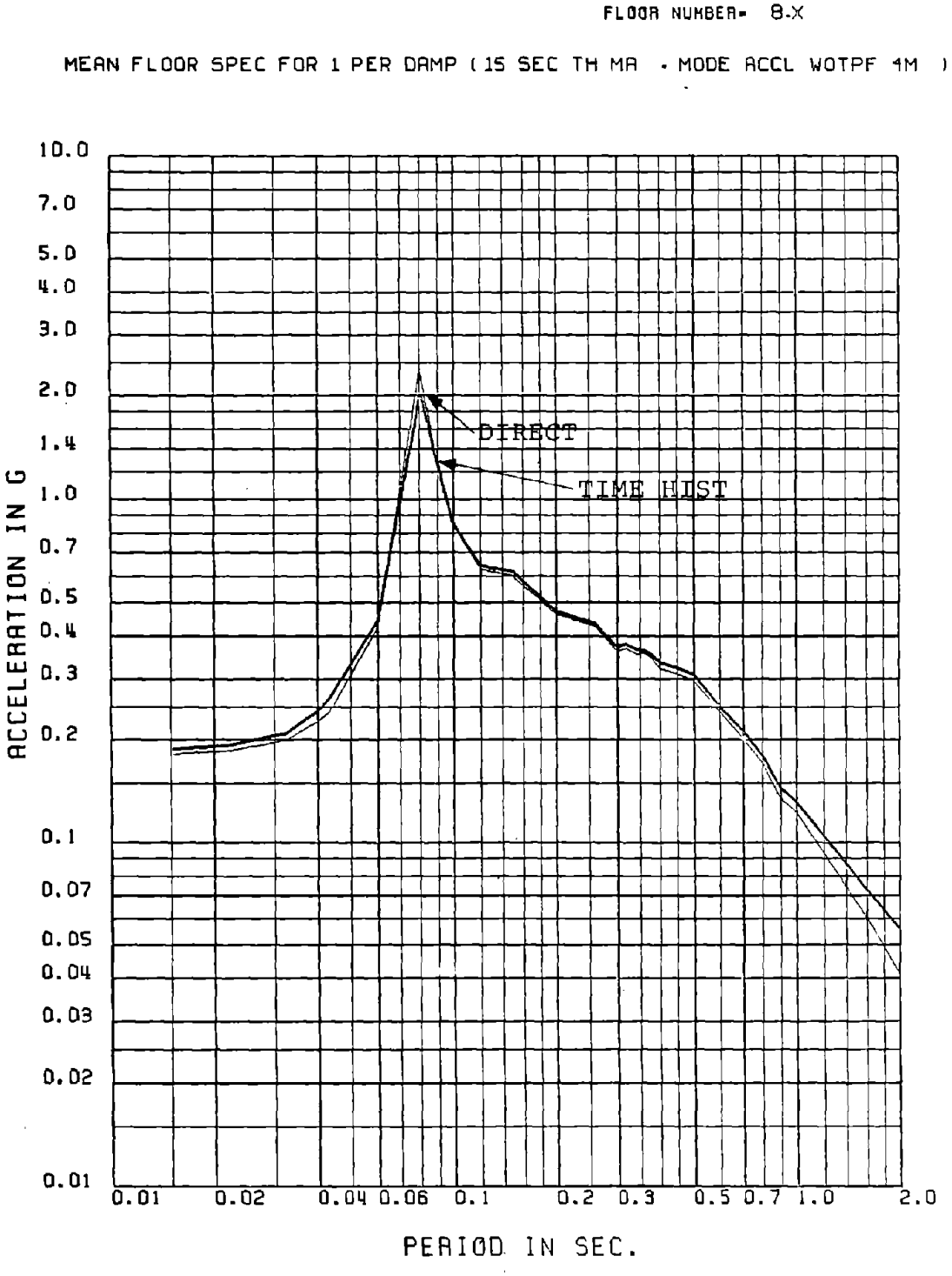

Fig. 4.20 Comparison of Floor Spectra Obtained by Mode Acceleration Approach with 4 Modes and by Time History Analysis for 1% Damping: Mean Spectra, 15-sec TH, Floor No. 8-X, 30-D.O.F. Model

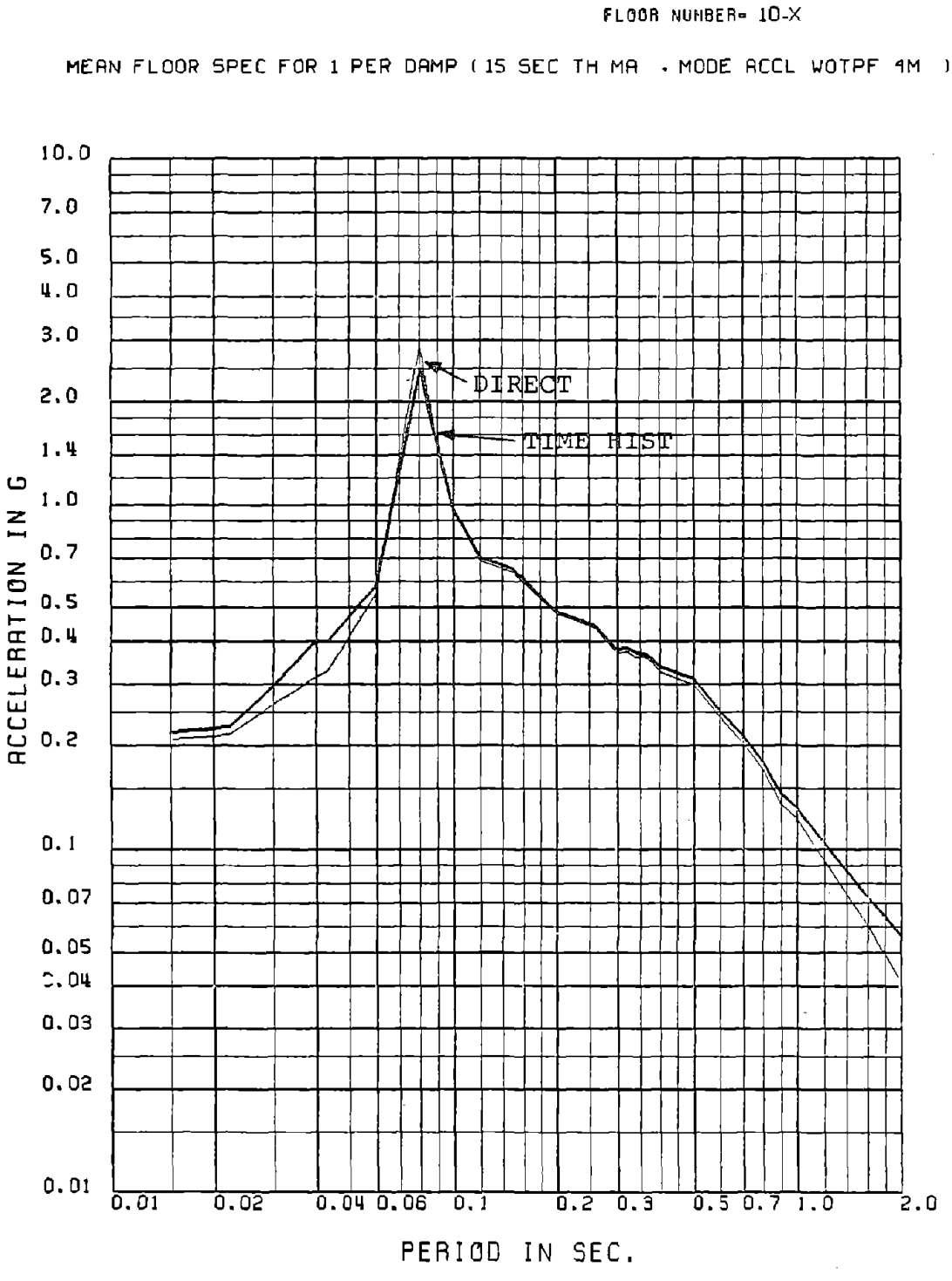

Fig. 4.21 Comparison of Floor Spectra Obtained by Mode Acceleration Approach with 4 Modes and by Time History Analysis for 1% Damping: Mean Spectra, 15-sec TH, Floor No. 10-X, 30-D.O.F. Model

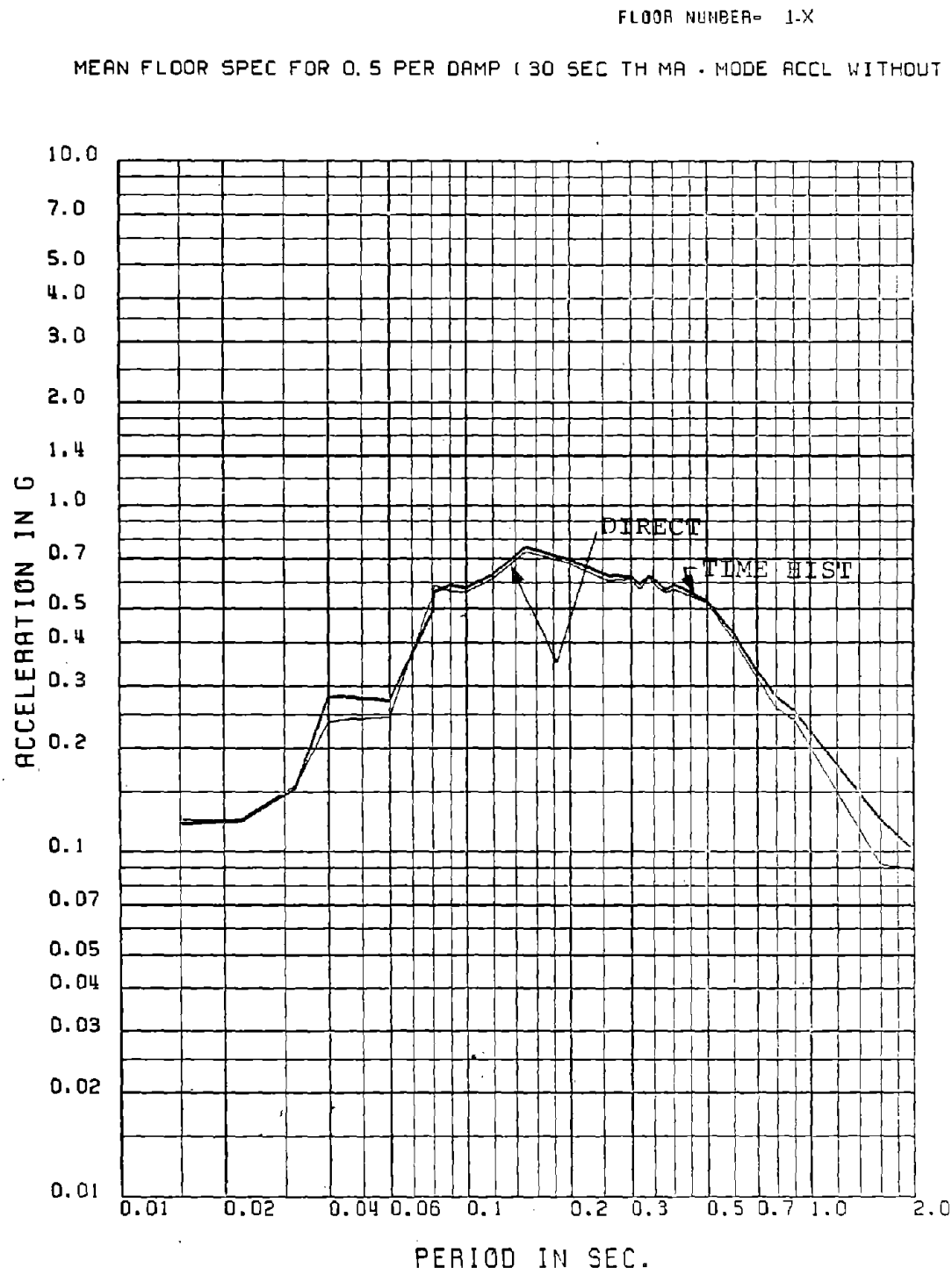

Fig. 4.22 Comparison of Floor Spectra Obtained by Mode Acceleration Approach with 4 Modes and by Time History Analysis for 0.5% Damping: Mean Spectra, 30-sec TH, Floor No. 1-X, 30-D.O.F. Model

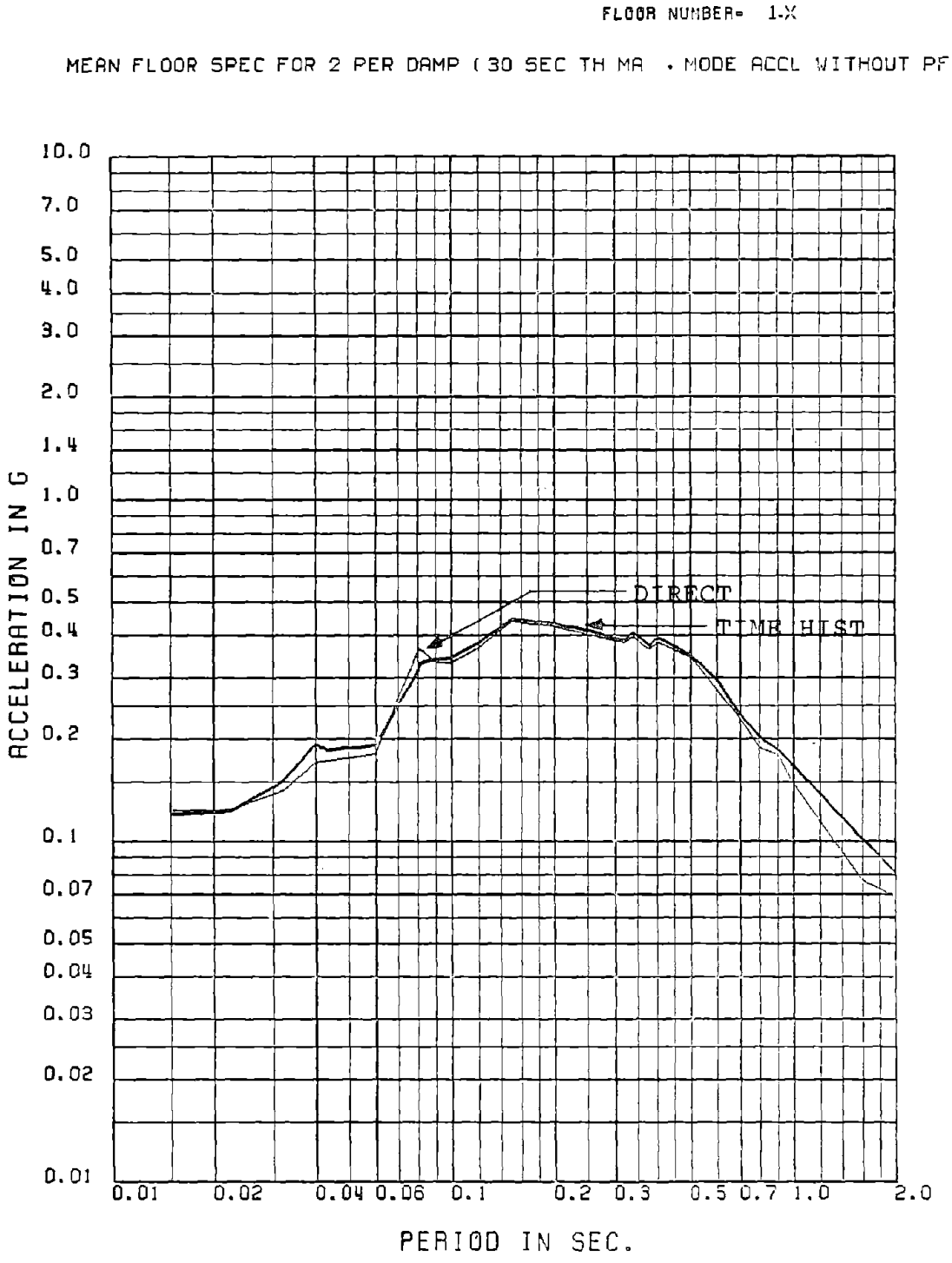

Fig. 4.23 Comparison of Floor Spectra Obtained by Mode Acceleration Approach with 4 Modes and by Time History Analysis for 2% Damping: Mean Spectra, 30-sec TH, Floor No. 1-X, 30-D.O.F. Model

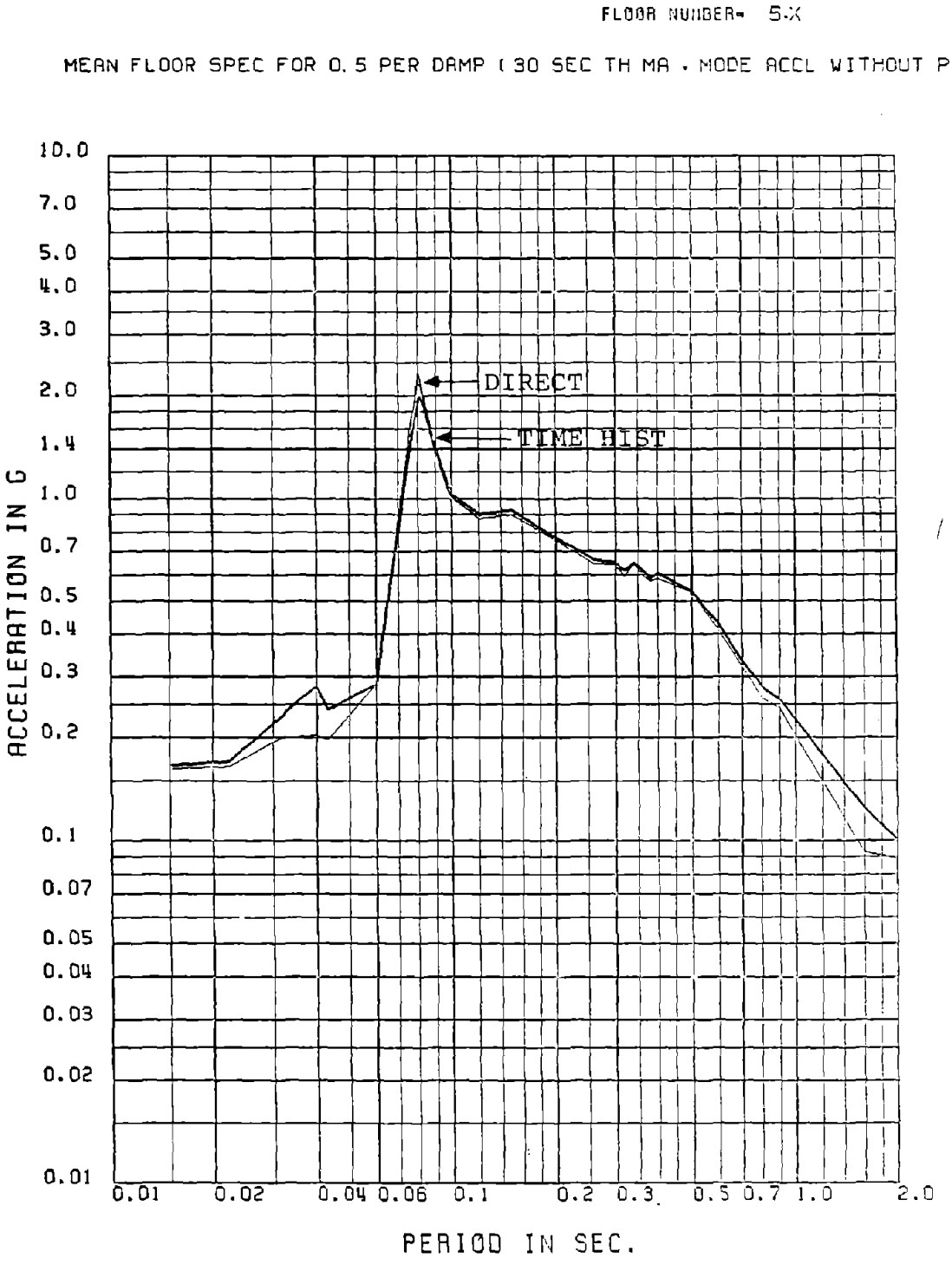

Fig. 4.24 Comparison of Floor Spectra Obtained by Mode Acceleration Approach with 4 Modes and by Time History Analysis for 0.5% Damping: Mean Spectra, 30-sec TH, Floor No. 5-X, 30-D.O.F. Model

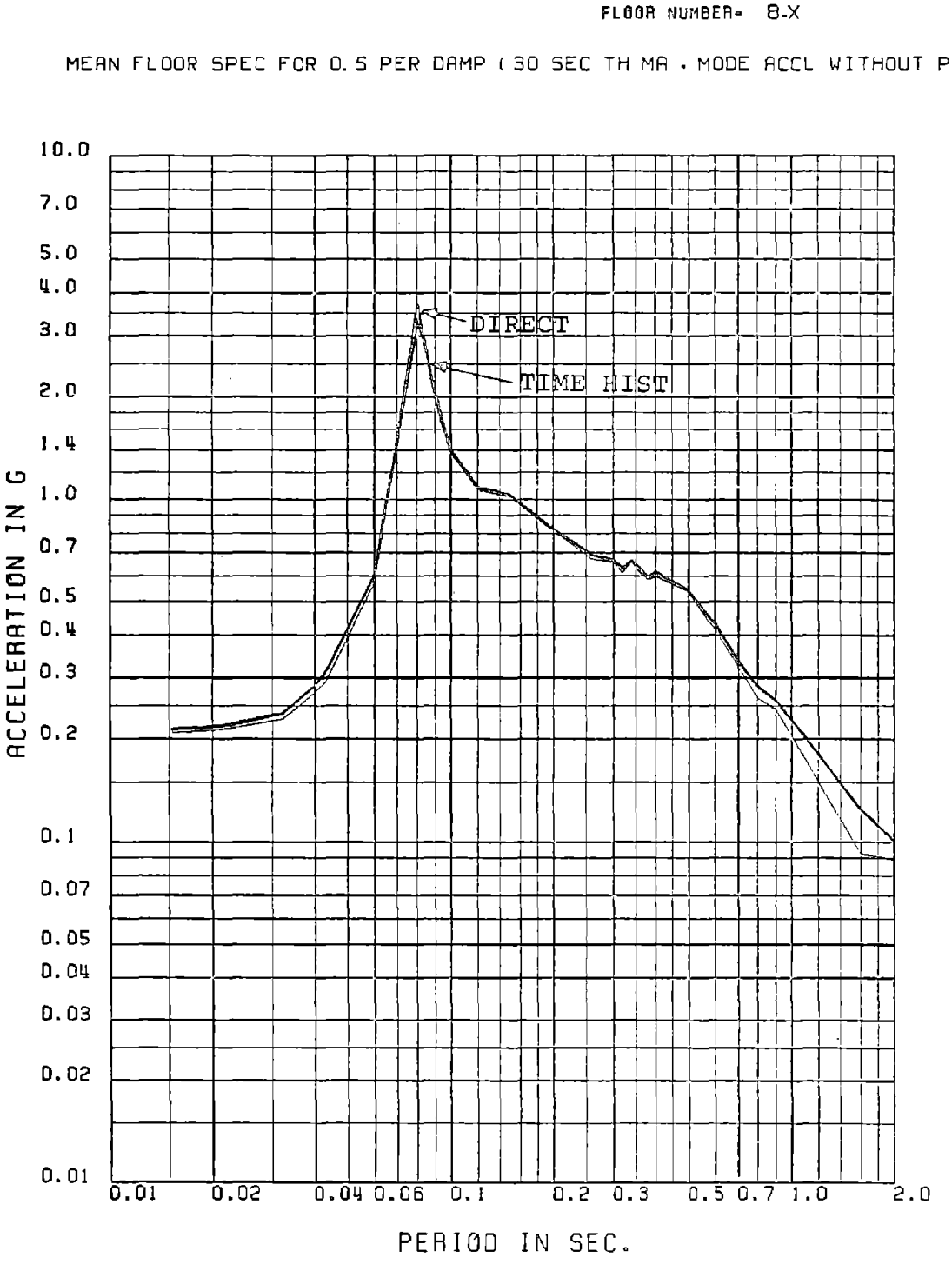

Fig. 4.25 Comparison of Floor Spectra Obtained by Mode Acceleration Approach with 4 Modes and by Time History Analysis for 0.5% Damping: Mean Spectra, 30-sec TH, Floor No. 8-X, 30-D.O.F. Model

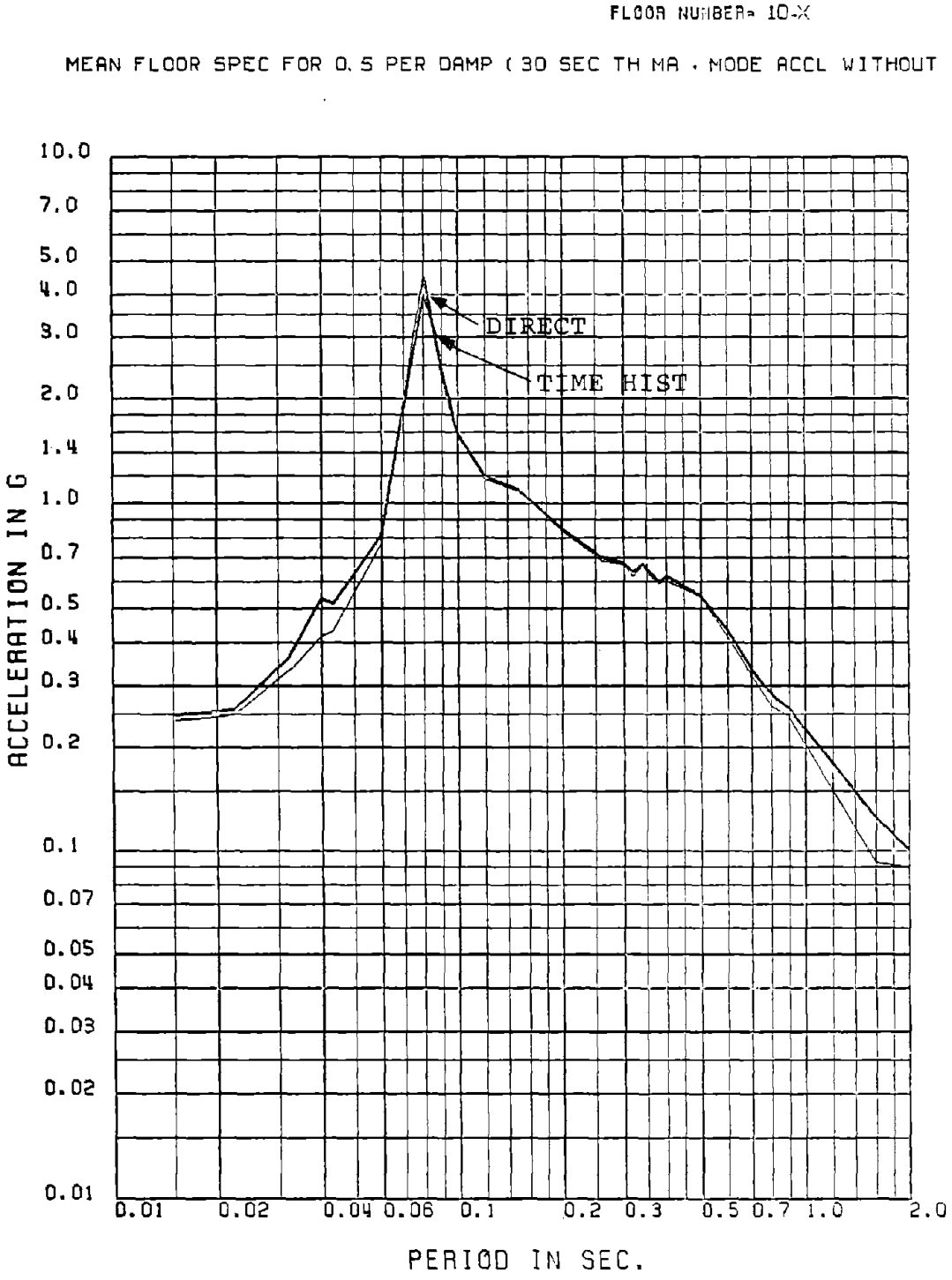

Fig. 4.26 Comparison of Floor Spectra Obtained by Mode Acceleration Approach with 4 Modes and by Time History Analysis for 0.5% Damping: Mean Spectra, 30-sec TH, Floor No. 10-X, 30-D.O.F. Model

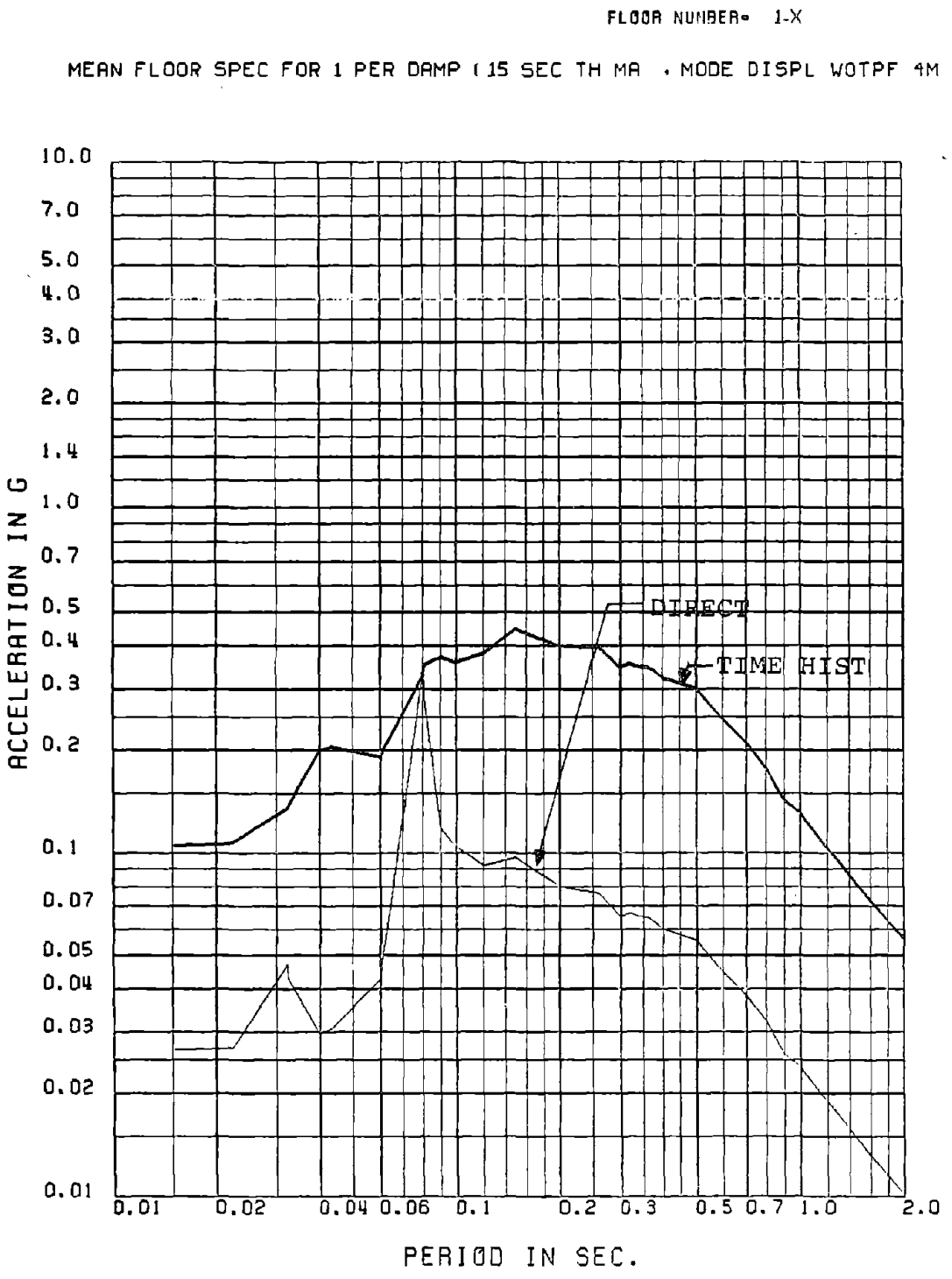

Fig. 4.27 Comparison of Floor Spectra Obtained by Mode Displacement Approach with 10 Modes and by Time History Analysis for 1% Damping: Mean Spectra, 15-sec TH, Floor No. 1-X, 30-D.O.F. Model

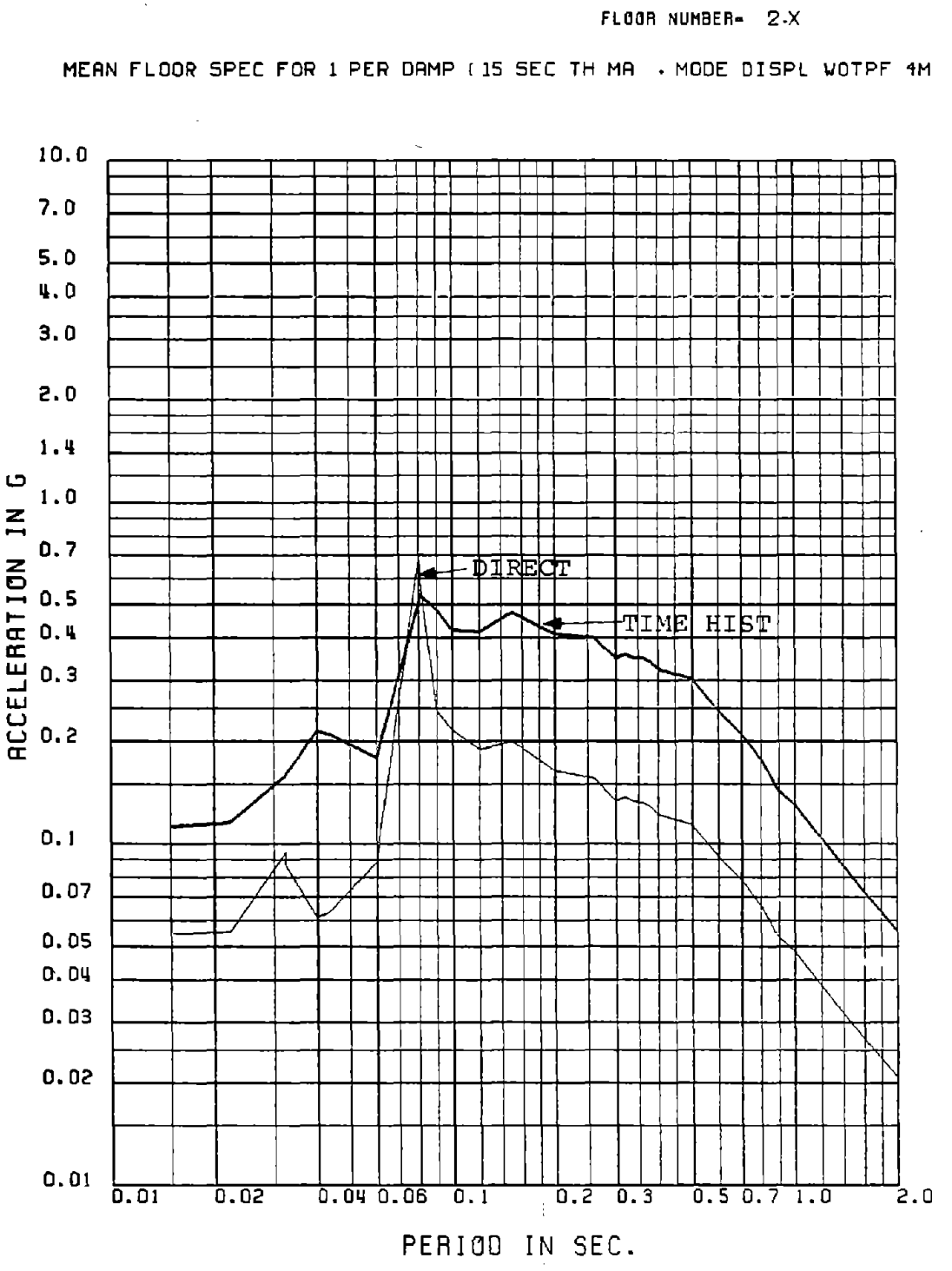

Fig. 4.28 Comparison of Floor Spectra Obtained by Mode Displacement Approach with 4 Modes and by Time History Analysis for 1% Damping: Mean Spectra, 15-sec TH, Floor No. 2-X, 30-D.O.F. Model

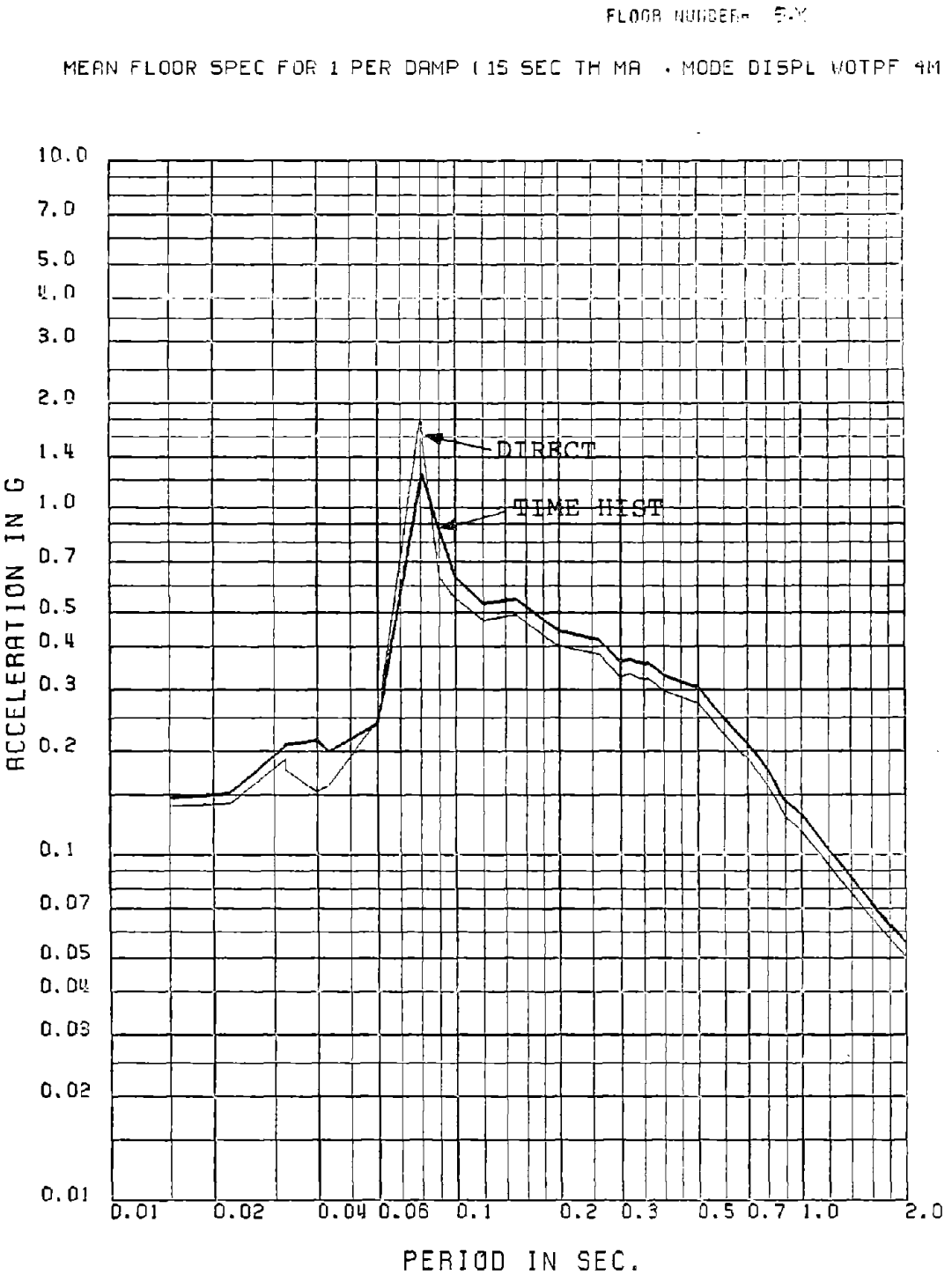

Fig. 4.29 Comparison of Floor Spectra Obtained by Mode Displacement Approach with 4 Modes and by Time History Analysis for 1% Damping: Mean Spectra, 15-sec TH, Floor No. 5-X, 30-D.O.F. Model

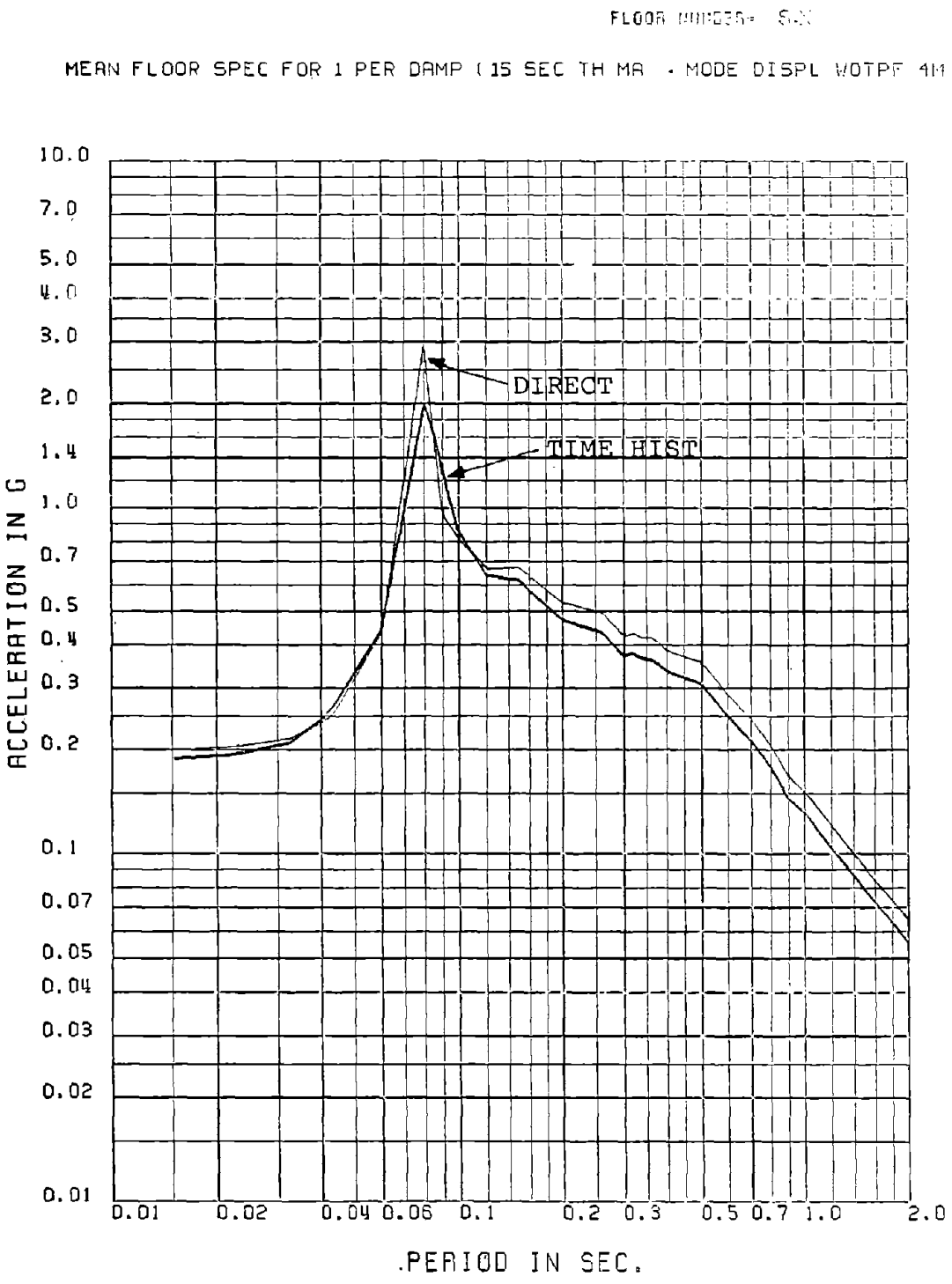

Fig. 4.30 Comparison of Floor Spectra Obtained by Mode Displacement Approach with 4 Modes and by Time History Analysis for 1% Damping: Mean Spectra, 15-sec TH, Floor No. 8-X, 30-D.O.F. Model

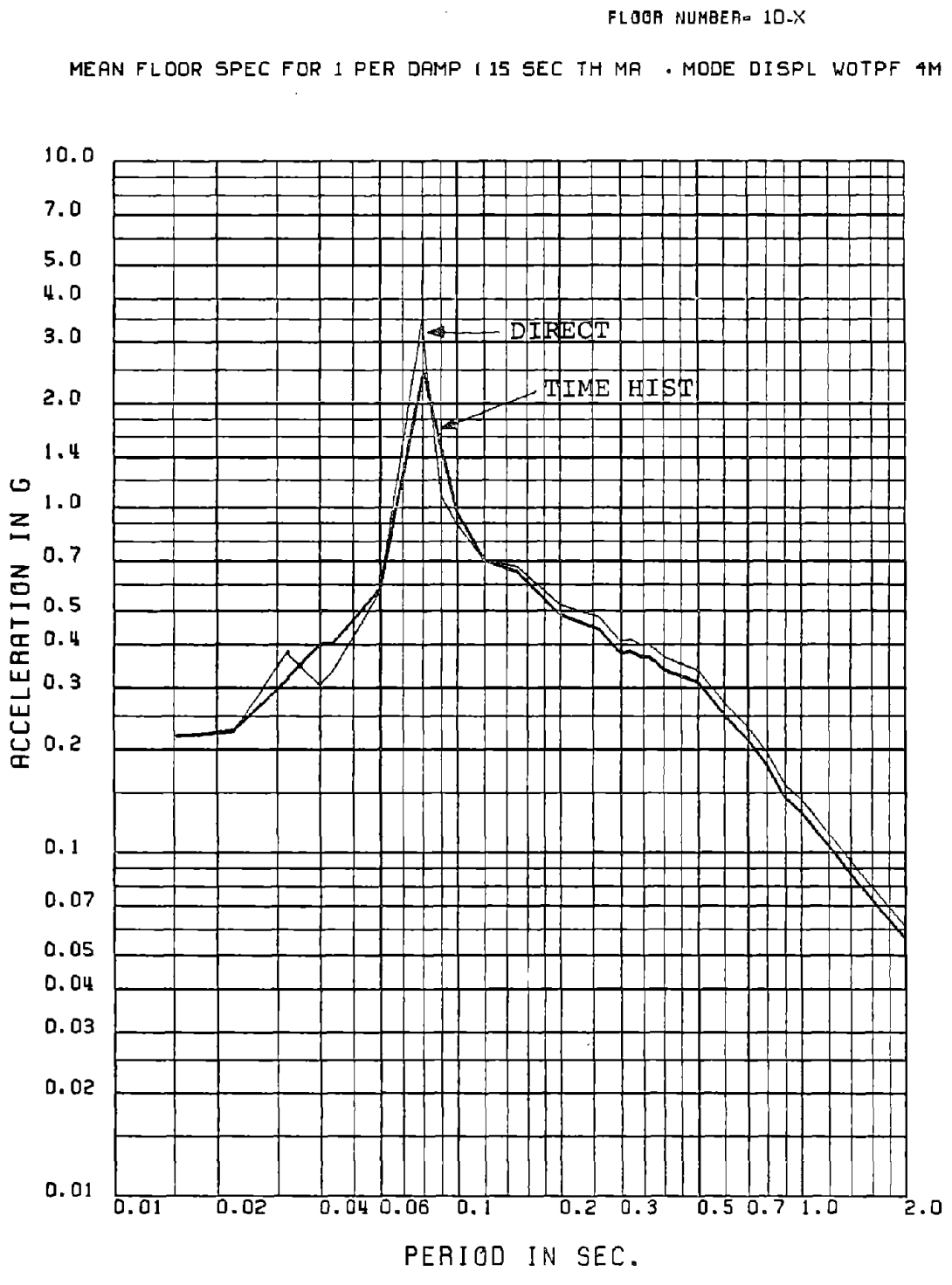

Fig. 4.31 Comparison of Floor Spectra Obtained by Mode Displacement Approach with 4 Modes and by Time History Analysis for 1% Damping: Mean Spectra, 15-sec TH, Floor No. 10-X, 30-D.O.F. Model

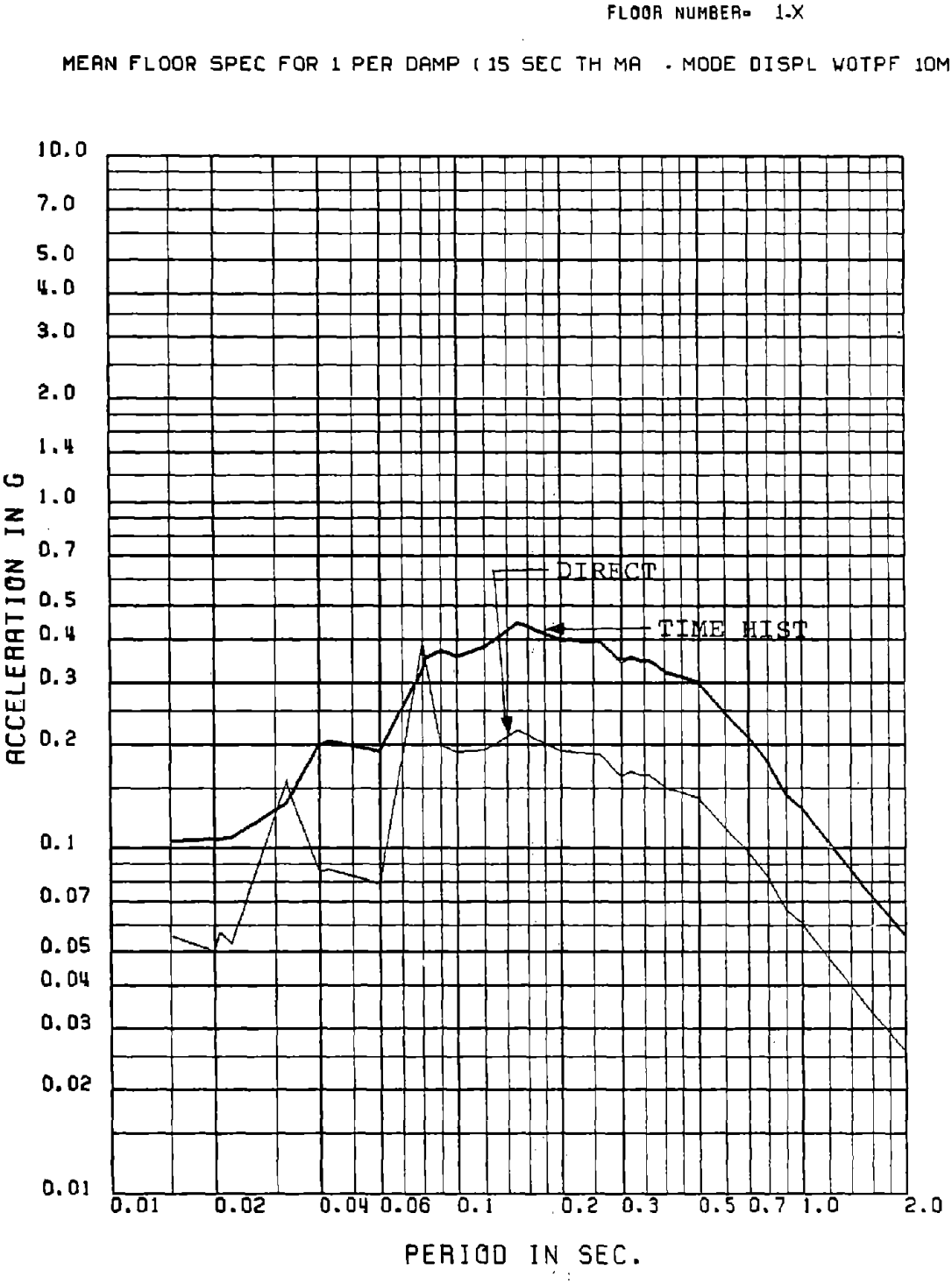

Fig. 4.32 Comparison of Floor Spectra Obtained by Mode Displacement Approach with 10 Modes and by Time History Analysis for 1% Damping: Mean Spectra, 15-sec TH, Floor No. 1-X, 30-D.O.F. Model

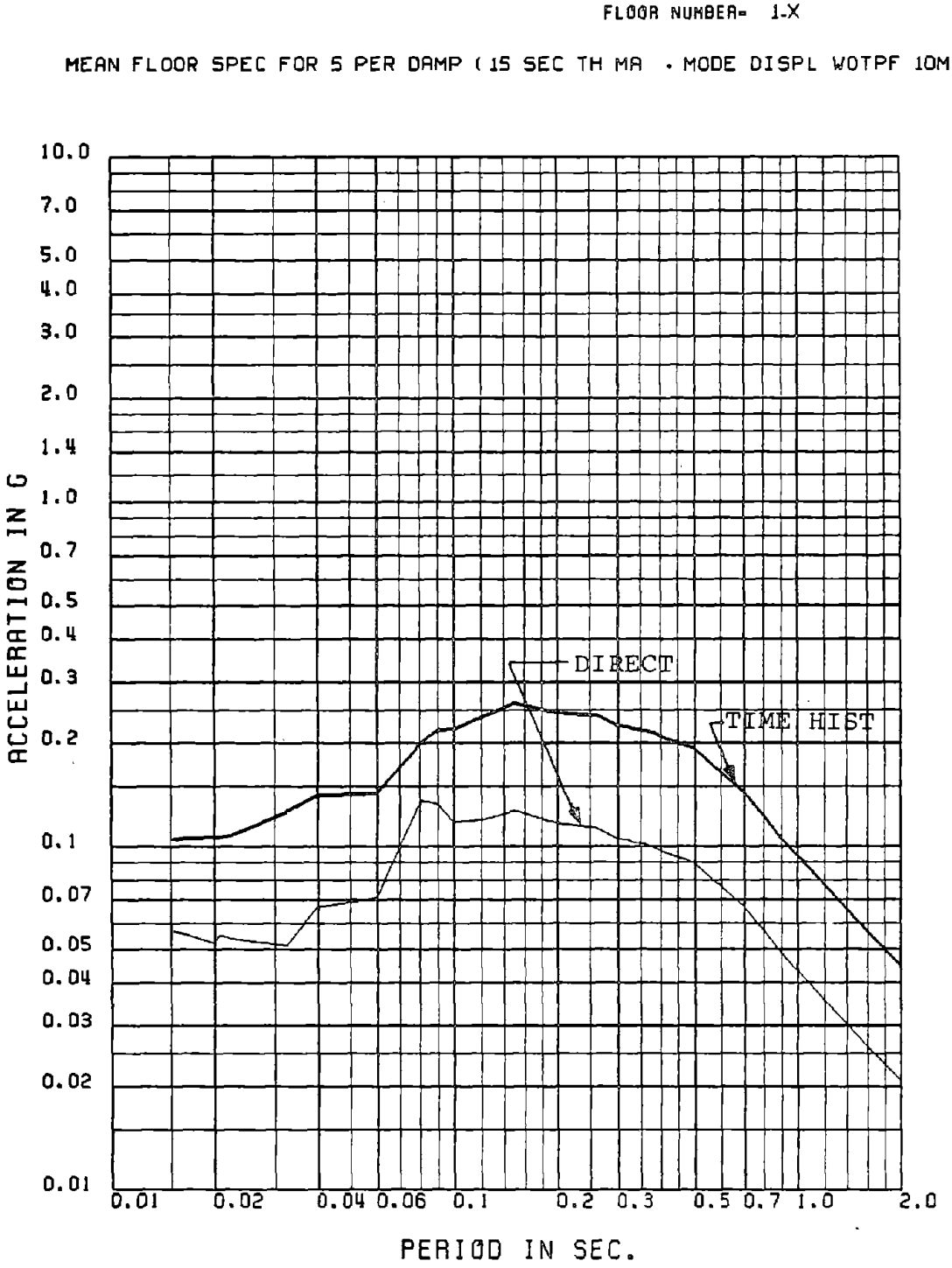

Fig. 4.33 Comparison of Floor Spectra Obtained by Mode Displacement Approach with 10 Modes and by Time History Analysis for 5% Damping: Mean Spectra, 15-sec TH, Floor No. 1-X, 30-D.O.F. Model

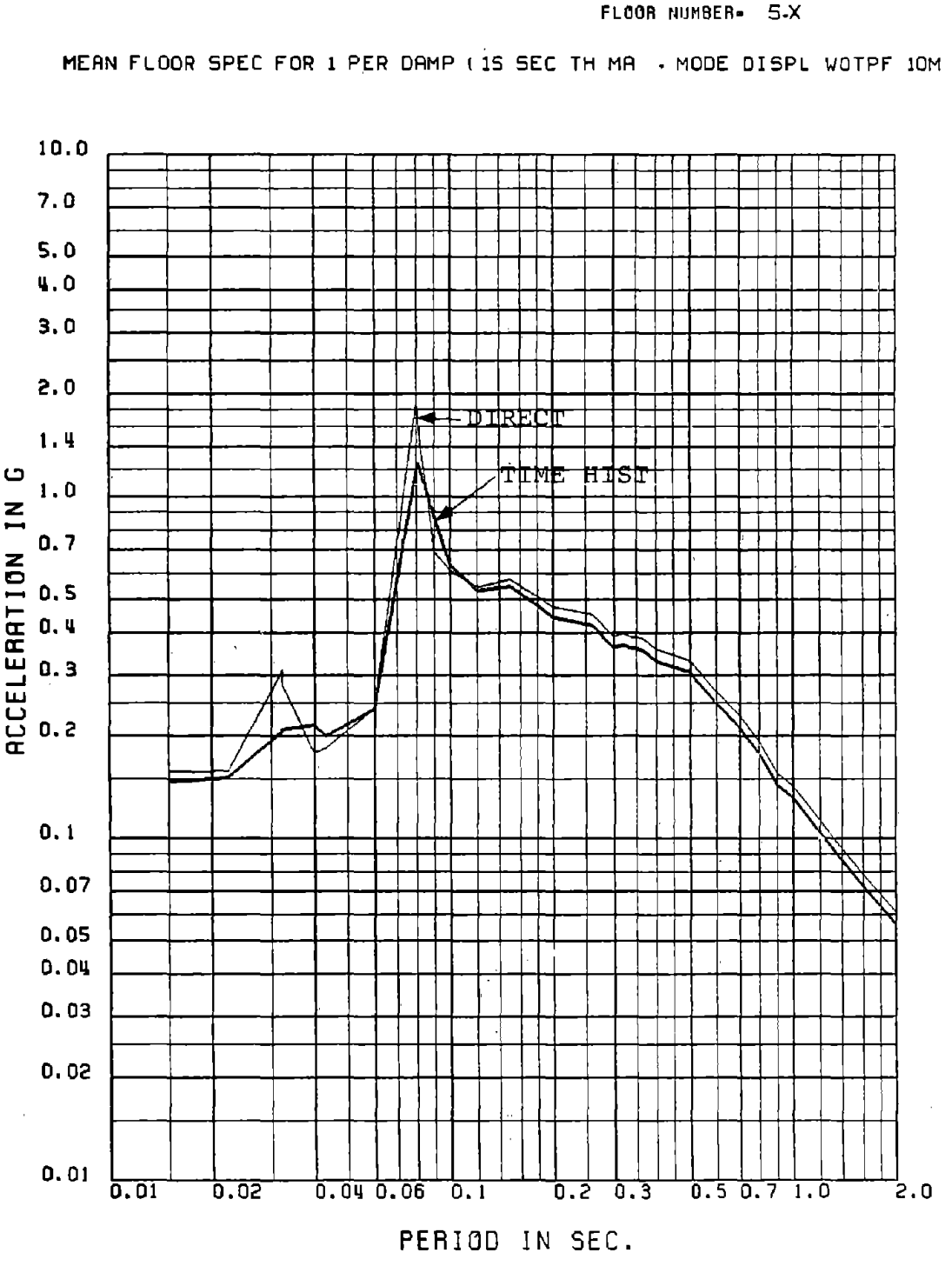

Fig. 4.34 Comparison of Floor Spectra Obtained by Mode Displacement Approach with 10 Modes and by Time History Analysis for 1% Damping: Mean Spectra, 15-sec TH, Floor No. 5-X, 30-D.O.F. Model

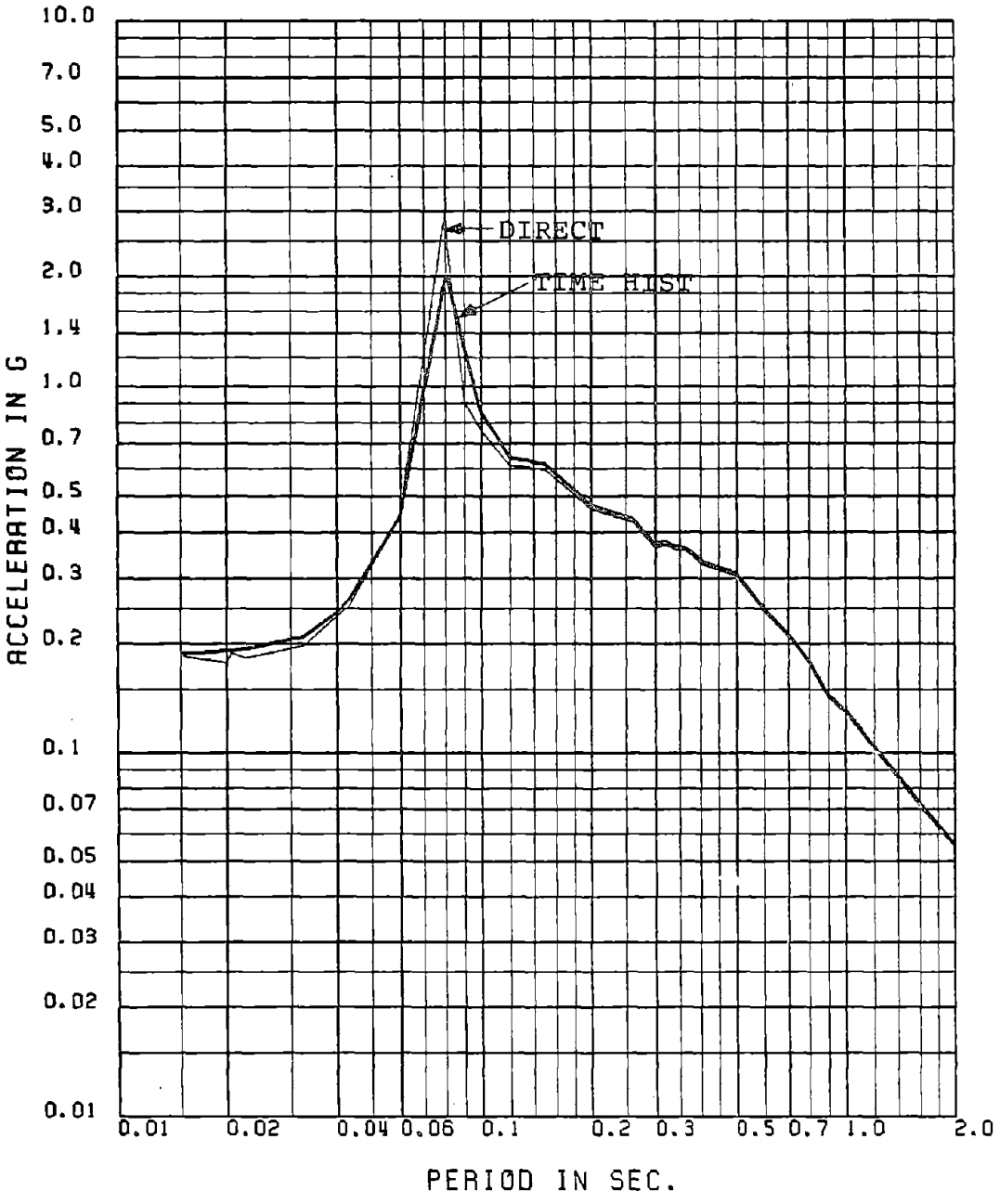

Fig. 4.35 Comparison of Floor Spectra Obtained by Mode Displacement Approach with 10 Modes and by Time History Analysis for 1% Damping: Mean Spectra, 15-sec TH, Floor No. 8-X, 30-D.O.F. Model

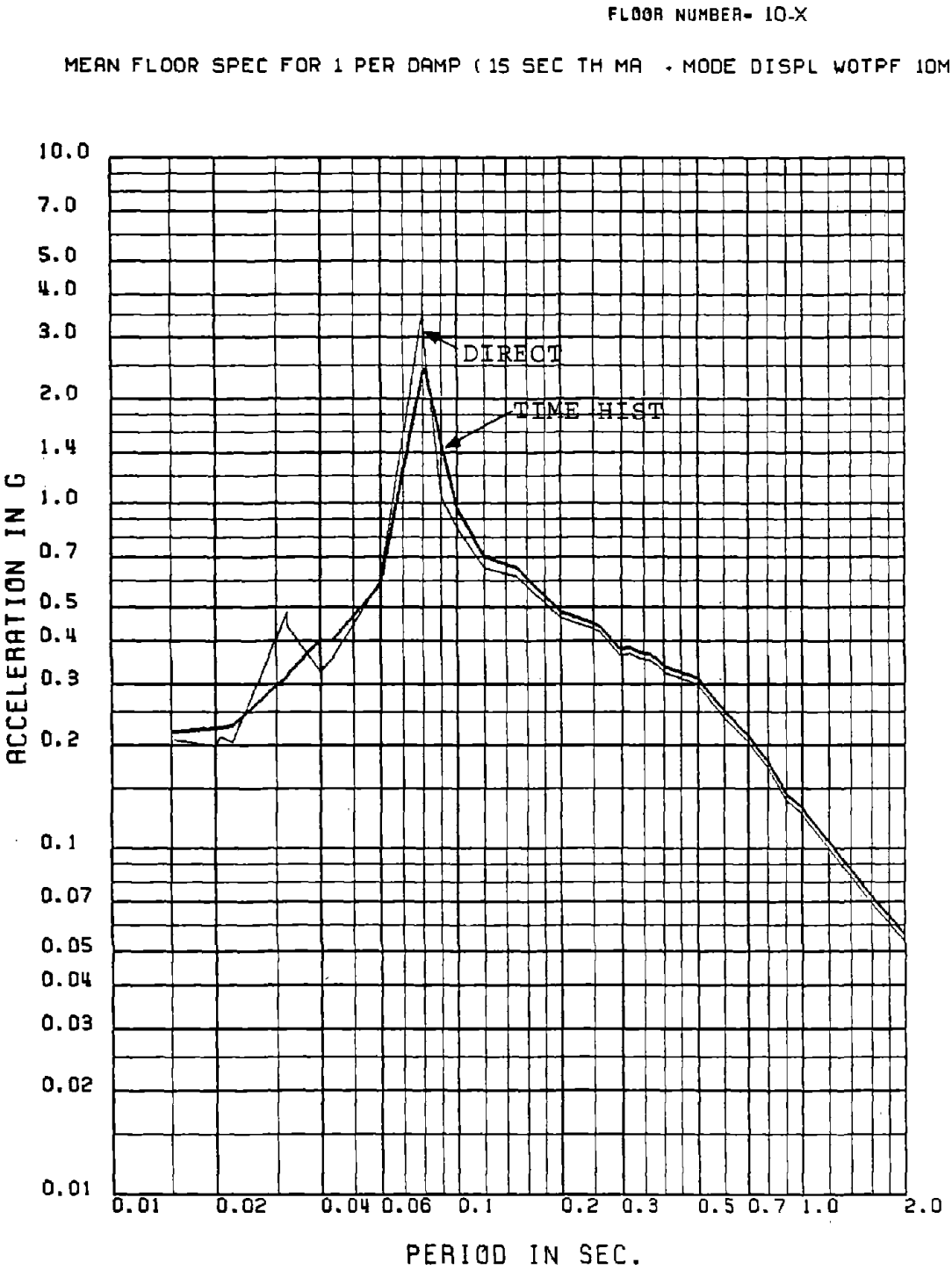

Fig. 4.36 Comparison of Floor Spectra Obtained by Mode Displacement Approach with 10 Modes and by Time History Analysis for 1% Damping: Mean Spectra, 15-sec TH, Floor No. 10-X, 30-D.O.F. Model

FIGURES FOR CHAPTER 5

NONCLASSICALLY DAMPED SYSTEMS: MODE ACCELERATION METHOD

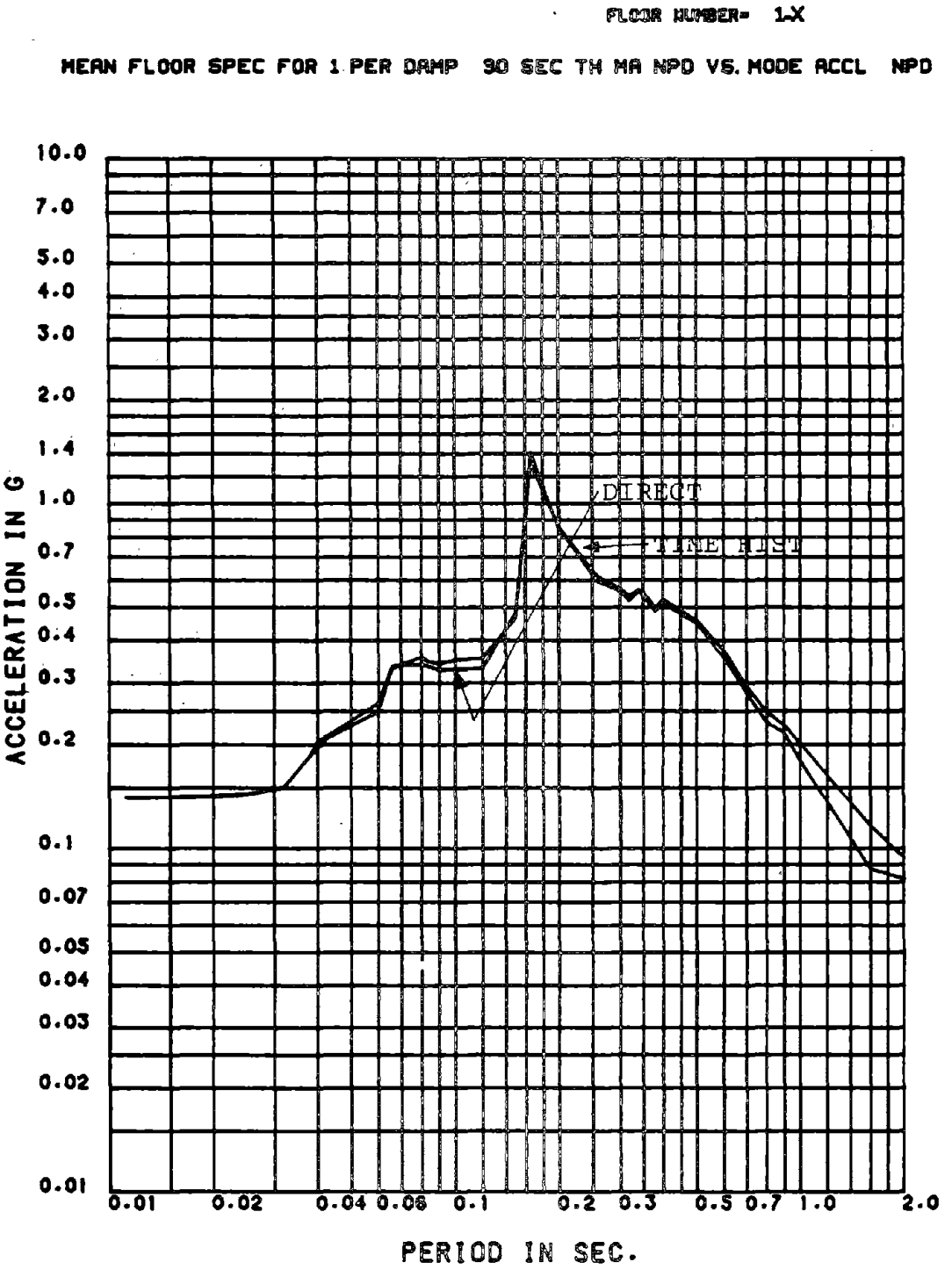

Fig. 5.1 Comparison of Floor Spectra Obtained by Mode Acceleration Approach and Time History Analysis for 1% Damping: Mean Spectra, 30-sec TH, Floor No. 1-X, Nonproportionally Damped 15-D.O.F. Model

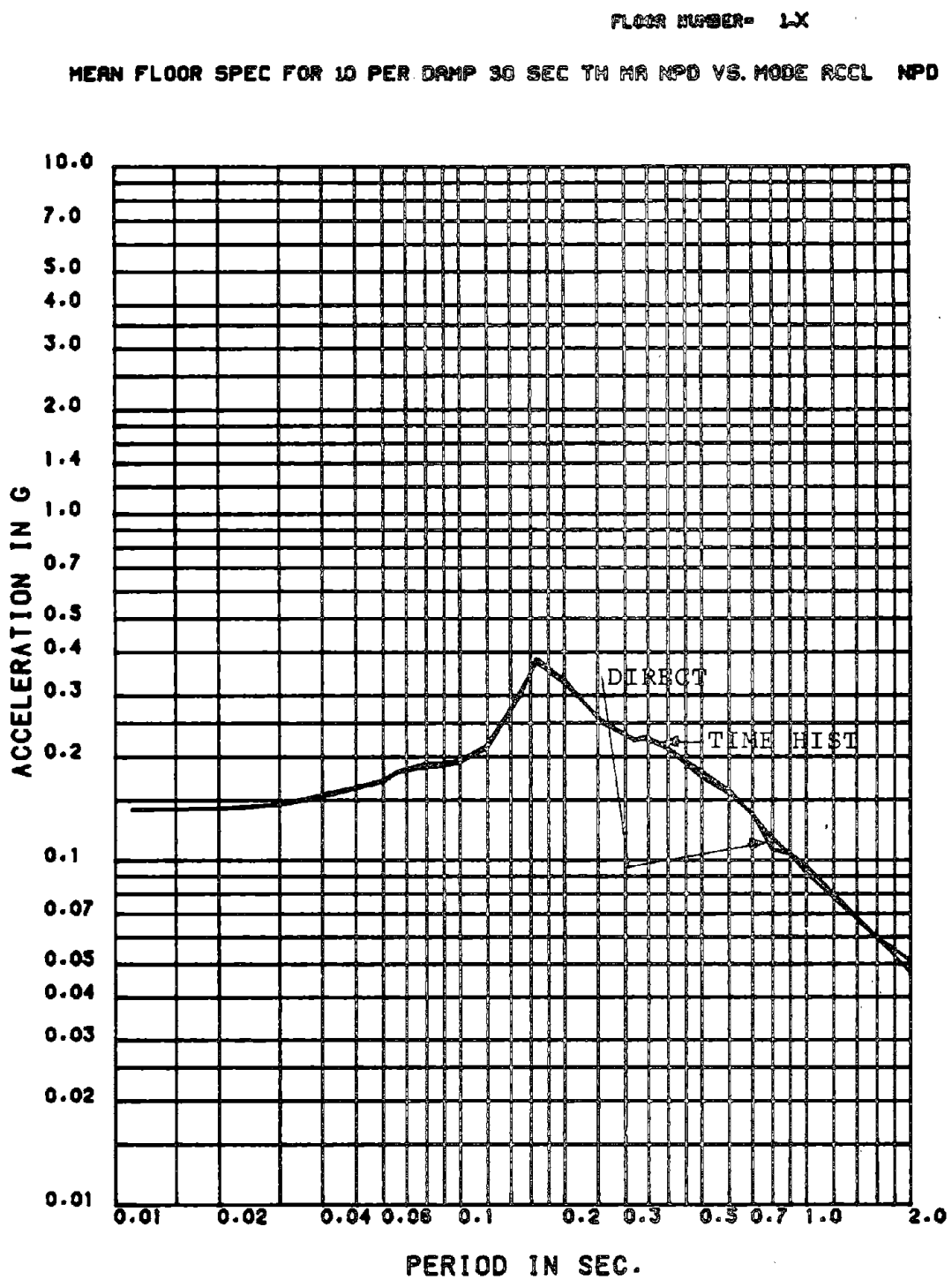

Fig. 5.2 Comparison of Floor Spectra Obtained by Mode Acceleration Approach and Time History Analysis for 10% Damping: Mean Spectra, 30-sec TH, Floor No. 1-X, Nonproportionally Damped 15-D.O.F. Model

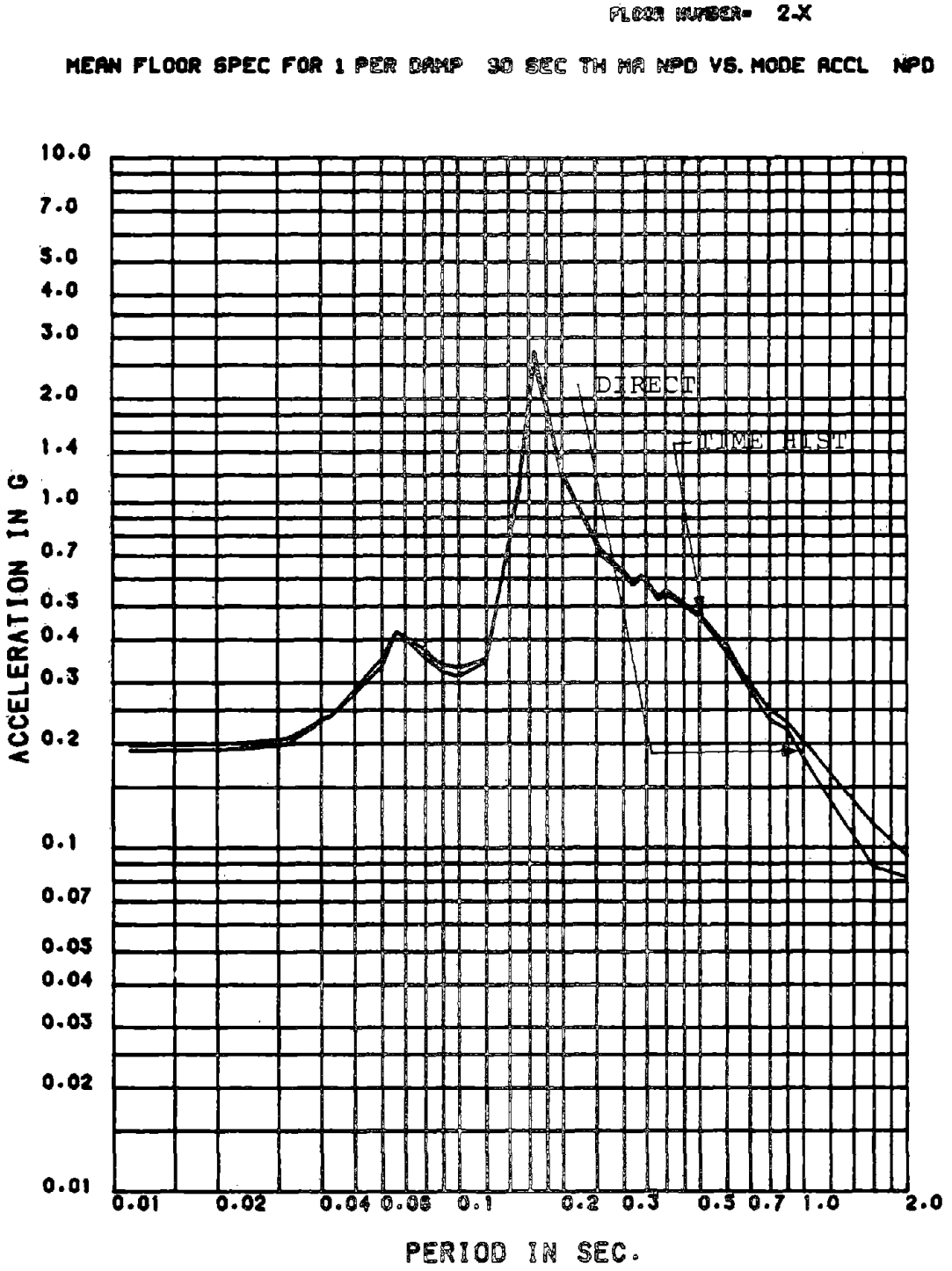

Fig. 5.3 Comparison of Floor Spectra Obtained by Mode Acceleration Approach and Time History Analysis for 1% Damping: Mean Spectra, 30-sec TH, Floor No. 2-X, Nonproportionally Damped 15-D.O.F. Model

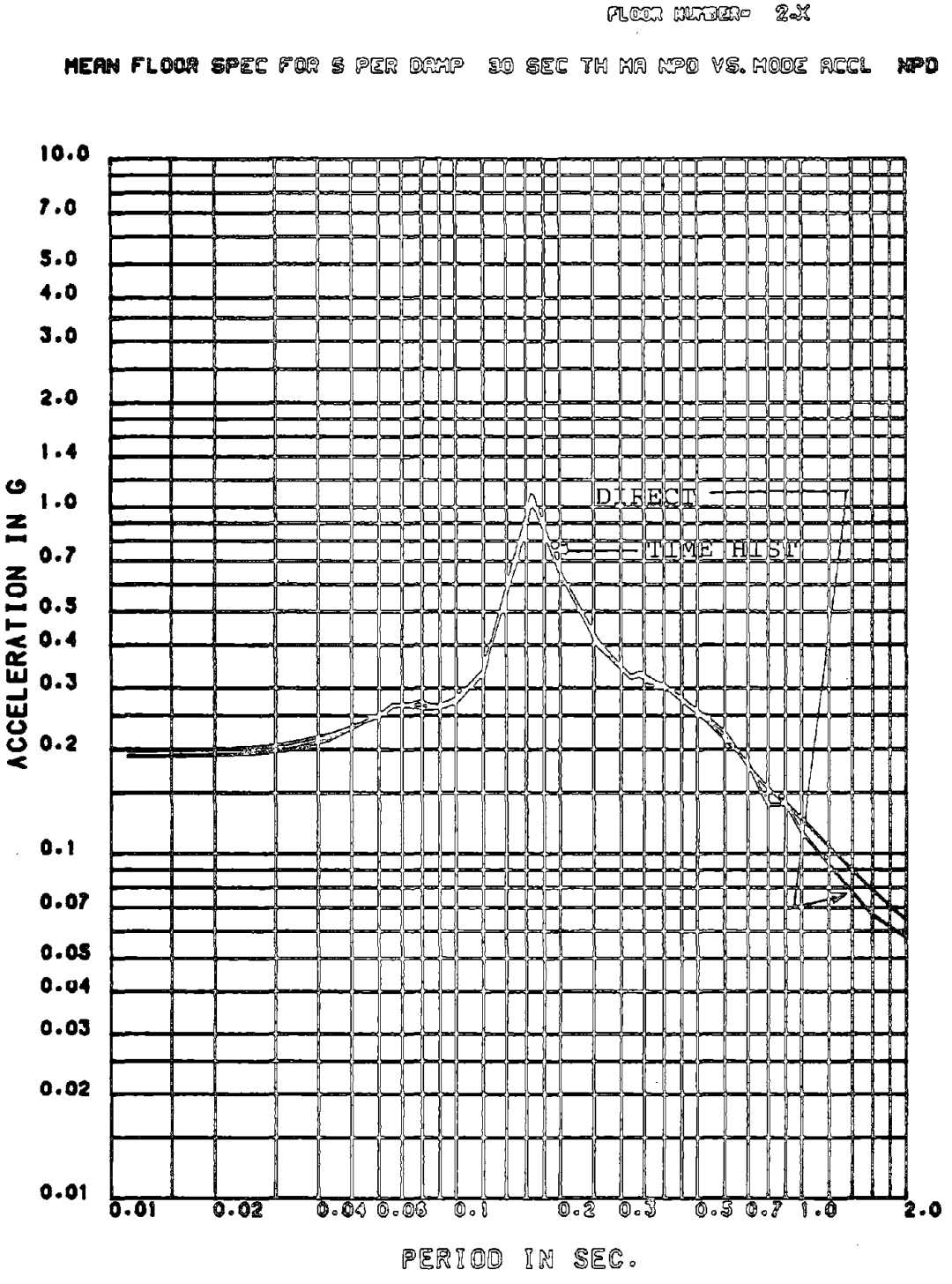

Fig. 5.4 Comparison of Floor Spectra Obtained by Mode Acceleration Approach and Time History Analysis for 5% Damping: Mean Spectra, 30-sec TH, Floor No. 2-X, Nonproportionally Damped 15-D.O.F. Model

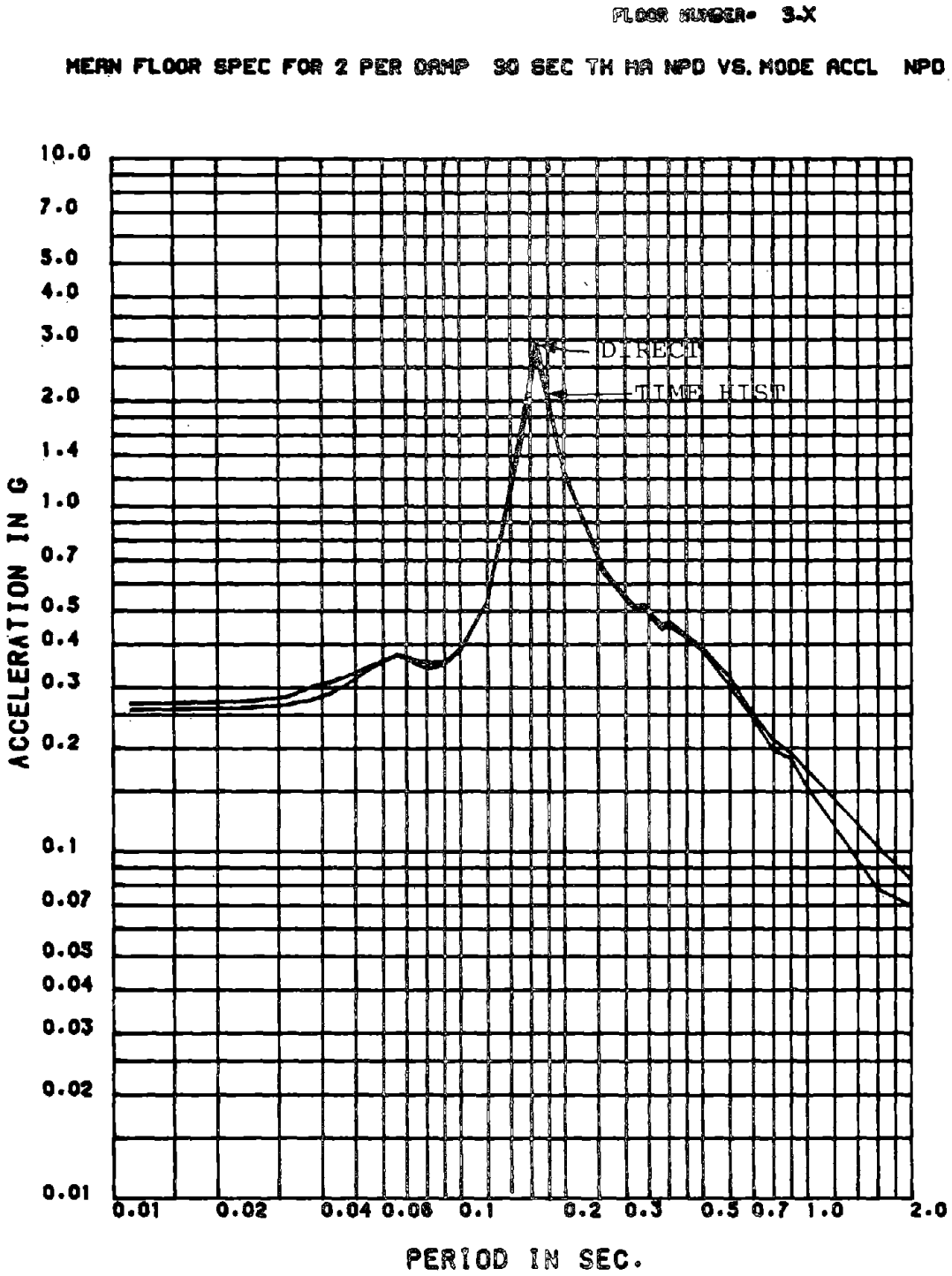

Fig. 5.5 Comparison of Floor Spectra Obtained by Mode Acceleration Approach and Time History Analysis for 2% Damping: Mean Spectra, 30-sec TH, Floor No. 3-X, Nonproportionally Damped 15-D.O.F. Model

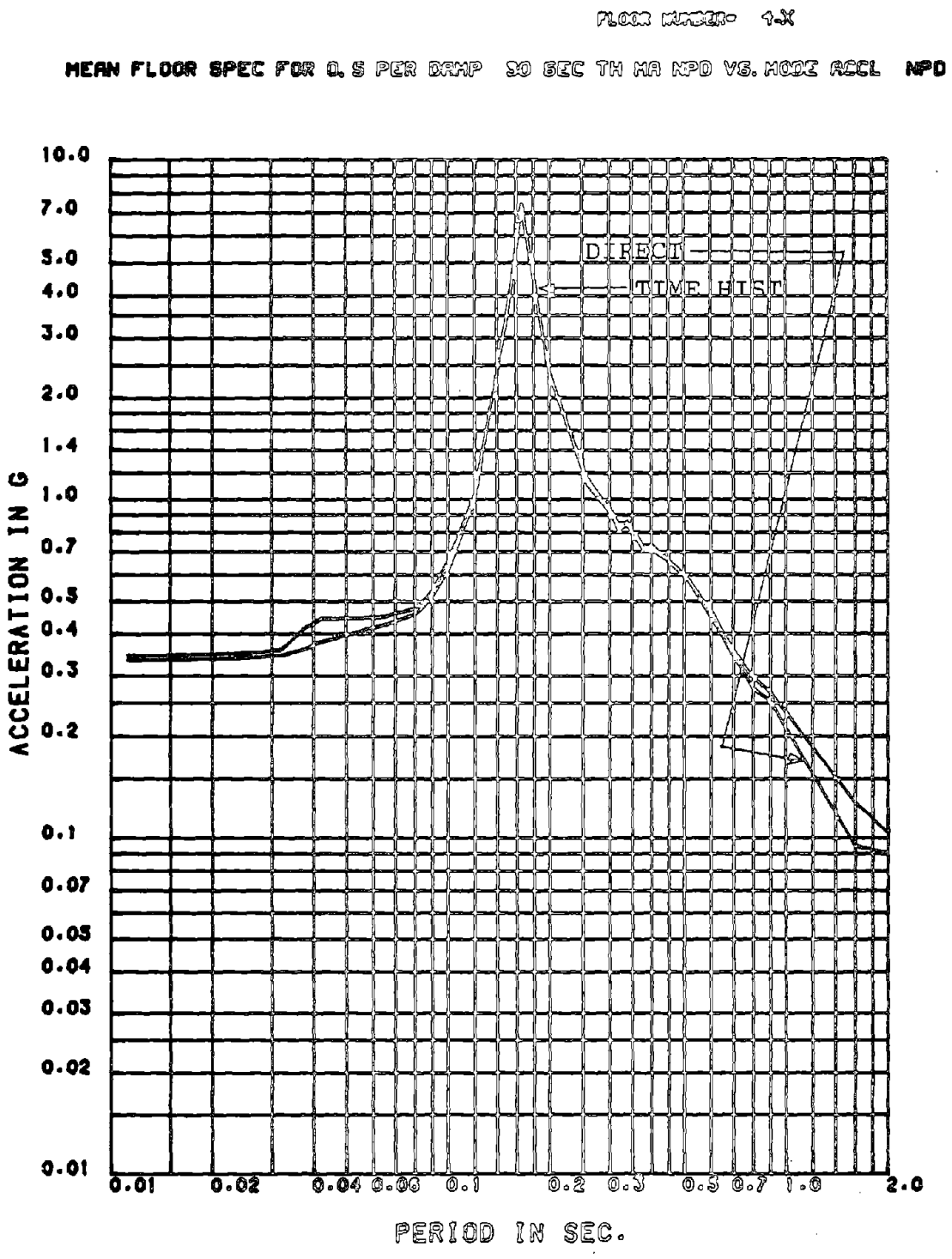

Fig. 5.6 Comparison of Floor Spectra Obtained by Mode Acceleration Approach and Time History Analysis for 0.5% Damping: Mean Spectra, 30-sec TH, Floor No. 4-X, Nonproportionally Damped 15-D.O.F. Model

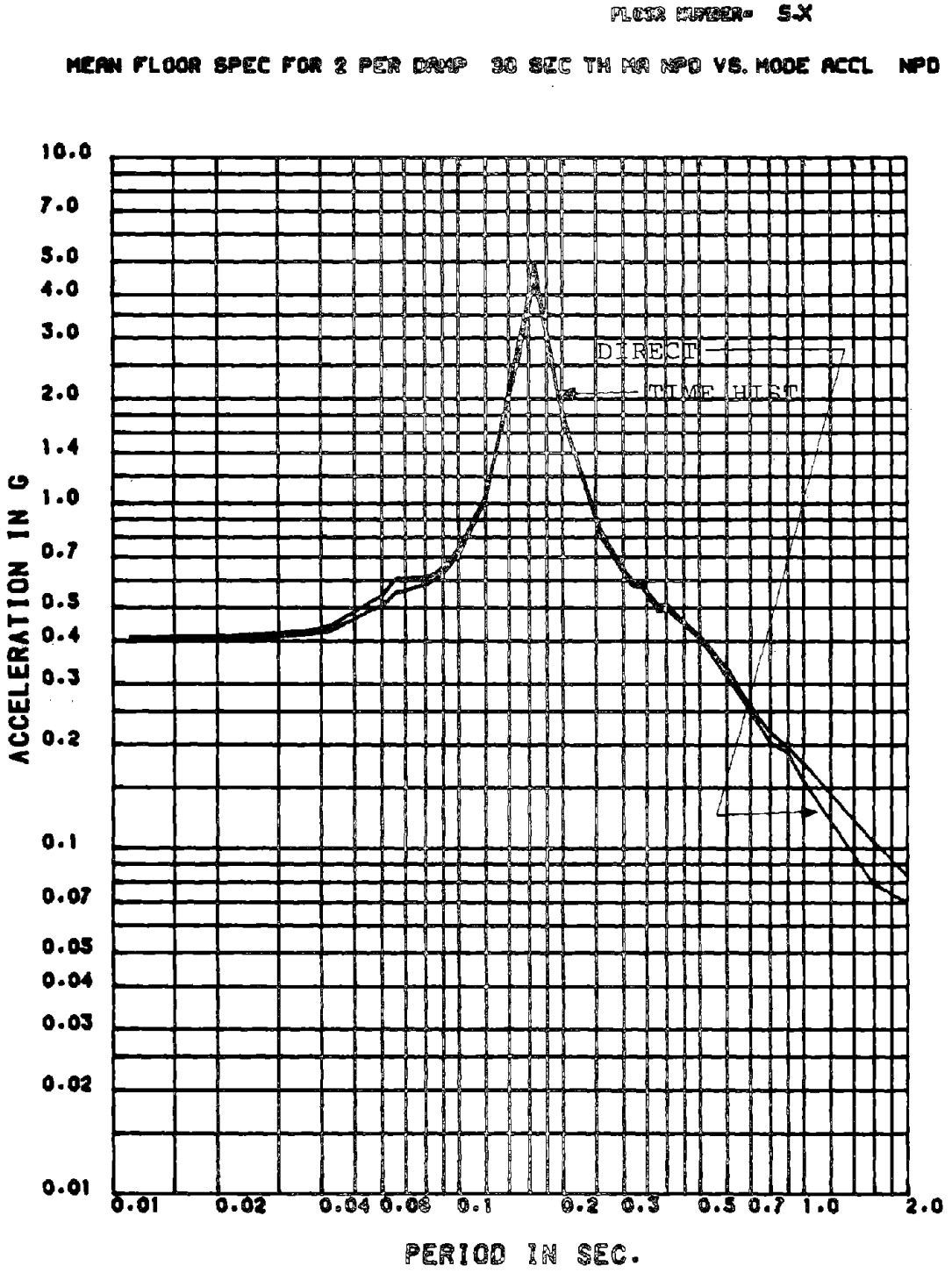

Fig. 5.7 Comparison of Floor Spectra Obtained by Mode Acceleration Approach and Time History Analysis for 2% Damping: Mean Spectra, 30-sec TH, Floor No. 5-X, Nonproportionally Damped 15-D.O.F. Model

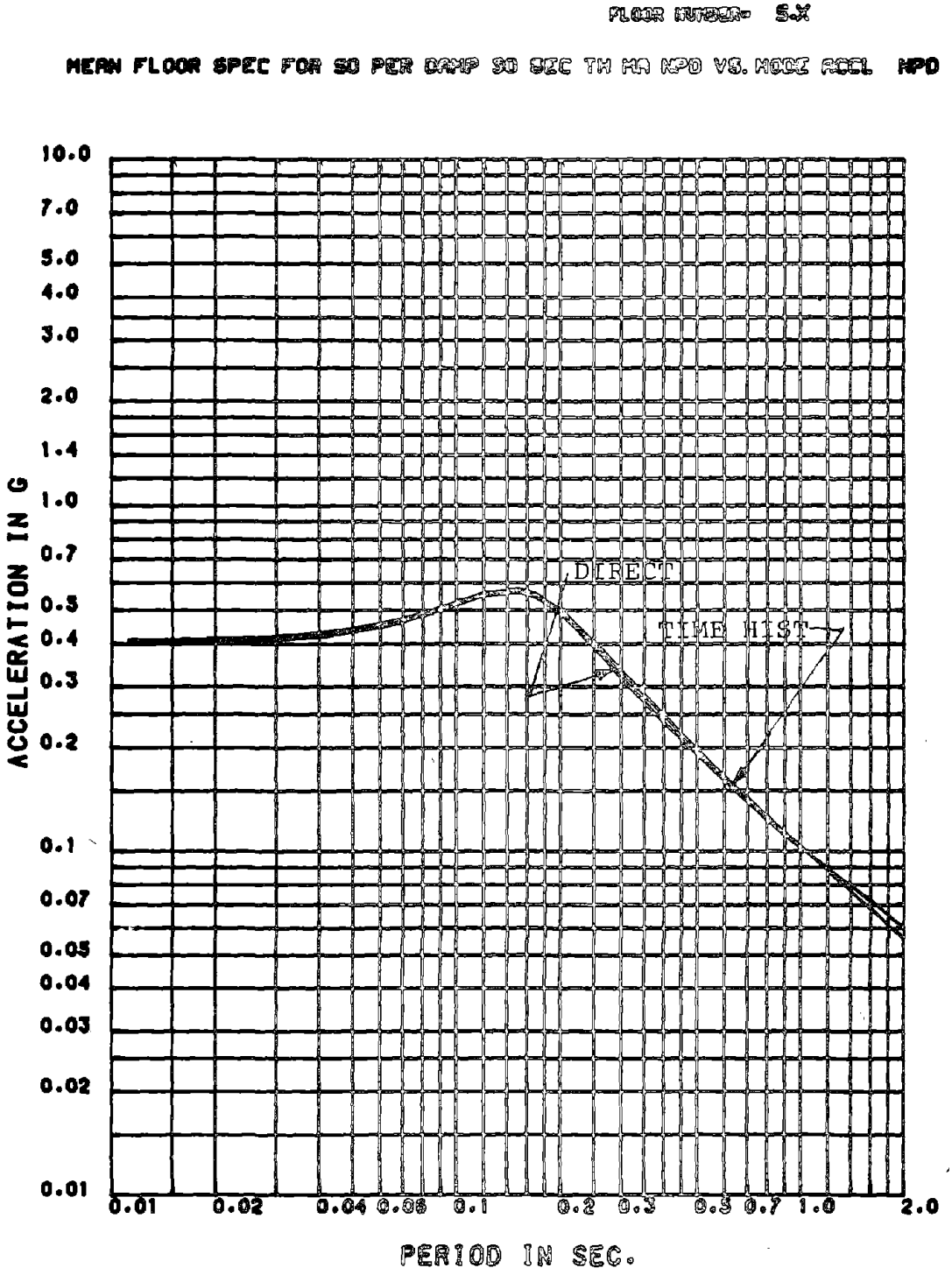

Fig. 5.8 Comparison of Floor Spectra Obtained by Mode Acceleration Approach and Time History Analysis for 50% Damping: Mean Spectra, 30-sec TH, Floor No. 5-X, Nonproportionally Damped 15-D.O.F. Model

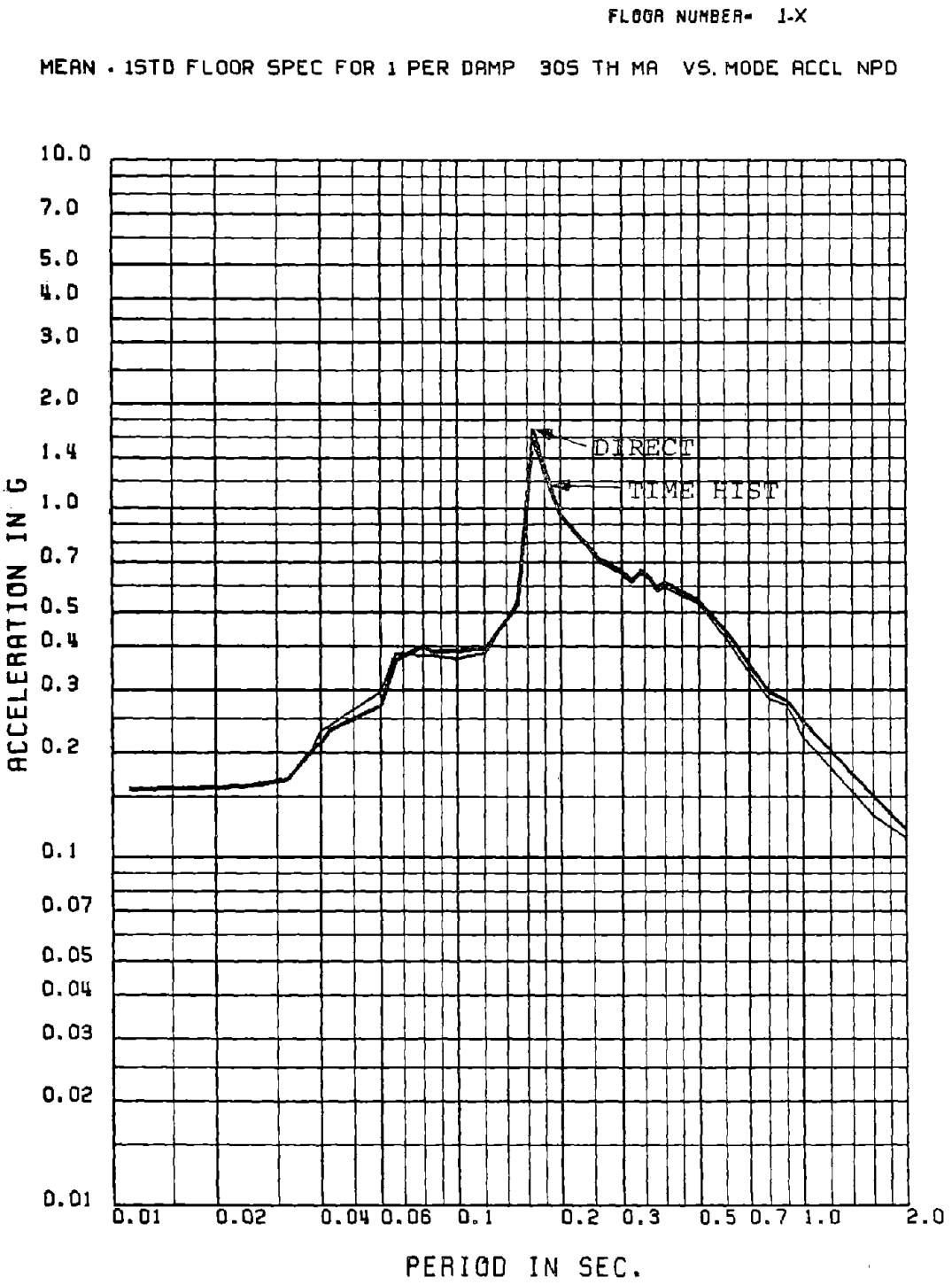

Fig. 5.9 Comparison of Floor Spectra Obtained by Mode Acceleration Approach and Time History Analysis for 1% Damping: Mean + 1 Standard Deviation Spectra, 30-sec TH, Floor No. 1-X, Nonproportionally Damped 15-D.O.F. Model

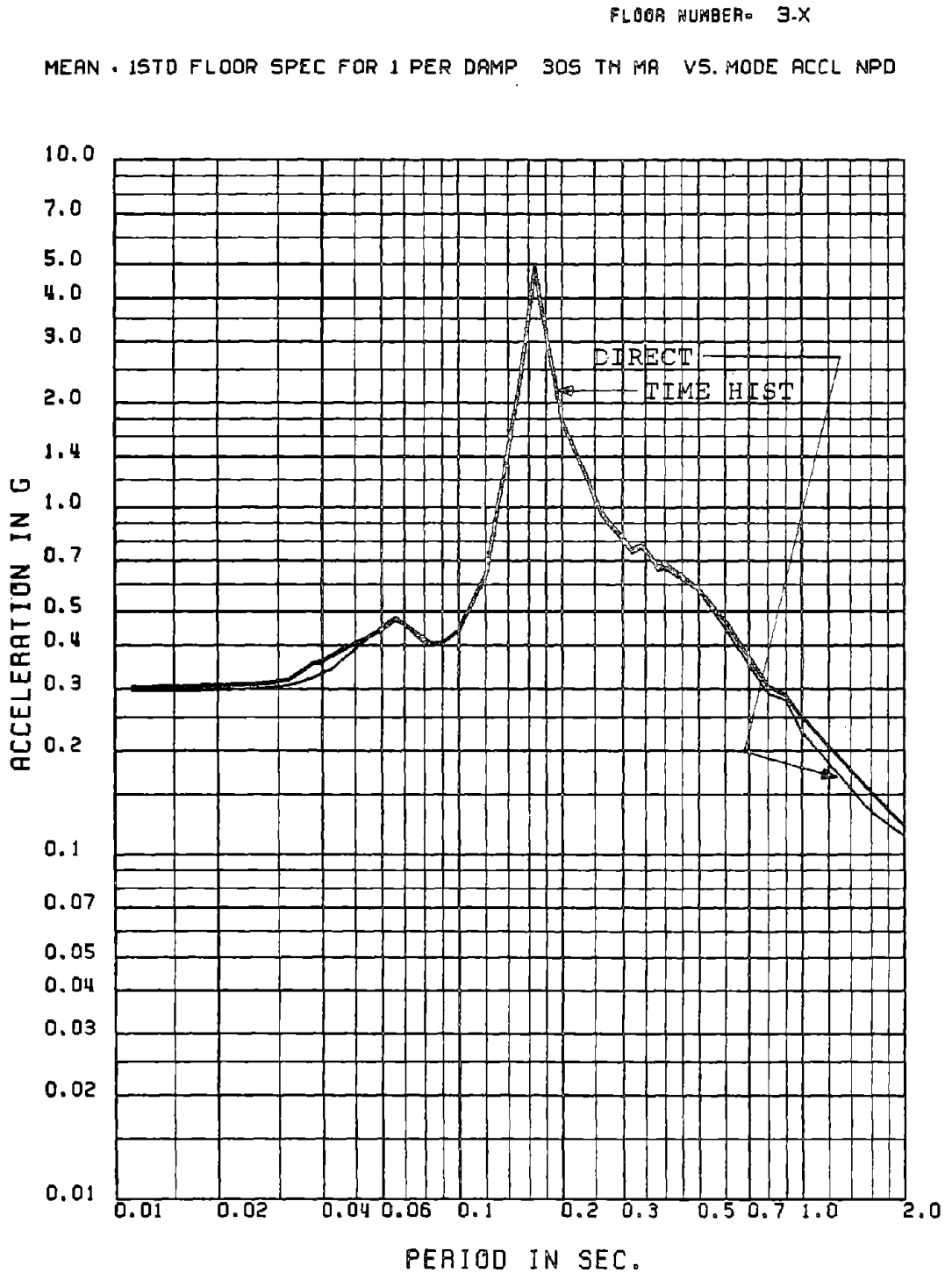

Fig. 5.10 Comparison of Floor Spectra Obtained by Mode Acceleration Approach and Time History Analysis for 1% Damping: Mean + 1 Standard Deviation Spectra, 30-sec TH, Floor No. 3-X, Nonproportionally Damped 15-D.O.F. Model

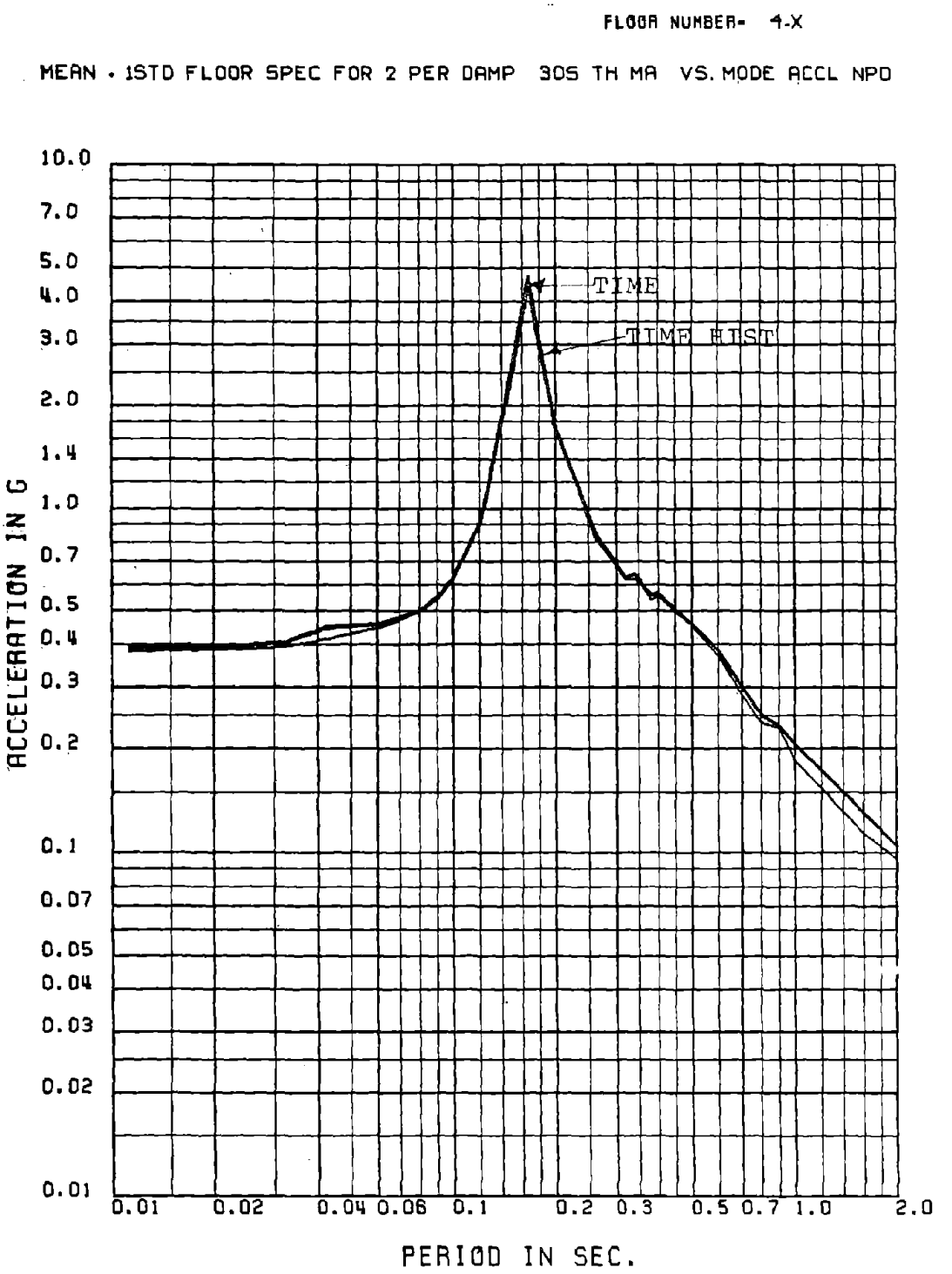

Fig. 5.11 Comparison of Floor Spectra Obtained by Mode Acceleration Approach and Time History Analysis for 1% Damping: Mean + 1 Standard Deviation Spectra, 30-sec TH, Floor No. 4-X, Nonproportionally Damped 15-D.O.F. Model

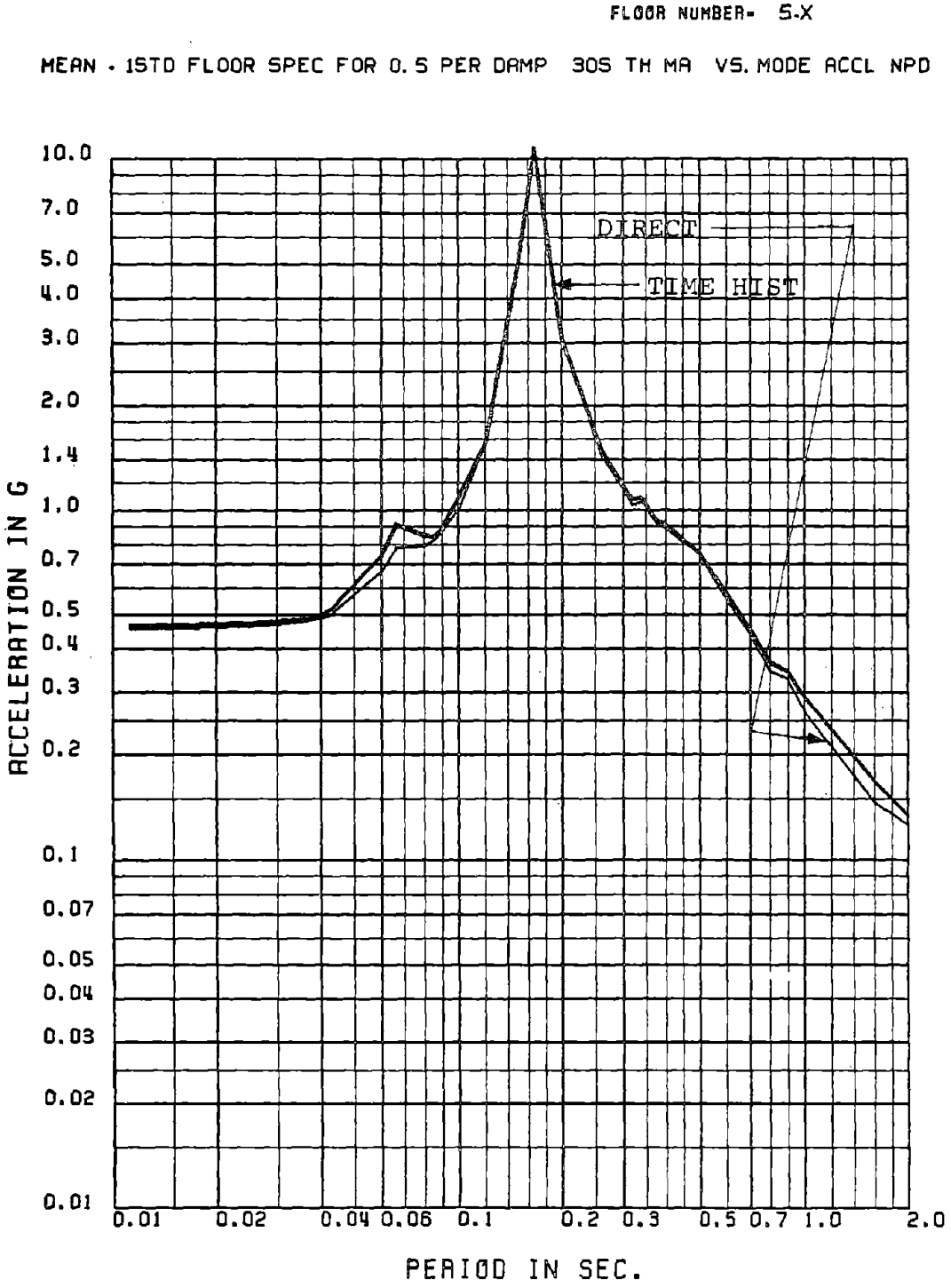

Fig. 5.12 Comparison of Floor Spectra Obtained by Mode Acceleration Approach and Time History Analysis for 0.5% Damping: Mean + 1 Standard Deviation Spectra, 30-sec TH, Floor No. 5-X, Nonproportionally Damped 15-D.O.F. Model

Appendix I

CLASSICAL DAMPING: MODE DISPLACEMENT METHOD

I-A EXPECTED VALUES

The expected values required in Eq. 2.10 are obtained as follows.

The solution of Eq. 2.3 is given by

$$z_j(t) = - \int_0^\tau \ddot{X}_g(\tau)\ h_j(t-\tau)\ d\tau \qquad (I.1)$$

where $h_j(t)$ is the impulse response function of Eq. 2.3. Using Eq. I.1, the expected value

$$E[z_j(t_1)\ z_k(t_2)] = \int_0^{t_1} \int_0^{t_2} E[\ddot{X}_g(\tau_1)\ \ddot{X}_g(\tau_2)] \cdot h_j(t_1-\tau_1)\ h_k(t_2-\tau_2)\ d\tau_1\ d\tau_2 \qquad (I.2)$$

in which the autocorrelation, $E[\ddot{X}_g(\tau_1)\ \ddot{X}_g(\tau_2)]$, is defined as

$$E[\ddot{X}_g(\tau_1)\ \ddot{X}_g(\tau_2)] = \int_{-\infty}^{\infty} \Phi_g(\omega)\ e^{i\omega(t_1-t_2)}\ d\omega \qquad (I.3)$$

Using Eq. I.3 in I.2, and changing the order of integration, the following is obtained

$$E[z_j(t_1)\ z_k(t_2)] = \int_{-\infty}^{\infty} \Phi_g(\omega)\ d\omega \cdot \int_0^{t_1} e^{i\omega t_1}\ h_j(t_1-\tau_1)d\tau_1$$

$$\cdot \int_0^{t_2} e^{i\omega t_2}\ h_k(t_2-\tau_2)d\tau \qquad (I.4)$$

For stationary response, when $t_1 \to \infty$, $t_2 \to \infty$ and $t_1 - t_2 = \tau$, Eq. I.4 can be written as

$$E[z_j(t_1)\ z_k(t_2)] = \int_{-\infty}^{\infty} \Phi_g(\omega)\ H_j\ H_k^*\ e^{i\omega\tau}\ d\omega \qquad (I.5)$$

where H_j is the complex frequency response function defined by Eq. 2.13. Also it can be shown that

$$E[\dot{z}_j(t_1)\ z_k(t_2)] = i \int_{-\infty}^{\infty} \omega\ \Phi_g(\omega)\ H_j\ H_k^*\ e^{i\omega\tau}\ d\omega$$

$$= -\ E[z_j(t_1)\ \dot{z}_k(t_2)] \qquad (I.6a)$$

$$E[\dot{z}_j(t_1)\ \dot{z}_k(t_2)] = \int_{-\infty}^{\infty} \omega^2\ \Phi_g(\omega)\ H_j\ H_k^*\ e^{i\omega\tau}\ d\tau \qquad (I.6b)$$

I-B AMPLIFICATION FACTORS

The factors A_1, A_2, A_3, A_4 in Eq. 2.19 are obtained as the solution of the following simultaneous equations:

$$[P]\ \{A_j\} = \{W_1\} \qquad (I.7)$$

where

$$\{A_j\}^T = (A_1, A_2, A_3, A_4) \tag{I.8}$$

the elements of matrix [P] are defined as

$$[P] = \begin{bmatrix} 0 & 1 & 0 & 1 \\ 1 & u & 1 & x \\ u & v & x & y \\ v & 0 & y & 0 \end{bmatrix} \tag{I.9}$$

in which

$$u = -2\, r_1^2\, (1 - 2\, \beta_j^2)\ ;\ v = r_1^4\ ,\ x = -2\, (1 - 2\, \beta_o^2)\ ;$$
$$y = 1\ ;\ r_1 = \omega_j/\omega_o \tag{I.10}$$

Also

$$W_1(1) = 0\ ;\ W_1(2) = 16\, \beta_o^2\, \beta_j^2\, r_1^2\ ;$$
$$W_1(3) = 4\, r_1^2\, (\beta_o^2\, r_1^2 + \beta_j^2)\ ;\ W_1(3) = r_1^4 \tag{I.11}$$

The factors $B_1, B_2, \ldots, B_4$ and $C_1, \ldots, C_4$ which appear in cross-terms under double summation terms in Eq. 2.27 are obtained from the following simultaneous equations:

$$[P]\ \{B_j\} = \{W_2\} \quad \text{and} \quad [P']\ \{C_j\} = \{W_3\} \tag{I.12}$$

where

$$\{B_j\}^T = (B_1, B_2, B_3, B_4) \text{ and } \{C_j\}^T = (C_1, C_2, C_3, C_4) \tag{I.13}$$

and the elements of [P] are defined in Eq. I.9. Also,

$$W_2(1) = 0 \; ; \; W_2(2) = 4 \; B_r \; \beta_o^2 \; ; \; W_2(3) = 4 \; A_r \; \beta_o^2 + B_r \; ;$$
$$W_2(4) = A_r \qquad (I.14)$$

The elements of the matrix [P'] are defined as

$$[P'] = \begin{bmatrix} 0 & 1 & 0 & 1 \\ 1 & u' & 1 & x \\ u' & v' & x & y \\ v' & 0 & y & 0 \end{bmatrix} \qquad (I.15)$$

in which $u' = -2 \; r_2^2 \; (1 - \beta_k^2)$, $v' = r_2^4$, $r_2 = \omega_k/\omega_o$, and x,y are the same as in Eq. I.9. Also,

$$W_3(1) = 0 \; ; \; W_3(2) = 4 \; D_r \; \beta_o^2 \; ; \; W_3(3) = 4 \; C_r \; \beta_o^2 + D_r \; ;$$
$$W_3(4) = C_r \qquad (I.16)$$

whereas the coefficients A_r, B_r, C_r, D_r in Eqs. I.14 and I.16 are obtained as the solution of the following simultaneous equations:

$$[P''] \; \{A\} = \{W_4\} \qquad (I.17)$$

where $\{A\}^T = (A_r, \; B_r, \; C_r, \; D_r)$ (I.18)

and the elements of [P''] matrix are defined as

$$[P''] = \begin{bmatrix} 0 & 1 & 0 & 1 \\ 1 & u'' & 1 & x'' \\ u'' & v'' & x'' & y'' \\ v'' & 0 & y'' & 0 \end{bmatrix} \tag{I.19}$$

in which

$$u'' = -2\, r_2^2\, (1 - 2\, \beta_k^2)\ ,\ v'' = r_2^4\ ,$$
$$x'' = -2\, r_1^2\, (1 - 2\, \beta_j^2)\ ,\ y'' = r_1^4 \tag{I.20}$$

and the vector $\{W_4\}$ is defined as

$$W_4(1) = 4\, \beta_j\, \beta_k\, r_1\, r_2\ ;\ W_4(2) = r_1^2\, r_2^2\, [1 - 4\, (\beta_j^2 + \beta_k^2) + 16\, \beta_j^2\, \beta_k^2]\ ,\ W_4(3) = -\, r_1^4\, r_2^2\, (1 - 4\, \beta_k^2) - r_1^2\, r_2^4\, (1 - 4\, \beta_j^2)\ ;\ W_4(4) = r_1^4\, r_2^4 \tag{I.21}$$

I.C FREQUENCY INTEGRALS

The closed form integration for the form are required in the evaluation of integrals in the resonance case.

$$I_{c1} = \int_{-\omega_c}^{\omega_c} (a_o\, \omega_o^2\, \omega^6 + a_1\, \omega_o^4\, \omega^2 + a_2\, \omega_o^6\, \omega^2 + a_3\, \omega_o^8)\, |H_o|^4\, d\omega$$
$$= \omega_c\, A_m(r,\, \beta_o,\, a_o,\, a_1,\, a_2,\, a_3) = \omega_c\, A_m \tag{I.22}$$

where a_o, a_1, a_2 and a_3 are constants, $r = \omega_o/\omega_c$ and for brevity A_m is used for $A_m(r,\, \beta_o,\, a_o,\, a_1,\, a_2,\, a_3)$

throughout this work.

In Eq. I.22, A_m is defined as

$$A_m = \frac{M_1}{2}\left\{\ell n\left[\frac{1 - 2i\,\beta_o\, r - r^2}{1 + 2i\,\beta_o\, r - r^2}\right] - \ell n\left[\frac{1 + 2i\,\beta_o\, r - r^2}{1 - 2i\,\beta_o\, r - r^2}\right]\right\}$$

$$+ \frac{2N_1 + m_1}{2r\sqrt{1 - \beta_o^2}}\ \ell n\left\{\frac{(1+r^2) - 2r\sqrt{1 - \beta_o^2}}{(1+r^2) + 2r\sqrt{1 - \beta_o^2}}\right\}$$

$$- \frac{2N_2\ \{(1-r^2) + 2\,\beta_o^2\, r^2\} - m_2/2(1+r^2)}{r^2(1 - \beta_o^2)\ \{(1-r^2)^2 + 4\,\beta_o^2\, r^2\}}$$

$$- \frac{2N_2 + M_2/2}{4r^3(1-\beta_o^2)\sqrt{1-\beta_o^2}}\ \ell n\left\{\frac{1+r^2 - 2r\sqrt{1 - \beta_o^2}}{1+r^2 + 2r\sqrt{1 - \beta_o^2}}\right\} \qquad \text{(I.23)}$$

where

$$N_1 = -\frac{1}{8r^2\,\beta_o^2}\left\{\frac{r^4}{2}\left[a_o(1-4\,\beta_o^2) + a_1 + a_2\right.\right.$$

$$\left.\left. + a_4(1+4\beta_o^2)\right]\right\}\ ;$$

$$N_2 = -\frac{1}{8\,\beta_o^2}\left\{\frac{r^4}{2}\left[(a_o + a_3)(1 - 4\,\beta_o^2) + a_1 + a_2\right]\right\}\ ;$$

$$m_1 = \frac{1}{8\,\beta_o^2\, r^2}\left\{\frac{r^4}{2}\left[(a_o + a_3)(1 + 4\,\beta_o^2) + a_1 + a_2\right\}\right.\ ;$$

$$m_2 = \frac{r^4}{2}\left[2(1 - 2\,\beta_o^2)\,a_o + a_1 - a_3\right]\ ;$$

$$M_1 = m_1/2i\,\beta_o\, r\ ;\ \text{and}\ M_2 = m_2/4i\,\beta_o\, r \qquad \text{(I.24)}$$

The first term in Eq. I.23 depends on the ratio r, and can be evaluated as follows

$$I' = \frac{M_1}{2} \left\{ \ell n \left(\frac{1 - 2i\ \beta_o\ r - r^2}{1 + 2i\ \beta_o\ r - r^2} \right) - \ell n \left(\frac{1 + 2i\ \beta_o\ r - r^2}{1 - 2i\ \beta_o\ r - r^2} \right) \right\}$$

$$= \frac{m_1}{2\ \beta_o\ r}\ Q_r \qquad \text{(I.25)}$$

where

$$\begin{aligned} Q_r &= 2(\pi - \theta) && r < 1 \\ &= \pi && r = 0 \\ &= 2\theta && r > 1 \end{aligned} \qquad \text{(I.26)}$$

in which $\theta = \tan^{-1} \dfrac{2\ \beta_o\ r}{|1-r|^2}$.

The closed form integration for the following forms are also required.

$$I_{c2} = \int_{-\omega_c}^{\omega_c} (a_o\ \omega_o^2\ \omega^2 + a_1\ \omega_o^4)\ |H_o|^2\ d\omega$$

$$= \omega_c \cdot B_m(r,\ \beta_o,\ a_o,\ a_1) = \omega_c \cdot B_m \qquad \text{(I.27)}$$

where a_o and a_1 are constants and for brevity B_m is used for $B_m(r,\ \beta_o,\ a_o,\ a_1)$. In Eq. I.26, B_m is defined as

$$B_m = \frac{m_1}{2\ \beta_o\ r} P_r + \frac{2N_1 + m_1}{2r\sqrt{1 - \beta_o^2}} \ln \left\{ \frac{1+r^2 - 2r\sqrt{1 - \beta_o^2}}{1+r^2 + 2r\sqrt{1 - \beta_o^2}} \right\} \tag{I.28}$$

in which the coefficients m_1 and N_1 are defined as follows

$$m_1 = \frac{a_o + a_1}{2} r^2 \quad ; \quad N_1 = -\frac{a_1}{2} r^2 \tag{I.29}$$

The coefficient P_r depends on the value of r and can be obtained as

$$\begin{aligned} P_r &= 2(\pi-\theta) && r < 1 \\ &= \pi && r = 1 \\ &= 2\theta && r > 1 \end{aligned} \tag{I.30}$$

where $\theta = \tan^{-1} \dfrac{2\ \beta_o\ r}{|1-r^2|}$.

I-D COEFFICIENTS AT RESONANCE

For $\omega_c = \infty$, the factors A_m, B_m, and A_m' in Eq. 2.43 are defined as

$$\left.\begin{aligned} A_m &= \frac{1 + 12\ \beta_o^2 + 16\ \beta_o^4}{8\ \beta_o^3} \\ B_m &= (1 - 4\ \beta_o/\pi) \\ A_m' &= (A_m - 4\ \beta_o/3\pi)/B_m \end{aligned}\right\} \tag{I.31}$$

Also the factor C_m and C_m' in Eq. 2.46 are defined as

$$\left.\begin{aligned} C_m &= \frac{(1 + 4\ \beta_o^2)(A_r + B_r) + 4\ \beta_o^3\ A_r}{8\ \beta_o^3} \\ C_m' &= (C_m - 4\ \beta_o\ A_r/\pi)/B_m \end{aligned}\right\} \qquad \text{(I.32)}$$

Appendix II

NONCLASSICAL DAMPING: MODE DISPLACEMENT METHOD

II-A EXPECTED VALUES

In Eq. 3.28, the expected values are evaluated as follows:

$$E[z_j(t_1)\ z_k(t_2)] = \int_0^{t_1}\int_0^{t_2} F_j\ F_k\ E[\ddot{X}_g(\tau_1)\ \ddot{X}_g(\tau_2)]\ e^{p_j(t_1-\tau_1)}\ e^{p_k(t_2-\tau_2)}\ d\tau_1\ d\tau_2 \qquad (II.1)$$

which can be written as

$$E[z_j(t_1)\cdot z_k(t_2)] = \int_{-\infty}^{\infty} F_j\ F_k\ \Phi_g(\omega)\ e^{p_j t_1}\ e^{p_k t_2}\ d\omega \cdot \int_0^{t_1} e^{(-p_j+i\omega)\tau_1}\ d\tau_1 \int_0^{t_2} e^{(-p_k-i\omega)\tau_2}\ d\tau_2$$

Considering stationary response, with $t_1 \to \infty$, $t_2 \to \infty$ and $(t_1-t_2) \to \tau$, the above equation can be written as

$$E[z_j(t_1)\ z_k(t_2)] = \int_{-\infty}^{\infty} \frac{F_j\ F_k\ \Phi_g(\omega)\ e^{i\omega\tau}}{(-p_j+i\omega)(-p_k-i\omega)}\ d\omega \qquad (II.2a)$$

For j = k

$$E[z_j(t)\ z_j(t_2)] = \int_{-\infty}^{\infty} \frac{F_j^2\ \Phi_g(\omega)\ e^{i\omega\tau}}{(p_j^2 + \omega^2)}\ d\omega \qquad \text{(II.2b)}$$

Similarly other expected values required in Eq. 3.31 can be obtained as follows:

$$E[z_j(t_1)\cdot z_k^*(t_2)] = F_j\ F_k^* \int_{-\infty}^{\infty} \frac{\Phi_g(\omega)\ e^{i\omega\tau}}{(-p_j+i\omega)(-p_k^*-i\omega)}\ d\omega \qquad \text{(II.3a)}$$

For j = k

$$E[z_j(t_1)\ z_j^*(t_2)] = F_j\ F_j^* \int_{-\infty}^{\infty} \frac{\Phi_g(\omega)\ e^{i\omega\tau}}{(-p_j+i\omega)(-p_j^*-i\omega)}\ d\omega \qquad \text{(II.3b)}$$

Also

$$E[z_j^*(t_1)\ z_k(t_2)] = F_j^*\ F_k \int_{-\infty}^{\infty} \frac{\Phi_g(\omega)\ e^{i\omega\tau}}{(-p_j^*+i\omega)(-p_k-i\omega)}\ d\omega \qquad \text{(II.4a)}$$

For j = k

$$E[z_j^*(t_1)\ z_j(t_2)] = F_j^*\ F_j \int_{-\infty}^{\infty} \frac{\Phi_g(\omega)\ e^{i\omega\tau}}{(-p_j^*+i\omega)(-p_j-i\omega)}\ d\omega \qquad \text{(II.4b)}$$

and finally

$$E[z_j^*(t_1)\ z_k^*(t_2)] = F_j^*\ F_k^* \int_{-\infty}^{\infty} \frac{\Phi_g(\omega)\ e^{i\omega\tau}}{(-p_j^*+i\omega)(-p_k^*-i\omega)}\ d\omega \qquad \text{(II.5a)}$$

For $j = k$

$$E[z_j^*(t_1)\ z_j^*(t_2)] = F_j^{*2} \int_{-\infty}^{\infty} \frac{\Phi_g(\omega)\ e^{i\omega\tau}}{(p_j^{*2} + \omega^2)}\ d\omega \qquad \text{(II.5b)}$$

II.D AMPLIFICATION FACTORS

The coefficients A_1, B_1, C_1 and D_1 in Eq. 3.48 are obtained as the solution of the following simultaneous equation

$$[P]\ \{A\} = \{W_1\} \qquad \text{(II.6)}$$

where

$$\{A\}^T = (A_1,\ A_2,\ A_3,\ A_4) \qquad \text{(II.7)}$$

and [P] is a 4×4 matrix whose elements are

$$[P] = \begin{bmatrix} 0 & 1 & 0 & 1 \\ 1 & u & 1 & x \\ u & v & x & y \\ v & 0 & y & 0 \end{bmatrix} \qquad \text{(II.8)}$$

in which $u = -2(1 - 2\beta_o^2)$, $v = 1$, $x = -2\,r_1^2\,(1 - 2\beta_j^2)$, and $y = r_1^4$. Also,

$$W_1(1) = 0\ ,\ W_1(2) = 4\,\beta_o^2\,C_j'\ ,\ W_1(3) = C_j' + 4\,\beta_o^2\,D_j'\ ,$$
$$W_1(4) = D_j' \qquad \text{(II.9)}$$

The factors A_j, B_j, ..., A_k, B_k, ..., etc. in Eq. 3.48 are obtained as the solution of the following simultaneous equations:

$$[P]\ \{A_j\} = \{W_2\} \quad \text{and} \quad [P']\ \{A_k\} = \{W_4\} \tag{II.10}$$

where

$$\{A_j\}^T = (A_j,\ B_j,\ C_j,\ D_j) \text{ and } \{A_k\}^T = (A_k,\ B_k,\ C_k,\ D_k) \tag{II.11}$$

and the elements of [P] are the same as in Eq. II.8 and the matrix [P'] is defined as

$$[P'] = \begin{bmatrix} 0 & 1 & 0 & 1 \\ 1 & u & 1 & x' \\ u & v & x' & y' \\ v & 0 & y' & 0 \end{bmatrix} \tag{II.12}$$

in which $x' = -2\, r_2^2\, (1 - 2\, \beta_k^2)$ and $y' = r_2^4$, u and v are the same as defined in Eq. II.8. Also

$$W_2(1) = 0\ ,\ W_2(2) = 4\, F_2\, \beta_o^2\ ,\ W_2(3) = 4\, F_1\, \beta_o^2 + F_2\ ,$$
$$W_2(4) = F_1$$
$$W_3(1) = 0\ ,\ W_3(2) = 4\, F_4\, \beta_o^2\ ,\ W_3(3) = 4\, F_3\, \beta_o^2 + F_4\ ,$$
$$W_3(4) = F_3 \tag{II.13}$$

Whereas the coefficients F_1, F_2, F_3, and F_4 in Eq. II.13 are obtained as the solution of the following simultaneous equations

$$[P''] \{F\} = \{W_4\} \tag{II.14}$$

where

$$\{F\}^T = (F_1, F_2, F_3, F_4)$$

and the elements of 4×4 matrix [P''] are defined as

$$[P''] = \begin{bmatrix} 0 & 1 & 0 & 1 \\ 1 & u'' & 1 & x'' \\ u'' & v'' & x'' & y'' \\ v'' & 0 & y'' & 0 \end{bmatrix} \tag{II.15}$$

in which

$$u'' = -2 r_2^2 (1 - 2 \beta_k^2) \ , \ v'' = r_2^4 \ ,$$

$$x = -2 r_1^2 (1 - 2 \beta_j^2) \ , \text{ and } y = r_1^4 \tag{II.16}$$

Also

$$W_4(1) = D_1 \ , \ W_4(2) = C_1 D_1 + D_2 + E_2 \ ,$$

$$W_4(3) = C_1 D_2 + C_2 D_1 + E_3 \ , \text{ and } W_4(4) = C_2 D_2 \tag{II.17}$$

In Eq. II.17, the coefficients C_1, C_2, D_1, D_2, E_2, E_3 are defined as follows:

$$C_1 = -(\gamma_1^2 + \gamma_2^2 - 4\,\gamma_1\,\gamma_2\,\beta_j\,\beta_k)\ ;\ C_2 = \gamma_1^2\,\gamma_2^2\ ;$$

$$D_1 = 4\,\gamma_1\,\gamma_2\,[a_k\,a_j\,\beta_k\,\beta_j + b_k\,b_j\sqrt{1-\beta_k^2}\sqrt{1-\beta_j^2}$$

$$+ a_k\,b_j\,\beta_k\sqrt{1-\beta_j^2} + a_j\,b_k\,\beta_j\sqrt{1-\beta_k^2}\,]\ ;$$

$$D_2 = 4\,\gamma_1^2\,\gamma_2^2\,a_k\,a_j\ ;\ E_2 = 8\cdot E_1\cdot(\gamma_1\,\beta_j - \gamma_2\,\beta_k)\ ;$$

$$E_3 = 8\cdot E_1\,\gamma_1\,\gamma_2\,(\gamma_1\,\beta_k - \gamma_2\,\beta_j)\ ;$$

$$E_1 = -\gamma_1\,\gamma_2\,[a_j\,a_k\,(\gamma_2\,\beta_j - \gamma_1\,\beta_k)$$

$$- a_j\,b_k\,\gamma_1\sqrt{1-\beta_k^2} + a_k\,b_j\,\gamma_2\sqrt{1-\beta_j^2}\,] \qquad \text{(II.18)}$$

II-C COEFFICIENTS IN RESONANCE CASE

In Eq. 3.52, A_m is defined using Eq. I.22 in Appendix I-C as follows:

$$A_m = A_m(r,\ \beta_o,\ b_o,\ b_1,\ b_2,\ b_3) \qquad \text{(II.19)}$$

in which

$$b_o = 0\ ;\ b_1 = 4\,\beta_o^2\,C_j'/\omega_o^2\ ;\ b_2 = (C_j'/\omega_o^2 + 4\,\beta_o^2\,D_j/\omega_o^4)\ ;$$

$$b_3 = D_j' \qquad \text{(II.20)}$$

The coefficient D_m in Eq. 3.57 is also defined using Eq. I.22 in Appendix I-C as follows:

$$D_m = A_m(r,\ \beta_o,\ c_o,\ c_1,\ c_2,\ c_3) \qquad \text{(II.21)}$$

where

$$c_o = 0 \ , \ c_1 = 4 \ \beta_o^2 \ F_2 \ , \ c_2 = F_2 + 4 \ \beta_o^2 \ F_1 \ ,$$

$$c_3 = F_1 \qquad \text{(II.22)}$$

Appendix III

CLASSICAL DAMPING: MODE ACCELERATION METHOD

III-A EXPECTED VALUES

For stationary response, the expected values required in Eq. 4.13 can be obtained by following the procedure described in Appendix I-A. Thus, it can be shown that

$$E[\ddot{X}_g(t_1)\ \ddot{z}_k(t_2)] = \int_{-\infty}^{\infty} \Phi_g(\omega)\ \omega^2\ H_k^*\ e^{i\omega\tau}\ d\omega \qquad \text{(III.1)}$$

$$E[\ddot{z}_j(t_1)\ \ddot{X}_g(t_2)] = \int_{-\infty}^{\infty} \Phi_g(\omega)\ \omega^2\ H_j\ e^{i\omega\tau}\ d\omega \qquad \text{(III.2)}$$

$$E[\ddot{z}_j(t_1)\ \ddot{z}_k(t_2)] = \int_{-\infty}^{\infty} \Phi_g(\omega)\ \omega^4\ H_j\ H_k^*\ e^{i\omega\tau}\ d\omega \qquad \text{(III.3)}$$

Other expected values required in Eq. 4.13 are given in Appendix I-A.

III-B AMPLIFICATION FACTORS

The coefficients A_1, B_1, C_1 and D_1 in Eq. 4.12 are obtained from the solution of the following simultaneous equations:

$$[P]\ \{A_j\} = \{W_1\} \qquad \text{(III.4)}$$

where

$$\{A_j\}^T = \{A_1,\ B_1,\ C_1,\ D_1\} \qquad \text{(III.5)}$$

and [P] is a 4×4 matrix whose elements are the same as defined in Eq. I.9. Also

$$W_1(1) = 0\ ,\ W_1(2) = -\ 4\ \beta_o^2\ ,\ W_1(3) = 4\ \beta_o^2\ r_1^2 - 1\ ,$$
$$W_1(4) = r_1^2 \qquad \text{(III.6)}$$

The factors A_2, B_2, C_2, D_2 in Eq. 4.15 are obtained as the solution of the following simultaneous equations:

$$[P]\ \{A_k\} = \{W_2\} \qquad \text{(III.7)}$$

where

$$\{A_k\}^T = \{A_2,\ B_2,\ C_2,\ D_2\} \qquad \text{(III.8)}$$

and

$$W_2(1) = 0\ ,\ W_2(2) = 4\ \beta_o^2\ ,\ W_2(3) = 1\ ,\ W_2(4) = 0 \qquad \text{(III.9)}$$

Matrix [P] is the same as defined in Eq. I.9.

The coefficients $A_j \ldots D_j$ and $A_k \ldots D_k$ which appear in cross-terms under double summation in Eq. 4.21 are obtained from the solution of the following simultaneous equations:

$$[P]\ \{A_{oj}\} = \{W_3\} \quad \text{and} \quad [P']\ \{A_{ok}\} = \{W_4\} \qquad \text{(III.10)}$$

where

$$\{A_{oj}\}^T = (A_j, B_j, C_j, D_j)$$

and (III.11)

$$\{A_{ok}\}^T = (A_k, B_k, C_k, D_k)$$

and the elements of [P] are the same as given in Eq. I.9 and the elements of matrix [P'] are the same as defined in Eq. I.15. Also,

$$W_3(1) = 0 \ , \ W_3(2) = 4 \ \beta_o^2 \ B_r \ , \ W_3(3) = 4 \ A_r \ \beta_o^2 + B \ ,$$

$$W_3(4) = A_r$$

$$W_4(1) = 0 \ , \ W_4(2) = 4 \ \beta_o^2 \ D_r \ , \ W_4(3) = 4 \ \beta_o^2 \ C_r + D \ ,$$

$$W_4(4) = C_r \qquad \text{(III.12)}$$

whereas the coefficients A_r, B_r, C_r, D_r in Eqs. 4.20 and III.10 are obtained as the solution of the following simultaneous equations:

$$[P''] \ \{A\} = \{W_5\} \qquad \text{(III.13)}$$

where

$$\{A\}^T = (A_r, B_r, C_r, D_r) \qquad \text{(III.14)}$$

and the elements of 4×4 matrix [P''] are the same as defined in Eq. I.19. Also,

$$W_5(1) = 1 \ , \ W_5(2) = 4 \ \beta_j \ \beta_k \ r_1 \ r_2 - r_1^2 - r_2^2 \ ,$$

$$W_5(3) = r_1^2 \ r_2^2 \ , \ W_5(4) = 0 \qquad \text{(III.15)}$$

III-C COEFFICIENTS IN RESONANCE CASE

In Eq. 4.28, V_m is defined as

$$V_m = \omega_o^2 \cdot B_m(r, \beta_o, a_o, a_1) \qquad \text{(III.16)}$$

in which $a_o = 1$, $a_1 = 0$ and B_m is defined by Eq. I.27 in Appendix I-C.

The coefficient, F_m in Eq. 4.29, is defined as

$$F_m = A_m(r, \beta_o, b_o, b_1, b_2, b_3) \qquad \text{(III.17)}$$

in which $b_o = -4\beta_o^2$; $b_1 = -(1 - 4\beta_o^2)$; $b_2 = 1$; $b_3 = 0$; and A_m is defined by Eq. I.22 in Appendix I-C.

In Eq. 4.34, the coefficient G_m is defined as

$$G_m = A_m(r, \beta_o, b_o', b_1', b_2', b_3') \qquad \text{(III.18)}$$

wherein $b_o' = 4\beta_o^2$, $b_1' = 1$, $b_2' = 0$, $b_3' = 0$.

The factor H_m which appears in Eq. 4.41 is obtained by the following equation

$$H_m = A_m(r, \beta_o, c_o, c_1, c_2, c_3) \qquad \text{(III.19)}$$

in which $c_o = 4\beta_o^2 B_r$; $c_1 = B_r + 4\beta_o^2 A_r$; $c_2 = A_r$; $c_3 = 0$ and the factor, A_m in Eqs. III.18 and III.19 is defined by Eq. I.22 in Appendix I-C.

Appendix IV

NONCLASSICAL DAMPING: MODE ACCELERATION METHOD

IV-A EXPECTED VALUES

Following the description in Appendix II-A, the expected values required in Eq. 5.5 can be obtained as follows:

$$E[\ddot{X}_g(t_1)\ z_k(t_2)] = -\int_0^{t_2} F_k\ e^{p_k(t_2-\tau_2)} \cdot E[\ddot{X}_g(t_1)\ \ddot{X}_g(\tau_2)]\ d\tau_2 \qquad \text{(IV.1)}$$

Substituting $t_2 - \tau_2 = u$ and $d\tau_2 = -du$, Eq. IV.1 can be written as

$$E[\ddot{X}_g(t_1)\ z_k(t_2)] = -F_k \int_0^{t_2} e^{p_k u} \cdot E[\ddot{X}_g(t_1)\ \ddot{X}_g(t_2-u)]\ du \qquad \text{(IV.2)}$$

Using Eq. I.3, and after some algebraic manipulations Eq. IV.2 can be written as

$$E[\ddot{X}_g(t_1)\ z_k(t)] = -F_k \int_{-\omega}^{\omega} \Phi_g(\omega)\ e^{i\omega t_1} \cdot \frac{e^{p_k t_2} - e^{-i\omega t_2}}{p_k + i\omega}\ d\omega \qquad \text{(IV.3)}$$

Now

$$E[\ddot{X}_g(t_1)\ \ddot{z}_k(t_2)] = \partial^2/\partial t_2^2\ \{E[\ddot{X}_g(t_1)\ z_k(t)]\}$$

$$= -\ F_k \int_{-\infty}^{\infty} \Phi_g(\omega)\ e^{i\omega t_1}$$

$$\frac{p_k^2\ e^{p_k t_2} + \omega^2\ e^{-i\omega t_2}}{p_k + i\omega}\ d\omega \qquad \text{(IV.4)}$$

For stationary response, $t_1 \to \infty$, $t_2 \to \infty$, $(t_1 - t_2) \to \tau$, hence

$$E[\ddot{X}_g(t_1)\ \ddot{z}_k(t_2)] = -\ F_k \int_{-\infty}^{\infty} \omega^2\ \Phi_g(\omega)\ \frac{e^{i\omega\tau}}{(p_k + i\omega)}\ d\omega \qquad \text{(IV.5)}$$

Similarly the other expected values in Eq. 5.5 can be shown to be as follows:

$$E[\ddot{X}_g(t_1)\ \ddot{z}_k^*(t_2)] = -\ F_k^* \int_{-\infty}^{\infty} \Phi_g(\omega) \cdot \omega^2\ \frac{e^{i\omega\tau}}{(p_k^* + i\omega)}\ d\omega \qquad \text{(IV.6)}$$

$$E[\ddot{X}_g(t_2)\ \ddot{z}_j(t_1)] = -\ F_j \int_{-\infty}^{\infty} \Phi_g(\omega)\ \omega^2\ \frac{e^{i\omega\tau}}{(p_j - i\omega)}\ d\omega \qquad \text{(IV.7)}$$

$$E[\ddot{X}_g(t_2)\ \ddot{z}_j^*(t_1)] = -\ F_j^* \int_{-\infty}^{\infty} \Phi_g(\omega)\ \omega^2\ \frac{e^{i\omega\tau}}{(p_j^* - i\omega)}\ d\omega \qquad \text{(IV.8)}$$

Using the following:

$$E[\ddot{z}_j(t_1)\ \ddot{z}_k(t_2)] = \frac{\partial^2}{\partial t_1^2}\ \frac{\partial^2}{\partial t_2^2}\ E[z_j(t_1)\ z_k(t_2)] \qquad \text{(IV.9)}$$

Other expected values required in Eq. 5.5 can be obtained from Appendix II-A.

IV-B AMPLIFICATION FACTORS

The coefficients A_1, A_2, A_3, A_4 in Eq. 5.21 are obtained from the solution of the following simultaneous equations

$$[P]\ \{R_j\} = \{W_1\} \tag{IV.10}$$

where

$$\{R_j\}^T = (A_1,\ A_2,\ A_3,\ A_4) \tag{IV.11}$$

and the elements of matrix [P] are the same as defined in Eq. II.8. Also

$$W_1(1) = 0;\ W_1(2) = 4\ \beta_o^2\ t_1;\ W_1(3) = t_1 + 4\ \beta_o^2\ t_3;$$
$$W_1(4) = t_3 \tag{IV.12}$$

The coefficients B_1, B_2, B_3, B_4 which appear in Eq. 5.23 are obtained as the solution of the following equations

$$[P]\ \{R_j'\} = \{W_2\} \tag{IV.13}$$

in which

$$\{R_j'\}^T = (B_1,\ B_2,\ B_3,\ B_4) \tag{IV.14}$$

and

$$W_2(1) = 4\ \beta_o^2\ a_j^2;\ W_2(2) = a_j^2 + 4\ \beta_o^2\ A_j';$$

$$W_2(3) = A_j';\ W_2(4) = 0 \qquad \text{(IV.15)}$$

Matrix [P] is the same as defined in Eq. IV.10.

The coefficients A_j, B_j, A_k, B_k, etc. which appear in the cross-terms in Eq. 5. are obtained as the solution of the following simultaneous equations:

$$[P]\ \{A_j\} = \{W_3\} \quad \text{and} \quad [P']\ \{A_k\} = \{W_4\} \qquad \text{(IV.16)}$$

where

$$\{A_j\}^T = (A_j,\ B_j,\ C_j,\ D_j)$$

and (IV.17)

$$\{A_k\}^T = (A_k,\ B_k,\ C_k,\ D_k)$$

The elements of matrix [P] are the same as defined in Eq. IV.10 and the matrix [P'] is the same as defined in Eq. II.12. Also

$$W_3(1) = 4\ F_2\ \beta_o^2\ ,\ W_3(2) = 4\ \beta_o^2\ F_1 + F_2\ ,\ W_3(3) = F_1\ ,$$

$$W_3(4) = 0$$

$$W_4(1) = 4\ F_4\ \beta_o^2\ ,\ W_4(2) = 4\ \beta_o^2\ F_3 + F_4\ ,\ W_4(3) = F_3\ ,$$

$$W_4(4) = 0 \qquad \text{(IV.18)}$$

whereas the coefficients F_1, F_2, F_3 and F_4 in Eq. IV.18 are obtained as the solution of the following simultaneous equations

$$[P''] \{F_k\} = \{W_5\} \tag{IV.19}$$

where

$$\{F_k\}^T = (F_1, F_2, F_3, F_4) \tag{IV.20}$$

The elements of matrix [P''] are the same as defined in Eq. II.15, and

$$W_5(1) = D_1;\ W_5(2) = C_1 D_1 + D_2 + E_2;$$
$$W_5(3) = C_1 D_2 + C_2 D_1 + E_3;\ W_5(4) = C_2 D_2 \tag{IV.21}$$

In Eq. IV.21, the coefficients C_1, C_2, D_1, D_2, E_2 and E_3 are defined as follows:

$$C_1 = -(\gamma_1^2 + \gamma_2^2 - 4\gamma_1\gamma_2\beta_j\beta_k)\ ;\ C_2 = \gamma_1^2\gamma_2^2\ ;$$
$$D_1 = 4 a_j a_k\ ;\ D_2 = 4\gamma_1\gamma_2 [a_j a_k \beta_j \beta_k$$
$$+ b_j b_k \sqrt{1-\beta_j^2}\sqrt{1-\beta_k^2} - a_j b_k \beta_j \sqrt{1-\beta_k^2}$$
$$- a_k b_j \beta_k \sqrt{1-\beta_j^2}];\ E_2 = 8 \cdot E_1(\gamma_1\beta_j - \gamma_2\beta_k)\ ;$$
$$E_3 = 8\gamma_1\gamma_2 E_1(\gamma_1\beta_k - \gamma_2\beta_j)\ ;\ E_1 = -a_j a_k (\gamma_2\beta_k$$
$$- \gamma_1\beta_j) + a_j b_k \gamma_2\sqrt{1-\beta_k^2} - a_k b_j \gamma_1\sqrt{1-\beta_j^2} \tag{IV.22}$$

IV-C COEFFICIENTS IN RESONANCE CASE

In the first single summation term denoted by I_s', as given by Eq. 5.25, A_m is defined as:

$$A_m = A_m(\gamma_c, \beta_o, a_o, a_1, a_2, a_3) \tag{IV.23}$$

where

$$a_o = 4\ \beta_o^2\ \omega_o^2\ t_1\ ,\ a_1 = t_1 + 4\ \beta_o^2\ t_3/\omega_o^2\ ,$$

$$a_2 = t_3/\omega_o^2\ ,\ a_3 = 0 \tag{IV.24}$$

In the second single summation term, I_s'' given by Eq. 5.31, the factor B_m is defined as

$$B_m = B_m(\gamma_c, \beta_o, b_o, b_1, b_2, b_3) \tag{IV.25}$$

in which

$$b_o = a_j^2\ \{1 + 16\ \beta_o^2(1 - 2\ \beta_o^2)\} + 4\ A_j\ \beta_o^2\ ;$$

$$b_1 = A_j - 8\ a_j^2\ \beta_o^2\ \{1 + 2\ (1 - 2\ \beta_o^2)^2\}\ ;$$

$$b_2 = 16\ a_j^2\ \beta_o^2\ (1 - 2\ \beta_o^2)\ ;\ b_3 = -\ 4\ a_j^2\ \beta_o^2 \tag{IV.26}$$

In Eq. 5.36, the factor C_m is defined as

$$C_m = C_m(\gamma_c, \beta_o, c_o, c_1, c_2, c_3) \tag{IV.27}$$

in which

$$c_o = 4\,\beta_o^2\,F_1 + F_2\,\{1 + 16\,\beta_o^2\,(1 - 2\,\beta_o^2)\}\;;$$

$$c_1 = F_1 - 8\,\beta_o^2\,F_2\,\{1 + 2\,(1 - 2\,\beta_o^2)^2\}\;;$$

$$c_2 = 16\,\beta_o^2\,F_2\,(1 - 2\,\beta_o^2)\;;\; c_3 = -\,4\,\beta_o^2\,F_2 \qquad \text{(IV.28)}$$

NOMENCLATURE

$[A]$ = real symmetric matrix of order 2n, defined by Eq. 3.2

$\{A_{oj}\},\{A_{ok}\}$ = vectors defined in Eq. III.10

A_j, B_j, C_j, D_j = coefficients of partial fractions defined by Eqs. II.10, III.11 and IV.16

A_g = maximum ground acceleration

A'_j = constant defined by Eqs. 3.33 and 5.12

A^*_j, B^*_j = diagonal elements of matrices: $[\phi]^T[A][\phi]$ and $[\phi]^T[B][\phi]$ respectively

A_k, B_k, C_k, D_k = coefficients of partial fractions

A_r, B_r, C_r, D_r = coefficients of partial fractions

A_1, A_2, A_3, A_4 = coefficients of partial fractions

$A_m, C_m, D_m, E_m, G_m, H_m$ = frequency integrals defined by Eq. I.22

A'_m = a factor function of frequency integrals

a_j, b_j = real and imaginary parts of the jth element of complex eigenvector $\{\phi_j\}$

a_o, a_1, a_2, a_3 = constants

a'_o, a'_1, a'_2, a'_3 = constants

$[B]$ = real symmetric matrix of order 2n, defined by Eq. 3.2

B_1, B_2, B_3, B_4 = coefficients of partial fractions

B_m = frequency integral defined by Eq. I.27

b_o, b_1, b_2, b_3 = constants

b'_o, b'_1, b'_2, b'_3 = constants

$[C]$ = damping matrices

C_1, C_2, C_3, C_4 = coefficients of partial fractions

c_o, c_1, c_2, c_3 = constants

c'_o, c'_1, c'_2, c'_3 = constants

[D] = real symmetric matrix of order 2n defined by Eq. 3.2

D_1, D_2 = constants of partial fractions

$E[\cdot]$ = expected value

E_1, E_2, E_3 = constants of partial fractions defined in Eqs. II.18 and IV.22

e/r = eccentricity ratio

{F} = complex symmetric matrix defined by Eq. 3.9

$\{F_k\}$ = vector of unknowns defined by Eq. IV.20

F_j = jth element of {F} defined by Eq. 3.10

$F(\omega_o)$ = ratio of frequency integrals defined by Eq. 2.38

H_j = complex frequency response function defined by Eq. 2.13

h_j = impulse response function

I_1, I_2, I_3 = frequency integrals defined by Eqs. 2.22, 2.23 and 4.9, respectively

I_b, I_{b2} = frequency integrals defined by Eqs. 2.34

I_d, I_{dd} = frequency integrals in double summation terms

$I'_d, I_d(\omega_o)$ = frequency integrals in double summation terms

I_g = frequency integral defined by Eq. 4.8

$I_s, I'_s(\omega_o)$ = frequency integrals in single summation terms

I'_s, I''_s = frequency integrals in single summation terms

$I_s(\omega_o)$ = frequency integral in single summation terms

I_{s1}, I_{s2} = frequency integrals in single summation terms

$i = \sqrt{-1}$

[K] = stiffness matrix

K, K_1, K_2 = constants of proportionality

$[M]$ = mass matrix

N, N_1, N_2 = functions to define the integrands

n = number of degrees of freedom

$[P], [P'], [P'']$ = matrices of order 4x4 used in Appendix I, II, III and IV

$P_F(\omega_o)$ = peak factor in floor spectra

p = probability of nonexceedance

p_j = jth complex eigenvalue

p_j^* = jth complex conjugate eigenvalue

$R_a(\omega_o, \beta_o)$ = floor response spectrum value at frequence ω_o and damping β_o

$\{R_j'\}$ = vector of unknowns as defined in Eq. I.14

R_d, R_{dd} = frequency integrals in the double summation terms

R_p = pseudo acceleration spectra

R_r = relative velocity spectra

$R_s, R_s', R_s'', R_{s1}, R_{s2}$ = frequency integrals in single summation terms

R_v = relative velocity spectra

$\{r\}$ = displacement influence vector

r_m = mth element of displacement vector $\{r\}$

S_g = peak factor for ground acceleration

S_p = peak factor for pseudo acceleration

S_r = peak factor for relative acceleration

S_v = peak factor for relative velocity

t_1, t_2, t_3 = coefficients defined by Eq. 5.9

U_{jk}, V_{jk} = coefficients defined

V_m = frequency integral defined by Eqs. III.16

X_{jk}, Y_{jk} = coefficients defined by Eqs. 3.43

X'_{jk}, Y'_{jk} = factors defined by Eqs. 3.40, 3.41 and 5.15, 5.16

$\ddot{X}_g(t)$ = ground acceleration time history

$\ddot{X}_a, \ddot{X}_{am}$ = absolute acceleration of floor

$\ddot{x}_a$ = relative acceleration of floor

$\{x\}$ = relative displacement vector

$\{y\}$ = 2n-dimensional state vector defined by Eq. 3.3

$\{z\}$ = vector of complex value principal coordinates

$\{z'\}$ = vector of principal coordinates

z_j = jth element of $\{z\}$

α = decay rate defined by Eq. 2.49

β_j = jth modal damping ratio

β_o = oscillator damping ratio

γ_j = jth participation factor

δ, δ_e = band with parameters, defined by Eqs. 2.51 and 2.52

ξ_j = real part of complex eigenvalue p_j

$\eta, \dot{\eta}, \ddot{\eta}$ = relative displacement, velocity and acceleration of the oscillator, respectively

$\ddot{\eta}_a$ = absolute acceleration of the oscillator

θ_j = imaginary part of p_j

λ = eigenvalue

λ_k = spectral moements defined by Eq. 2.53

$\lambda_{f\ell}$ = moments of floor response defined by Eq. 2.68

$\lambda_{p\ell}$ = moments pseudo acceleration response defined by Eq. 2.54

$\lambda_{v\ell}$ = moments of relative velocity response defined by Eq. 2.55

$\{\rho\}$ = a vector defined by Eq. 3.18

$\sigma_{\ddot{\eta}_a}$ = standard deviation of $\ddot{\eta}_a$

$\Phi_g(\omega)$ = spectral density of ground motion defined by Eq. 2.105

Φ_m = spectral density function of floor motion

$[\phi]$ = modal matrix

$\{\phi_j\}$ = jth eigenvector of $[\phi]$

$\{\phi_j\}_\ell$ = lower half part of complex eigenvector

$\{\phi_j\}_u$ = upper half part of complex eigenvector

ϕ_j = mth element of eigenvector $\{\phi_j\}$

ω = natural circular frequency

ω_j = jth natural frequency

ω_o = oscillator frequency

ν_a = level crossing rate defined by Eq. 2.50

BIBLIOGRAPHIC DATA SHEET	1. Report No. VPI-E-83-44	2.	3. Recipient's Accession No. PB84 191675
4. Title and Subtitle DIRECT GENERATION OF SEISMIC FLOOR RESPONSE SPECTRA FOR CLASSICALLY AND NONCLASSICALLY DAMPED STRUCTURES			5. Report Date November 1983 6.
7. Author(s) Anil M. Sharma and Mahendra P. Singh			8. Performing Organization Rept. No.
9. Performing Organization Name and Address DEPARTMENT OF ENGINEERING SCIENCE AND MECHANICS VIRGINIA POLYTECHNIC INSTITUTE AND STATE UNIVERSITY BLACKSBURG, VA 24061			10. Project/Task/Work Unit No. 11. Contract/Grant No. CEE-8109100
12. Sponsoring Organization Name and Address National Science Foundation Washington, D.C. 20550			13. Type of Report & Period Covered Final 14.

15. Supplementary Notes

16. Abstracts

Floor response spectra are commonly used as seismic inputs for the design of secondary systems. Here several direct approaches based on the method of mode displacement as well as mode acceleration have been developed for generation of floor spectra for classically and non-classically damped systems. The mode displacement approaches require pseudo acceleration and relative velocity spectra whereas the mode acceleration approaches require relative acceleration and velocity spectra as their seismic inputs. These proposed approaches have been validated by a comprehensive numerical simulation study involving several ensembles of time histories.

For structural systems with dominant high frequency modes, the mode displacement approaches may give inaccurate results if only a first few modes are used in the analysis, whereas the mode acceleration approaches will still predict the response accurately. Therefore, the mode acceleration approaches are proposed as better alternatives to the mode displacement approaches which are currently used.

17. Key Words and Document Analysis. 17a. Descriptors

Earthquakes: Structural Dynamics; Seismic Response
Floor Specra; Secondary Systems; Vibrations;
Response Spectra; Structural Analysis; Proportional Damping;
Nonproportional Damping

17b. Identifiers/Open-Ended Terms

17c. COSATI Field/Group

18. Availability Statement	19. Security Class (This Report)	21. No. of Pages
Distribution Unlimited	UNCLASSIFIED	
	20. Security Class (This Page) UNCLASSIFIED	22. Price

ACKNOWLEDGEMENTS

This report is the dissertation of Anil M. Sharma which was completed under the supervision of M. P. Singh as his Major Advisor. This dissertation was submitted to Virginia Polytechnic Institute and State University in November 1983 in partial fulfillment of the requirements of the degree of Doctor of Philosophy in Engineering Mechanics.

The work on this report was funded by the National Science Foundation Grant No. CEE-8109100 with Dr. M. P. Gaus and Dr. J. E. Goldberg as its Program Directors. This support is gratefully acknowledged. Any opinion, findings and conclusions or recommendations expressed in this report are those of the writers and do not necessarily reflect the views of the National Science Foundation.